Erythropoietin as a driver of neurodifferentiation, neuroplasticity and cognition – A continuum view of the neuronal lineage

by

Debia Wakhloo

Born in Kashmir, India

Dissertation

for the award of the degree

Doctor of Philosophy (Ph.D.)

In the doctoral program Center for Systems Neuroscience

of the Georg-August-Universität Göttingen

Göttingen 2019

Doctoral thesis committee:

Prof. Dr. Dr. Hannelore Ehrenreich (Supervisor – 1st Referee)	Department of Clinical Neuroscience, Max Planck Institute of Experimental Medicine, Göttingen.
Prof. Dr. Dörthe Katschinski (2nd Referee)	Department of Cardiovascular Physiology Universitätsmedizin Göttingen, Göttingen.
Prof. Dr. Ralf Heinrich	Department of Cellular Neurobiology, Schwann-Schleiden Research Centre, Göttingen.
Prof. Dr. Wolfram-Hubertus Zimmermann	Institute of Pharmacology and Toxicology, Universitätsmedizin Göttingen, Göttingen.

Examination committee:

Prof. Dr. Klaus-Armin Nave	Max Planck Institute of Experimental Medicine, Clinical Neuroscience, Göttingen.
Prof. Dr. Susann Boretius	Department of Functional Imaging, German Primate Center, Göttingen.

Date of thesis submission: 30.09.2019
Date of dissertation defense: 19.11.2019

Declaration

I hereby declare that this Ph.D. thesis "***Erythropoietin as a driver of neurodifferentiation, neuroplasticity and cognition – A continuum view of the neuronal lineage***" has been written independently and is an outcome of my own work with no other sources and aids unless cited.

The second and third chapter of my result section is adapted from the manuscript "***Functional hypoxia drives neuroplasticity and neurogenesis via brain erythropoietin***", currently submitted in a peer-review journal, which summarizes my own contribution to the manuscript.

Debia Wakhloo
Göttingen 2019

Dedicated to my parents

"Sic parvis magna"

"Greatness from small beginnings"

"नम्र शुरुआत से महत्त्वपूर्ण उपलब्धियों की ओर"

- Sir Francis Drake (Nathan Drake)

‘True progress is when you begin with one question and end up having million more’

Acknowledgements

‘‘We often take for granted the very things that most deserve our gratitude.”

– Cynthia Ozick

I would like to dedicate this thesis to my parents, Amrita Wakhloo and Rajnath Wakhloo, who have provided me with a great platform despite several difficulties they had to face. I hope to make them proud.

The last four years have been an integral part of my life. I owe my gratitude to many people and I hope to carry them in my memories forever.

I begin with expressing my deepest gratitude towards my supervisor, Prof. Dr. Dr. Hannelore Ehrenreich for giving me an opportunity to work on a project that is very close to her heart. This has been an exciting yet a challenging project. She always encouraged me to develop as a researcher and more importantly, an independent thinker. Despite our difference in opinions on certain aspects, she always encouraged me to voice my opinion that made my scientific journey more beautiful and immensely educational. I am greatly indebted for her wisdom and her zealous nature, which has led me to be a better version of myself. I have immense admiration for her as a strong driven woman and I hope to mirror some of her qualities in the tough journey of life, which lies ahead.

I am also thankful to Prof. Dr. Klaus-Armin Nave for giving me an opportunity to join this prestigious institute. I am sincerely grateful for his constructive criticism and insightful discussions throughout the project. His collaboration has been of tremendous help.

I would also like to thank my thesis committee members Prof. Dr. Dörthe Katschinski, Prof. Dr. Ralf Heinrich and Prof. Dr. Wolfram-Hubertus Zimmermann, who have always taken time to give their scientific input and provide immense support during my PhD. I would also like to thank my examination board members, Prof. Dr. Klaus-Armin Nave and Prof. Dr. Susann Boretius for taking the time to consider and judge my work.

The journey of a PhD student is exciting but riddled with difficult times. I want to express my sincere love towards my colleagues, without whom, this journey would

have been impossible to complete. I am thankful to Anja Ronnenberg and Sahab Arinrad who were always present to lift me up, when I felt like I had hit rock bottom. A good chat with them over coffee or alcohol has always helped me to strive harder and accomplish more. I am sorry that they had to be the primary victims of my erratic behavior at times. I am also immensely thankful to my project team, Dr. Franziska Scharkowski, Yasmina Curto and Agnes Steixner for their support and generous contributions to the work. I feel blessed to have the opportunity to work with them. I would like to thank the entire technical assistance team who doing an incredible job, especially the animal caretaker Steffi Thiel who has been extremely helpful. I would also like to thank Wiebke Timner, Nadine Schopf and Viktoria Pfander (Danke für die Deutsche Übung) and especially for providing me with emotional support, in my numerous times of need. You all have been my family away from home.

I am especially grateful for my PhD gang members Hong Pan and Jan Seidel with whom I have had my most memorable moments in the past four years. *'Misery Loves Company'* never fitted perfectly than in our case and this journey would have been much more difficult without their lovely companionship.

Not only has the pristine beauty of Austria smote me, but also I feel lucky to have met amazing souls like my Austrian sweethearts – Sandra Kogler and Agnes Steixner. Thank you for being a constant source of motivation to make me strive harder and accomplish more. More importantly, reminding me to believe in myself, when things looked dire. I will miss our crazy fun moments like adopting 'Franz and Kafka', the 'shady cab ride', the Hemmingway cocktails and my funny swimming lessons.

Last but not least, I would like to thank my entire family and my friends back home in India for their constant support and helping me to maintain my sanity. I have missed them dearly in the past four years.

Above all, I would like to express my deepest appreciation to my dear husband Dr. Sameehan Mahajani, who has been a constant support in my life. I would say that he almost did a second PhD with me, due to our constant scientific discussions. I thank you for proof reading my thesis and your immense support, care and love.

Table of contents

Number	Title	Page Number
I.	**Declaration**	II
II.	**Acknowledgement**	V
III.	**Table of Contents**	1
IV.	**List of Figures**	4
V.	**List of Tables**	7
VI.	**List of Boxes**	7
VII.	**Abstract**	8
1.	***Introduction***	9
1.1.	**Neurogenesis**	10
1.1.1.	Evolutionary aspects of neurogenesis.	10
1.1.2.	Embryonic neurogenesis.	11
1.1.3.	Adult neurogenesis.	15
1.1.4.	Migration and synaptic integration of newly generated neurons in the adult brain.	18
1.1.5.	Tracking adult neurogenesis and limitations.	20
1.1.6.	Other Neurogenic zones.	22
1.1.7.	Importance of adult hippocampal neurogenesis.	24
1.1.8.	Factors involved in neurogenesis.	26
1.2.	**Hypoxia.**	32
1.2.1.	Hypoxia as a critical microenvironment in neurogenic niches.	32
1.2.2.	Hypoxic neurogenic niches in humans and rodents.	35
1.2.3.	Importance of hypoxia in regulating 'Stemness'.	36
1.2.4.	Hypoxia induced transcriptional control.	38
1.2.5.	Hypoxic upregulation of erythropoietin.	40
1.3.	**Erythropoietin.**	42
1.3.1	History of EPO.	42
1.3.2.	EPO and the blood brain barrier.	44
1.3.3.	Importance of EPO.	45
1.3.4.	Role on EPO on neurogenesis.	47
2.	***Rationale and Research Aims***	48
3.	***Materials and Methods***	51
3.1.	**Experimental models and mouse genetics.**	52
3.1.1.	Mouse strains.	52
3.1.2.	Breeding strategy.	54
3.1.3.	Genotyping.	55
3.2.	***In-vitro* cell cultures.**	58
3.2.1.	Hippocampal neuronal culture.	58
3.2.2.	Microglia culture.	58

3.2.3.	Oligodendrocyte culture.	59
3.2.4.	Astrocyte culture.	59
3.3.	**Quantitative Real-Time PCR (qRT-PCR).**	60
3.3.1	RNA extraction.	60
3.3.2.	cDNA synthesis and qRT-PCR.	60
3.4.	**Mouse treatments.**	61
3.4.1.	Tamoxifen.	61
3.4.2.	EPO.	61
3.4.3.	Hypoxia.	62
3.4.4.	Complex running wheels (CRW).	62
3.5.	**Immunohistochemistry (IHC).**	63
3.6.	**Imaging and analysis.**	65
3.6.1.	Pyramidal neurons.	65
3.6.2.	Dendritic spines.	66
3.6.3.	RNAscope in-situ hybridization (ISH).	66
3.7.	**Drop sequencing.**	67
3.7.1.	Tissue dissociation.	67
3.7.2.	Single-cell barcoding and library preparation.	67
3.7.3.	Single cell RNA-seq processing.	68
3.7.4.	Filtering and data normalization.	68
3.7.5.	Canonical correlation analysis.	69
3.7.6.	Clustering and visualization.	69
3.7.7.	Cell trajectory (pseudotime) analysis.	69
3.7.8.	Differential expression and gene ontology (GO) analyses.	69
3.8.	**Quantification and statistical analysis.**	70
4.	***Results***	71
4.1.	**Effect of EPO on neural precursors.**	72
4.1.1.	EPO induced increase in pyramidal neurons is not mediated via Nestin positive precursors.	72
4.1.2.	EPO regulates the differentiation of Gli positive precursors into astrocytes, but not neurons.	75
4.1.3.	EPO induced increase in pyramidal neurons could potentially be via Sox2 positive precursors.	81
4.2.	**Effect of EPO on pyramidal neurons.**	87
4.2.1.	Substantial generation of pyramidal neurons in the CA1 of adult mice and its amplification by EPO.	87
4.2.2.	EPO leads to an increase in the dendrites and spine density of pyramidal neurons in the CA1.	89
4.2.3.	EPO mediated increase in neurons is accompanied by changes in other cell types in the CA1.	92
4.2.4.	Drop-sequencing analysis demonstrates increase in the number of immature glutamatergic neurons after EPO treatment.	96
4.2.5.	EPO drives maturation of immature neurons as revealed by Monocle analysis.	100

4.2.6.	EPO increases the expression of immature neuronal markers such as Tbr1 and Tle4.	103
4.2.7.	EPO increases the expression of Lnc-RNA 'RMST' in immature glutamatergic neuronal cluster.	106
4.3.	**Effect of EPO and Hypoxia on cognitive learning.**	110
4.3.1.	Elevated expression of EPO and EPOR in pyramidal neurons upon Complex Running Wheel (CRW).	110
4.3.2.	Hypoxia inducible gene EPO and its EPOR are master regulators of enhanced learning.	112
4.3.3.	Labelling of increased hypoxic neurons in the CA1 upon CRW.	113
4.3.4.	Exogenous mild hypoxia acts synergistically with CRW on generation of pyramidal neurons in the CA1.	115
4.3.5.	Targeted deletion of EPO and EPOR in pyramidal neurons attenuates hypoxia-induced motor learning and endurance.	117
5.	***Discussion***	121
5.1.	Role of EPO on neuronal precursors situated in adult hippocampus.	122
5.2.	EPO acts on multiple precursors analogous to the hematopoietic system.	127
5.3.	EPO mediates neurogenesis in the hippocampus.	128
5.4.	EPO supports a continuum view for neuronal lineage.	130
5.5.	EPO mediated enhancement in synaptic plasticity.	131
5.6.	Mechanism of EPO action – Activity mediated adult hippocampal neurogenesis.	134
5.7.	EPO/EPOR system central to physiological hypoxia induced hippocampal neurogenesis.	135
6.	***References***	139
7.	***Appendices***	166
7.1.	List of Abbreviations	166

List of Figures

Figure	Title	Page Number
1.	***Introduction***	
Fig. 1	Symmetric and asymmetric divisions of progenitor cells.	11
Fig. 2	Symmetric divisions of progenitor cells.	12
Fig. 3	Examples of canonical progenitor cell lineages to neurons in developing neocortex.	13
Fig. 4	Differentiation of embryonic neuroepithelial cells of the neural tube to radial glial cells.	14
Fig. 5	Schematic representation of adult neurogenesis.	17
Fig. 6	Maturation of Granule cells.	19
Fig. 7	Consequences of species differences in the course of neurogenesis.	21
Fig. 8	Neurogenesis mediates cognitive flexibility by allowing the formation of new memory traces.	25
Fig. 9	Potential cellular intrinsic signaling pathways regulating adult neurogenesis.	27
Fig. 10	Role of Sox2 positive NSCs in adult neurogenesis.	29
Fig. 11	Involvement of Pax6 positive radial glial cells to adult neurogenesis.	29
Fig. 12	Mechanism of Sox2-RMST during neurogenesis.	32
Fig. 13	Postnatal brain stem cells and surrounding niche.	34
Fig. 14	Oxygen tension measurements in different stem cell compartments.	36
Fig. 15	Role of hypoxia and HIF-1a in astrocyte differentiation and neurogenesis.	37
Fig. 16	Influence of oxygen levels on proliferation and lineage specification of NSCs.	38
Fig. 17	Cellular responses to hypoxia.	39
Fig. 18	Schematic representation of EPO and factors controlling hypoxic EPO induction.	40
Fig. 19	Regulation of EPO under hypoxia in kidney and liver.	41
Fig. 20	Main sites of EPO production.	43
3.	***Materials and Methods***	
Fig. 21	Generation of $EPOR^{fl/fl}$ mice.	53
Fig. 22	Breeding strategy for the generation of inducible double transgenic mice.	55
Fig. 23	Hypoxia chamber used for experiments in this thesis.	62
4.	***Results***	

Fig. 24	Multiple EPO treatment does not give rise to TdTomato positive neurons in NestinCreERT2::TdTomato mice, but decreases the Nestin cell numbers in the SVZ of the DG.	73
Fig. 25	Fate mapping of NestinCreERT2::TdTomato mice upon single dose of EPO does not give rise to neurons in the CA1.	74
Fig. 26	Multiple EPO injections lead to an increase in Gli labelled TdTomato positive cells in the GliCreERT2::TdTomato mice without proliferation, but does not give rise to CA1 neurons.	76
Fig. 27	Fate mapping over time of GliCreERT2::TdTomato mice upon single dose of EPO does not give rise to neurons in the CA1.	78
Fig. 28	No unspecific TdTomato expression observed in Oil injected control GliCreERT2::TdTomato mice.	79
Fig. 29	TdTomato labelled Gli positive cells co-localize with other cell types in the hippocampus upon multiple placebo or EPO injections.	80
Fig. 30	EPO administration led to a significant decrease in the number of Sox2 positive cells in the CA1 region of GliCreERT2::TdTomato mice.	82
Fig. 31	EPO administration led to an increase in the number of TdTomato labelled Sox2 positive cells in the CA1 region of Sox2CreERT2::TdTomato mice.	83
Fig. 32	Unspecific TdTomato expression observed in Oil injected control Sox2CreERT2::TdTomato mice.	85
Fig. 33	EPO increases number of pyramidal neurons in the CA1 region of the hippocampus.	88
Fig. 34	EPO increases the dendritic and total spine density in the CA1 region of the hippocampus.	90
Fig. 35	EPO increases the density of immature stubby spine type in the CA1 region of the hippocampus.	91
Fig. 36	EPO decreases the number of Iba1 positive microglia in juvenile mice in the CA1 region of the hippocampus.	93
Fig. 37	Endogenous mRNA levels of EPOR in cultured neurons, microglia, astrocytes and oligodendrocytes.	95
Fig. 38	Determination of major hippocampal cell types and cell type-specific gene markers.	97
Fig. 39	Drop-Sequencing analysis demonstrates increase in the number of immature glutamatergic neurons after EPO treatment.	99
Fig. 40	Trajectory analysis (Monocle) demonstrates EPO induced maturation of immature glutamatergic neurons.	102
Fig. 41	EPO treatment increases the expression of immature neuronal marker gene Tbr1.	104
Fig. 42	EPO treatment increases the expression of immature neuronal marker gene Tle4.	105
Fig. 43	EPO treatment increases the expression of long noncoding RNA `RMST`.	107

Fig. 44 EPO treatment increases the expression of immature neuronal marker gene Dcx, Satb1 and Sox5. 108
Fig. 45 EPO increases the local expression of EPO/EPOR in pyramidal neurons in the CA1 region of the hippocampus. 111
Fig. 46 Learning improved upon EPO treatment. 113
Fig. 47 Voluntary running induces hypoxia in pyramidal neurons. 114
Fig. 48 Voluntary running induced hypoxia gives rise to new pyramidal neurons in CA1 region. 116
Fig. 49 Voluntary running induced learning is mediated by EPOR. 119

5. *Discussion*

Fig. 50 Complexity of neuronal lineage as compared to oligodendrocytic lineage. 123
Fig. 51 EPO induced generation of newly differentiated neurons in the CA1 region of the hippocampus. 130
Fig. 52 Model illustrating suggested mechanisms and effects of EPO/EPOR in the CA1. 137

List of Tables

Table	Title	Page Number
1.	***Introduction***	
Table. 1	Results depicting positive and negative results of adult neurogenesis in different brain regions.	23
Table. 2	Effect of growth factors on adult hippocampal neurogenesis.	28
Table. 3	Effect of low Oxygen tension on proliferation and differentiation of human neural stem cells.	38
3.	***Materials and Methods***	
Table. 4	Various transgenic mouse model used in this thesis.	54
Table. 5	Composition of contents for genotyping.	56
Table. 6	Sizes of expected bands after genotyping.	56
Table. 7	PCR procedure.	57
Table. 8	Forward and reverse primers for genotyping of all mouse lines.	57
Table. 9	qRT-PCR procedure.	61
Table. 10	Forward and Reverse primers used for RT-PCR.	61
Table. 11	List of primary antibodies used in this thesis.	64

List of Boxes

Box	Title	Page Number
1.	***Introduction***	
Box. 1	Neural Stem Cells.	12
Box. 2	Apical progenitor cells, Basal progenitor cells and Transit-amplifying cells	15
Box. 3	Radial Glial Cells.	16
Box. 4	BrdU.	20
Box. 5	Cre-loxP recombination.	22
Box. 6	Morphogens.	26
Box. 7	Hypoxia and Normoxia.	34
3.	***Materials and Methods***	
Box. 8	Cre-ERT2	54

Abstract.

Erythropoietin (EPO), named after its role in hematopoiesis, has been best studied in the hematopoietic system. Studies emphasizing the expression of EPO in the central nervous system have sparked an interest in its role in the brain. Interestingly, EPO has consistently led to improved cognition in animal models and in patients suffering from neuropsychiatric disorders such as schizophrenia. However, the mechanism by which EPO mediates its effects on cognition have remained obscure. The present work focuses on EPO mediated action on the Central Nervous System (CNS). This thesis replicated the EPO mediated increase in pyramidal neuron numbers of the CA1 region previously published by our group (Hassouna et al, 2016) and extended this finding using a novel approach. Moreover, this thesis demonstrated EPO mediated increase in neurodifferentiation (NexCreERT2) and neuroplasticity (Thy1-YFP) in young and adult mice. Single cell sequencing after EPO injection also revealed and strengthened these findings on a transcriptome level. These results represent a new perspective of EPO mediated neuronal differentiation. Despite technical limitations of using transgenic mouse lines, the present work could hypothesize that EPO induces the differentiation of precursors into different progenies (GliCreERT2) in other regions of the brain (NestinCreERT2) or differentiate into neurons (Sox2CreERT2). These findings reveal a continuum like view of neuronal lineage and demonstrate that EPO acts on multiple precursors known or unknown, alone or synergistically, to contribute to the increase in the number of pyramidal neurons in the CA1, and thereby improving cognition. The present work in addition provides a cellular mechanistic insight, which hypothesized that exposure to a learning paradigm such as complex running wheel (CRW) could upregulate EPO/EPOR in pyramidal neurons of the CA1. As EPO is a hypoxia inducible gene, this thesis demonstrated that neuronal networks engaged in cognitive tasks undergo hypoxia (CAGCreERT2ODD). EPO mediated improved learning is imitated by exposure to mild exogenous/inspiratory hypoxia. The present work provides the first evidence that EPO/EPOR are central to cognitive improvement upon physiological/mild exogenous hypoxia as the effects are attenuated in conditional knockout mice lacking EPO (NexCre::EPO-KO) or EPOR (NexCre::EPOR-KO) gene. Taken together, these results indicate a novel model of neuronal plasticity where neuronal networks challenged by cognitive tasks drift into transient hypoxia triggering neuronal EPO/EPOR expression. This provides insight for the importance of EPO in cognition and perhaps its relevance for new treatment strategies of cognitive improvement.

INTRODUCTION

1. Introduction

1.1. Neurogenesis.

1.1.1. Evolutionary aspects of neurogenesis.

The capability of the evolutionary primitive organisms to regrow significant body parts *(Fuchs & Segre, 2000)* made them highly intriguing and therefore, researchers wondered if this regenerative potential could also be a feature of evolutionarily complex, high-order organisms. Over the past years, it has been evident that the complex organisms retain this capacity to repair tissue damage throughout adult life but to a limited extent. This potential of regeneration is bestowed upon 'stem cells', which have been implicated to give rise to various cell types *(Barker et al., 2010; Morrison & Spradling, 2008)*. The hematopoietic system is the most well studied system with a great stem cell potential wherein adult stem cells can fully reconstitute all cell types for a tissue *(Ye et al., 2017)*.

For numerous years, the adult central nervous system was thought to lack any regenerative potential and therefore, was postulated to be not required or even detrimental to normal brain function *(Rakic, 1985)*. Santiago Ramón y Cajal, who extensively depicted pyramidal neurons and their dendritic arborizations in the brain for the first time, famously quoted that the mature central nervous system was a place where "*everything may die and nothing may be regenerated*" *(Cajal and May, 1913).*

However, several years later, Altman and Das challenged this theory and provided the first evidence of putative proliferating cells in the rat hippocampus. They suggested that neurogenesis occurs in the adult mammalian brain, which goes way beyond early embryonic development *(Altman & Das, 1965)*. This publication led to increased optimism in the field that endogenous neurogenesis could be harnessed to repair the injured or diseased brain. Adult hippocampal neurogenesis has been demonstrated in primates, including marmosets *(Gould et al., 1998)* as well as in macaques *(Gould et al., 1999; Kornack & Rakic, 1999)*. When compared to rodents, the rate of adult hippocampal neurogenesis was observed to be approximately 10 fold lower in adult macaques *(Kornack et al., 1999)*. Leuner and colleagues also demonstrated that the

rate of neurogenesis in the Sub-Granular Zone (SGZ) of the hippocampus was lower in older macaques as compared to younger ones and the rate subsequently decreased linearly with age *(Leuner et al., 2007)*. This decline was also observed in older rats and mice, which occurred in midlife before the onset of 'old age' *(Leuner et al., 2007)*. The majority of these newly born cells mature into neurons, which was observed in primates as well as in rodents *(Gould et al., 2001)*.

In the past two decades, there has been increasing evidence suggesting that adult mammalian brains possess stem cells and can generate new, functional cells. These findings open new avenues for the field of regenerative medicine.

1.1.2. Embryonic neurogenesis.

The generation of new neurons by differentiation of stem cells is known as neurogenesis. A 'Neurogenic Zone' is the region of the brain, which supports neurogenesis. This zone demonstrates the presence of immature progenitor cells (stem cells) and a microenvironment secreting various factors that is permissive for the generation of new neurons. The widely accepted neurogenic zones where majority of neurogenesis takes place are the Sub-Ventricular Zone (SVZ) and the Sub-Granular Zone (SGZ) of the hippocampus *(Balu & Lucki, 2009)*. Three hypothesis concerning the pattern of neurogenesis were considered *(Kriegstein & Alvarez-Buylla, 2009)*. The first hypothesis consisted of the presence of a founder Neural Stem Cells (NSCs; Box. 1), which undergoes multiple symmetric divisions to give rise to other NSCs, which could further differentiate into neurons (Fig. 1).

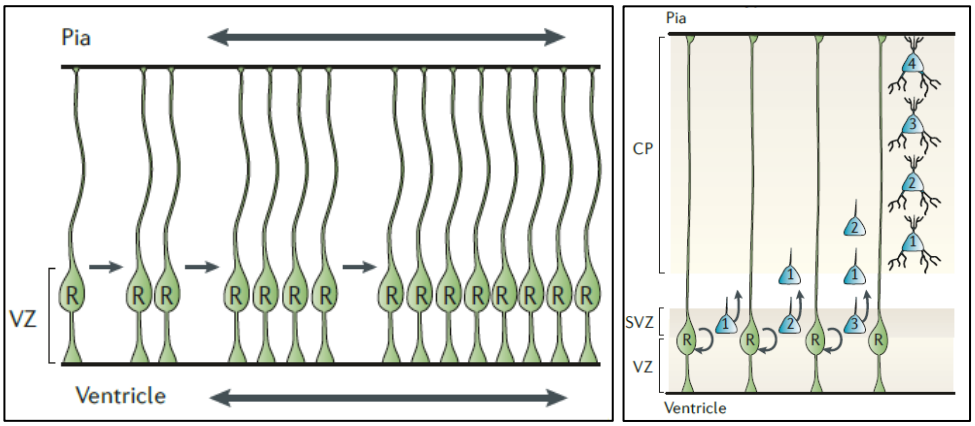

Figure 1. Symmetric and asymmetric divisions of progenitor cells. *(Left) Schematic illustrations of radial glial (R) cells undergoing symmetric divisions in the ventricular zone during embryonic cortex development. (Right) Schematic illustrations of radial glial (R) cells undergoing asymmetric divisions in the ventricular zone during embryonic cortex development, giving rise to radial glial cells (R) and neurons (blue). Adapted from Kriegstein et al, 2006.*

The second hypothesis suggested the presence of NSCs, which undergo asymmetric division, giving rise to one daughter NSC as well as another intermediate NSC, which differentiates into neurons (Fig. 1).

Box. 1. Neural Stem Cells.

Neural stem cells are multipotent adult stem cells present in the adult central nervous system that can self-renew, and give rise to new neurons, oligodendrocytes and astrocytes.

The third and the last hypothesis suggested the presence of NSCs, which undergo symmetric division, giving rise to one daughter NSC as well as one intermediate progenitor cell, which can undergo further proliferation and differentiation into neurons (Fig. 2).

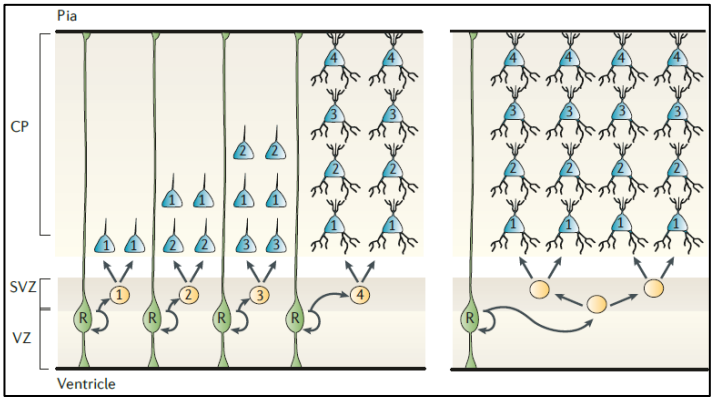

Figure 2. Symmetric divisions of progenitor cells. *Schematic illustrations of radial glial (R) cells undergoing symmetric divisions in the ventricular zone during embryonic cortex development, giving rise to radial glial cells (R) and intermediate progenitors (yellow). These intermediate progenitor cells differentiate into neurons (blue). Adapted from Kriegstein et al, 2006.*

The neurogenesis in rodents and in primates follow a different mode as seen in Fig. 3 *(Namba & Huttner, 2017)*.

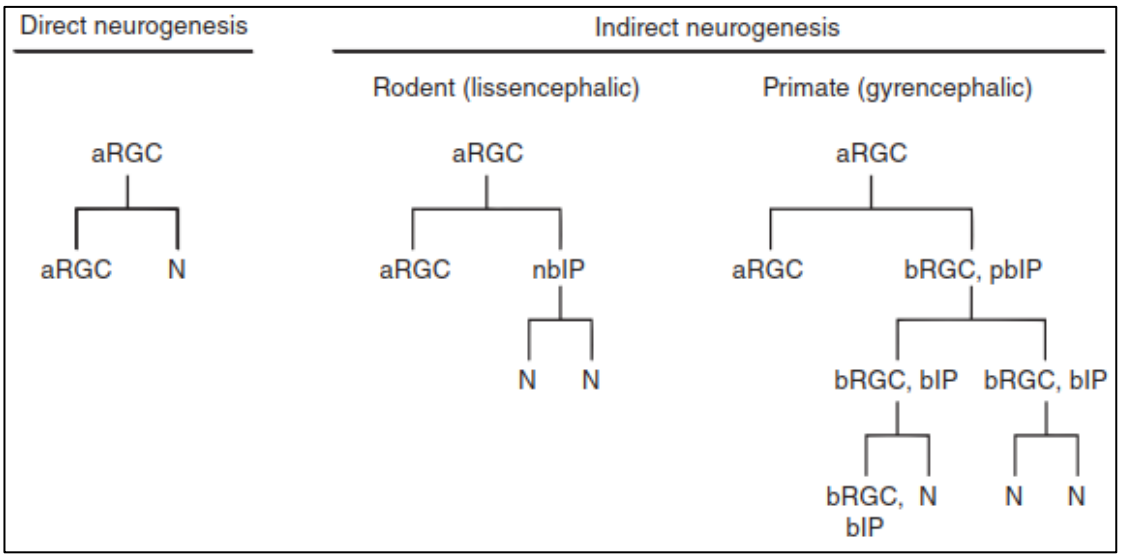

Figure 3. Examples of canonical progenitor cell lineages to neurons in developing neocortex. *Direct neurogenesis via asymmetric divisions of Radial Glial Cells (aRGCs) to give rise to another aRGC and a daughter neuron (N; Left). In rodent (Middle), an aRGC undergoes asymmetric division to give rise to an intermediate progenitor (nbIP), which further undergoes symmetric divisions to give rise to two neurons (N). In primates (Right), an aRGC undergoes asymmetric division to give rise to another RGC or IP, which further undergo symmetric proliferative division to give rise to two RGCs/IPs. They can further undergo symmetric or asymmetric divisions to give rise to neurons. Adapted from Namba and Huttner, 2017.*

In rodents, during early corticogenesis, the progenitor cells of the SVZ make the switch from symmetric to asymmetric cell division *(Gotz & Huttner, 2005)*. At this time, there is a considerable reduction in the number of progenitor cells as they proliferate asymmetrically to differentiate into cortical neurons. However, the differentiated cortical neurons accumulate above the sub-plate (SP) in an inverted 'inside-out' sequence. That is, the earliest born neurons are destined to become a part of the innermost layer 6 whereas the neurons born at a later stage forms the outer layer 2 of the cortical plate *(Statler et al., 2007)*. Apical progenitor cells and basal progenitor cells (Box. 2) in the SVZ accumulate to become the major source of pyramidal neurons (Fig. 4).

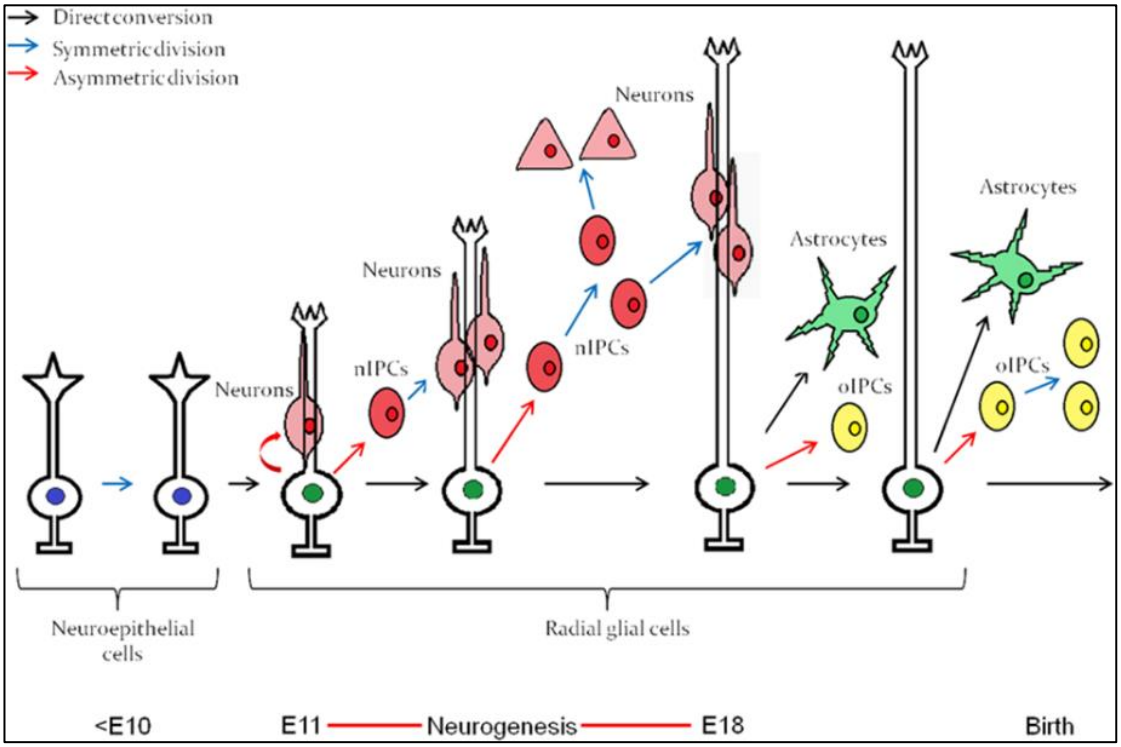

Figure 4. Differentiation of embryonic neuroepithelial cells of the neural tube to radial glial cells. *Neurogenesis takes place from E11 to E18. The neuroepithelial cells first differentiate into radial glial cells, which further differentiates into neurons. Astrocytic differentiation starts after neurogenesis is over at E18. Adapated from Mitrousis et al., 2015.*

However, during human brain development, neurogenesis involves a highly precise orchestrated sequence of cellular events. The brain development begins with the formation of the neocortex at the rostral end of the neural tube, near the embryonic cerebral vesicle *(Sidman & Rakic, 1973)*. The neural tube closes at embryonic day 30 i.e. during the fifth week of gestation *(O'Rahilly & Muller, 2010)*. After the fifth week of gestation, the amniotic fluid is trapped within the central canal and the ventricular system begins to form. Rapid brain enlargement begins when a rise in intraventricular fluid pressure is initiated by neural tube closure *(Budday et al., 2015)*. Based on the above-mentioned literature, the embryonic neurogenesis in rodents and humans follow a similar pattern with NSCs in the SVZ playing a critical role.

Box. 2. Apical progenitor cells.

The term apical progenitor cells (APs) refer to cells undergoing mitosis at the apical surface of the ventricular zone. There are three types of apical progenitors: neuroepithelial cells, and the derivative apical radial glia and apical intermediate progenitors.

Basal progenitor cells.

The term Basal progenitor cells (BPs) refer to cells, which undergo mitosis in the secondary germinal zone located basally, compared to the ventricular zone. BPs are generated by divisions of apical radial glia and move basally via a process known as delamination. There are two types of basal progenitors: basal intermediate progenitors and basal radial glia.

Transit-amplifying cells.

These cells are known as neural progenitor cells, which are differentiation committed cells derived from the asymmetric division of stem cells and endowed by elevated proliferative but no self-renewal capacity.

1.1.3. Adult neurogenesis.

Using rodents as experimental models, multiple reports have led to increasing our understanding of the origin of the newly generated neurons, their maturation, and their integration into the existing neuronal circuitry in the adult hippocampus *(Geil et al., 2014)*. The SGZ and the SVZ are the most well studied zones for adult neurogenesis. The newly generated neurons, during development, show the expression of temporally ordered expression of stage-specific markers and changes in morphological and functional properties *(Costa et al., 2015)*. For example, during early neurogenic lineage commitment, the transient amplifying Type II cells express various markers including Sox2. However, at later stages of differentiation, the progenitors express neuronal transcription factors like NeuroD *(Kronenberg et al., 2003; Seki, 2002)* and immature neurons express Doublecortin *(Brown et al., 2003)* and the microtubule associated

protein. The expression of immediate early genes such as c-FOS and ARC, a molecular marker of neuronal activity, provides the evidence of newly generated neurons actively integrating into the existing circuitry *(Costa et al., 2015)*.

Genetic fate mapping studies have demonstrated that neuronal progenitor cells are situated in the SGZ between the granular cell layer and the hilus. These neuronal progenitor cells are the main source of newly generated neurons in the dentate gyrus (DG) of the hippocampus *(Dhaliwal & Lagace, 2011)*. These cells are commonly referred to as radial glial Type I cells (Box. 3). These cells possess radial processes spanning through the molecular layer and express radial glia marker expressing glial fibrillary acidic protein GFAP *(Kriegstein et al., 2009)*.

Box. 3. Radial Glial Cells.

These neurogenic cortical progenitors can undergo either symmetric or asymmetric divisions to give rise to neurons and to undergo self-renewal. Radial Glial Cells (RGCs) are situated in the cortical Ventricular Zone (VZ). These cells show a distinctive polarized morphology characterized by an apical process towards the Ventricle and a long basal process towards the pial surface.

Type I cells, when active, give rise to transient amplifying neural precursor cells (NPCs), which are referred to as Type II cells. These Type II cells further mature into granular neurons in the hippocampus *(Sierra et al., 2010)*.

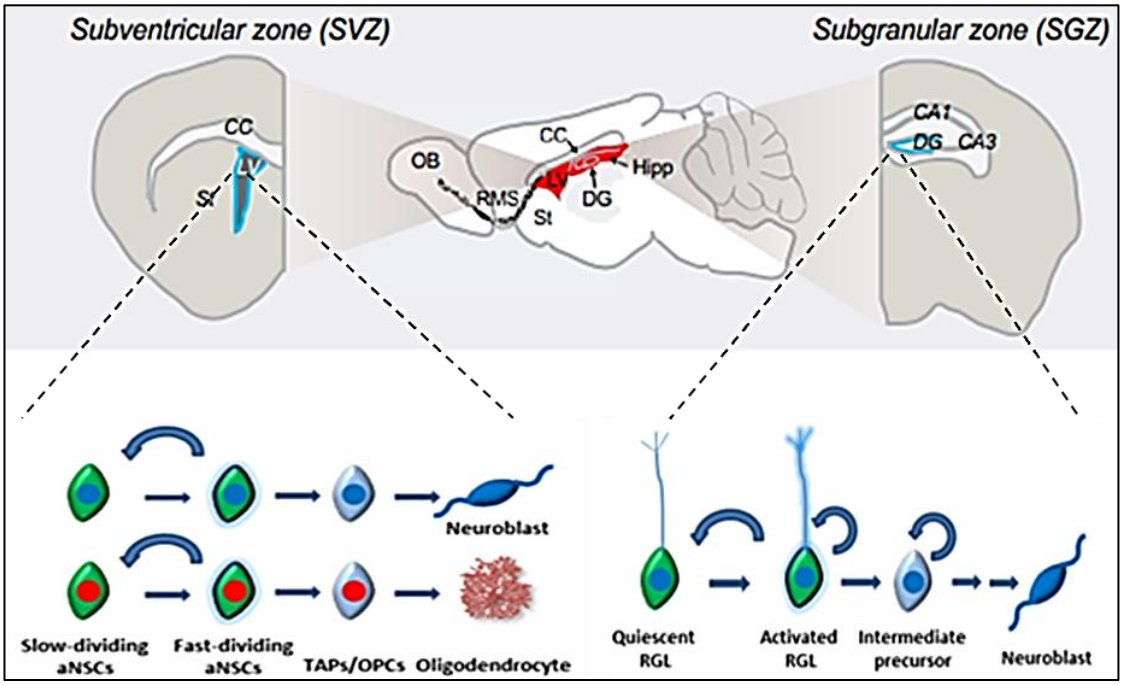

Figure 5. Schematic representation of adult neurogenesis. *Two adult neurogenic niches i.e. Sub-ventricular zone (SVZ; Left) and Sub-granular zone (SGZ; Right), where neurogenesis takes place. In the SVZ, slow dividing quiescent NSCs give rise to fast dividing NSCs that subsequently generates transit amplifying progenitors (TAPs) and finally neuroblasts. However, in the SGZ, quiescent radial glial like (RGL) progenitors become activated to give rise to intermediate progenitors and neuroblasts. Modified from Ortega and Costa, 2016.*

Maturation of these granular neurons are marked by the development of dendritic trees into the molecular layer of the DG and the projection of axons towards CA3 to become functionally integrated *(Hastings & Gould, 1999; Toni et al., 2007)*. Bonaguidi and colleagues have also demonstrated that other non-radial precursors cells located within the SGZ can give rise to newly generated neurons *(Fig. 6; Bonaguidi et al., 2012)*. It is also interesting to highlight that majority of these newly generated neurons in rodent hippocampus die within the first four days of their birth *(Sierra et al., 2010)* or within one to three weeks after birth *(Tashiro et al., 2006)*. After this scheduled apoptosis, less than 25% of the newly generated neurons survive to mature and form functional synapses with other surviving neurons.

1.1.4. Migration and synaptic integration of newly generated neurons in the adult brain.

In the SVZ, during adult neurogenesis, the newly generated neurons migrate through the rostral migratory stream (RMS) to reach the olfactory bulb and further settle into different layers of the cortical plate *(Statler et al., 2007)* through radial migration. Various molecules such as β1-integrin, PSA-NCAM, GABA and Slits act as environmental extracellular cues to regulate the stability, mobility and the direction of these migrating neurons *(Ming & Song, 2005; Zhao et al., 2008)*. However, in the hippocampus, the newly generated neurons in the DG migrate locally into the inner granular cell layer. The newly generated neurons from the SGZ rapidly extend their axons through the hilus region to reach the CA1 region within two weeks after birth, while their dendrites reach the molecular layer (i.e. CA1) within the next week *(Ge et al., 2006; Zhao et al., 2006)*. The migration of newly generated neurons from the SGZ is not well defined as compared to the migration of newborn neurons in the SVZ *(Duan et al., 2008)*.

The dorsal and ventral hippocampus has been reported to be implicated in learning and memory. Altman and colleagues suggested that newly generated neurons are essential for continued learning and memory formation *(Altman & Das, 1967)*. Jessberger and colleagues demonstrated that ambient GABA activates the neural progenitors and immature neurons before receiving functional synaptic inputs during neurogenesis in both SVZ and SGZ *(Fig. 6; Jessberger et al., 2005)*.

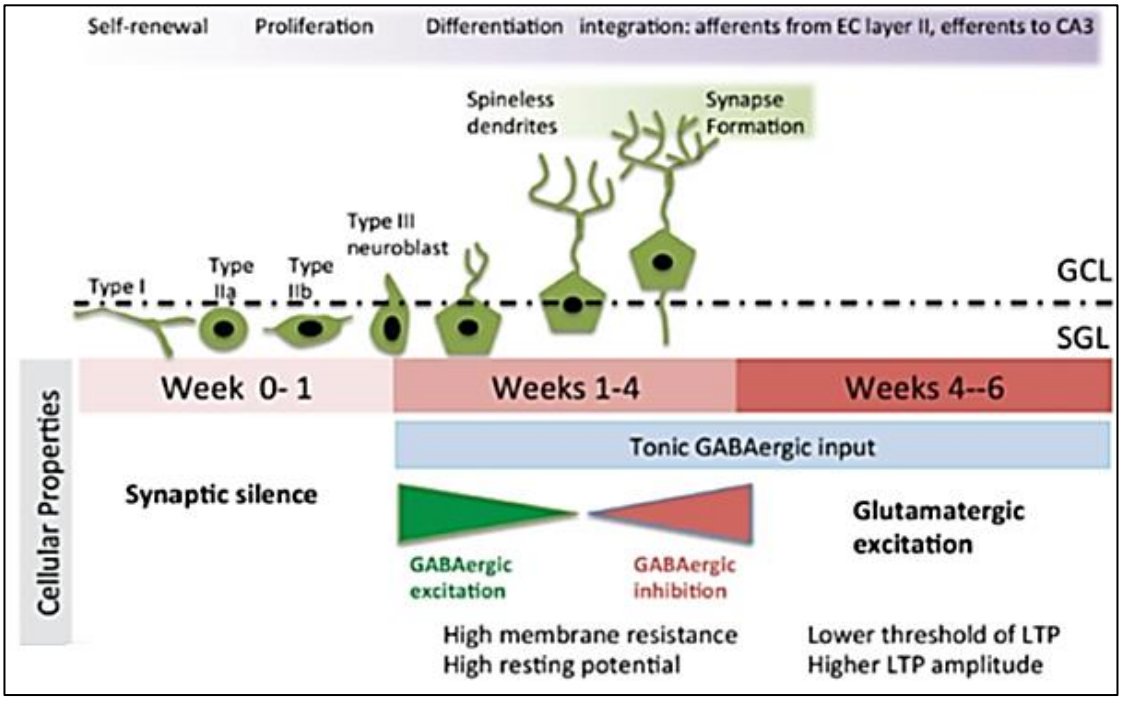

Figure 6. Maturation of Granule cells. *In the first week after birth, the neural progenitors are characterized by irregular shape, immature spikes and no synaptic activity. The next week, the cells migrate into the granule cell layer and develop dendrites lacking spines. They also show slow GABAergic synaptic inputs. The week after, they start to form afferent connections from the performant pathway of the cortex and the CA3. At this stage, there is a transition from GABAergic to glutamatergic synaptic inputs. Adapted from Toni et al., 2007.*

Once the neuronal maturation begins, GABA depolarizes the newly generated neurons due to the high chloride content and promotes the formation of GABAergic and glutamatergic synaptic inputs *(Ge et al., 2006)*. These newly generated neurons exhibit hyper-excitability and enhanced synaptic plasticity of their glutamatergic inputs during maturation in the hippocampus. This enables the newly generated neurons to integrate into the existing architecture and make unique contributions to information processing. At cellular level, long-term potentiation (LTP) of evoked field potentials is abolished by radiation to abrogate adult neurogenesis *(Snyder et al., 2001)*. Many have reported that even a small number of neurons can influence behavior *(Brecht et al., 2004; Shadlen et al., 1996)*.

1.1.5. Tracking adult neurogenesis and limitations.

For almost two decades, the DG was considered as the only brain region where adult neurogenesis takes place in humans *(Eriksson et al., 1998)*. However, novel techniques for retrospective cellular birth dating in humans provided the first evidence that robust neurogenesis takes place in the adult human striatum *(Ernst et al., 2014)*. This cellular birth dating was performed using isotope Carbon-14 (14C). The level of 14C in genomic DNA was used to reliably determine the time at which DNA was synthesized and populations of cells were generated without the use of exogenous markers *(Spalding et al., 2005)*. Adult neurogenesis was found to be remarkably similar across various species, but dramatically different in the rates of neurogenesis *(Jakovcevski et al., 2011)*. Contradicting reports suggest that it is difficult to determine how rates of neurogenesis compare within species, as 14C birth dating cannot be employed in rodents due to their short lifespan, whereas bromodeoxyuridine (BrdU) (Box. 4) is never used in humans due to its toxic nature. Therefore, immunohistochemistry for endogenous markers of immature neurons have been useful in identifying newly generated neurons in different species and their various brain regions *(Liu et al., 2009)*. However, this technique still is unsuitable for cross-species rate comparisons due to different rates of cell death, maturation, downregulation of endogenous immature neuronal markers as well as postmortem stability across different species *(Amrein et al., 2014; Snyder et al., 2009)*.

Box. 4. BrdU.

Bromodeoxyuridine (5-bromo-2'-deoxyuridine and BrdU) is an analog of thymidine and a synthetic nucleoside. BrdU is used in the detection of proliferating cells in living tissues. BrdU can be introduced into the newly synthesized DNA of replicating cells and can substitute for thymidine during DNA replication. Specific antibodies can then detect the incorporated BrdU (see immunohistochemistry), thereby demonstrating newly generated cells.

The major disadvantages of radioactive thymidine labelling include the uptake by cells undergoing DNA repair as well as it can cause DNA strand breaks. It is also diluted after every replication cycle and therefore cannot be used for a longer period if labelling of progenitor cells is performed *(Breunig et al., 2007)*. Similarly, BrdU labelling also has its disadvantages such as causing DNA breaks, DNA transcription errors, toxic in higher doses as well as dilutes after every replication cycle *(Breunig et al., 2007)*.

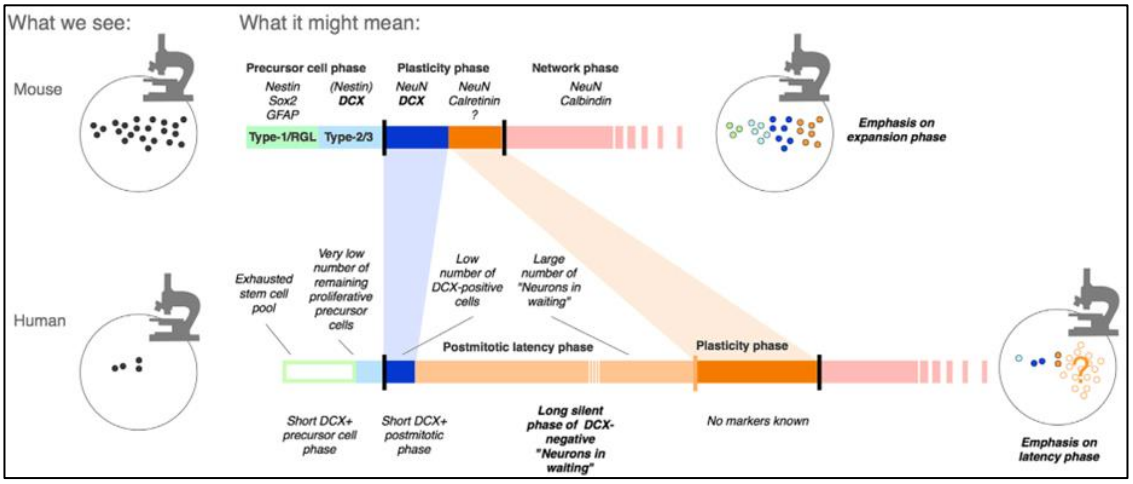

Figure 7. Consequences of Species differences in the course of neurogenesis. *Among methodological considerations, a hypothetical concept of a temporal decoupling of the stages of adult neurogenesis and species differences in marker expression. This could partially explain the differences observed in rodent and human experiments. Adapted from Kempermann et al., 2018.*

Certain experiments using Cre-LoxP (Box. 5) suggested that astrocytes expressing GFAP show radial glial properties and are adult NSCs *(Alvarez-Buylla & Lim, 2004)*. However, a limitation of using wide range of animal models and marker genes is that several of these markers are not specific to quiescent or cycling progenitors as revealed by single cell RNA Sequencing *(Hochgerner et al., 2018)*. Moreover, many of these transgenic mouse lines have shown variable levels of unspecific signal, thereby limiting our understanding of adult neurogenesis.

Box. 5. Cre-loxP recombination.

Cre-Lox recombination is a technology that can be used for carrying out deletions, insertions, translocations and inversions at various specific sites in the DNA sequence of eukaryotic or prokaryotic cells. DNA modifications can be targeted to a cell type or be triggered by an external stimulus (e.g. Tamoxifen). The system consists of an enzyme, Cre recombinase that recombines with a pair of short sequences. These sequences are called the Lox sequences. Lox sequences are appropriately placed so as to allow genes to be activated, repressed, or exchanged for other genes. These DNA changes are targeted and are specifically useful in lineage tracing, where global mutants are embryonic lethal.

Contradictory reports suggest the existence of adult hippocampal neurogenesis in humans. Sorrells and colleagues reported that humans uniquely appear to lack adult hippocampal neurogenesis *(Sorrells et al., 2018)*. The authors used well-known markers of neural progenitors and immature neurons in post mortem brain sections, and observed that neurogenesis rapidly decreased with advancing age, with no signs of neurogenesis observed in individuals older than 13 years. On the other hand, Boldrini and colleagues demonstrated that adult hippocampal neurogenesis does occur in humans and it does not decline with age *(Boldrini et al., 2018)*. Even though the authors used similar markers to detect adult neurogenesis as *Sorrells et al., 2018*, they used a stereological approach to quantify the total cell numbers observed in the entire DG region. Moreno-Jimenez and colleagues, in part corroborated these results by demonstrating numerous immature neurons in the DG region of healthy humans up to 90 years of age *(Moreno-Jimenez et al., 2019)*. These contradicting results provide insight on the technical difficulties and variations in determining the extent of adult hippocampal neurogenesis in humans.

1.1.6. Other Neurogenic zones.

There is immense controversy in the field of adult neurogenesis as mentioned above due to the methodological limitations. There have been multiple reports of constitutive neurogenesis in various regions of the brain of primates and rodents such as neocortex *(Dayer et al., 2005; Gould et al., 1999; Gould & Kamnasaran, 2011; Kaplan, 1981)*, in

the dorsal vagal complex of the brainstem *(Bauer et al., 2005)* and in the spinal cord *(Yamamoto et al., 2001)*. Other regions of the brain where reported neurogenesis takes place are the substantia nigra *(Zhao et al., 2003)*, the amygdala *(Bernier et al., 2002)* and rodent CA1 region of the hippocampus *(Rietze et al., 2000)*.

Even though numerous reports have indicated that adult neurogenesis takes place specifically in the SVZ and SGZ, other regions containing NSCs should not be underestimated *(Ortega & Costa, 2016)*. For example, multipotent NSCs have been isolated from uninjured postnatal mouse cerebral cortex *(Belachew et al., 2003; Costa et al., 2007; Marmur et al., 1998; Seaberg et al., 2005)* or after inducing traumatic injury *(Buffo et al., 2008; Sirko et al., 2013)*. The inner core of the olfactory bulb (OB) of rodents and humans have also been described to possess adult NSCs *(Ortega et al., 2016)*. Reports have also demonstrated that injuries and pathological stimuli such as stroke activate neurogenesis outside the two established neurogenic zones *(Ming et al., 2005)*. Similar reports have shown that adult neurogenesis also takes place in the peripheral nervous system (PNS), such as the generation of olfactory neurons in the olfactory epithelium *(Leung et al., 2007)* and neural crest lineages in the carotid bodies *(Pardal et al., 2007)*. More recent evidence suggests that lesions may also activate `dormant` or `quiescent` NSCs via release of certain signaling molecules such as Vascular Endothelial Growth Factor (VEGF), basic Fibroblast Growth Factor (bFGF) and sonic hedgehog *(Luo et al., 2015; Sirko et al., 2013)*. However, the contribution of these `dormant` NSCs to any periodical or unnoticed turnover of various neuronal populations remain to be demonstrated.

Brain region	Positive (model)	Negative (model)	Technique
Neocortex	Rat, Hamster and Macaque	Mouse	BrdU and neuronal markers
Striatum	Rat, Rabbit and Macaque	Mouse	BrdU and neuronal markers
Amygdala	Vole and Macaque	Rat	BrdU and neuronal markers
Piriform cortex	Rat		BrdU and neuronal markers
Olfactory tubercle	Squirrel monkey and Macaque		BrdU and neuronal markers
Hypothalamus	Hamster, Vole and Mouse		BrdU and neuronal markers
Substantia nigra	Mouse	Rat	BrdU and neuronal markers
Brainstem	Rat		BrdU and neuronal markers

Table 1. Results depicting positive and negative results of adult neurogenesis in different brain regions (Adapted from Gould, 2007).

1.1.7. Importance of adult hippocampal neurogenesis.

Adult hippocampal neurogenesis can contribute indirectly to brain function via alteration in structural properties of the circuitry *(Geil et al., 2014)*. At a systemic level, a variety of computational models of adult neurogenesis has demonstrated that newly generated neurons alter neural network properties *(Aimone & Gage, 2011)*. Multiple reports have demonstrated that the newly generated neurons show enhanced synaptic plasticity for a limited time after their differentiation *(Ge et al., 2007)*. This enhanced synaptic plasticity is crucial for their role in mediating pattern separation in memory formation and cognition in rodents *(Clelland et al., 2009; Nakashiba et al., 2012; Sahay et al., 2011)*. Various reports have demonstrated that adult hippocampal neurogenesis facilitates cognitive flexibility by the formation of new distinct memories *(Dupret et al., 2008; Epp et al., 2016; Garthe et al., 2009)*. In an experiment, where mice were first exposed to Morris water maze, they were able to find the safety platform without difficulties. However, mice with higher rate of adult hippocampal neurogenesis were able to find the safety platform even when its position was changed. The mice with lower rate of adult hippocampal neurogenesis were unable to find the changed safety platform and were observed to be searching for the platform in its prior location. The authors suggest that due to the higher rate of adult hippocampal neurogenesis; the earlier memory of the safety platform was cleared quickly, which enabled the mice to find the new location of the platform. They term this phenomenon cognitive flexibility. In contrast, the mice with lower rate of adult hippocampal neurogenesis show cognitive inflexibility, were unable to clear the earlier memory, and therefore could not find the new position of the platform (Fig. 8).

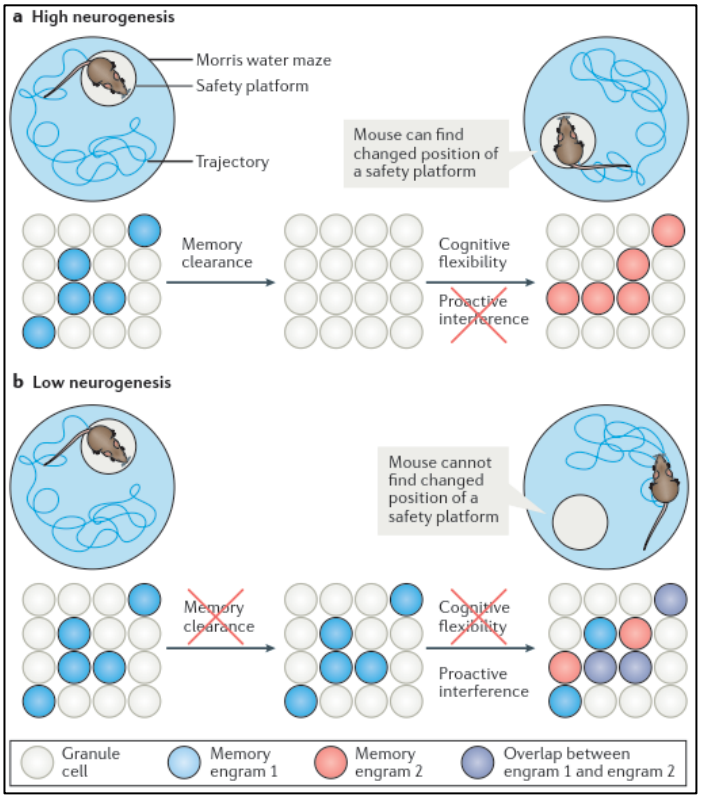

Figure 8. Neurogenesis mediates cognitive flexibility by allowing the formation of new memory traces. *(a) With high neurogenesis, engrams are cleared faster. This efficient memory clearance reduces proactive interference between the memory of the previous location and the ability to encode a new location. This facilitates cognitive flexibility and promote the finding of the new location of the platform. (b) With low neurogenesis, engrams of previous memories are not cleared. Due to this, new memory engrams might not be encoded properly, thereby increasing proactive interference and reduce cognitive flexibility and impair the ability to find the new location of the platform. Adapted from Anacker et al., 2018.*

Toni and colleagues demonstrated that adult neurogenesis could disrupt the existing synapses of mature neurons due to the competition during new neuron synaptic integration *(Toni et al., 2008; Toni et al., 2007)*. Moreover, adult neurogenesis in the hippocampus leads to an increased number of astrocytes that migrate into the hilus, the granular cell layer and the molecular layer *(Bonaguidi et al., 2011; Encinas et al., 2011)*. Multiple reports have further demonstrated that adult hippocampal neurogenesis influences experience and mood *(Sahay & Hen, 2007)* and is implicated in neurological disorders such as depression, schizophrenia and cognitive dysfunction. An interesting question in the field, which suggests that increasing adult hippocampal neurogenesis would be sufficient to improve memory and cognition, remains to be determined *(Sahay et al., 2011)*. Based on the above-mentioned literature, it is evident that upregulation or downregulation of adult hippocampal neurogenesis could led to various neuropsychiatric disorders.

1.1.8. Factors involved in neurogenesis.

Various morphogens (Box. 6) such as Bone Morphogenetic Protein (BMPs), Notch, WNT and Sonic Hedge-Hog (SHH) are reported to be extremely critical for tissue patterning and specification during embryonic development (Fig. 9). They also continue to regulate adult NSCs *(Faigle & Song, 2013)*. BMP signaling negatively regulates SVZ neurogenesis by promoting the differentiation of NSCs to astrocytes as well as causing quiescence in NSCs of the SGZ *(Bonaguidi et al., 2005; Mira et al., 2010)*. On the other hand, Notch signaling can induce proliferation and maintenance of NSCs in both adult niches (SVZ and SGZ), but the inhibition of Notch signaling triggers the NSCs to exit the cell cycle and transition to a progenitor cell stage *(Breunig et al., 2007; Ehm et al., 2010)*.

Box. 6. Morphogens.

The term morphogen describes a type of signaling molecule that can act on cells to induce distinct cellular responses in a concentration-dependent manner. During development, various cells differentiate according to the morphogens induced positional information. Morphogens act as signaling molecules that originate from a region and distribute from their source to form a concentration gradient. The fate of other cells in the field depend on the morphogen concentration and the gradient defines the pattern of development.

Similarly, SHH signaling is essential to maintain the NSCs in the SVZ, however, upregulated signaling promotes symmetric division leading to expansion of NSCs but ultimately depleting their numbers *(Ferent et al., 2014)*. Another factor important for maintenance of NSCs is WNT signaling. Use of WNT signaling inhibitors such as Dickkopf-1 (Dkk1) and secreted frizzled related protein 3 (sFRP3) promotes NSCs quiescence along with the maturation of newborn neurons *(Jang et al., 2013)*. Other factors such as growth factors and neurotrophins play an important role in regulating late stage progenitors, but their impact of NSCs is not well defined *(Faigle et al., 2013)*.

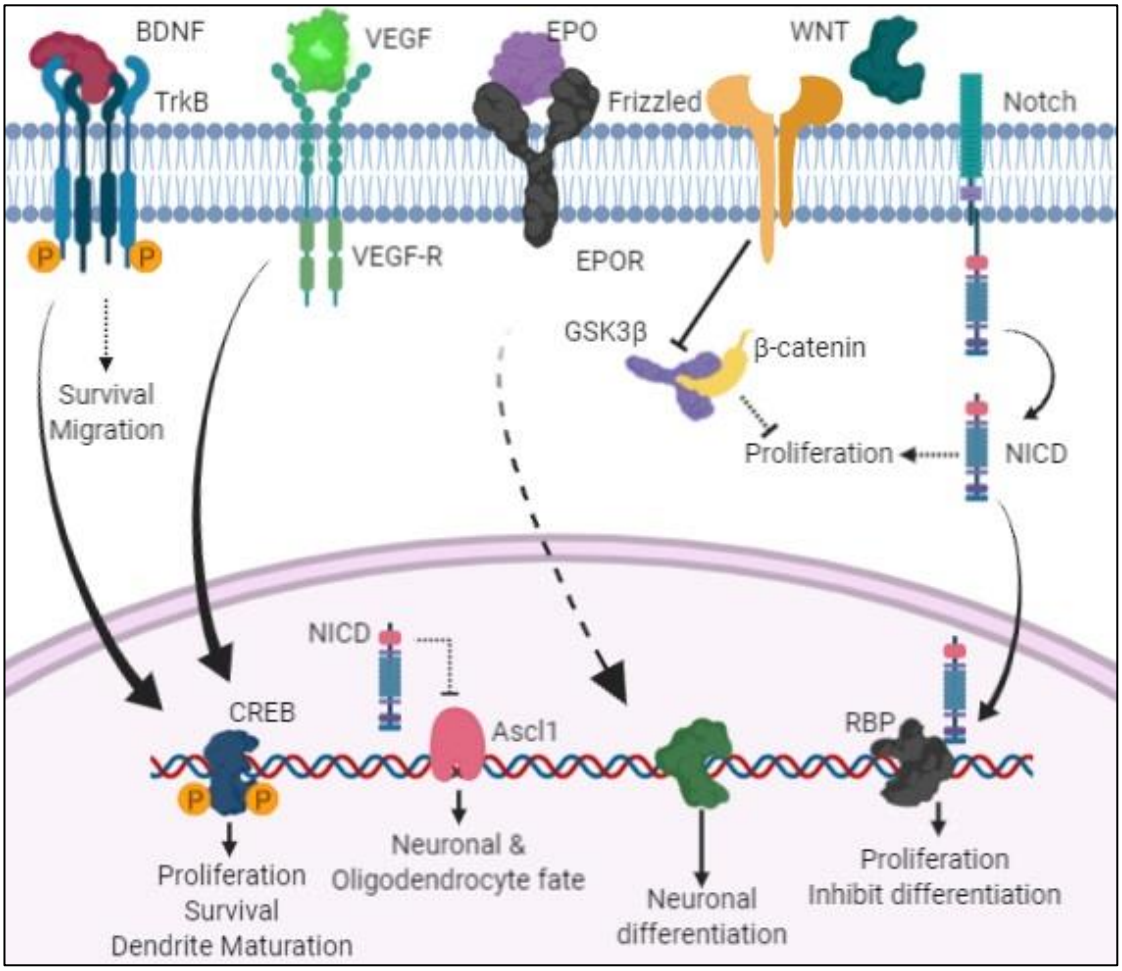

Figure 9. Potential cellular intrinsic signaling pathways regulating adult neurogenesis. *A schematic of a single cell proposes a hypothesis that different intrinsic signaling pathways may act in concert or in opposition to regulate different stages of adult neurogenesis. Solid lines indicate direct signaling, whereas dashed lines show indirect signaling. These signaling pathways could influence differentiation, proliferation, survival and maturation. Modified from Johnson et al., 2009.*

Lot of signaling molecules such as epidermal growth factor (EGF), fibroblast growth factor-2 (FGF-2), brain derived neurotrophic factor (BDNF), glial cell line derived neurotrophic factor (GDNF), stem cell factor (SCF), vascular endothelial growth factor (VEGF), insulin like growth factor-1 (IGF-1), nitric oxide (NO) and erythropoietin (EPO) have been reported to be involved in neurogenesis *(Kokaia & Lindvall, 2003; Wiltrout et al., 2007)*. Moreover, most of these above-mentioned factors regulate neurogenesis by inducing or interacting with important transcription factors (TFs).

Regulatory factor	State	Event	Reference
Notch	Active	Maintains quiescence	Ables et al, 2010; Ehm et al, 2010; Lugert et al, 2010.
SHH	Down regulated	Maintains quiescence	Lau et al, 2003; Breunig et al, 2008; Favaro et al, 2009.
BMP	Active	Maintains quiescence	Bonaguidi et al, 2005; Mira et al, 2010.
WNT	Down regulated	Maintains quiescence	Lie et al, 2005; Jang et al, 2013; Varela-Nallar and Inestrosa, 2013.
Ephrin-B2	Active	Promotes neuronal differentiation	Astron et al, 2012.
TLRs	Active	Regulates proliferation and differentiation	Rolls et al, 2007.
EGF	Active	Regulates proliferation	Khun et al, 1997.
FGF-2	Active	Inhibits neuronal differentiation	Zhao et al, 2007.
IGF-1	Active	Promotes neuronal differentiation	Aberg et al, 2000; Aberg et al, 2003.
VEGF	Active	Promotes NSCs proliferation	Jin et al, 2002.
EPO	Active	Promotes neuronal differentiation	Hassouna et al, 2016.

Table 2. Effect of growth factors on adult hippocampal neurogenesis *(Modified from Balu and Lucki, 2009).*

Transcription factors regulate neurogenesis in embryonic as well as adult NSCs *(Hsieh, 2012)*. TFs promoting neuronal progenitor cell proliferation and/or neuronal cell fate commitment could increase the generation of new neurons. However, at normal physiological condition, certain TFs control proliferation, while others affect differentiation of NSCs towards either a neuronal or a glial phenotype *(Tonchev & Yamashima, 2007)*.

Sox2. One such transcription factor is Sex determining region Y – box 2 (Sox2). Sox family proteins bind to DNA via their high-mobility group (HMG) domains that are conserved TFs which play an important role in cell fate specification and differentiation of many tissues *(A. B. Abraham et al., 2013; B. J. Abraham et al., 2013; Kamachi & Kondoh, 2013)*. Sox2 has also been characterized as one of the essential `Yamanaka factors` required for the generation of induced pluripotent stem cells (iPSCs) from fibroblasts *(Takahashi & Yamanaka, 2006)*. Moreover, Sox2 is highly expressed in embryonic and adult NSCs of both niches and reduction in its expression leads to depletion in the numbers of NSCs. Sox2 is also expressed in Embryonic stem (ES) cells and neural epithelial cells during development *(Avilion et al., 2003; Ferri et al., 2004; Zappone et al., 2000)*. Various reports have demonstrated that NSCs also express Sox2 *in vitro (Bylund et al., 2003; Ferri et al., 2004; Graham et al., 2003)*. Suh and colleagues, *in vivo*, demonstrated that Sox2 was expressed by a population of cells in the SGZ of the DG in the hippocampus, capable of producing differentiated neural cells as well as identical Sox2 positive cells *(Suh et al., 2007)*. These results indicate that Sox2 positive

cells possess the ability to proliferate as well as differentiate into neurons. The authors also demonstrate that Sox2 positive precursors undergo symmetric division (Fig. 10) i.e. the size of Sox2 positive NSCs pool remains unchanged *(Suh et al., 2007)*.

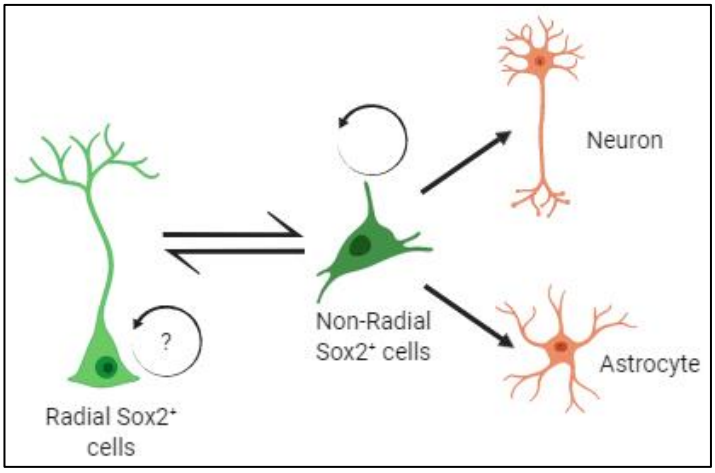

Figure 10. Role of Sox2 positive NSCs in adult neurogenesis. *Radial Sox2 positive NSCs can proliferate and differentiate to give rise to non-radial Sox2 positive NSCs. These cells have the ability to proliferate to produce more non-radial Sox2 positive NSCs. They can also differentiate to give rise to neurons or astrocytes. Modified from Suh et al., 2007.*

Pax6. Paired-box 6 (Pax6) is another conserved TF which is highly expressed in cells originating from embryonic neural development and adult neurogenic zones *(Betizeau et al., 2013; Florio & Huttner, 2014).* Pax6 is required for regulating neurogenesis and proliferation of NSCs *(Haubst et al., 2004)*. Upon Pax6 expression, several TFs such as Neurogenin 2 (Ngn2), T-box brain gene 2 (Tbr2), Neurogenic differentiation 1 (NeuroD) and T-box brain gene 1 (Tbr1) are activated. These TFs are expressed sequentially (Pax6 -> Ngn2 -> Tbr2 -> NeuroD -> Tbr1), which lead to neuronal differentiation (Fig. 11; *Haubst et al., 2004*).

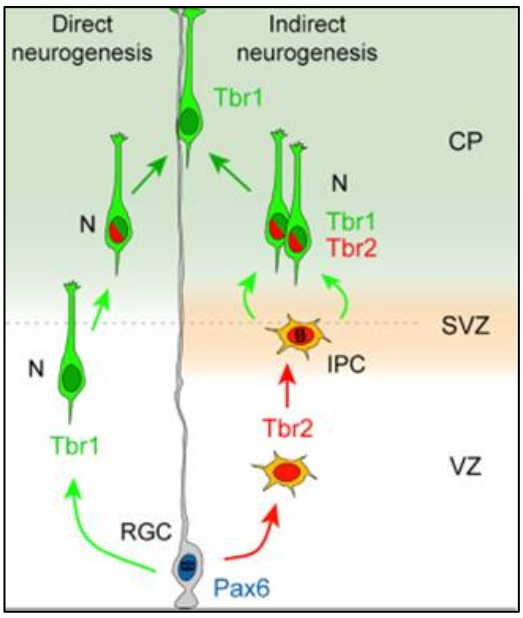

Figure 11. Involvement of Pax6 positive radial glial cells in adult neurogenesis. *Differentiation of Pax6 positive RGC to neurons can take place via either direct or indirect approach of neurogenesis. In direct neurogenesis, Pax6 positive RGCs differentiated into Tbr1 positive neurons directly, whereas in indirect neurogenesis approach, these Pax6 positive RGCs first differentiate into an intermediate stage, which express Tbr2, which then further differentiates into Tbr1 positive neurons. Adapted from Haubst et al., 2004.*

Gli1. Gliotactin 1 (Gli1) is a transcription factor, which is activated by sonic hedgehog (SHH) signaling pathway *(Lai et al., 2003; Machold et al., 2003)*. Gli1, therefore, has been routinely used as a sensitive readout of SHH activity in cells *(Rimkus et al., 2016)*. SHH responsive NSCs have been reported to possess the ability of proliferation and differentiation into neurons, thereby increasing in number as well as generating more neurons *(Ahn & Joyner, 2005)*. In the SVZ, the stem cells (B – cells) give rise to amplifying cells (C – cells) which act as progenitors to form neuroblasts (A – cells). Gli1 is expressed in B – cells and C – cells, which was confirmed with single cell RT-PCR *(Palma et al., 2005)* as well as analysis of transgenic Gli1-nLacZ mice *(Ahn et al., 2005)*. Immunohistochemistry on this mice showed that Gli1 was expressed in the SVZ, specifically in NSCs (B – cells) and their progenies (C – cells). However, in the SGZ, SHH administration increased the number of proliferating cells *(Lai et al., 2003; Machold et al., 2003)*, thereby indicating that SHH acts as a regulator of adult hippocampal NSCs. In this case as well, Gli1 was found to be transcriptionally induced after the activation of SHH pathway in the SGZ *(Galvin et al., 2008)*. Further, Encinas and collaborators crossed Gli1CreERT2 mouse line with a reporter Rosa26 (CMV-LoxP-stop-LoxP-GFP) mouse line *(Balordi & Fishell, 2007)*, to drive the expression of GFP exclusively in the NSCs of the SGZ *(Encinas et al., 2011)*. These labeled NSCs were first quiescent in nature, which undergo asymmetric division to give rise to amplifying NSCs.

Tle4. Gro/Tle4 proteins are transcriptional corepressors, which are active in many cells during development. Tle4 is also known to suppress Notch signaling. However, Tle do not directly bind to the DNA, but they are recruited via a protein-protein interaction with specific DNA binding proteins such as bHLH and Fox Family proteins, Tcf/LEF, Hhex and Runx1 *(Buscarlet & Stifani, 2007; Jennings & Ish-Horowicz, 2008)*. Tle4 and Tle3 are expressed in ESC *(Cloonan et al., 2008)*, indicating its importance in the proliferation of ESCs. Tle3/4 acts by displacing Tcf3 from β-catenin, a byproduct of Wnt signaling. It directly interacts with Tcf3 on Nanog *(Pereira et al., 2006)* and Oct4 *(Tam et al., 2008)* promoters. Tle3/4 can also regulate differentiation in ESCs by interacting with various corepressors such as FoxD3 and Hes1 *(Liu & Labosky, 2008; Zhou et al., 2013)*.

Tbr1. The T-box brain 1 (Tbr1) is expressed in the developing cerebral cortex, hippocampus and the olfactory bulb *(Bulfone et al., 1995; Puelles, 2017)*. Tbr1 is a transcription factor, which promotes frontal identity in post mitotic neurons as well as implementing fate to initially specified radial progenitors cells. Several reports have demonstrated that Tbr1 is expressed downstream of Pax6, Tbr2 and NeuroD1, which implies its role in late stage glutamatergic neuronal differentiation *(Hevner et al., 2006; Hodge et al., 2008; Roybon et al., 2009; Schuurmans et al., 2004)*. Moreover, overexpression of Tbr1 resulted in the inhibition of astrocyte production in the developing olfactory bulb as well as promoting neuronal and oligodendrocytic differentiation *in vitro*. Puelles and colleagues demonstrated that evolutionarily, Tbr1 and Dcx positive cells are present in the pallial derivatives (homologous to the amygdala) of reptiles *(Puelles, 2017)*. This was in congruence with the proposal put forth by Luzzati and colleagues regarding the presence of a conserved pallial cell type, indicating the possibility of a population of slowly maturing DCX positive cells shared by multiple domains, which remain conserved during evolution *(Luzzati, 2015)*.

Lnc-RNAs. The above mentioned signaling mechanisms activate certain transcriptional programs in part by interacting with cellular epigenetic mechanisms including their interaction with chromatin remodeling enzymes and regulating fate of NSCs with the help of non-coding RNAs *(Mercer et al., 2008; Puthanveettil et al., 2013)*. In recent years, the role of long non-coding RNAs (lnc-RNAs) in adult neurogenesis has been highlighted. Barry and colleagues reported that lnc-RNAs have been previously linked to embryonic neurogenesis *(Barry et al., 2015)*. Moreover, several lnc-RNAs such as MALAT1, BCYRN1, MIAT, SOX2-OT, TUG1 and RMST were expressed in the SVZ of the adult human brain *(Barry et al., 2015)*. Various other lnc-RNAs such as DLX1AS, SIX3OS and PNKY were also demonstrated to be functionally essential in adult mouse neurogenesis *(Ramos et al., 2015; Ramos et al., 2013; Spalding et al., 2013)*. It is highly likely that any alteration in the levels of these essential lnc-RNAs could have pronounced effect on NSCs proliferation, amplification, differentiation into neuroblasts and potentially leading to impaired neurogenesis. Lnc-RNAs are greater than 200 nucleotides in size and can aid in regulating gene transcription, post-transcriptional mRNA processing and epigenetic modifications *(Llorens-Bobadilla et al.,*

2015). Lnc-RNAs could also drive neurogenic fate of NSCs, as shown *(Ng et al., 2013)*. The authors demonstrate that knockdown of lnc-RNA RMST inhibits neuronal differentiation and is essential for the binding of Sox2 to promoter regions of neurogenic transcription factors *(Fig. 12; Ng et al., 2013)*.

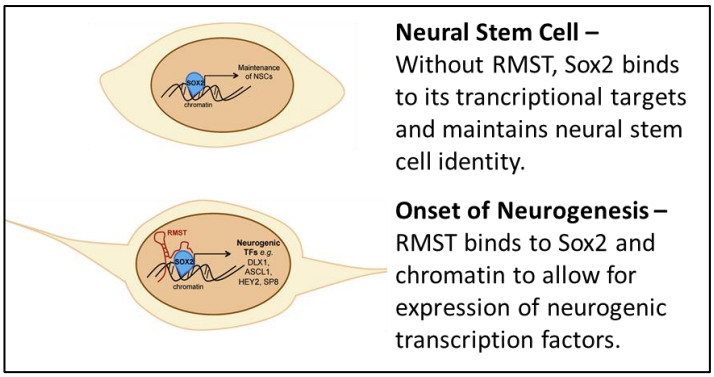

Figure 12. Mechanism of Sox2-RMST during neurogenesis. *In NSCs, when RMST is absent, Sox2 binds to its transcriptional targets to maintain NSC identity. However, during the onset of neurogenesis, RMST binds to Sox2 to allow the expression of neurogenic transcription factors. Adapted from Ng et al., 2013.*

In 2015, single cell RNA-Sequencing analysis of adult NSCs dynamics demonstrated that activation of quiescent NSCs is accompanied by downregulation of glycolytic metabolism accompanied by upregulation of mitochondrial oxidation in both neurogenic niches (SVZ and SGZ; *Shin et al., 2015*).

HIF-1. HIF-1, a heterodimer composed of HIF-1α and HIF-1β, is a transcription factor *(Cummins & Taylor, 2005)*. HIF-1α is oxygen-regulated protein, which is continuously synthesized and degraded. It is absent in normoxic cells. Studies have demonstrated that a link exists between hypoxia, HIFs and certain crucial differentiation regulating molecules such as OCT4 and c-Myc, which act in a HIF-dependent system to regulate stem cell function *(Maherali et al., 2007; Okita et al., 2007; Wernig et al., 2007)*.

1.2. Hypoxia.

1.2.1. Hypoxia as a critical microenvironment in neurogenic niches.

A critical question regarding what constitutes a niche for stem cell has often-troubled researchers. Over several years, this concept has been better understood. It is defined as a compartment containing cellular as well as acellular components, which release signals to create a microenvironment that regulates stem cells *(Scadden, 2006)*. The most basic element of a niche is contact and communication between these various

elements. As mentioned before, the Sub-Ventricular zone (SVZ) is the major neurogenic zone during early corticogenesis in rodents. This zone is populated by a variety of heterogeneous cell types. Doetsch and colleagues demonstrated that the multipotent NSCs (Type B cells) show linear progression to become proliferating, transit-amplifying cells (Type C cells) which would further lead to neuronal progenitors *(Doetsch et al., 1993)*. The Type B cells always maintain contact with both the ependymal cells as well as the basal lamina of the endothelial cells. The basal lamina of the endothelial cells is a component of the surrounding blood vasculature *(Alvarez-Buylla et al., 2004)*. In addition to that, the Type B cells also contains ciliated processes that maintain contact with the cerebrospinal fluid (CSF) present in the ventricle (Fig. 13). In the SVZ, the endothelial, ependymal cells and the choroid plexus together constitute a niche. They are the main sources of instructive signals for the stem cells present in the SVZ. Similar niches have been observed in postnatal human brains *(Quinones-Hinojosa et al., 2006)*. Each component of the niche plays a critical role in neurogenesis. The presence of astrocytes around the capillaries play a significant role in the proliferation of adult NSCs *(Palmer et al., 2000)*. The endothelial cells release soluble factors, which promote the proliferation of adult NSCs *(Shen et al., 2004; Shen et al., 2008)*. On the other hand, ependymal cells secrete Noggin, which promotes neurogenesis by activating Type B cells *(Lim et al., 2000)*. Noggin acts as a receptor for BMPs, which is a known differentiating factor. Vascular endothelial cells differentially control oxygen perfusion to either maintain or release NSCs from quiescence (Fig. 13). Even though adult NSCs are known for their extensive and long-term proliferative capacities, they possess the unique characteristic to remain quiescent (i.e. non-diving) for long periods. These quiescent NSCs thereby provide a regenerative reserve for age-related cell loss *(Li & Clevers, 2010)*. This 'stand by' mode preserves the stem cells from uncontrolled expansion and premature exhaustion while leaving them poised to reactivate in case of need *(Rodgers et al., 2014)*. These quiescent stem cells are located in niches with low oxygen tension *(Gopinath et al., 2014)*, suggesting that the availability of oxygen could determine the fate of the cell. Milosevic and colleagues demonstrated that lower oxygen levels (2-5%) reduced the level of apoptosis, improved the long-term expansion

of NSCs *(Milosevic et al., 2005)* and prevented neuronal differentiation *(Gustafsson et al., 2005)*.

Box. 7. Hypoxia.

It is a state of reduced oxygen pressure below a certain threshold, which induces adaptive gene expression and if severe, restricts the function of organs, tissues or cells. It also has an important role in maintaining stem cell behavior.

Normoxia.

A normal state of oxygen pressure i.e. in the range of 2-9% of oxygen in most adult cells in vivo is termed physiological normoxia.

Reports have described that this response of a cell to hypoxia involves a shutdown of oxidative phosphorylation thereby stopping proliferation to be brought about by hypoxia-inducible factors (HIFs). These factors are activated when there is low oxygen availability *(Majmundar et al., 2010)*. The authors also indicate that the hypoxic signaling helps in maintenance of NSCs, by reinforcing cell quiescence and/or promoting proliferation at the expense of differentiation. Decreasing the oxygen levels can activate quiescent NSCs to proliferate, yielding Type C cells that eventually differentiate in specific regions where oxygen levels are higher.

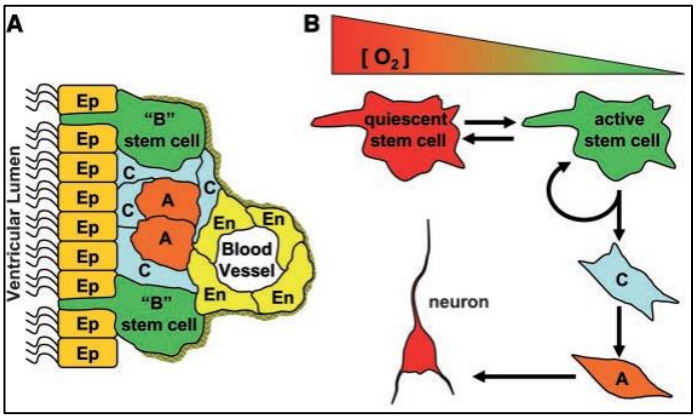

Figure 13. Postnatal brain stem cells and surrounding niche. *(a) Stem cells maintain contact with ependymal (Ep) cells, endothelial (En) cells and with the ventricular lumen. (b) Changing oxygen tension regulates stem cell quiescence and activation to generate transit amplifying cells and their differentiated progeny. Adapted from Panchision, 2009.*

One of the major advantage of stem cells located in a hypoxic niche is that the cells can maintain slow-cycling proliferation rates while avoiding the oxidative stress, yielding

Type C cells that eventually differentiate in specific regions where oxygen levels are higher *(Cipolleschi et al., 1993; Eliasson & Jonsson, 2010; Lekli et al., 2009)*.

1.2.2. Hypoxic neurogenic niches in humans and rodents.

With all the reports published so far, researchers have started manipulating oxygen levels to demonstrate that lower oxygen levels significantly influence both embryonic and adult stem cells *(Eliasson et al., 2010; Panchision, 2009)*. In humans, the neural, mesenchymal and hematopoietic are the three niches where different stem cells reside. The hematopoietic stem cell niche is one of the best characterized niches in humans *(Yin & Li, 2006)*. In the bone marrow, the hematopoietic stem cell niche showed the oxygen levels to be approximately 1-6% O_2 *(Grant and Root, 1947; Cipolleschi et al., 1993; Eliasson and Jonsson, 2010)*. The architecture of the medullary sinuses and arterial blood flow are responsible for generating an oxygen gradient within the bone marrow. Cipolleschi, Parmar and colleagues demonstrated that HSCs are naturally distributed within the oxygen gradient in the bone marrow, with HSCs mostly residing in the most hypoxic niches *(Cipolleschi et al., 1993; Parmar et al., 2007)*. Following multiple reports, the oxygen levels in mesenchymal stem cell niche present in the adipose tissue was found to be approximately 2-8% O_2 *(Harrison et al., 2002; Kofoed et al., 1985; Matsumoto et al., 2006; Pasarica et al., 2009)*. In the SVZ, direct measurements from the neural stem cell niche has never been performed, but various regions of the rodent brain have shown the oxygen levels to be as low as 0.55% O_2 *(Dings et al., 1998; Erecinska & Silver, 2001; Panchision, 2009)*. In rodent brain, the pressure of oxygen is significantly lower and ranges from 0.55% in the mesencephalon to 8% at the surface of the brain *(Erecinska et al., 2001)*. However, in comparison, the pressure of oxygen in the human brain as measured by catheter electrodes varies from approximately 3% at a location of 22-27mm deep at the dura to 4% at 7-12mm under the dura *(Dings et al., 1998)*. This demonstrates that physiological oxygen gradient is observed at its highest in the alveolar space and lowest in tissues (Fig. 14). These data altogether provide evidence that NSCs in the human brain are located in a hypoxic environment.

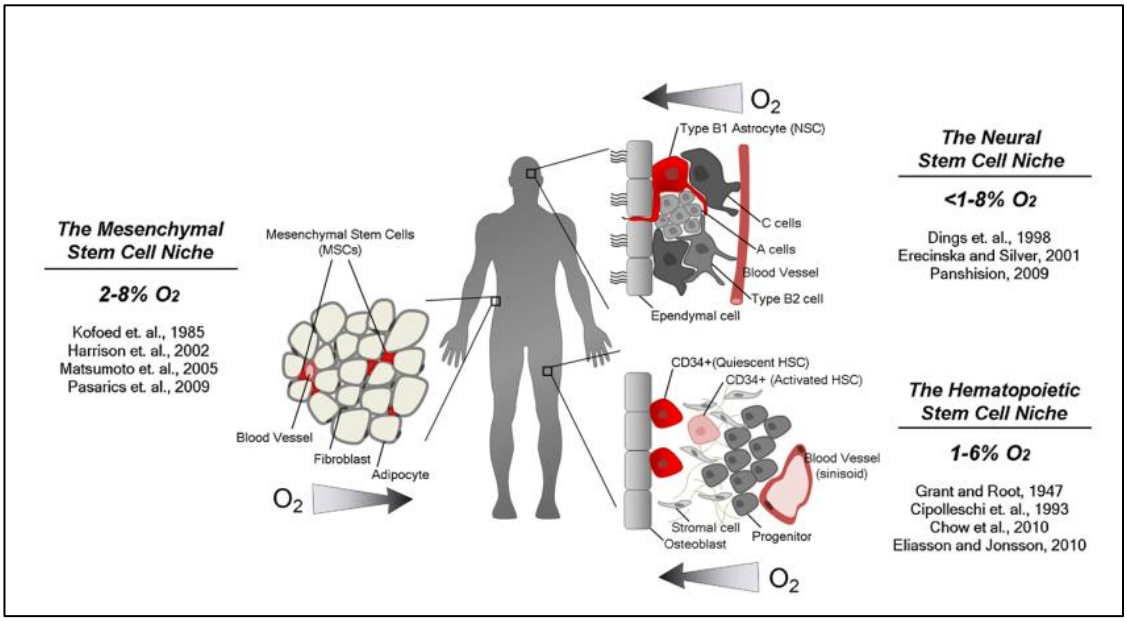

Figure 14. Oxygen tension measurements in different stem cell compartments. *Schematic models based on available literature for hematopoietic, mesenchymal and neural stem cells in their respective niches namely, bone marrow, adipose tissue and the sub-ventricular zone. Adapted from Mohyeldin et al., 2010.*

1.2.3. Importance of hypoxia in regulating 'Stemness'.

During development, cortical vascular network formation occurs simultaneously with neurogenesis. During corticogenesis at E10.5 in rodents, a hypoxic environment induces and maintains high levels of HIF-1a in radial glial cells, due to the absence of blood vessels at this time point. Due to such a low oxygen level, the radial glial cells undergo symmetric divisions, thereby increasing their numbers rapidly. At this time, the presence of high levels of HIF-1a restricts the radial glial cells to prematurely commit to produce differentiated progeny. However, at a later stage at E13.5, HIF-1a levels are needed for the blood vessel formation, since it has been reported to be impaired in the absence of HIF-1a *(Morante-Redolat & Farinas, 2016)*. This blood vessel formation thereby increases the oxygen levels in the tissue.

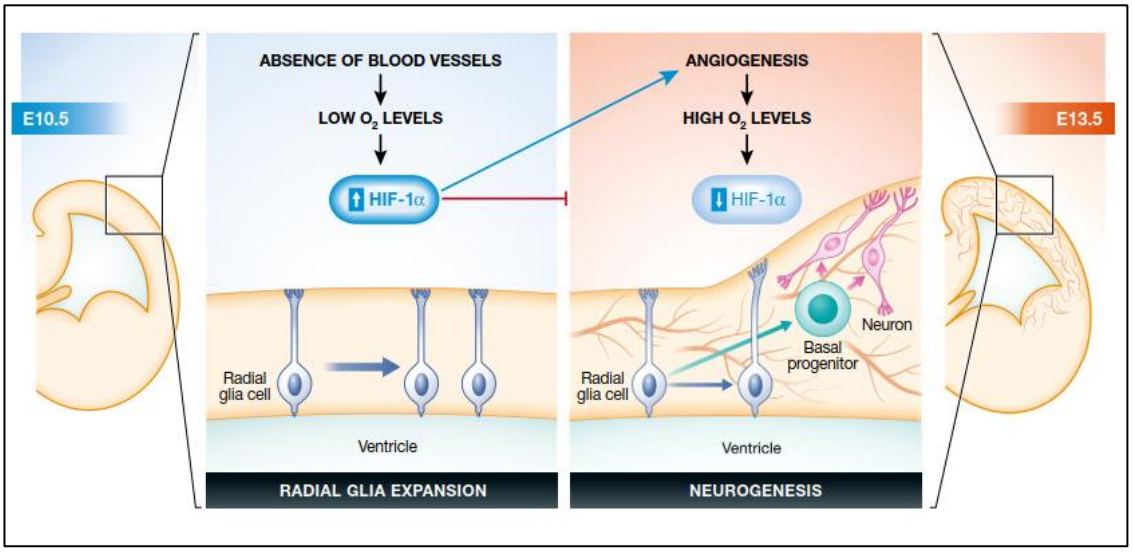

Figure 15. Role of hypoxia and HIF-1a in astrocyte differentiation and neurogenesis. *At E10.5, the absence of blood vessels results in a hypoxic environment that induces and maintains high levels of HIF-1a in radial glial cells. However, at E13.5 the growth of blood vessels leads to an increase in the oxygen levels in the tissue. Due to this, HIF-1a is degraded and this initiates neurogenesis. Adapted from Morante-Redolat and Farinas, 2016).*

Due to this sudden rise in the oxygen levels, HIF-1a is degraded and its downregulation leads the radial glial cells to undergo asymmetric divisions and initiate neurogenesis *(Morante-Redolate and Farinas, 2016)*. This shows that hypoxia and HIF-1a creates an auto-regulatory loop ensuring initial radial glial expansion via proliferation and subsequent induction of their asymmetric divisions to generate higher number of neurons (Fig. 15). Hypoxia during early developmental stages thereby regulates differentiation and tissue repair *(Burton et al., 2017; Zhang et al., 2016)*. This has been demonstrated *in vitro* as well (Table. 3).

Cells	Oxygen tension (%)	Effect on proliferation	Effect on neuro-differentiation	References
Fetal Mesencephalix precursors	3 %	Increase	Increase	Storch et al, 2001
Forebrain precursors	3 %	Modest Increase	No effect	Storch et al, 2001
Fetal NSCs	1 %	Decrease	Increase	Santilli et al, 2010
Fetal NSCs	2.5 %	Increase	Increase	Santilli et al, 2010
Fetal NSCs	5 %	Increase	Increase	Santilli et al, 2010
Postnatal CD133+; Nestin+ precursors	5 %	Increase	No effect	Pistollato et al, 2007
Fetal neural progenitors	3 %	Increase	Increase	Giese et al, 2010

Table 3. In-vitro effect of low Oxygen tension on proliferation and differentiation of human neural stem cells (De Filippis & Delia, 2011).

In rodents, there have been reports suggesting the fine-tuned control of hypoxia on neurogenesis as demonstrated *(Xie & Lowry, 2018).*

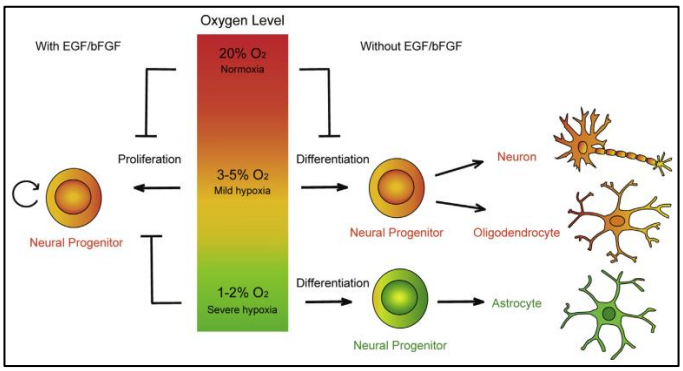

Figure 16. Influence of oxygen levels on proliferation and lineage specification of NSCs. *Mild hypoxia promotes neurogenesis and oligodendrocyte differentiation, whereas severe hypoxia induces the generation of astrocytic differentiation. Adapted from Xie and Lowry, 2018.*

1.2.4. Hypoxia induced transcriptional control.

All cells need a continuous supply of oxygen, even the cells present within the fetus. Oxygen is delivered to all cells by red blood cells through the vasculature. Cells usually activate mechanisms, which are essential for their optimal function in response to either reduction or increase in oxygen levels *(Semenza, 2010)*. Reduction in oxygen levels leads the cells to trigger enhanced mechanisms to promote the delivery of oxygen. One such mechanism is centered on the upregulation of transcription factor complex known as Hypoxia Inducible Factor *(Bruick et al., 2010)*. HIF consists of two subunits, one acts as a regulatory subunit sensitive to oxygen and other is constitutively

expressed oxygen insensitive b-subunit (HIF-1b). HIF-1b is also known as Aryl Hydrocarbon Receptor Translocator (ARNT). There are three subunit genes present in the mammalian genome, namely; HIF-1a, HIF-2a and HIF-3a. HIF-1a is the most widely studied and possess the broadest tissue distribution as compared to the others. In the presence of low oxygen levels, HIF-1a protein is stabilized which allows it to interact with ARNT and further recruit the coactivators such as CREB binding protein (CBP), E1A binding protein p300 (EP300). This complex then also binds to the hypoxia regulatory elements (HREs) associated with other target genes which further encode proteins that help the cell to regulate adaptations to hypoxia *(Kaelin & Ratcliffe, 2008)*. However, when oxygen levels are back to normal, HIF-1a subunits undergo hydroxylation on the prolyl residues by a family of oxygen sensitive prolyl hydroxylases (PHD1, PHD2 and PHD3). This hydroxylation then facilitates the HIF-1a subunit to associate with the Von-Hippel-Lindau (VHL) protein, thereby leading to its ubiquitination, followed by its subsequent proteasome-mediated degradation (Fig. 17; *Kaelin and Ratcliffe, 2008*).

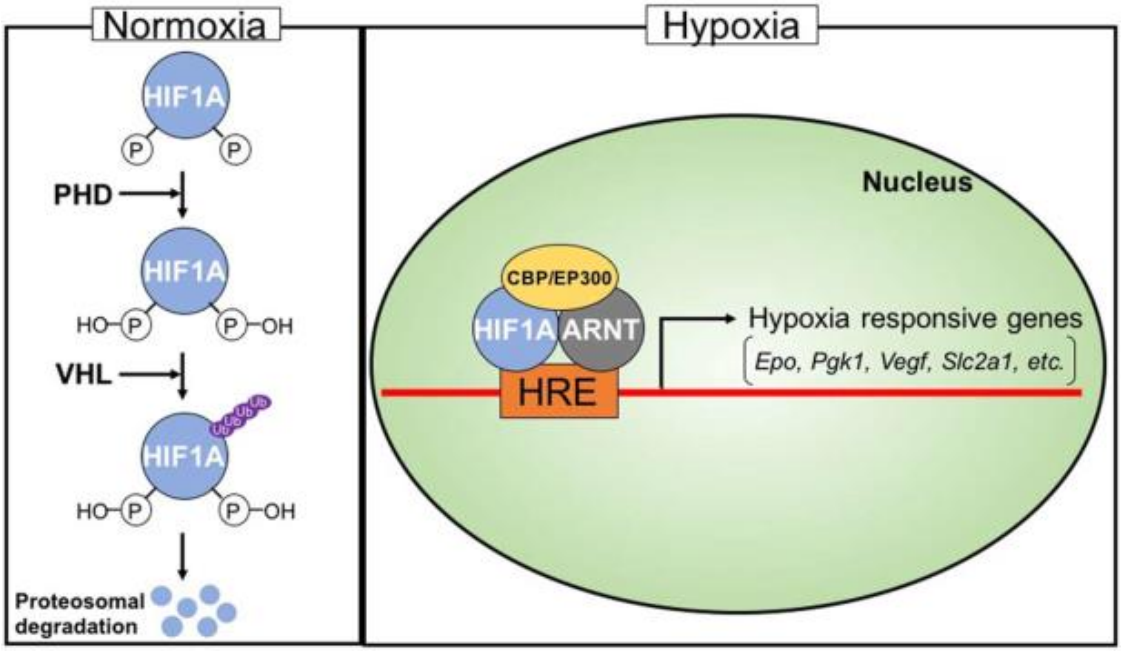

Figure 17. Cellular responses to hypoxia. *In normoxia, PHD hydroxylate HIF-1a allowing VHL protein to ubiquitinate HIF-1a resulting in degradation of HIF-1a. However, in hypoxia, HIF-1a is stable and can dimerize with ARNT, also recruit CBP/EP300 and bind to hypoxia/HIF response elements (HRE). The binding induces hypoxia responsive genes encoding proteins required for the adaptation. Adapted from Soares et al., 2017.*

In response to induced or endogenous hypoxia, gene-expression studies have revealed that over thousands of genes are activated by HIF1-a. Majority of those genes are involved in pathways that control O_2 consumption and delivery, inhibition of growth and development, and promotion of anaerobic metabolism *(Bruick, 2003; Carmeliet et al., 1998; Iyer et al., 1998)*. Vascular endothelial growth factor (VEGF), glucose transporters (Slc2a1) and erythropoietin (EPO) are some of the examples of oxygen-regulated genes, which are activated by HIF1-a *(Loike et al., 1992; Shweiki et al., 1992)*.

1.2.5. Hypoxic upregulation of erythropoietin.

As mentioned before, there is a strong induction of HIF-1a in the brain during hypoxia, which leads to a transcriptional regulation of target genes *(Chavez et al., 2000)*. Stroka and colleagues demonstrated that sustained high levels of HIF-1a lead to an upregulation of erythropoietin (EPO) during hypoxic exposure *(Stroka et al., 2001)*. EPO is one of the examples of a gene regulated in an oxygen dependent manner. Semenza and Wang, identified EPO to be the first target gene of HIF-1 *(Semenza & Wang, 1992)*. The discovery of HIF was found by studies on the DNA-protein interactions at the 3' hypoxia response element (HRE) of erythropoietin (Fig. 18; *Wang and Sememza, 1995*).

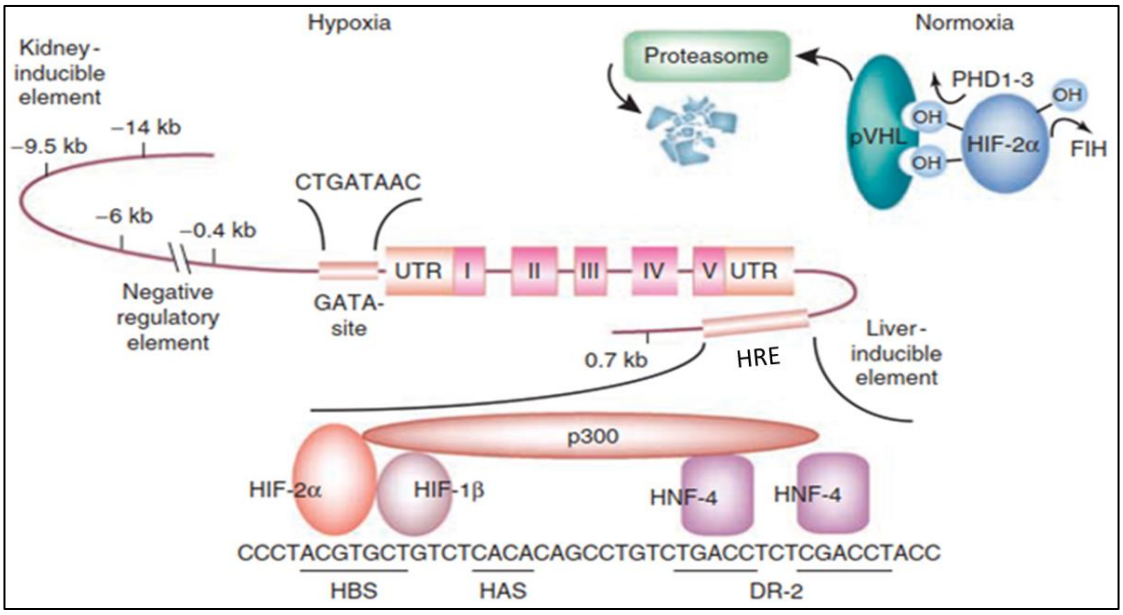

Figure 18. Schematic representation of EPO and factors controlling hypoxic EPO induction. *Under hypoxic condition, HIF-2a is stabilized and binds with HIF-1ß, translocate to the nucleus where it binds to the HRE region in the 3- enhancer. Modified from Weidemann and Johnson, 2009.*

As the severity of hypoxia increases, the mRNA expression of EPO increases from 3 to 20 fold in the brain as compared to 200 fold in the kidney *(Marti et al., 1996)*. However, the temporal pattern is different. EPO expression upon hypoxia in liver and kidney is transient between 6 to 24 hours *in vivo* and 6 hours *in vitro* (Fig. 19), depending on the severity of hypoxia *(Fandrey et al., 1990)*. In the brain, the mRNA levels of EPOR are observed to be elevated throughout the hypoxic exposure. Researchers discovered that relative hypoxic conditions were sufficient to increase the expression level of EPO mRNA and maintain an elevated level for at least 12 hours *(Morita et al., 2003)*. When mice were exposed to hypoxic conditions, Yeo and colleagues suggested that the EPO transcription in the brain was primarily induced by HIF-2a instead of HIF-1a. They also demonstrated that EPO was present in the nuclei after 1 hour of hypoxia exposure *(Yeo et al., 2008)*. This was one contradicting report suggesting that EPO is induced by HIF-2a; whereas multiple other reports corroborate the evidence, indicating HIF-1a induces an upregulation in EPO *(Manalo et al., 2005; Sharp et al., 2004)*.

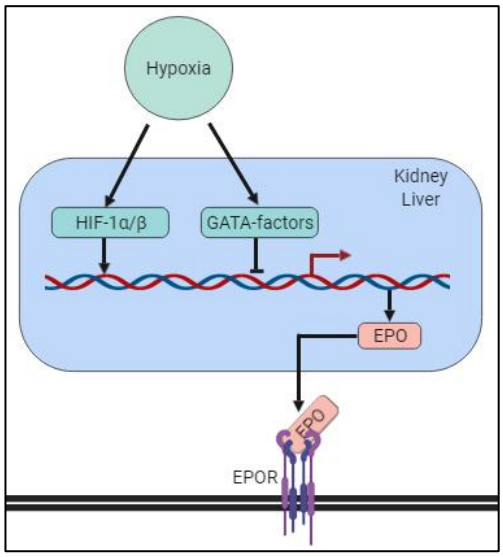

Figure 19. Regulation of EPO under hypoxia in kidney and liver. *Schematic representation of hypoxia regulated upregulation of HIF-1a/HIF-1β, which further leads to an upregulation of EPO that can bind to its receptor EPOR. Modified from Chateauvieux et al., 2011.*

With the help of more *in vitro* studies, cultured primary mouse astrocytes showed approx. 100-fold increase in EPO mRNA expression after hypoxia exposure *(Marti et al., 1996)*. Youssoufian and colleagues used *in vitro* cultures of NSCs to show that after treatment with hypoxia, the expression of EPO was significantly increased *(Youssoufian et al., 1993)*. Similar increase in the expression of EPO mRNA was observed in cultured neurons after hypoxia treatment *(Bernaudin et al., 2000)*. Cultured hippocampal

neurons after exposure to hypoxia showed an upregulation of EPOR mRNA expression *(Lewczuk et al., 2000)*. Shingo and colleagues suggested that hypoxia induced upregulation of EPO could act directly on NSCs, by promoting neurogenesis after hypoxia *(Shingo et al., 2001)*. Similarly, VEGF expression is also observed to be upregulated via hypoxia, thereby increasing adult neurogenesis *(Jin et al., 2002; Shweiki et al., 1992)*. Moreover, EPO treatment also enhanced the survival and differentiation of dopaminergic neurons from NSCs *in vitro (Studer et al., 2000)*. In terms of NSCs maintenance, hypoxia has been proven to increase proliferation of NSCs through EPO *in vitro* and *in vivo* via the NF-κB signaling. Upon activation, there is a significant increase in the expression of Mash1, a transcription factor promoting neurogenesis *(Shingo et al., 2001)*. The increased expression of receptors for EPO in the developing rodents and human CNSs after hypoxia/ischemic exposure *(Juul et al., 1998; Juul et al., 1999; Liu et al., 1997; Siren et al., 2001; Siren et al., 2006)* supports a possible role for EPO in the CNS development.

1.3. Erythropoietin.

1.3.1. History of EPO.

Paul Bert, the pioneer of aviation medicine, first recognized an increase in the red blood cells at reduced oxygen levels *(Bert, 1882)*. He looked at the animals surviving at higher altitudes and hypothesized the existence of a genetic reason for their elevated oxygen capacity of the blood. Another researcher also recognized that acute exposure to high altitude could increase the number of erythrocytes *(Viault, 1890)*. Further, down the line, Paul Carnot and Deflandre first proposed the regulation of erythropoiesis *(Carnot and Deflandre, 1906)*. Following that, in 1948, Bonsdorff and Jalavisto coined the name 'erythropoietin' (EPO; *Bonsdorff, 1949*). EPO is primarily found to be produced in the kidney or liver of adults and in the liver of fetal and neonatal mammals *(Jacobs et al., 1985)*. Jelkmann in 1992 demonstrated the functionality of EPO, where he demonstrated that EPO is essential for the maintenance and renewal of red blood cells *(Jelkmann, 1992)*. Although initially thought to be restricted to the hematopoietic system, research during the last 20 years has revealed important functions of EPO outside the hematopoietic system, EPO production has been identified in the central

nervous system *(Masuda et al., 1994; Siren et al., 2001; Marti et al., 2004; Siren et al., 2006; Noguchi et al., 2008)*. EPO is produced in three main sites in mammals namely, the central nervous system, the liver and the kidney. In the CNS, EPO is produced by astrocytes and neurons to exert neuroprotective effects. In the liver, EPO is produced in Ito-cells and in hepatocytes, where HIF-2a is the main regulator of hypoxic EPO induction. However, in the kidney, majority of EPO expression is influenced by the hypoxic response of the skin *(Weidemann & Johnson, 2009)*.

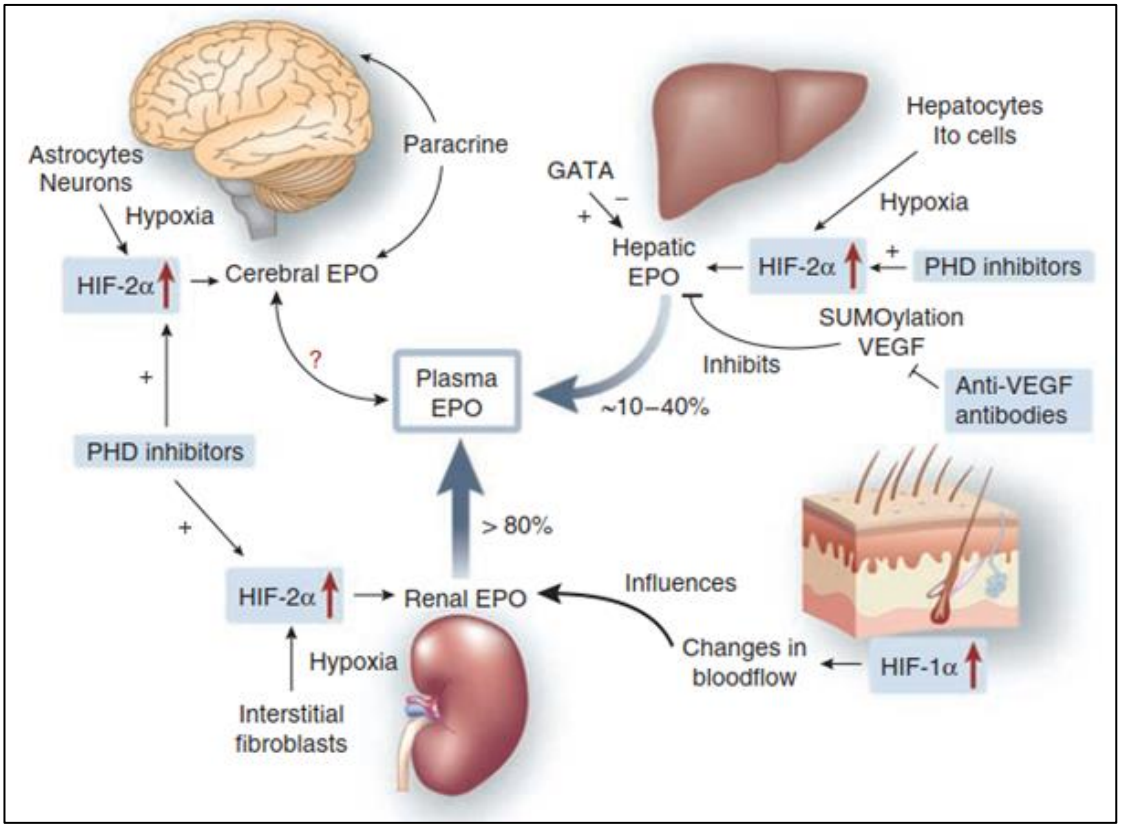

Figure 20. Main sites of EPO production. *EPO is produced in three main sites in mammals namely, the central nervous system, the liver and the kidney. In the CNS, EPO is produced by astrocytes and neurons to exert neuroprotective effects. In the liver, EPO is produced in Ito-cells and in hepatocytes, where HIF-2a is the main regulator of hypoxic EPO induction. However, in the kidney, majority of EPO expression is influenced by the hypoxic response of the skin. Adapted from Weidermann and Johnson, 2009.*

The mRNA expression levels of EPO were found to be at comparable levels in the brain of mice *(Digicaylioglu et al., 1995)*, monkeys and humans *(Marti et al., 1996)*. EPO, at its protein level, was detected in the cortex and hippocampus of human and rodent brain *(Bernaudin et al., 1999; Siren et al., 2001)*. Critical role of EPO in development and maintenance of the CNS was demonstrated by its importance in neurogenesis and

neuroblasts migration *(Tsai et al., 2006; Yu et al., 2002)*, neuronal differentiation *(Park et al., 2006)*, oligodendrocyte differentiation and maturation *(Iwai et al., 2010; Sugawa et al., 2002)*. EPO mediates its effect through binding to its receptor EPOR. This suggested that EPOR must be expressed at various sites in the CNS to enable EPO to initiate its effects. To prove this, several researchers demonstrated that the expression of EPOR mRNA and protein was observed in the brains of mouse, rat, monkey and humans *(Digicaylioglu et al., 1995; Liu et al., 1997; Marti et al., 1996)*. Most types of neural cells express EPOR, including neurons, oligodendroglia lineage cells, astrocytes and microglia *(Bernaudin et al., 2000; Bernaudin et al., 1999; Hasselblatt et al., 2006; Ott et al., 2015; Siren et al., 2001; Sugawa et al., 2002)*.

1.3.2. EPO and the blood brain barrier.

EPO is a 166 amino acid glycoprotein, which is a member of the type I cytokine superfamily *(Brines & Cerami, 2005; Noguchi et al., 2008; Youssoufian et al., 1993)*. EPO consists of four α-helices connected through two disulfide bridges between cysteines 6 and 161 and cysteines 29 and 33 *(Lai et al., 1986)*. It consists of about 60% protein and 40% carbohydrate *(Noguchi et al., 2008)* and has three N-glycosylation sites and one O-glycosylation site *(Sasaki et al., 1987)*. The molecular weight of EPO is approximately 30.4 kD, which is significantly higher than the threshold for lipid mediated transport across the blood brain barrier (BBB). Brines and colleagues demonstrated that EPOR was expressed in brain capillaries facilitating the transport of EPO across the blood-brain barrier *(Brines et al., 2000)*. The brain uptake of EPO was calculated to be approx. 0.05-0.1% of the total injected dose per gram of the brain, which peaked at 3 hours after injection. Using rodent model, biotinylated EPO was administered and biotin localization was observed around the capillaries in mouse brain 5 hours after injection. This was subsequently eliminated by an increase of unlabeled exogenous EPO, indicating a specific receptor-mediated transport of EPO in the brain *(Banks et al., 2004)*. An increase of EPO in the serum could suggest the dysfunction of BBB, whereas increase of EPO in CSF indicates the synthesis of EPO in the CNS *(Marti et al., 1997)*. To corroborate this finding, when humans were given high doses of EPO, there as a significant increase of EPO in the CSF at 3 hours after

administration. This provided the first evidence that EPO transport inside the brain takes place via a first order transmembrane or a non-receptor mediated mechanism *(Xenocostas et al., 2005)*. Moreover, intravenous injection of 111-labeled EPO in healthy individuals and patients led to the detection of significant radioactivity in the brain, which peaked at 4 hours after injection and was maintained constant for 2 days *(Ehrenreich et al., 2004)*. These reports together provide evidence that EPO crosses the BBB in a dose-dependent manner and is found to be increased after brain injury *(Statler et al., 2007)*.

1.3.3. Importance of EPO.

In a neonatal stroke model using P10 rats, the expression of HIF-1a and EPO was observed to have peaked 8 hours after ischemia *(Mu et al., 2005)*. It was also reported that EPO treated animals showed earlier restored cognitive functions after traumatic head injury *(Brines et al., 2000; Meng et al., 2012).* EPO treatment in mouse cortical lesion model prevented long-term behavioral alterations like impaired learning and brain atrophy *(Dayyat et al., 2012)*. As mentioned above, high-dose EPO is able to cross the blood brain barrier in mice and man *(Brines et al., 2000; Ehrenreich et al., 2004)*. Cerebral EPO has therefore drawn much attention as a neurotrophic and a neuroprotective factor for cerebral diseases including Alzheimer's *(Maurice et al., 2013)*, depression *(Miskowiak et al., 2010)*, epilepsy *(Castaneda-Arellano et al., 2014)* and ischemia *(Nguyen et al., 2014)*. Pioneering work done in humans by Ehrenreich and colleagues, demonstrated a greater clinical significance. In clinical trials, high dose EPO treatment in patients with chronic progressive multiple sclerosis (MS) is both beneficial and safe *(Ehrenreich, et al., 2007)*. Moreover, EPO treatment showed improvement in cognitive functions in chronic schizophrenic patients *(Ehrenreich, et al., 2007)* and in therapy resistant major depression patients as well *(Miskowiak, et al., 2014)*. Kästner and colleagues identified novel association of EPO and EPOR genotypes with cognition *(Kästner et al, 2012)* in schizophrenic patients. As gray matter loss is one of main characteristics of schizophrenia, it was also reported that EPO would delay cortical atrophy in chronic schizophrenic patients *(Wustenberg et al., 2011)*. Further studies showed that EPO could reduce brain matter loss specifically in the CA1 and CA3 regions

of the hippocampus in affective disorder patients *(Miskowiak, et al., 2014)*. These studies when interpreted together could indicate that loss of neurons could give rise to cognitive defects in these patients. EPO treatment and cognitive function studies in patients with schizophrenia and multiple sclerosis have shown that 8–12 weeks of high-dose EPO treatment improved cognitive functioning that lasted up to 6 months after treatment completion, which exceeds the red blood cell normalization *(Ehrenreich, et al., 2007; Ehrenreich, et al., 2007)*. This suggests that the pro-cognitive effects of EPO are not related to changes in the hematopoietic system. On the contrary, EPO induced effects on neuro-cognition in humans seem to be mediated through neurobiological actions rather than indirect increase in the number of red blood cells *(Miskowiak et al., 2007a; Miskowiak et al., 2007b)*. These clinical trials demonstrated that one high dose of EPO as compared to saline was capable of improving neural and cognitive measures of memory and executive functioning in healthy volunteers without affecting the number of red blood cells. Miskowiak and colleagues performed a clinical trial to examine the effects of EPO on mood symptoms and cognitive dysfunction in Treatment Resistant Depression (TRD) and Bipolar Disorder *(Kimura et al., 2015)* patients. The results indicated that EPO treatment significantly improved verbal memory in TRD patients and speed of complex cognitive processing across attention, memory and executive function in BD patients *(Miskowiak, et al., 2014a; Miskowiak, et al., 2014b)*. Further analysis revealed a structural hippocampal increase and task-related neural activity change correlated with the observed improvements in EPO-treated patients' cognitive functions. These improvements had no relation with the number of red blood cells, mood symptoms, age or gender of the patients treated *(Miskowiak, et al., 2016a; Miskowiak, et al., 2016b; Miskowiak et al., 2015)*.

Ehrenreich and colleagues conducted clinical trial for stroke patients. In the double bind proof of concept trial, the authors demonstrated that injecting of EPO daily for the first three days after stroke led to a significant increase in the functional outcome (determined by Barthel Index) and prominent reduction in neurological defects in EPO treated stroke patients *(Ehrenreich et al., 2002)* as well as in schizophrenic patients *(Ehrenreich et al., 2004)*.

In conclusion, EPO, as a candidate, has been demonstrated to be hypoxia-inducible, which could provide neuroprotection in rodents by targeting variety of mechanisms involving neuronal, glial and endothelial cellular functions. These results pointed towards the hypoxic regulation of the EPO gene and its implication on hippocampal neuro-differentiation and thereby enhancing cognition.

1.3.4. Role on EPO on neurogenesis.

Erythropoietin role in the differentiation of stem cells in the hematopoietic system was widely studied. Early fate maps of hematopoiesis depicted one initial hematopoietic stem cell (HSC) population differentiating into blood and immune cells. Hematopoietic progenitor cells (HPCs) are their progeny that have been `chosen` to differentiate rather than proliferate *(Ceredig et al., 2009; Hattangadi et al., 2011)*. However, since the finding of EPO and EPOR in the CNS, our group wondered whether similar mechanisms might also apply in the central nervous system. Previous work from our lab, demonstrated that EPO administration in mice led to 20% increase in the number of pyramidal neurons and oligodendrocytes in the CA1 and CA3 region of the hippocampus of young mice, without undergoing proliferation, resembling similarities from the hematopoietic system. Enhanced pyramidal neuron numbers induced by EPO in young mice were shown to be maintained under conditions of ongoing cognitive challenge using the touch-screen paradigm but this effect was not observed in the absence of a cognitive challenge. This led to the hypothesis of `use-it-or-lose-it`. However, as opposed to the precursor identification in the oligodendrocyte cell lineage, the neuronal lineage was much more broad and complicated.

Rationale and Research Aims

2. Rationale and research aims.

Previous work from our group has demonstrated that EPO treatment induces an increase in the number of pyramidal neurons in the CA1 region of the hippocampus *(Hassouna et al., 2015)*. Understanding the endogenous mechanisms by which EPO mediates this increase in the brain may open new avenues for the development of therapeutic strategies for modulation of adult neural precursor cells. Harnessing this mechanism for the treatment of various cognitive decline disorders led to the research aims of my PhD work.

The main objectives of my PhD study were as follows:

1. ***To locate the neuronal progenitor cells which respond to EPO and lead to an increase in the number of pyramidal neurons in the CA1.*** The increase in neurons upon EPO had to be attributed to certain neural precursors. Given the complexity of the neuronal lineage, This thesis attempted to determine the influence of EPO on number of progenitor cells as well as fate map these cells using transgenic mouse models like NestinCreERT2, GliCreERT2 and Sox2CreERT2 mice crossed with a reporter mouse line (R26R-TdTomato).
2. ***To replicate and extend the previous findings of increased neuron numbers using a novel sophisticated method.*** One way of addressing the question of adult neurogenesis is by using precursor marker labelled additive method. However, a subtractive approach was employed where a transgenic mouse (NexCreERT2) was crossed with a reporter mouse line (R26R-TdTomato) and effects were studied in juvenile and adult mice. Yet another approach, to strengthen these claims was to observe the effect of EPO on RNA transcriptome level. Single cell Drop-Sequencing method was employed to elucidate the effect of a single high-dose of EPO on different cell populations in the CA1 region of the hippocampus.
3. ***To elucidate the effect of EPO on synaptic connectivity of pyramidal neurons in the CA1 region of juvenile and adult mice.*** Having observed increased pyramidal neuronal numbers, next aim was to evaluate the role of EPO in neuroplasticity. To achieve this, a transgenic mouse model (Thy1) was crossed with a reporter mouse

line (EGFP) to label dendrites and spines of sparsely labelled pyramidal neurons in the CA1.

4. ***To evaluate the endogenous mechanisms by which EPO mediated these neuroplastic effects.*** Exogenous EPO led to an increase in neuroplasticity but EPO being a hypoxia-regulated gene should be able to deliver similar effects upon hypoxia exposure was reasoned. Therefore, to understand the physiological underpinnings, a hypothesis was put forth that a learning/cognitive challenge such as Complex Running Wheel (CRW) could lead to an increase in the levels of EPO, its receptor EPOR and cause an increase in endogenous functional hypoxia in pyramidal neurons. This was achieved using a hypoxia sensitive transgenic mouse model (CAG-ODD) crossed with a reporter mouse line (R26R-TdTomato). Further, this thesis aimed to determine the effect of physiological hypoxia (via Complex Running wheel) and/or exogenous hypoxia (via exposing mice to 12% Oxygen in chambers) on the number of pyramidal neurons as well as to determine whether any enhancement in cognitive learning and endurance is observed. Moreover, to specifically understand the importance of EPO and EPOR in the brain, the present work investigated the effect of a specific deletion of EPO or EPOR in pyramidal neurons. For this purpose, conditional transgenic pyramidal knockout mouse models like NexCre::$EPO^{fl/fl}$ or NexCre::$EPOR^{fl/fl}$ mice were generated.

Materials and Methods

3. Materials and methods

3.1.1. Experimental models and mouse genetics.

3.1.2. Mouse strains.

All experiments were approved by and conducted in accordance with the regulations of the local Animal Care and Use Committee (Niedersächsisches Landesamt für Verbraucherschutz und Lebensmittelsicherheit, LAVES). NestinCreERT2 (Jackson Laboratory; 016261), GliCreERT2 (Jackson Laboratory; 007913), SoxCreERT2 (Jackson Laboratory; 007593), WT C57BL/6N (Charles River), NexCreERT2 *(Agarwal et al., 2011)*, R26R-TdTomato *(Madisen et al., 2010)*, Thy1-YFP (*Feng et al., 2000*; Jackson Laboratory, 003782), CAGCreERT2-ODD *(Kimura et al., 2015)*, NexCre *(Goebbels et al., 2006)*, Ella-Cre *(Holzenberger et al., 2000)*, EPOR-floxed ($EPOR^{fl/fl}$) and EPO-floxed ($EPO^{fl/fl}$) mice were used for the experiments. Juvenile (P23) and adult (3 months old) mice were used in this study. For labelling radial glial like precursor cells, Sox2CreERT2 and other precursors cells, NestinCreERT2 and GliCreERT2 mice were bred with Rosa26 floxed-stop TdTomato (R26R-TdTomato) reporter mice to generate Sox2CreERT2::TdTomato, NestinCreERT2::TdTomato and GliCreERT2::TdTomato mice. For genetic labelling of projection neurons, NexCreERT2 mice were bred with Rosa26 floxed-stop TdTomato (R26R-TdTomato) reporter mice to generate NexCreERT2::R26R-TdTomato mice. For labelling cells undergoing hypoxia, CAGCreERT2-ODD mice were employed *(Kimura et al., 2015)*. Briefly, a fusion protein consisting of the ODD domain of Hif1α and a ubiquitous CAGCreERT2 is expressed upon tamoxifen induction. CAGCreERT2-ODD were bred with R26R-TdTomato to generate CAGCreERT2-ODD::TdTomato reporter mice. Upon tamoxifen induction, cells are irreversibly labeled with TdTomato containing stabilized Hif-1α. NexCre::$Epor^{fl/fl}$ mice were generated to specifically delete *Epor* in projection neurons. For the generation of $Epor^{fl/fl}$ mice, embryonic stem cells (ES) harboring an engineered allele *($Epor^{tm1a(KOMP)Wtsi}$)* of the *Epor* gene were acquired from the Knockout Mouse Project (KOMP, University of California, Davis CA 95618, USA). ES cells were microinjected into blastocysts derived from C57BL/6N mice and the embryos were transferred to pseudo-pregnant foster mothers, yielding chimeric males. For ES clone *EPD0316_5_A03*, germline transmission was achieved upon breeding with C57BL/6N females, generating mice harboring the

Epor$^{tm1a(KOMP)Wtsi}$ allele (termed *Epor*$^{lacZ\text{-}neo}$). The lacZ-neo cassette was excised *in vivo* upon interbreeding with mice expressing FLIP recombinase (*129S4/SvJaeSor-Gt(ROSA)26Sor*$^{tm1(FLP1)Dym/J}$; backcrossed into C57BL/6N), yielding mice carrying the *Epor*$^{tm1c(KOMP)Wtsi}$ allele (termed *Epor*^{flox}). The construct validity of this mouse line was established using a deleter Ella-Cre mouse line. Breeding the Epor$^{fl/fl}$ mice with Ella-Cre mice for two generations led to a global knockout of EPOR in all cells. To recombine the *Epor* gene specifically in projection neurons, exons 3-6 were excised *in vivo* upon appropriate interbreedings of *Epor*$^{tm1c(KOMP)Wtsi}$ mice with mice expressing Cre recombinase under control of the *Nex/Neurod6* promoter *(Goebbels et al., 2006)*, generating mice carrying the *Epor*$^{tm1d(KOMP)Wtsi}$ allele (*NexCre::Epor*$^{fl/fl}$ mice).

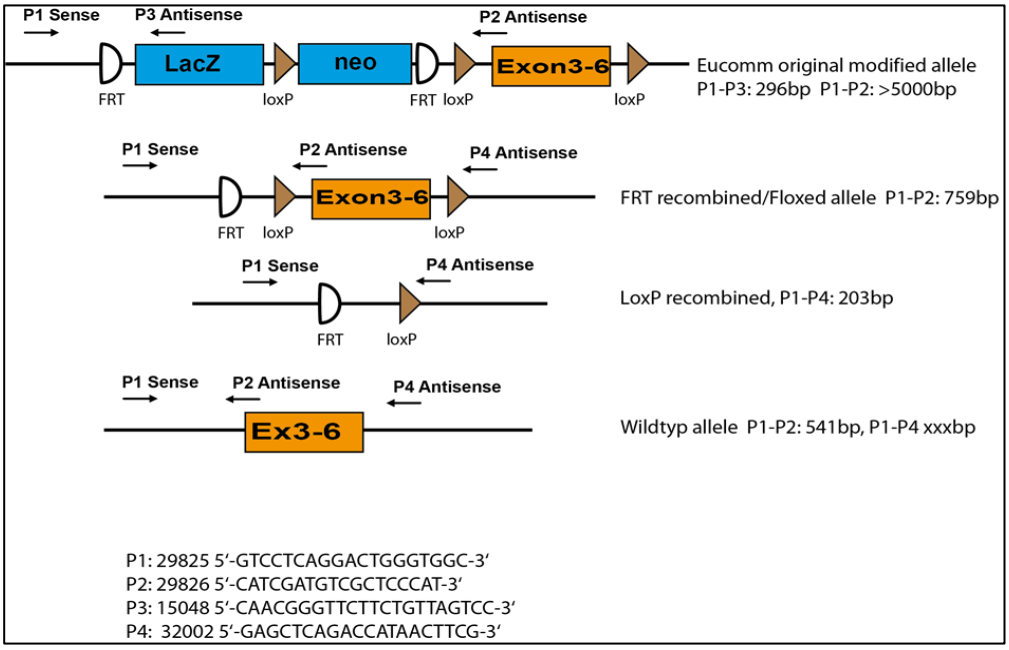

Figure 21. *Generation of EPOR*$^{fl/fl}$ *mice.*

All mice were housed in a temperature-controlled environment (21±2°C) on a 12h light–dark cycle with food and water available *ad libitum*. Male mice of the same age were used for the experiments, unless stated otherwise.

Summary of the mouse lines used in the project is listed below.

Mice	Allele Type	Brief description	Reference
R26R-TdTomato	Transgenic	Tamoxifen under the control of the ubiquitous Rosa 26 promoter	Madisen et al., 2010
NestinCreERT2	Targeted Knock-in	Tamoxifen-inducible form of Cre recombinase under the control of Nestin promoter	Lagace et al., 2007
GliCreERT2	Transgenic	Tamoxifen-inducible form of Cre recombinase under the control of Gli promoter	Ahn et al., 2005
Sox2CreERT2	Transgenic	Tamoxifen-inducible form of Cre recombinase under the control of Sox2 promoter	Arnold et al., 2011
NexCreERT2	Transgenic	Tamoxifen-inducible form of Cre recombinase under the control of Nex promoter	Agarwal et al., 2011
Thy1-EGFP	Transgenic	EGFP expression specifically in dendrites of pyramidal neurons	Feng et al, 2000
CAGCreERT2-ODD	Transgenic	Tamoxifen-inducible form of Cre recombinase under the control of CAG-ODD promoter	Kimura et al., 2015
EIIaCre	Transgenic	The adenovirus EIIa promoter directs expression of Cre recombinase in preimplantation mouse embryos.	Holzenberger et al, 2000
$EPOR^{fl/fl}$	Targeted knockout-out	Targeted disruption of the coding region of EPO	
$EPOR^{fl/fl}$	Targeted knockout-out	Targeted disruption of the coding region of EPO receptor (EPOR)	
$NexCreEPOR^{fl/fl}$	Targeted conditional knockout-out	Targeted disruption of the coding region of EPO receptor (EPOR) specifically in pyramidal neurons	
C57Bl/6N		Wild type mice	

Table 4. Various transgenic mouse models used in this thesis.

3.1.2. Breeding strategy.

Multiple transgenic (CreERT2) mice were used, in which CreERT2 recombinase (Box. 8) is functionally active in the presence of its ligand, i.e. tamoxifen.

Box. 8. Cre-ERT2

Cre-ERT2 is a ligand dependent chimeric Cre recombinase where a mutated form of human estrogen receptor (ER) ligand binding domain (LBD) is fused to Cre-recombinase (Feil et al., 1997; Indra et al., 1999). In the chosen mutant Cre-ERT2, the mutation is such that Cre-ERT2 can be activated by the synthetic ligands Oestrogen 4-hydroxytamoxifen (OHT), ICI or tamoxifen (TM), but remains insensitive to E2 (17ß-oestradiol), which is endogenous present in mice. Like Cre-recombinase, Cre-ERT2 is a site-specific recombinase that recognizes and binds to specific sites called LoxP (Nagy, 2000). Two loxP sites recombine in the presence of Cre, allowing the DNA cloned between two such sites to be removed by Cre-mediated recombination after TM treatment. The mechanism by which this process occurs is schematically represented below.

This CreERT2 recombinase is placed under the control of a regulatory element of a cell type specific gene. These mice were bred with a reporter mouse, which contains an inactive TdTomato reporter gene that upon tamoxifen administration is activated in cells that express Cre-recombinase. This breeding led to double-transgenic offspring.

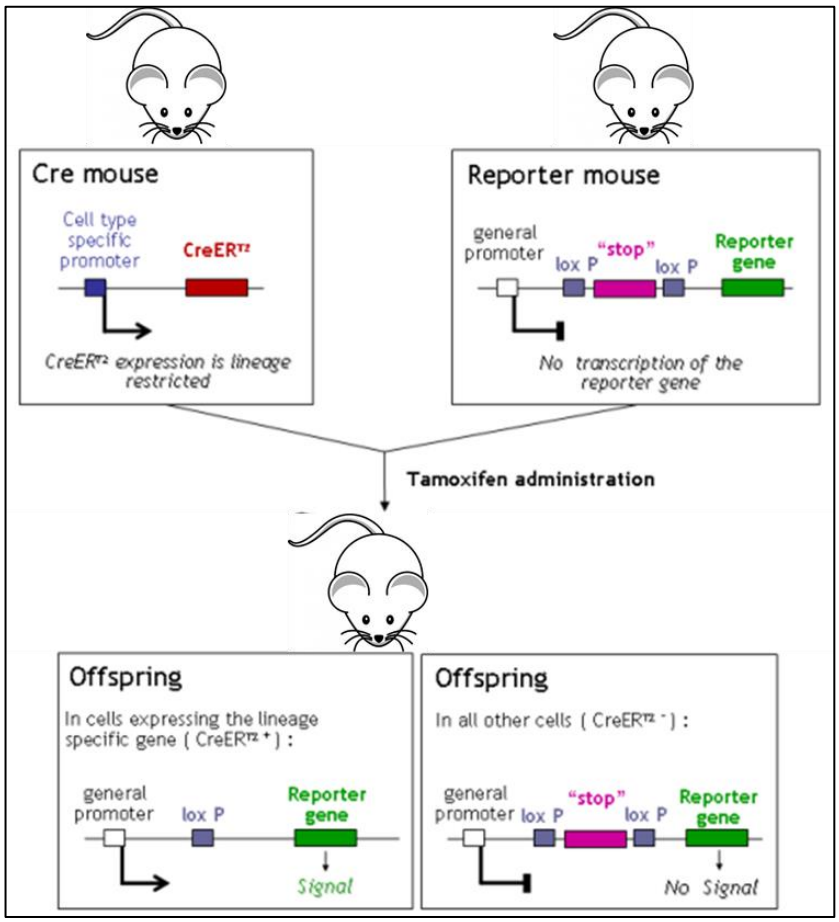

Figure 22. *Breeding strategy for the generation of inducible double transgenic mice.*

3.1.3. Genotyping.

The genotypes of newborn pups were determined using specific primers. The DNA was extracted from the tail tips or ear biopsies as per the manufacturer's protocol. Briefly, the biopsies or tail tips were cut into 25mg pieces and pre-lysis was performed at 56°C for 1-3 hours in the presence of 180µl T1 buffer supplemented with 25µl Proteinase K solution, with constant shaking. 200µl of B3 buffer was added to the samples and kept at 70°C for 10min. To enable DNA binding, 210µl of 96-100% ethanol was added to the samples and vortexed vigorously. Next, the sample was loaded in a Nucleospin® Tissue Column placed in the collection tube and centrifuged for 1min at 11000xg. Subsequent

washes with 500µl of BW buffer and 600µl of B5 buffer were performed followed by centrifugation at 11000xg after each wash. Residual ethanol is removed by centrifugation for 1min at 11000xg. The DNA was eluted by adding 100µl of pre-warmed (70°C) BE buffer to the column which was maintained at room temperature for 1min followed by centrifugation at 11000xg for 1min.

Mice / Contents	TdTomato mice	NexCre ERT2 mice	NestinCre ERT2 mice	SoxCre ERT2 mice	GliCre ERT2 mice	EIIaCre mice	$EPOR^{fl/fl}$ mice	$EPO^{fl/fl}$ mice
DNA (sample)	1 µl	0.5 µl	1 µl	1 µl	1 µl	1 µl	1 µl	0.5 µl
PCR buffer	2 µl (10X)	4 µl	4 µl	4 µl	4 µl	2 µl	4.2 µl	4.2 µl
DNTPs (2mM)	2 µl	2.1 µl	0.2 µl	2.1 µl	0.2 µl	2 µl	2.1 µl	2.1 µl
Primers (10pmol/µl)	1 µl	1 µl	1 µl	1.5 µl	1 µl	1 µl	1.5 µl	1.5 µl
Taq Polymerase	1 µl	0.15 µl	0.2 µl	0.2 µl	0.2 µl	2 µl	0.07 µl	0.07 µl
Dnase free water	11 µl	9.65 µl	8 µl	9.95 µl	9 µl	12 µl	11.13 µl	12.13 µl
$MgCl_2$ (25mM)	-	1.25 µl	1.6 µl	1.25 µl	1.6 µl	-	-	-

Table 5. Composition of contents for genotyping.

Mice / Allelle	TdTomato mice	NexCre ERT2 mice	NestinCre ERT2 mice	SoxCre ERT2 mice	GliCre ERT2 mice	EllaCre mice	$EPOR^{fl/fl}$ mice	$EPO^{fl/fl}$ mice
Transgene (bp)	250	100	100	100	100	400	203	290
Wildtype (bp)	330	-	-	-	136	-	541	429
Flox (bp)	-	-	-	-	-	-	759	613

Table 6. Sizes of expected bands after genotyping.

Steps \ Mice	TdTomato mice	NexCre ERT2 mice	NestinCre ERT2 mice	SoxCre ERT2 mice	GliCre ERT2 mice	EllaCre mice	EPOR$^{fl/fl}$ mice	EPO$^{fl/fl}$ mice
94 °C	5 min	-	-	3:30 min	3 min	-	-	-
95 °C	-	3:30 min	2:30 min	-	0:30 min	2 min	3 min	3 min
51.7 °C	-	-	-	1 min	-	-	-	-
54.5 °C	-	-	0:30 min	-	-	-	-	-
55 °C	-	-	-	-	-	0:45 min	-	-
56 °C	-	-	-	-	-	-	-	0:30 min
56.4 °C	-	-	-	-	1 min	-	-	-
58 °C	0:30 min	0:30 min	-	-	-	-	-	-
62 °C	-	-	-	-	-	-	0:30 min	-
72 °C	1:20 min	1 min	1 min	1 min	0:30 min	1 min	1 min	1 min
Cycles	30	39	30	35	35	40	35	37
72 °C	2 min	2 min	5 min	2 min	5 min	10 min	5 min	10 min
4 °C	forever	forever	forever	forever	forever	forever	forever	forever

Table 7. PCR procedure.

Mice	Forward Primer	Reverse Primer
TdTomato mice	CTCTGCTGCCTCCTGGCTTCT – Rosa 10	TCAATGGGCGGGGGTCGTT – Rosa 4 CGAGGCGGATCACAAGCAATA – Rosa 11
NexcreERT2 mice	GAGTCCTGGAATCAGTCTTTTTC – Nex	AGAATGTGGAGTAGGGTGAC – Nex CCGCATAACCAGTGAAACAG – Cre
NestincreERT2 mice	GCGGTCTGGCAGTAAAAACTATC – Cre	GTGAAACAGCATTGCTGTCACTT – Cre
SoxcreERT2 mice	GCGGTCTGGCAGTAAAAACTATC – Cre	GTGAAACAGCATTGCTGTCACTT – Cre
GlicreERT2 mice	GCGGTCTGGCAGTAAAAACTATC – Cre GGGATCTGTGCCTGAAACTG – Wildtype	GTGAAACAGCATTGCTGTCACTT – Cre CTTGTGGTGGAGTCATTGGA – Wildtype
EPOR$^{fl/fl}$ mice	GTCCTCAGGACTGGGTGGC	CATCGATGTCGCTCCCAT GAGCTCAGACCATAACTTCG
EPO$^{fl/fl}$ mice	CAGCCTCCACGTGCACTAAG	GCAGGGTGGGACGTTCTG

Table 8. Forward and reverse primers for genotyping of all mouse lines.

3.2. *In-vitro* cell cultures.

3.2.1. Hippocampal neuronal culture.

Pregnant mice were sacrificed by cervical dislocation and hippocampal neurons were isolated from embryos at E17 (Embryonic day 17). Firstly, the embryos were decapitated and placed into a dish with Hanks balanced salt solution (HBBS) (Invitrogen, 14060-40) containing 1% Penicillin/Streptomycin (PAA, P11-010) and 0.7% 1M HEPES buffer (Invitrogen, 15630-056). The hippocampi were isolated and dissociated with pre-warmed trypsin (Invitrogen, 25300-054) solution for 5min at 37°C. Following washes with warm HBBS, the hippocampi were mechanically titurated and added to the MEM medium (Invitrogen, 21430-020) supplemented with 0.2% Sodium Bicarbonate (Invitrogen, 25080-060), 0.6% Glucose (Sigma, G-6152, anhydrous), 1mM Sodium Pyruvate (Invitrogen, 11360-039), 1% Pen/Strep (PAA, P11-010), 1% L-Glutamine (PAA, M11-004) and 2% B27 (Invitrogen, 17504-044). Single dissociated cells (25,000 cells/well) were then plated on glass coverslips pre-coated with 0.05mg/ml Poly D-Lysine (Sigma, 7280) and incubated with complete MEM medium for 5 days at 37°C with 5% CO_2.

3.2.2. Microglia culture.

Microglia were isolated from the brains of P1 (post-natal day 1) mice. The meninges and cerebellum were excluded and the brain was digested using 0.05% trypsin/EDTA for 10min at 37°C. Following the trypsinization procedure, the cells were washed with pre-warmed HBBS and mechanically triturated with DMEM (Invitrogen, 41965-039) microglia medium containing 10% horse serum (Invitrogen, 26050-070) and 0.5% Pen/Strep and supplemented with 400 IU/brain of DNaseI (Invitrogen, 18068015). The dissociated cells were then centrifuged for 10min at 150g at room temperature. The cells were plated in 75cm^2 flask pre-coated with 50µg/ml Poly D-Lysine. The cells were maintained in complete DMEM microglia medium at 37°C, 5% CO_2. The medium was replaced every 2-3 days. On day 5 and day 7, microglia cultures were treated with L929 mouse fibroblast culture conditioned DMEM medium (1:3; 10% Fetal Calf Serum and 1% Pen/Strep). The microglia were then detached by manual shaking of the flasks and

centrifuged for 10min at 800rpm. The cells were then seeded in DMEM medium supplemented with 1mM Sodium Pyruvate and 0.5% Pen/Strep until further analyzed.

3.2.3. Oligodendrocyte culture.

Oligodendrocytes were isolated from the brains of P1 newborn mice. The meninges and cerebellum were excluded and the brain was digested using 0.05% trypsin/EDTA for 10min at 37°C. Following trypsinization, the cells were washed with pre-warmed HBBS and mechanically triturated to obtain single cells. The cells were then plated in 75cm^2 flasks pre-coated with 50µg/ml Poly D-Lysine containing BME medium (Invitrogen, 41010-026) supplemented with 10% horse serum, 0.5% Pen/Strep and 1% Glutamax (Invitrogen, 35050-038). The cells were then maintained at 37°C, 5% CO_2 and half of the medium was replaced every 3-4 days. On DIV 8, the oligodendrocytes were detached by manual shaking of the flasks and centrifuged for 10min at 900rpm. The cell number was quantified and 30,000 cells/well were plated on coverslips pre-coated with 50µg/ml Poly D-Lysine. The cells were maintained in Super-SATO medium containing DMEM medium, 2% B27, 1% Glutamax, 0.5% Pen/Strep, 1% horse serum, 1% Pyruvate (Invitrogen, 11360-039) solution, 0.01% Triiodthyronin (Calbiochem, 64245) solution and 0.013% L-Thryonin (Sigma, T1775) solution until further analyzed.

3.2.4. Astrocyte culture.

Astrocytes were isolated from the brains of P1 newborn mice. The meninges and cerebellum were excluded and the brain was digested using 0.05% trypsin/EDTA for 10min at 37°C. Following trypsinization, the cells were washed with pre-warmed HBBS and mechanically triturated to obtain single cells. The cells were then plated in 75cm^2 flasks pre-coated with 50µg/ml Poly D-Lysine containing Astrocytes DMEM medium (Invitrogen, BE12707F) supplemented with 20% Fetal Calf Serum (FCS; heat inactivated) and 0.5% Pen/Strep. The cells were then maintained at 37°C, 5% CO_2 and half of the medium was replaced every 2 days. On DIV 14, the astrocytes were detached by manual shaking of the flasks and centrifuged for 5min at 800rpm. The cell number was quantified and 150,000 cells/well were plated in flasks pre-coated with 50µg/ml

Poly D-Lysine. The cells were maintained in Astrocytes DMEM medium supplemented with 10% FCS and 0.5% Pen/Strep until further analyzed.

3.3. Quantitative Real-Time PCR (qRT-PCR).

3.3.1. RNA extraction.

After 6h of treatment with either placebo or EPO, P28 old mice were anesthetised with 0.5ml Avertin (1g tribromomethanol and 1ml of tetramylalcohol in 71.49ml millQ water). The hippocampi were dissected and stored at -80°C before RNA extraction. As a comparative study, RNA was also extracted from cultured cells (microglia, astrocytes, oligodendrocytes and E17 hippocampal neurons). The RNA extraction was performed via miRNeasy mini kit (Qiagen) following the manufacturer's instructions. Briefly, the tissue or cells were homogenised or lyzed in Qiazol via mechanical disruption (tissue) or passing through syringes (cells), followed by the addition of chloroform for 2-3min. The samples were then centrifuged at 12000xg for 15min at 4°C to separate the RNA from DNA and protein content. The RNA concentration was measured with a photometer to detect the sample absorbance at OD260nm and the purity of RNA was evaluated via the ratio of OD260/OD280.

3.3.2. cDNA synthesis and qRT-PCR.

RNA was reverse transcribed using a RNA concentration of 20ng/µl for cells and 100ng/µl for tissue, mixed with 0.6 pmol oligo dT-mix (AGCTlab, MPIem) and 50 pmol of hexamers (Invitrogen, N8080127). Annealing was performed at 70°C for 2min. The CDNA was then synthesized using SuperScript® III kit (Invitrogen, 18080051) according to manufacturer's guidelines. The resulting cDNA was diluted to 1:5 (cells) and 1:10 (tissue). 4µl of the diluted cDNA was used as template followed by the addition of 6µl of master mix containing specific primers (1pmol/µl) and 10µl of SYBR Green (Qiagen, 204143) mix. Triplicates for each sample along with housekeeping genes such as GAPDH or β-actin were used. This reaction was run in Roche Lightcycler 480 and results were analyzed using LightCycler® 480 Software. The PCR cycle used and the sequence of primers are listed below.

Steps	Procedure	Time/Cycles
1	Initiation at 50 °C	2 min
2	Denaturation at 90 °C	10 min
3	Cycle to step 2	45 cycles
4	Denaturation at 95 °C	15 sec
5	Annealing at 60 °C	60 sec

Table 9. qRT-PCR procedure.

Gene	Forward primer	Reverse primer
mEPOR	CCTCATCTCGTTGTTGCTGA	CAGGCCAGATCTTCTGCTG
mEphB4	AGTGGCTTCGAGCCATCAAGA	CTCCTGGCTTAGCTTGGGACTTC
mGAPDH	CAATGAATACGGCTACAGCAAC	TTACTCCTTGGAGGCCATGT
mβ-actin	CTTCCTCCCTGGAGAAGAGC	ATGCCACAGGATTCCATACC

Table 10. Forward and Reverse primers used for RT-PCR.

3.4. Mouse treatments.

3.4.1. Tamoxifen.

Tamoxifen solution (10mg/ml) was freshly prepared by dissolving tamoxifen freebase (Sigma) in corn oil (Sigma) at room temperature for 45min. Postnatal CreERT2 activity in NexCreERT2, GliCreERT2, NestinCreERT2 and SoxCreERT2 mice was induced by a total of 5 intraperitoneal injections (i.p.) of 100mg/kg tamoxifen over the course of 3days in juvenile mice. For CreERT2 induction in adult NexCreERT2 mice, a total of 10 i.p. injections of 100mg/kg tamoxifen were administered over the course of 10 consecutive days. For the desired induction of CreERT2 in CAGCreERT2-ODD mice, a single i.p. injection of 100mg/kg tamoxifen was sufficient.

3.4.2. EPO.

Male mice were i.p. injected with 5000IU/kg rhEPO (NeoRecormon, Roche) or placebo (solvent solution, 0.01ml/g). At 48h after the last tamoxifen injection, EPO/placebo treatment was initiated in P28 or 3months-old NexCreERT2, Thy1-YFPH mice and in P28 old WT and NexCreEPOR$^{fl/fl}$ mice, which was carried out every other day for 3 weeks.

For Drop-Seq analysis, EPO was administered once followed by tissue collection 6h later. Additionally, for labeling of proliferating cells, NexCreERT2 mice obtained 5-Ethynyl-2'-deoxyuridine (EdU; 0.2mg/ml; ThermoFisher) via drinking water (exchanged on all alternate days).

3.4.3. Hypoxia.

The hypoxia chamber was designed in cooperation with Coy Laboratory Products Inc. (Grass Lake, MI, USA) with the dimensions 164cm x 121cm x 112cm. The system includes an air filtration system consisting of carbolime and activated charcoal. The oxygen and carbon dioxide levels were constantly detected and controlled via online monitoring. A gradual reduction of 3% oxygen per day resulted in 12% oxygen level in 3 days and was maintained until the end of the experiment. During the course of the experiment, mice were treated with EdU via drinking water as described above.

Figure 23. *Hypoxia chamber used for experiments in this thesis.*

3.4.4. Complex running wheels (CRW).

Post weaning, mice were single-housed and tamoxifen treatment was initiated for NexCreERT2::TdTomato mice (described above). NexCreERT2::TdTomato, NexCreEPOR$^{fl/fl}$ mice were divided into 4 groups and monitored for 17 days. Groups included (1) normoxic room conditions (at 21% O_2) in standard cages, (2) normoxic conditions with voluntary running on CRW, (3) hypoxic conditions (hypoxia chamber to 12% O_2) in standard cages, (4) hypoxic conditions with voluntary running on CRW.

CRW (TSE Systems, Bad Homburg, Germany) is characterized by randomized missing bars as previously described (Hibbits et al., 2009; Liebetanz et al., 2007; McKenzie et al., 2014). The testing period of 17 days was followed by 1 week of normal conditions for all groups (no running, normoxia). The mice that were previously running (in normoxic or hypoxic conditions) were finally exposed again to CRW for 4h (as cFos inducing challenge) before being sacrificed. For *in-situ* hybridization experiments, male WT mice (P55) were exposed to 5h, 9h, or 13h of CRW. For the experiment involving CAGCreERT2-ODD::TdTomato mice, animals were exposed to overnight complex wheel running. Running was voluntary at all times with *ad libidum* access to food and water. Control mice (no running) were housed in standard cages. Mice were sacrificed, perfused and brains collected as described below. Running was tracked automatically via Phenomaster software (TSE Systems, Germany) for the whole day. Since mice are mainly night-active (dark-phase), the total distance run between 6pm and 6am was summarized for every individual animal. The total distance run on each night was normalized to the average distance of each animal run in the first 3 nights (data expressed as % performance in relation to the first 3 nights). For the experiments involving EPO treatment, mice were treated with EPO (5000IU/kg, 11 i.p. injections on alternate days for 3 weeks), followed by 1 week break. They were then exposed to 12h of CRW overnight. Data for this experiment are expressed as distance run summarized for every 30min.

3.5. Immunohistochemistry (IHC).

Mice were anesthetized and perfused transcardially with 4% cold formaldehyde. Dissected brains were post-fixed in 4% formaldehyde at 4°C and equilibrated in 30% sucrose dissolved in phosphate-buffered saline (PBS) at 4°C overnight. Brains were then embedded in cryoprotectant (O.C.T.^{TM} Tissue-Tek, Sakura) and stored at -80°C. Whole mouse brains were cut into 30µm thick coronal sections (coordinates from bregma: −1.34 to −2.54mm posterior) using a cryostat (Leica) and stored in a cryoprotective solution (25% ethylene glycol and 25% glycerol in PBS) at -20°C until further use. For analysis of dendritic spines and MAP2 dendrites, the right hemisphere, destined to the neuronal structural analysis, was cut in 100µm coronal sections with a vibratome (Leica

VT 1000E, Leica), collected in 3 subseries and stored at 4ºC in PB 0.1M with sodium azide (0.05%).

For IHC, sections were permeabilized in PBS containing 0.3% Triton X-100 and blocked in 5% horse serum for 1h at room temperature. Brain sections were incubated with primary antibodies in blocking solution overnight at 4°C, followed by 2h incubation of appropriate fluorophore-conjugated secondary antibodies in blocking solution containing 3% horse serum (or 5% normal donkey serum) and counterstained with 4',6-diamidino-2-phenylindole (DAPI). The sections were then mounted on SuperFrostPlus Slides (ThermoFisher) with Aqua-Poly/mount (Polysciences, Inc). Primary antibodies used were: anti-Ctip2 (1:500; Guinea pig polyclonal; SYSY 325005), anti-Map2 (1:1000; mouse monoclonal; Sigma M9942), anti-TBR1 (1:200; rabbit monoclonal; Abcam ab183032), anti-Tle4 (1:200; rabbit polyclonal; Abcam ab64833) and anti-cFos (1:1000; rabbit polyclonal; SYSY 226003). Secondary antibodies used were: Alexa488 anti-Guinea pig (1:500; Jackson Immuno Research 706-548-148) and Alexa635 anti-mouse (1:400; ThermoFisher A31575). Depending on the need for a triple or a quadruple staining, Alexa405 anti-rabbit (1:1000; Abcam 175652) or Alexa647 anti-rabbit (1:500; ThermoFisher A31573) were used. Following IHC, sections were stained for EdU using Click-iT™ EdU Alexa Fluor™ 647 Imaging kit (ThermoFisher E10415), according to the manufacturer's instructions.

Antibody	Host Species	Dilution	IHC protocol requirement	Company
Ctip2	Guinea Pig	1:500	Fixed 3 nights	SYSY – 325005
Map2	Mouse	1:1000	Standard (i.e. o/n fixed tissue, o/n antibody incubation)	Sigma – M9942
cFOS	Rabbit	1:1000	Standard	SYSY – 226003
NeuN	Mouse	1:1000	Fixed 3 nights	Millipore – MAB377
GFAP	Guinea Pig	1:500	Standard	SYSY – 173004
S100β	Guinea Pig	1:1000	Standard	SYSY – 287004
PDGFRα	Rabbit	1:500	Antigen retrieval (3x -5min 10mM Citrate buffer; pH-6) followed by standard protocol	Cell signaling – 3174
Sox2	Mouse	1:250	Antigen retrieval (3x -5min 10mM Citrate buffer; pH-6) followed by standard protocol	Calbiochem – SC1002
IBA	Chicken	1:1000	Standard	SYSY – 234006
Tbr1	Rabbit	1:200	Standard	Abcam – ab183032
Tle4	Rabbit	1:200	Standard	Abcam – ab64833

Table 11. List of primary antibodies used in this thesis.

3.6. Imaging and analysis.

3.6.1. Pyramidal neurons.

Imaging was performed using the Andor Eclipse TiE microscope system (Nikon, Tokyo, Japan) with a 40x objective (Plan Apoλ40x, NA = 0.95) to image the hippocampal layers. Ctip2$^+$ cells among total neuron numbers were manually counted. Ctip2$^+$ and TdTomato$^-$ cells were characterized as newly generated neurons. Quantifications are expressed as number of newly generated neurons divided by the total area of CA1 *stratum pyramidale* (mm^2). For Ctip2 stainings, a total of 16 hippocampi with 8 sections per animal were used. Quadruple (TdTomato, Ctip2, cFos and EdU) stainings were acquired with a TCS SP5-II System (Leica) equipped with a 20x objective (NA=0.70). For total Ctip2 positive cell counts, 6 hippocampi from 3 sections per animal were used. Quantifications for CRW mice were expressed as percentage of Ctip2 positive cells normalized to their respective non-running controls. Whole hippocampi were imaged and analyzed by Fiji software. Neurons showing positive immunoreactivity for cFos were identified and quantified manually. These neurons were further sub-categorized into pre-existing (cFos$^+$, TdTomato$^+$, Ctip2$^+$) or newly generated (cFos$^+$, TdTomato$^-$, Ctip2$^+$) neurons. Again, quantifications are indicated as cFos$^+$ cells divided by the total area of the CA1 *stratum pyramidale* (mm^2). For cFos stainings, a total of 8 hippocampi with 4 sections per animal were used. For quantification of hypoxic neurons, whole hippocampus sections of CAGCreERT2-ODD::TdTomato mice were imaged. The TdTomato$^+$ cells were characterized as neurons undergoing hypoxia and manually quantified. Quantifications are expressed as number of hypoxic neurons divided by the total area of CA1 *stratum pyramidale* (mm^2). A total of 10 hippocampi with 5 sections per animal were used. The cFos$^+$ cells were also analyzed as described above. For Map2$^+$ dendritic density analysis, the *stratum radiatum* of the CA1 region was imaged using a laser scanning confocal microscope (Leica TCS SPE). Per animal, 3 dorsal hippocampal slices were selected starting at bregma -1.58mm. Confocal *z*-stacks (0.38µm intervals) of whole sections were taken using a 63x objective (NA=1.40). Per hippocampus, 3 images were captured, and 4 fields of the dimension 36.67µmx36.67µm were analyzed in each image (total 36 fields per animal). Images were processed using Fiji software and Map2$^+$ principal apical dendrites were manually

quantified. The quantifications are expressed as number of $Map2^+$ dendrites divided by the area of each image (1344.7μm^2).

3.6.2. Dendritic spines.

Images were captured using a 63x oil immersion objective (NA=1.40) and a 3.5x additional digital zoom to investigate the first 200µm of the principal apical dendrite in segments of 50µm. Confocal z-stacks (0.38µm intervals) of whole sections were performed. Dendrites included in the study were at least 200µm in length. Per animal, 6 such dendrites of 6 different Thy1-YFPH expressing pyramidal neurons were randomly selected from the CA1 region. The stitching plugin in Fiji software (2.0.0) was used to reconstruct 3D images of the apical dendrites. The spines were further sub-categorized as proximal (0–50µm), medial (50–100µm), medial-distal (100–150µm) and distal (150-200µm) segments of the dendrite, depending on their distance from the soma. The total density of spines was also analyzed. Based on their morphology (Guirado et al., 2013; Kasai et al., 2010), the spines were manually divided into (1) stubby, i.e. length of the protrusion was <1µm and no neck is observed; (2) mushroom, when a clear head-like structure could be observed (maximum diameter of the head was at least 1.5 times the average length of the neck) and the total length of the protrusion was <1.5µm; and (3) thin, i.e. the length of the protrusion was >1.5µm or the length was between 1 and 1.5µm and a clear head-like structure could not be distinguished.

3.6.3. RNAscope in-situ hybridization (ISH).

RNAscope® 2.5 HD Brown Reagent Kit (322300), Advanced Cell Diagnostics (ACD), Hayward, CA, USA was used for the detection of EPO and EPOR mRNA. ISH was performed according to the manufacturer's instructions. Briefly, coronal cryosections of 15µm thickness were mounted on SuperFrostPlus Slides, dried and stored at -80°C. Sections were then pretreated by dropwise addition of hydrogen peroxide and incubated for 10min at room temperature. Slides were immersed in boiling target retrieval buffer for 15min, followed by incubation with protease plus for 30min at 40°C. Sections were then hybridized with the corresponding target probe Mm-Epo-01 (444941) or Mm-Epor (412351) for 2h at 40°C, followed by a series of amplification and

washing steps. Chromogenic signal detection was performed with 3,3'-diaminobenzidine (DAB) incubation for 20min at room temperature. Sections were counterstained with 50% Mayer's hemalum (Merck) and mounted with EcoMount (BioCare Medical). Brown punctate dots in the CA1 were counted in a total of 12 hippocampi with 6 sections per animal using a light microscope (Olympus BX-50, Tokyo, Japan) equipped with a 100x oil immersion objective (NA=1.35) and normalized to the area of the respective region (mm^2). Sagittal 15µm sections from kidney (P55) and heart (E11.5) of WT mice were used as positive controls for EPO and EPOR, respectively. According to manufacturer's instructions, each dot represents a single molecule of mRNA in these sections. The quantification is normalized and presented as percentage of the mean dot number of groups and time points [% value = (number/mm^2)/(mean dot number/mm^2) *100].

3.7. Drop sequencing.

3.7.1. Tissue dissociation.

Juvenile male WT mice (P28; 3 mice/group) were injected i.p with EPO and sacrificed after 6h. The hippocampi were dissected and sliced into 600µm sections using McIlwain Tissue chopper (Cavey Laboratory Engineering Co. Ltd). The CA1 region was digested with a working solution of Papain/DNaseI in Earle's Balanced Salt Solution, according to manufacturer's instructions (Worthington Biochemical Corp). The samples were then incubated at 37°C for 40min with constant agitation before gentle manual trituration. The samples were centrifuged for 10min at 200g at 4°C. After discarding the Papain/DNaseI supernatant, cells were resuspended in 1mL of sterile DMEM/F12 (Sigma) without phenol-red containing 3% fetal bovine serum (FBS; Life Technologies) and the suspension was passed through a 40µm strainer cap (Corning) to yield a uniform single-cell suspension.

3.7.2. Single-cell barcoding and library preparation.

Barcoded single cells, or STAMPs (single-cell transcriptomes attached to microparticles), and cDNA libraries were generated following the protocol (Macosko et al., 2015). Briefly, single cell suspensions (100cells/µl), droplet generation oil (Bio-Rad) and barcoded microparticles (ChemGenes; 120beads/µl) were co-flowed through a

FlowJEM aquapel-treated DropSeq microfluidic device (FlowJEM) and droplets were generated for 15min. Captured RNA on the bead surface was recovered by washing the beads in saline-sodium citrate buffer (SSC) and perflurooctanol (PFO) solutions and then reverse transcribed using Maxima H minus reverse transcriptase kit (ThermoFisher). Excess primer on the surface of the bead uncaptured by an RNA molecule was digested using Exonucleases I kit (ThermoFisher). A cDNA amplification PCR was performed using 10µM SMART PCR primer and 2X Kapa HiFi HotStart ReadyMix (Kapa Biosystems) with 5000 beads per tube and amplified for 9 PCR cycles. The resulting samples were purified using AMPureXP beads (Beckman Coulter) and the quality and concentration of the cDNA was assessed using High sensitivity DNA bioanalyzer (Agilent Technologies). Library sizes were adjusted using the Nextera Amplicon Tagmentase enzyme and DNA was amplified for 14 cycles using 10µM New-P5-SMART PCR hybrid oligo, 10µM Nextera Index and the Nextera PCR mix (Nextera XT DNA Library Preparation kit; Illumina). Tagmented libraries were again purified (AMPureXP), quality controlled (high sensitivity DNA Bioanalyzer), quantified (Qubit dsDNA HS assay kit; Life Technologies) and sequenced (Illumina Hi-seq 2500). All assays mentioned above have been performed according to manufacturer's protocol.

3.7.3. Single cell RNA-seq processing.

Unique molecular identifier (UMI) gene counts for each group (placebo or EPO) was imported into R (v3.4.1). Seurat (v2.3.0) function within the R environment was used for filtering, normalization, canonical correlation analyses, unsupervised clustering, visualization and differential expression analyses.

3.7.4. Filtering and data normalization.

Cells with minimum and maximum of 1,000 and 8,000 genes expressed (≥ 1 count), respectively, and the genes that were expressed in at least 3 cells were retained. Cells with more than 40% of counts on mitochondrial genes were excluded. After filtering, there were 14,061 genes in 390 cells from placebo and 14,971 genes in 583 cells from EPO group. Gene UMI counts for each cell were normalized via natural-log normalization of gene UMI counts divided by total UMI counts per cell and scaled by

10000. After normalization, scaled expression (z-scores for each gene) for downstream analyses was calculated.

3.7.5. Canonical correlation analysis.

Integration of scRNA-seq data from two groups (placebo and EPO) was performed using canonical correlation analysis (CCA). Top 1000 highly variable genes from each group was used to calculate canonical correlation vectors (reduced dimension) and subsequently, first 20 vectors were aligned using dynamic time warping.

3.7.6. Clustering and visualization.

Clustering was performed using "*FindClusters*" function with default parameters with resolution set to 1 and first 20 CCA aligned dimensions were used in the construction of the shared-nearest neighbor (SNN) graph and to generate 2-dimensional embeddings for data visualization using t-SNE. Based on the visualization the glutamatergic cluster 0 and 1 were merged manually to represent a single cluster. The percentages of 'immature glutamatergic cells' for each mouse were placebo 1.6%, 2.3% and 4.3%, EPO 3.7%, 6.8% and 7.0%.

3.7.7. Cell trajectory (pseudotime) analysis.

Trajectory analysis of cells from the 'Immature Glutamatergic' and 'Mature Glutamatergic1' clusters (n=502) was performed in Monocle 223. The trajectory was constructed according to the documentation of Monocle 2. Prior to cell ordering, re-clustering was performed to confirm robust detection of the immature cluster across methods which revealed 3 clusters (1 cluster largely corresponding to Seurat's 'Immature Glutamatergic' cluster and 2 corresponding to Seurat's 'Mature Glutamatergic1' cluster; Supplementary Fig3a). Subsequently, dimension reduction using the 'DDRTree' method was performed. Differentially expressed genes ($q<0.01$) between the 3 clusters obtained by re-clustering in Monocle 2 were used as input for pseudotemporal ordering.

3.7.8. Differential expression and gene ontology (GO) analyses.

"*FindAllMarkers*" function was used with default parameters and tested genes with a detected threshold of minimum of 25% of cells in either of the 2 clusters. Genes with

an adjusted p value <0.01 were considered to be differentially expressed. GO analysis was conducted using WEB-based Gene SeT Analysis Toolkit (WebGestalt 2013). Entrez protein-coding genes were used as background. An adjusted p value <0.05 using the Benjamini–Hochberg method for controlling the false discovery rate was set as significant for GO terms in biological processes.

3.8. Quantification and statistical analysis.

All statistical analysis was performed using GraphPad Prism 5. For comparisons across multiple groups, a 2-way analysis of variance (ANOVA) was used. For comparisons across 2 groups, an unpaired Student's t test was performed. A p value<0.05 is considered statistically significant. Variance was similar between compared groups for their respective experiments. All values represent mean ± SEM (standard error of the mean). All analysis and quantification were performed in a double-blinded fashion.

Results

4. Results.

4.1. Effect of EPO on neural precursors.

4.1.1. EPO induced increase in pyramidal neurons is not mediated via Nestin positive precursors.

Nestin is an intermediate filament protein expressed by radial glial cells, neural stem cells (NSCs) and neural progenitor cells (NPCs). Most glutamatergic neurons arise from Nestin positive progenitors situated in the sub-ventricular zone (SVZ) lining the lateral ventricles and the sub-granular zone (SGZ) within the dentate gyrus (DG) of the hippocampus during embryogenesis . The Nestin positive progenitors located in these stem cell niches have the capacity to proliferate and differentiate into neurons. A significant increase in the number of pyramidal neurons in the CA1 region of P55 mice hippocampi, when EPO was intraperitoneally administered for three weeks was previously recorded *(Hassouna et al., 2016)*. Based on the literature, Nestin appeared to be a promising progenitor candidate that could give rise to these newly generated neurons under the influence of EPO. For this purpose, an inducible NestinCreERT2 mouse line was crossed with a TdTomato (R26R-TdTomato) reporter mouse line.

Following the similar treatment regimen as previously published by *Hassouna et al., 2016*, with minor modifications, creERT2 activity was induced in NestinCreERT2::TdTomato mice by injecting them with tamoxifen (100mg/kg; 1x injection daily from P23-P27; Fig. 24A). The tamoxifen treatment labelled Nestin positive cells with TdTomato reporter tag. The tamoxifen administration was followed by 11 injections of either placebo or EPO (5000IU/kg; on alternate days from P28-P48). The mice were sacrificed as mentioned in *Hassouna et al., 2016*; at P55. Upon sectioning and staining of P55 brains, no TdTomato positive cells (red) were observed in the CA1 region of the hippocampus of either placebo or EPO treated mice (Fig. 24B-C).

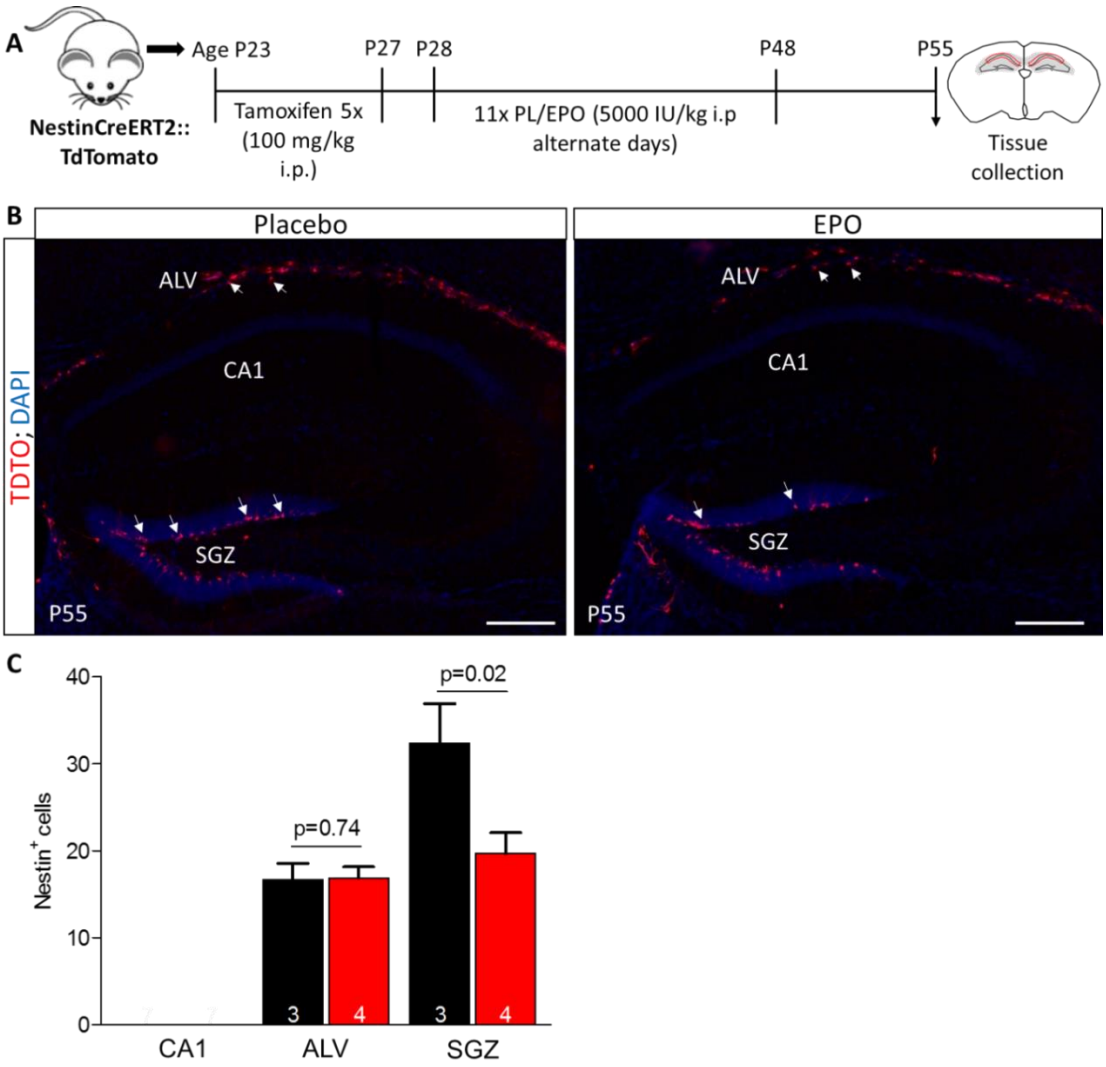

Figure 24. Multiple EPO treatment does not give rise to TdTomato positive neurons in NestinCreERT2::TdTomato mice, but decreases the Nestin cell numbers in the SVZ of the DG. *(A) Experimental schematic where 5 i.p. injections of tamoxifen were administered from P23-P27 in NestinCreERT2::TdTomato mice, followed by 11 i.p. injections of either placebo or EPO (on alternate days) from P28-P48. Mice were then sacrificed at P55. (B) Representative images of the hippocampus at P55 of placebo or EPO treated NestinCreERT2::TdTomato mice, showing positive signal for Nestin as labelled by TdTomato (red) in the alveus of hippocampus (ALV) and the Sub-Granular Zone (SVZ). Nuclei were counterstained using DAPI (blue). Scale bar: 100µm. (C) Quantification of TdTomato labelled Nestin positive cells at P55 in the CA1, ALV and SVZ of placebo (black) and EPO (red) treated NestinCreERT2::TdTomato mice. Data represents average number of cells ± SEM. Quantification performed from 3-4 independent mice and p-values presented via unpaired Student's t-test.*

Interestingly, after quantification of TdTomato positive cells, a significant decrease in the number of Nestin positive cells in the SGZ of the dentate gyrus of the EPO treated mice was observed as compared to the placebo treated group (Fig. 24C). Furthermore, no difference in the number of Nestin positive cells in the Alveus (ALV) of EPO or

placebo treated mice (Fig. 24C) was recorded. This data together, suggest that Nestin progenitors may give rise to neurons, which migrate to other regions of the brain, but not to the newly generated neurons found in the pyramidal layer of the CA1 upon EPO treatment. To completely rule out this possibility, another experiment was performed, where the hypothesis was that our approach might be too late for labelling the Nestin positive cells after 11 EPO or placebo injections, and therefore, decided to fate map the Nestin positive progenitors with only a single high dose of EPO. The mice were as before treated with 5x injections of tamoxifen (P23-P27), followed by 1x injection of placebo or EPO (P28), and the mice were sacrificed at P55 (Fig. 25A). However, after sectioning and staining, no TdTomato positive cells in the CA1 region of the hippocampi of EPO or placebo treated mice were observed (Fig. 25B).

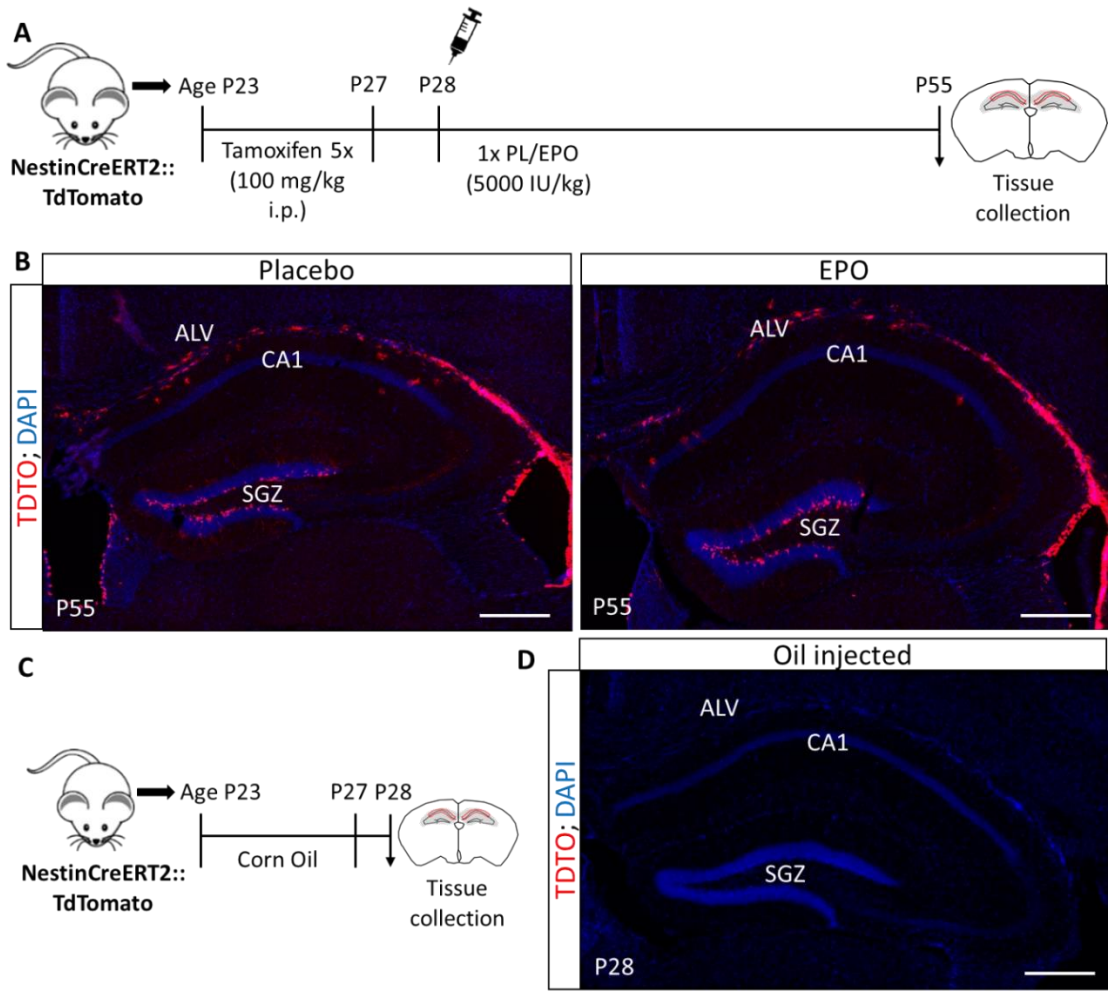

Figure 25. Fate mapping of NestinCreERT2::TdTomato mice upon single dose of EPO does not give rise to neurons in the CA1. *(A) Experimental schematic where 5 i.p. injections of tamoxifen were administered from P23-P27 in NestinCreERT2::TdTomato mice, followed by 1 i.p. injection of either placebo or EPO on P28. Mice were then sacrificed at P55. (B) Representative images of the hippocampus at P55 of placebo or EPO treated NestinCreERT2::TdTomato mice, showing positive signal for Nestin as labelled by TdTomato (red) in the Alveus (ALV) and the Sub-Granular Zone (SVZ). (C) Experimental schematic where 5 i.p. injections of corn oil were administered from P23-P27 and mice was sacrificed at P28. (D) Representative image of the hippocampus at P28 of oil-treated NestinCreERT2::TdTomato mice, showing no signal for TdTomato (red). Nuclei were counterstained using DAPI (blue). Scale bar: 100µm.*

These results suggest that the increase in the number of pyramidal neurons upon EPO administration might not be mediated by Nestin positive type II radial glial progenitors, at least the ones labelled by the transgenic Nestin mouse line used in this thesis. As a control experiment for ectopic expression and to determine the robustness and efficiency of the transgenic NestinCreERT2::TdTomato mouse line, these mice were injected with only a carrier solvent i.e. corn oil (1x injection daily from P23-P27), instead of tamoxifen (Fig. 25C), and observed no signal for any unspecific TdTomato expression when sacrificed and stained at P28 (Fig. 25D).

4.1.2. EPO regulates the differentiation of Gli positive precursors into astrocytes, but not neurons.

As mentioned in the introduction, Gli positive precursors located in the SGZ of the hippocampus are implicated in adult neurogenesis *(Ahn and Joyner, 2005)*. Sonic Hedgehog (SHH) signaling pathway plays a critical role during adult neurogenesis and acts a potent mitogen capable of giving rise to both neurons and oligodendrocytes *(Lai et al., 2003)*. These Gli positive SHH responsive NSCs have the ability to proliferate and differentiate into neurons *(Ahn et al., 2005)*. *In-vitro* experiments revealed the role of SHH signaling pathway in mediating the effects of EPO in regulating neuronal differentiation *(Wang et al., 2007)*. Considering the available literature, Gli was considered as a good candidate for *in-vivo* lineage tracing experiments using EPO as a stimulator. In order to accomplish these experiments, an inducible GliCreERT2 mouse line was obtained and crossed with a TdTomato (R26R-TdTomato) reporter mouse line.

Similar to previous experiments with NestinCreERT2::TdTomato mice, the protocol published by *Hassouna et al., 2016* was followed. The GliCreERT2::TdTomato mice were injected with tamoxifen (1x injection daily from P23-P27) to label Gli positive precursors with TdTomato reporter. This was followed by 11x i.p. injections of placebo or EPO (alternate days from P28-P48) and mice were sacrificed at P55 (Fig. 26A). Upon sectioning and staining, no Gli positive cells in the CA1 region of the hippocampus in either placebo or EPO treated mice were observed (Fig. 26B).

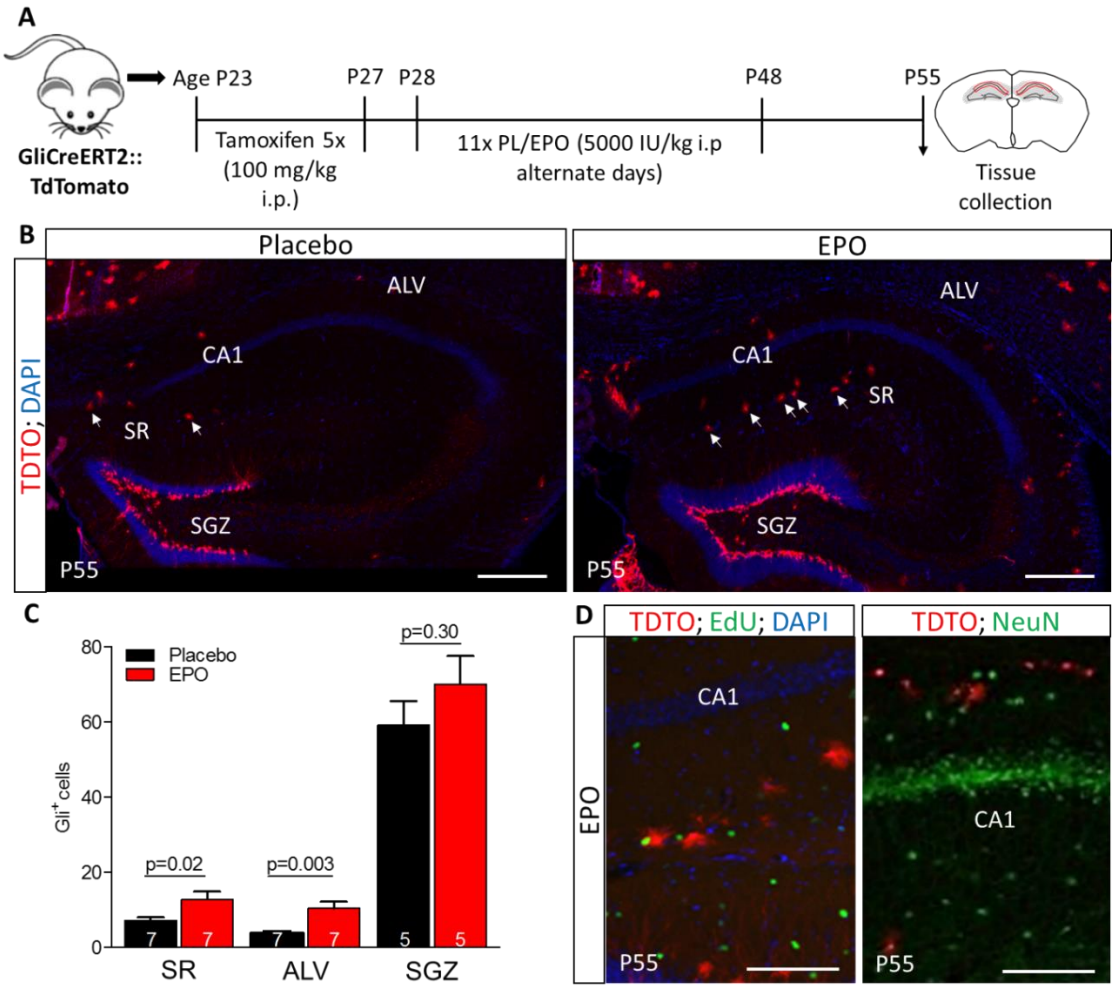

Figure 26. Multiple EPO injections lead to an increase in Gli labelled TdTomato positive cells in the GliCreERT2::TdTomato mice without proliferation, but does not give rise to CA1 neurons. *(A) Experimental schematic where 5 i.p. injections of tamoxifen were administered from P23-P27 in GliCreERT2::TdTomato mice, followed by 11 i.p. injections of either placebo or EPO (on alternate days) from P28-P48. Mice were then sacrificed at P55. (B) Representative images of the hippocampus at P55 of placebo or EPO treated GliCreERT2::TdTomato mice, showing positive signal for Gli as labelled by TdTomato (red) in the Stratum Radiatum (SR), Alveus of hippocampus (ALV) and the Sub-Granular Zone (SGZ). (C) Quantification of TdTomato labelled Gli positive cells at P55 in the SR, ALV and SGZ of placebo (black) and EPO (red) treated hippocampi of GliCreERT2:TdTomato mice. Data represents average number of cells ± SEM. Quantification performed from 5-7 independent mice and p-values presented via unpaired Student's t-test. (D) Representative image of the hippocampus at P55 of EPO treated GliCreERT2::TdTomato mice, showing positive signal for TdTomato (red) and neuronal marker NeuN (right panel; green) or proliferation marker EdU (left panel; green). Nuclei were counterstained with DAPI (blue). Scale bars: 100µm.*

Surprisingly, after quantification, a significant increase in the number of Gli positive cells in the *stratum radiatum* (SR) and in the alveus of hippocampus was recorded, but only an increased trend in the SGZ of the hippocampus after EPO treatment as compared to the placebo treated mice (Fig. 26C). However, upon staining these sections with a neuronal marker NeuN (green), none of the NeuN positive neurons showed TdTomato expression, suggesting that Gli positive precursors did not give rise to the newly generated neurons in the CA1 upon EPO treatment (Fig. 26D). Moreover, labeling with EdU (green) did not reveal any co-localization of Gli positive cells with EdU signal (Fig. 26D), suggesting that EPO administration led to a significant increase in the number of Gli positive cells without undergoing proliferation.

Similar to the experiment performed with Nestin mouse line; whether a single dose of EPO could have a similar effect on Gli positive precursors at different stages of mice development remained to be determined. To achieve this, GliCreERT2::TdTomato mice were treated with tamoxifen (P23-P27), followed by a single dose of placebo or EPO (P28) and sacrificed at P29, P55 and P120 (Fig. 27A).

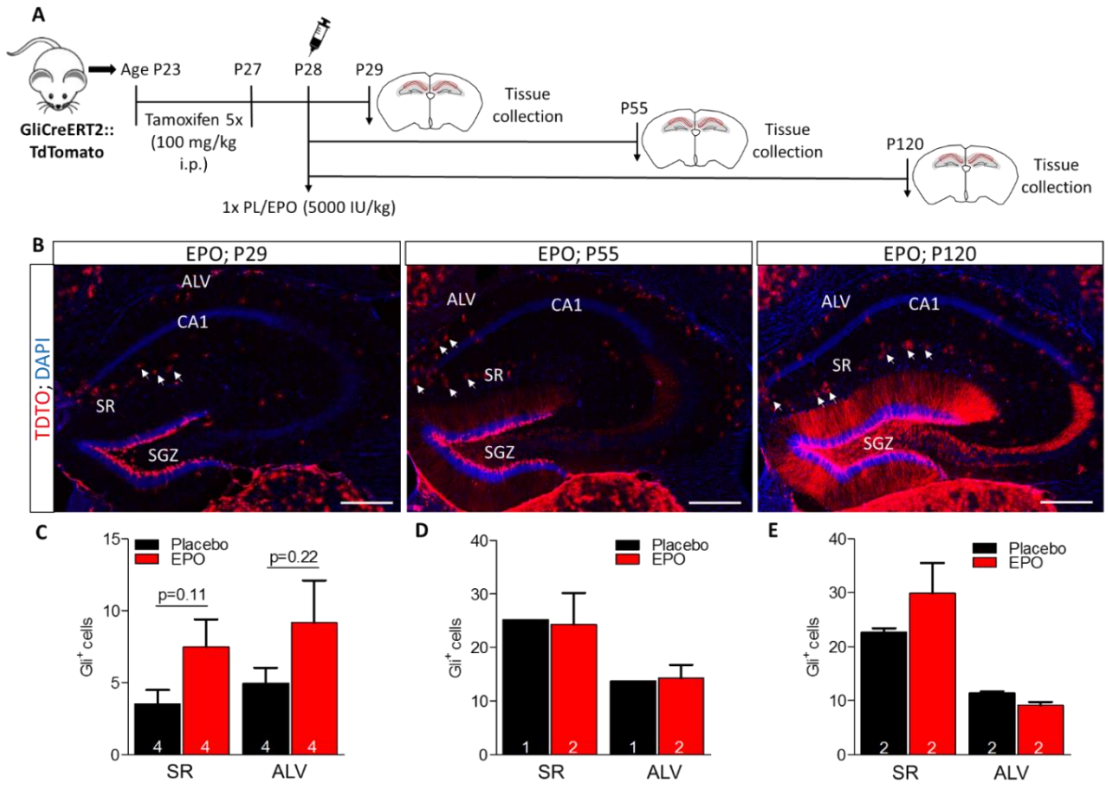

Figure 27. Fate mapping over time of GliCreERT2::TdTomato mice upon single dose of EPO does not give rise to neurons in the CA1. *(A) Experimental schematic where 5 i.p. injections of tamoxifen were administered from P23-P27 in GliCreERT2::TdTomato mice , followed by 1 i.p. injection of either placebo or EPO at P28. Mice were then sacrificed at P29, P55 or P120. (B) Representative images of the hippocampus at P29, P55 and P120 of EPO treated GliCreERT2::TdTomato mice, showing positive signal for Gli as labelled by TdTomato (red) in the Stratum radiatum (SR), Alveus of the hippocampus (ALV) and the Sub-Granular Zone (SGZ). Nuclei were counterstained using DAPI (blue). Scale bar: 100µm. (C, D, E) Quantification of TdTomato labelled Gli positive cells at P29 (C), P55 (D) and P120 (E) in the SR and ALV of placebo (black) and EPO (red) treated hippocampi of GliCreERT2::TdTomato mice. Data represents average number of cells ± SEM. Quantification performed from 1-4 independent mice and p-values presented via unpaired Student's t-test.*

Upon sectioning, staining (Fig. 27B) and quantification, an increase trend in Gli positive cells in SR of P29 (Fig. 27C) and P120 (Fig. 27E) mice treated with EPO was observed as compared to the age matched placebo control. Similar increased trend was also observed in the ALV of P29 (Fig. 27C) mice treated with EPO, but not in P55 (Fig. 27D) or P120 (Fig. 27E) EPO treated mice as compared to their respective age matched controls. As a control experiment to determine the robustness and efficiency of GliCreERT2::TdTomato mouse line, these mice were injected with a carrier solvent i.e.

corn oil (1x injection daily from P23-P27; Fig. 28A), and observed no signal for any unspecific TdTomato expression when sacrificed and stained at P28 (Fig. 28B).

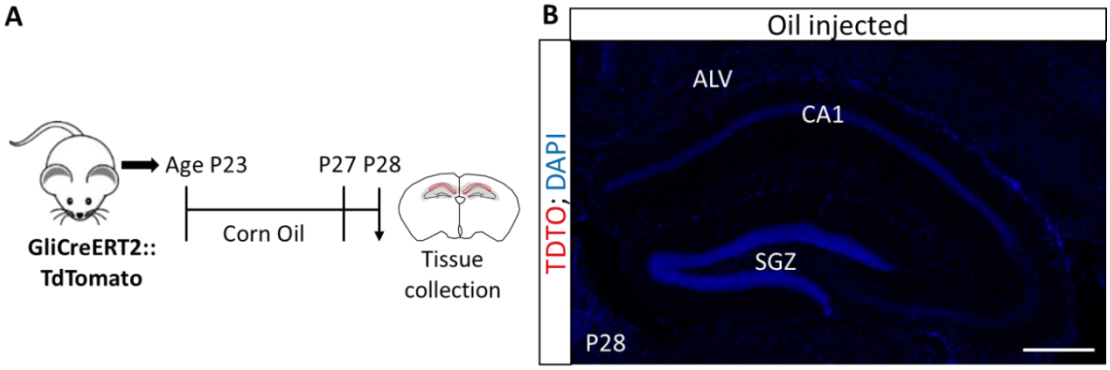

Figure 28. No unspecific TdTomato expression observed in Oil injected control GliCreERT2::TdTomato mice. *(A) Experimental schematic where 5 i.p. injections of corn oil were administered from P23-P27 and mice was sacrificed at P28. (B) Representative image of the hippocampus at P28 of corn oil-treated GliCreERT2::TdTomato mice, showing no signal for TdTomato (red). Nuclei were counterstained using DAPI (blue). Scale bar: 100µm.*

Although the Gli positive precursors did not give rise to any new neurons under the influence of EPO treatment, the identity of these Gli positive cells remained unknown. Following similar treatment regime as described previously by *Hassouna et al., 2016*, mice were injected with tamoxifen (P23-P27), followed by 11x injections of placebo or EPO (P28-P48) and sacrificed these mice at P55. Upon labelling these cells with astrocytic markers (GFAP and s100β; green) and oligodendrocyte maker (PDGFRα; green), TdTomato signal co-localized with these respective markers (Fig. 29A, 29C and 29E). After quantification of cells where signal of these markers and TdTomato co-localize, an increase trend in the number of $Gli^{+}/GFAP^{+}$ cells in the SR region (Fig. 29B) of the hippocampus of EPO treated mice was recorded as compared to the placebo treated mice.

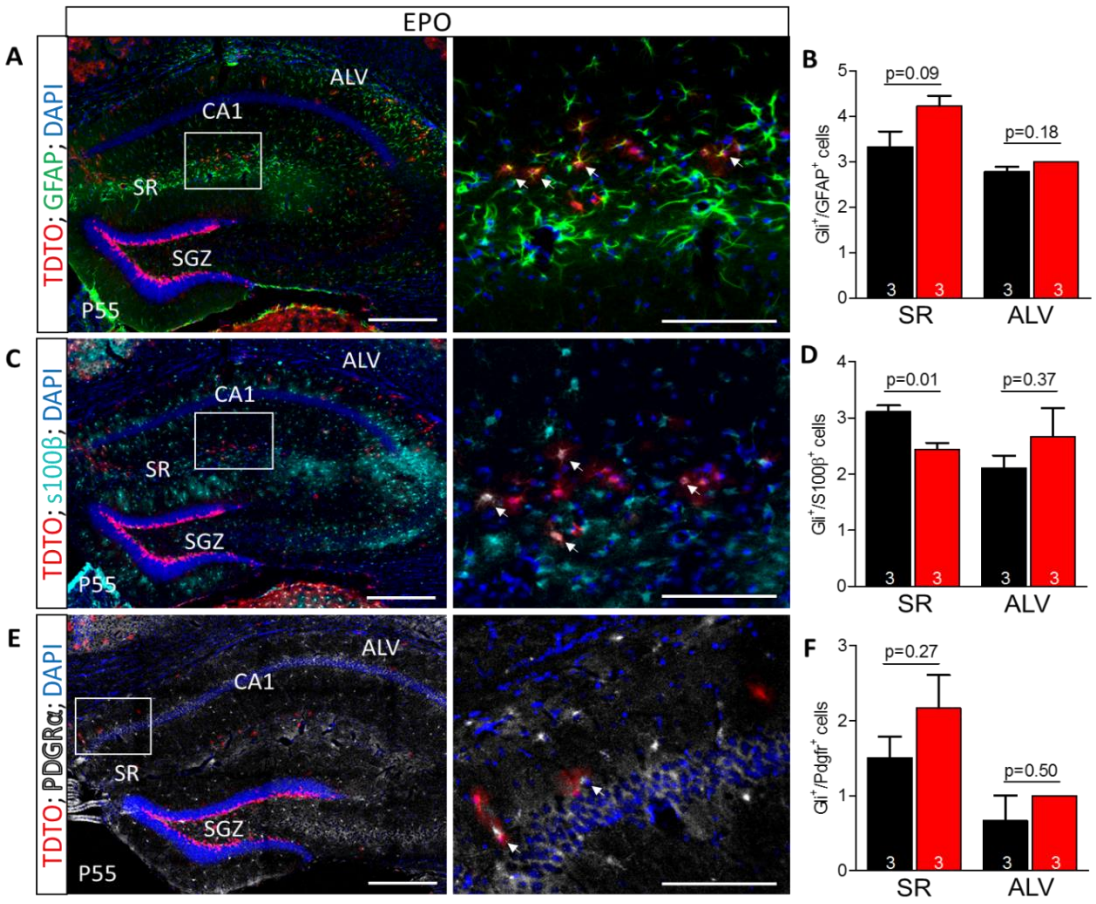

Figure 29. TdTomato labelled Gli positive cells co-localize with other cell types in the hippocampus upon multiple placebo or EPO injections. *(A; C; E) Representative images of the hippocampus at P55 of EPO treated GliCreERT2::TdTomato mice, showing positive signal for TdTomato (red) and immature astrocytic marker GFAP (green; A), mature astrocytic marker s100β (green; C) and oligodendrocytic precursor marker PDGFRα (green; E). Respective magnified images are shown in the right panel. Nuclei are counterstained with DAPI (blue). Scale bars: 100µm. (B; D; F) Quantification of TdTomato labelled Gli positive cells co-localizing with GFAP (B), s100β (D) and PDGFRα (F) at P55 in the SR and ALV of placebo (black) and EPO (red) treated hippocampi of GliCreERT2::TdTomato mice. Data represents average number of cells ± SEM. Quantification performed from 3 independent mice and p-values presented via unpaired Student's t-test.*

Moreover, significant reduction in the number of $Gli^+/s100\beta^+$ cells was observed in the SR region of the hippocampus after EPO treatment (Fig. 29D). On the other hand, no difference in the number of $Gli^+/PDGFR\alpha^+$ cells in the SR region of the hippocampus was observed after EPO treatment (Fig. 29F). Similarly, no difference was recorded in the number of positive cells in the ALV region of the hippocampus after EPO treatment (Fig. 29B, 29D and 29F). The increase trend in $Gli^+/GFAP^+$ cells in the SR region of the hippocampus was as expected because Gli, expressed primarily by type I and type II

radial glial cells, are also known to express GFAP *(Ahn and Joyner, 2005)*. Taken together, this data suggests that EPO does not regulate neurogenesis in the hippocampus via type II (Nestin and Gli) precursors.

4.1.3. EPO induced increase in pyramidal neurons could potentially be via Sox2 positive precursors.

Sox2, known as SRY (Sex determining region Y box 2) protein, is a transcription factor that plays a crucial role in cell fate commitment and differentiation *(Kamachi and Kondoh, 2013)*. Interestingly, Sox2 marks NSCs in embryonic and adult mice as well as type I radial glial cells. It is also one of the Yamanaka factors required for the generation of induced pluripotent stem cells (iPSCs) from human fibroblasts *(Takahashi and Yamanaka, 2006)*. Sox2 is involved in the maintenance of stem cells as well as their multipotent capabilities and self-renewal properties *(Arnold et al., 2011; Suh et al., 2007)*. Therefore, Sox2 was considered as a potential candidate, which could give rise to the increase in the pyramidal neurons upon EPO treatment.

To begin with, a commercially available Sox2 antibody was used to stain sections from GliCreERT2::TdTomato mice after similar treatment protocol as published by *Hassouna et al., 2016* (Fig. 30A-B).

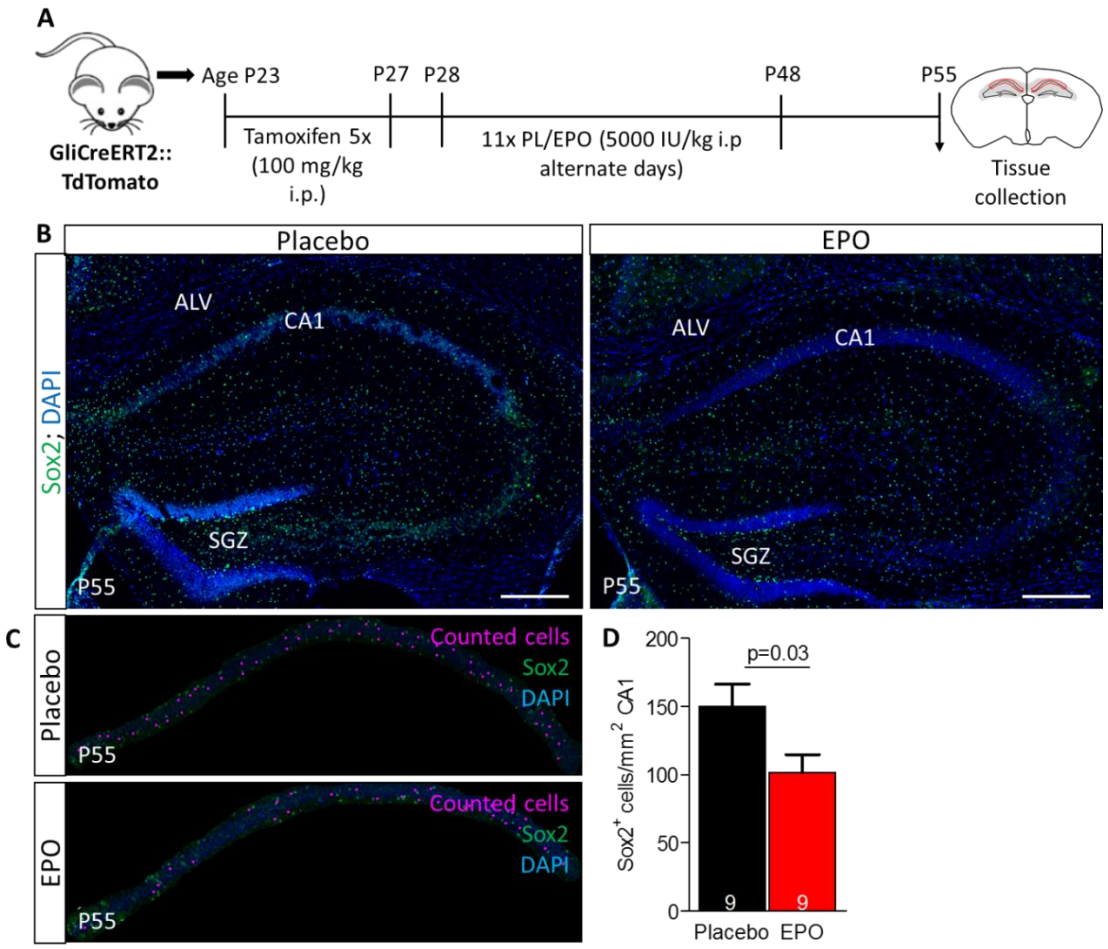

Figure 30. EPO administration led to a significant decrease in the number of Sox2 positive cells in the CA1 region of GliCreERT2::TdTomato mice. *(A) Experimental schematic where 5 i.p. injections of tamoxifen were administered from P23-P27 in GliCreERT2::TdTomato mice, followed by 11 i.p. injections of either placebo or EPO (on alternate days) from P28-P48. Mice were then sacrificed at P55. (B-C) Representative images of the hippocampus at P55 of placebo or EPO treated GliCreERT2::TdTomato mice and representation of cells that were quantified (C), showing positive signal for Sox2 (green) in the CA1 region of the hippocampus. Nuclei were counterstained using DAPI (blue). Scale bar: 100µm. (D) Quantification of Sox2-positive cells at P55 in the CA1 region of placebo (black) and EPO (red) treated hippocampi of GliCreERT2::TdTomato mice. Data represents average number of cells ± SEM. Quantification performed from 9 independent mice and p-values presented via unpaired Student's t-test.*

After staining using antigen retrieval, Sox2 positive cells were observed in the CA1 region of the hippocampus of placebo and EPO treated mice at P55. Upon quantification (Fig. 30C) of Sox2 positive cells, a significant decrease in the number of Sox2 positive cells in the pyramidal layer of the CA1 region of mice treated with EPO was quantified as compared to the placebo treated controls (Fig. 30D). This result

suggests that EPO could increase the number of pyramidal neurons by forcing Sox2 positive precursors to undergo asymmetrical differentiation.

In order to fate map the Sox2 positive cells after EPO treatment, an inducible Sox2CreERT2 transgenic mouse line was crossed with TdTomato reporter mouse line (R26R-TdTomato; *Madison et al., 2010*). Following the treatment regimen as published in *Hassouna et al., 2016*, Sox2CreERT2::TdTomato mice were treated with 5x injections of tamoxifen to label Sox2 positive precursors with TdTomato. Placebo or EPO injections (11x, on alternate days) were administered from P28-P48, followed by sacrificing the mice at P55 (Fig. 31A). Upon sectioning and staining, TdTomato positive cells in both placebo and EPO treated mice hippocampus (Fig. 31B) were observed.

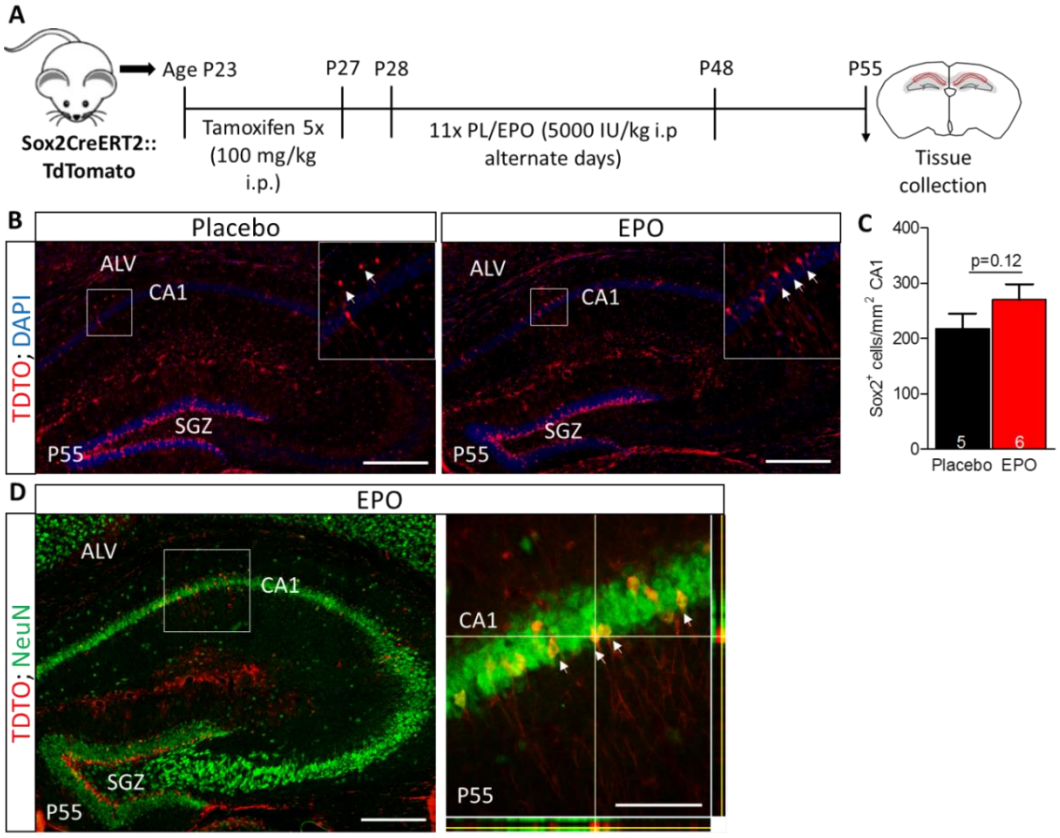

Figure 31. EPO administration led to an increase in the number of Tdtomato labelled Sox2 positive cells in the CA1 region of Sox2CreERT2::TdTomato mice. *(A) Experimental schematic where 5 i.p. injections of tamoxifen were administered from P23-P27, followed by 11 i.p. injections of either placebo or EPO (on alternate days) from P28-P48 in Sox2CreERT2::TdTomato mice. Mice were then sacrificed at P55. (B) Representative images of the hippocampus at P55 of placebo or EPO treated Sox2CreERT2::TdTomato mice, showing positive signal for TdTomato (red) in the CA1 region of the hippocampus. (C) Quantification of TdTomato labelled Sox2 positive cells in the CA1 region at P55 of placebo (black) and EPO (red) treated hippocampi of Sox2CreERT2::TdTomato mice. Data represents average number of cells ± SEM. Quantification performed from 5-6 independent mice and p-values presented via unpaired Student's t-test. (D) Representative images of the hippocampus at P55 of EPO treated Sox2CreERT2::TdTomato mice, showing positive signal for TdTomato (red) and neuronal marker NeuN (green) in the CA1 region of the hippocampus. Nuclei were counterstained using DAPI (blue). Scale bar: 100µm.*

Upon quantification of Sox2 positive cells, an increased trend in the CA1 region of EPO treated mice (p-value=0.12) was recorded as compared to the placebo treated mice (Fig. 31C). As TdTomato positive cells were present in the pyramidal layer of the CA1 region of treated mice, a co-staining with a neuronal marker NeuN (green) demonstrated that NeuN positive neurons also showed TdTomato expression in EPO (Fig. 31D) treated pyramidal layer of the CA1. Magnified images of co-localization of NeuN (green) and TdTomato (red) are depicted in Fig. 31D. As a control experiment to confirm the robustness and efficiency of Sox2CreERT2::TdTomato mice, these mice were injected with a carrier solvent i.e. corn oil (5x, P23-P27), followed by sacrificing the mice at P55 (Fig. 32A). After sectioning and staining, unfortunately, unspecific TdTomato expression in the hippocampus of oil treated mice at P55 was observed (Fig. 32B), suggesting that the Sox2CreERT2::TdTomato transgenic mice was leaky and could not be further used for these experiments.

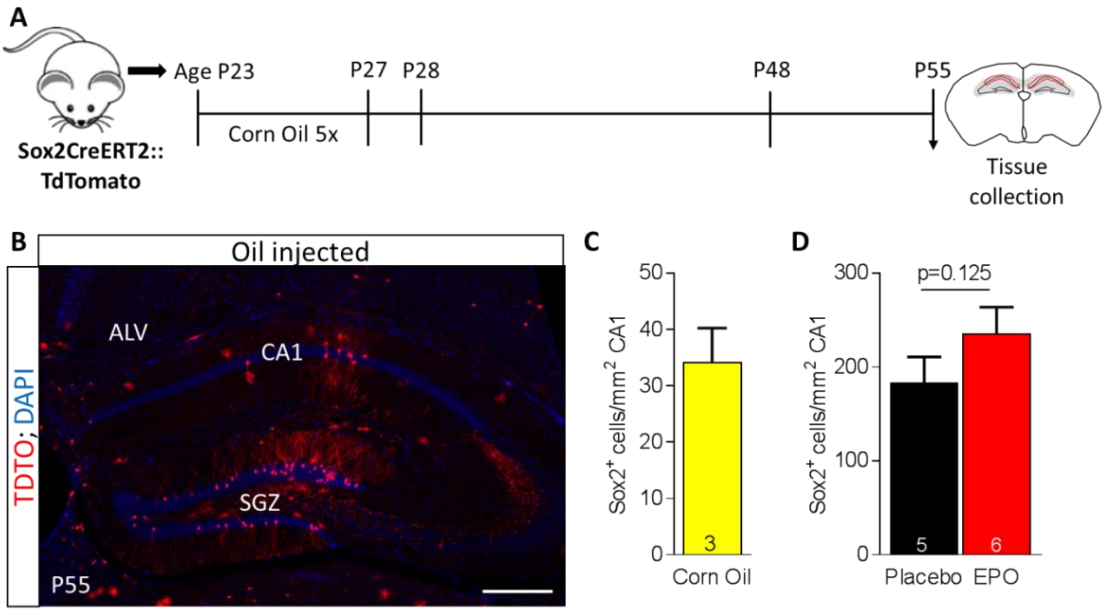

Figure 32. Unspecific TdTomato expression observed in Oil injected control Sox2CreERT2::TdTomato mice. *(A) Experimental schematic where corn oil was administered (i.p.) at P23-P27 in Sox2CreERT2::TdTomato mice and then sacrificed at P55. (B) Representative image of the hippocampus of corn oil treated Sox2CreERT2::TdTomato mice at P55, showing unspecific signal for TdTomato (red). Nuclei were counterstained using DAPI (blue). Scale bar: 100µm. (C) Quantification of TdTomato positive cells in the CA1 region at P55 of corn oil treated hippocampi of Sox2CreERT2::TdTomato mice. (D) Quantification of Sox2 positive cells obtained in Placebo (black) or EPO (red) treated mice after subtracting the number of unspecific positive cells observed in corn oil treated mice at the same time point. Data represents average number of cells ± SEM. Quantification performed from 9 independent mice and p-values presented via unpaired Student's t-test.*

Many transgenic mice have known to show a variable degree of leaky expression, although it is not always documented. However, the number of unspecific TdTomato positive cells obtained after corn oil treatment were still quantified (Fig. 32C) and subtracted from the number of TdTomato positive cells obtained after placebo or EPO treatment (Fig. 32D). In this case, a similar increase trend in the number of Sox2 positive cells after EPO treatment was observed as compared to the placebo treated mice (Fig. 32D). This data, however, cannot provide concrete evidence that EPO treatment leads to an increase in the number of pyramidal neurons mediated via Sox2 positive precursors.

Taking results and interpretations from all the three mouse lines used so far and the Doublecortin (Dcx) mouse line used in the past, this thesis can conclude that neuronal lineage commitment is comparatively more complex than the oligodendrocyte lineage

commitment (as shown by *Hassouna et al., 2016*). Various precursors, known or unknown, could differentiate, alone or synergistically, to contribute to the increased pyramidal neuronal number upon EPO administration. Interestingly, multiple studies have demonstrated that hematopoietic stem cells (HSCs) and multipotent precursors (MPPs) can circumvent distinct intermediate stages *(Haas et al., 2005; Pietras et al., 2015; Sanjuan-Pla et al., 2013; Yamamoto et al., 2013)*. Therefore, drawing parallels from the effect of EPO on the hematopoietic system, the present work could suggest that EPO could drive the neuro-differentiation without proliferation, possibly also skipping the intermediate stages. However, the data gathered so far from several experiments with different precursor makers like Sox9, Pax6, DCX *(Hassouna et al., 2016)*, Sox2 and from transgenic mouse lines for DCX, Nestin, Gli and Sox2, this thesis could suggest that EPO works on multiple precursors (Pax6, DCX, Sox2) in the brain to differentiate into new pyramidal neurons in the CA1 region.

4.2. Effect of EPO on pyramidal neurons.

4.2.1. Substantial generation of pyramidal neurons in the CA1 of adult mice and its amplification by EPO.

An increase (>20%) in pyramidal neurons upon 3-week treatment of juvenile mice (P55) with EPO, without evidence of proliferation or anti-apoptosis was recently demonstrated (*Hassouna et al., 2016)*. Due to the absence of any suitable reporter line (Fig. 24 – Fig. 32), which allowed us to fate map the importance of a single neuronal precursor, the above-mentioned observation remained difficult to corroborate. Several reports, fate-mapping neurons using additive labelling of progenitors and their progenies, have provided variable results *(Sun, 2014)*. Therefore, these type of studies are still in their infancy to provide reliable answer to the question of adult neurogenesis. Taking this into account, a subtractive approach was hypothesized that could enable us to elucidate the influence of EPO on adult neurogenesis. The idea behind this subtractive approach was to completely label embryonic born neurons in juvenile mice, which then could be distinguished from newly generated neurons. Using a novel approach to consolidate the finding *(Hassouna et al., 2016)*, almost all mature CA1 pyramidal neurons present at P27 were permanently pre-labeled with a tamoxifen inducible reporter TdTomato. This was performed by crossing a NexCreERT2 *(Agarwal et al., 2012)* with a inducible TdTomato; R26R-TdTomato *(Madisen et al., 2010)* transgenic mouse line. These NexCreERT2::TdTomato transgenic mice were treated with 5 or 10 i.p. injections of tamoxifen to completely label embryonic born neurons in juvenile mice and adult mice respectively (Fig. 33A). All neurons differentiating and maturing thereafter (i.e. start Nex/NeuroD6 expression) would not carry the TdTomato label, thereby enabling us to distinguish between pre-existing TdTomato labeled neurons and the newly generated neurons marked by a pyramidal neuronal marker Ctip2 (Chicken ovalbumin upstream promoter transcription factor-interacting protein 2). As a control experiment, a co-staining of TdTomato with Ctip2 was performed and approximately <3% of Ctip2 positive neurons were found *(data not shown)* to be not labelled with TdTomato ($TdTomato^-$, $Ctip2^+$). EPO or placebo treatment was initiated at P28, according to the previous injection scheme (5000U/kg, on alternate days from

P28-P48, followed by a treatment free week; *Hassouna et al., 2016*). The mice were then sacrificed at P55. Upon sectioning and staining (Fig. 33B), a significant increase in the number of newly generated neurons (TdTomato$^-$, Ctip2$^+$) in the CA1 after EPO treatment was measured as compared to the placebo treated mice (Fig. 33C).

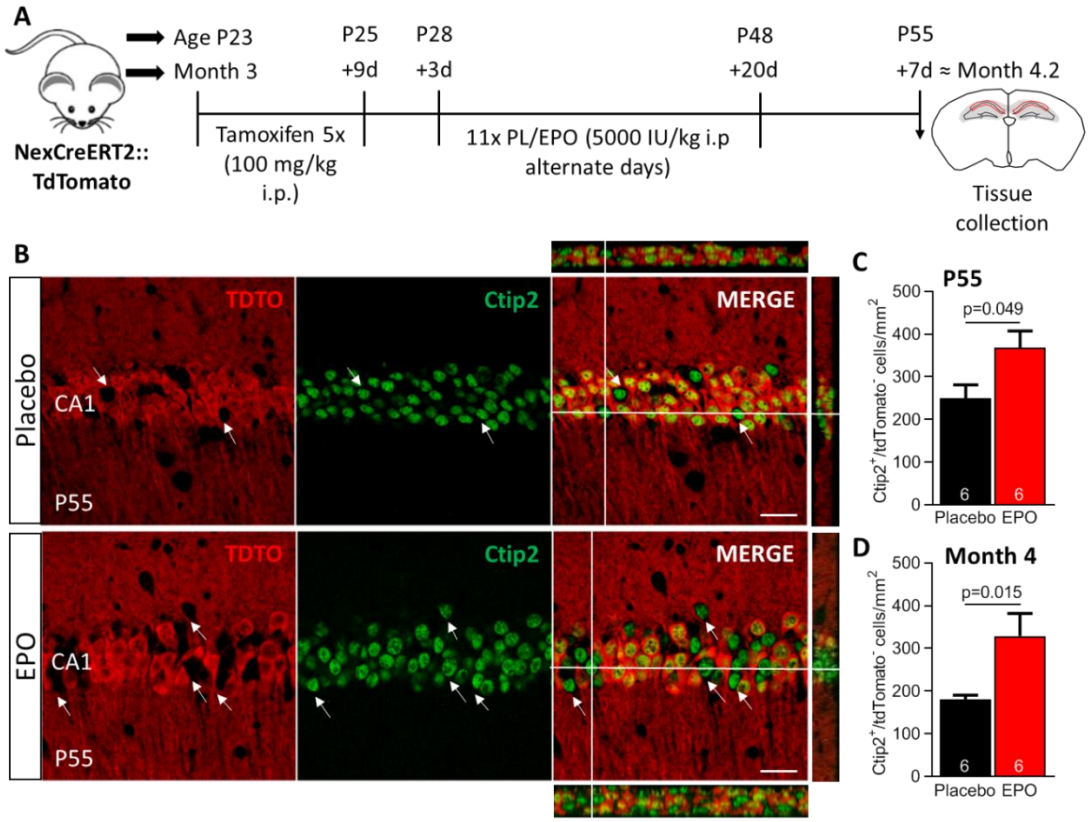

Figure 33. EPO increases number of pyramidal neurons in the CA1 region of the hippocampus. *(A) Experimental schematic to determine the effect of EPO on neuron number in NexCreERT2::TdTomato mice (starting at age P23 or month 3), where tamoxifen was administered either for 5 i.p. injections either in juvenile (P23) or 10x i.p. injections adult (Month 3) mice, followed by either placebo or EPO (11 i.p; on alternate days) for three weeks. Mice were then sacrificed at P55 or at approx. Month 4.2. (B) Representative images of the hippocampus at P55 of placebo or EPO treated NexCreERT2::TdTomato mice, showing positive signal for TdTomato (red) and excitatory neuronal marker Ctip2 (green) in the CA1 region of the hippocampus. White arrows indicate newly generated neurons. Scale bar: 50µm. (C-D) Quantification of newly generated Ctip2$^+$/TdTomato$^-$ neurons at P55 (C; juvenile) and at Month 4 (D; adult) in the CA1 of placebo (black) and EPO (red) treated hippocampi of NexCreERT2::TdTomato mice. Data represents average number of cells ± SEM. Quantification performed from 6 independent mice and p-values presented via unpaired Student's t-test.*

As previously reported *(Hassouna et al., 2016)*, these differentiated neurons did not show any evidence of recent generation from proliferating precursors (All EdU$^-$). Interestingly, using the same treatment schedule in adult mice, where the mice would

receive EPO or placebo starting at month 3 (Fig. 33A), a comparable increase in newly generated pyramidal neurons (TdTomato$^-$, Ctip2$^+$) upon EPO treatment (Fig. 33D) was recorded. Taken together, these data indicate that EPO induced substantial generation of pyramidal neurons not only in early developmental stages (juvenile mice), but also in adulthood. This, interestingly, represents a previously overlooked novel aspect of adult neurogenesis uncovered by the serendipity and validated with the subtractive approach in our EPO studies.

4.2.2. EPO leads to an increase in the dendrites and spine density of pyramidal neurons in the CA1.

Not only neuronal numbers, but also an increase in neuropil can theoretically contribute to enlargement of brain regions and cognitive improvements as previously observed under the influence of EPO *(Wüstenberg et al., 2011; Hassouna et al., 2016)*. A Thy1-EGFP transgenic mice *(Feng et al., 2010; Porrero et al., 2010)* was employed, where dendrites of pyramidal neurons are labelled with EGFP reporter. Following similar treatment regime *(Hassouna et al., 2016)*, Thy1-EGFP juvenile mice or Month 3 old adult mice were treated with placebo or EPO (11 i.p. injections, on alternate days) (Fig. 34A). Brain sections were stained with a dendritic marker Map2 (Fig. 34B-C) to determine the dendritic density after placebo or EPO treatment. Upon quantification, a significant increase in the dendritic density in juvenile (P55) and adult (4 months) mice after EPO treatment was quantified as compared to the placebo treated mice (Fig. 34D).

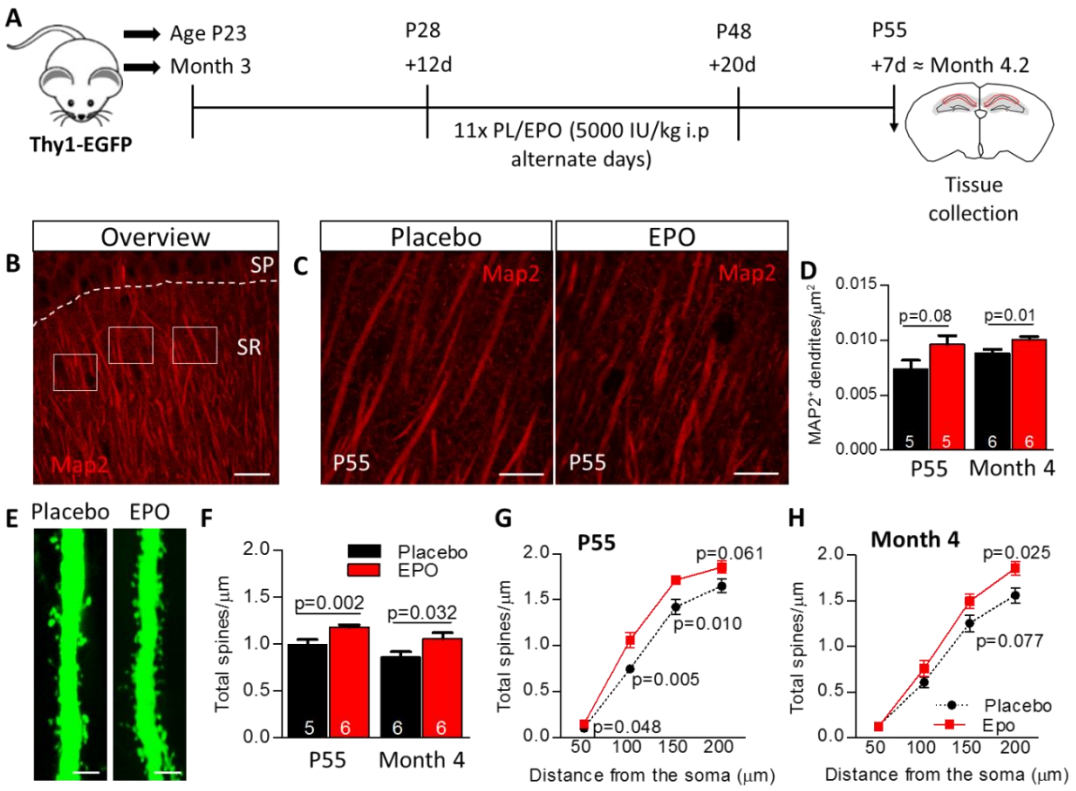

Figure 34. EPO increases the dendritic and total spine density in the CA1 region of the hippocampus. *(A) Experimental schematic where Thy1-EYFP juvenile (P23) or adult (Month 3) mice were treated with either placebo or EPO (11 i.p; on alternate days) for three weeks. Mice were then sacrificed at P55 or at approx. Month 4.2. (B) Representative overview image of the quantification method employed for determining the density of dendrites using dendritic marker MAP2 (red) in CA1 stratum radiatum (SR).White boxes denote areas of measurements. Scale bar: 20µm. (C) Representative images at P55 of the dendrites of pyramidal neurons of placebo or EPO treated Thy1-EGFP mice, showing positive signal for dendritic marker MAP2 (red) in the CA1 region of the hippocampus. Scale bar: 10µm (D) Quantification of total number of MAP2 positive dendrites of pyramidal neurons in the CA1 at P55 and at Month 4 of placebo (black) and EPO (red) treated hippocampi of Thy1-EGFP mice. Data represents average number of Map2 positive dendrites/µm² ± SEM. (E) Representative images of EYFP (green) expression in principal apical dendrites in CA1 of placebo or EPO treated Thy1-EYFP mice. Scale bar: 10µm. (F) Quantification of total number of apical dendritic spines at P55 (juvenile) or at Month 4 (adult) in placebo (black) or EPO (red) treated Thy1-EGFP mice hippocampus. Data represents average number of dendritic spines/µm ± SEM. (G-H) Line graphs depict the total number of spines mice at P55 (G; juvenile) or at Month 4 (H; adult) presenting their respective distance from the soma in placebo (black) or EPO (red) treated. Data represents average number of total dendritic spines/µm ± SEM in correlation with their respective distance from the soma (µm). Quantification performed from 5-6 independent mice and p-values presented via unpaired Student's t-test. This data was generated in collaboration with Yasmina Curto.*

Next, the total dendritic spine density of pyramidal neurons (labelled by EGFP) in placebo or EPO treated juvenile and adult mice was determined (Fig. 34E) and was observed to be enhanced after EPO treatment at both P55 and 4 months of age (Fig. 34F). Correlating the number of dendritic spines with their distance from the respective cell soma, a significantly higher number of spines located closer to their respective cell somas (Fig. 34G) after EPO treatment in juvenile mice was observed, whereas in adult mice, significantly higher number of spines were located further away from their respective cell somas (Fig. 34H). Taken together, this data suggests that EPO induces an increase in dendritic density as well as dendritic spine density in both juvenile mice (P55) and adult mice (4 months).

Previous reports have suggested that maturity of dendritic spines can be determined by observing their morphology *(Kasai et al., 2011)*. Therefore, following similar placebo or EPO treatment regime in Thy1-EGFP juvenile and adult mice (Fig. 35A), the morphology of labelled dendritic spines (Fig. 35B) was studied.

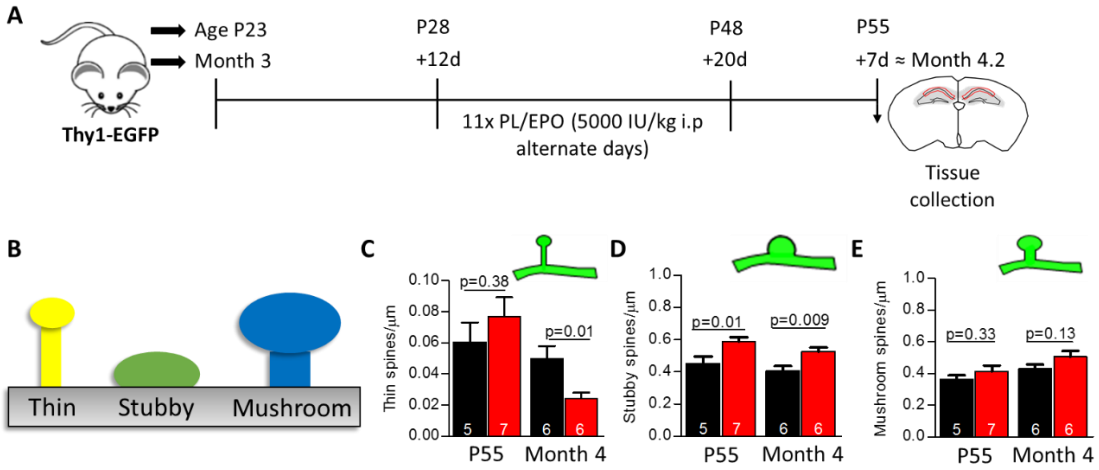

Figure 35. EPO increases the density of immature stubby spine type in the CA1 region of the hippocampus. *(A) Experimental schematic where Thy1-EYFP juvenile (P23) or adult (Month 3) mice were treated with either placebo or EPO (11 i.p; on alternate days) for three weeks. Mice were then sacrificed at P55 or at approx. Month 4.2. (B-D) Quantification of EYFP positive principal apical dendritic in the CA1 region of the hippocampus at P55 (C-E; juvenile) and at Month 4 (C-E; adult) based on their morphology as illustrated in (B) showing thin (C), stubby (D) or mushroom (E) morphology in placebo (black) and EPO (red) treated Thy1-EGFP mice. Data represents average number of dendritic spines/µm ± SEM. Quantification performed from 5-7 independent mice and p-values presented via unpaired Student's t-test. This data was generated in collaboration with Yasmina Curto.*

Upon quantification, a significant increase in stubby immature spines and a trend towards more of the mature mushroom spines upon EPO treatment (Fig. 35C-E) was measured. These findings indicate that in addition to more newly generated pyramidal neurons, other important aspects of neuroplasticity, supporting functional neuronal network complexity, are efficiently augmented by EPO.

4.2.3. EPO mediated increase in neurons is accompanied by changes in other cell types in the CA1.

After confirming a substantial increase in the number of pyramidal neurons in the CA1 upon EPO treatment, it was imperative to determine whether EPO mediated an interplay between other cell types present in the CA1 region of the hippocampus. In our previously published report, EPO has been demonstrated to play a crucial role in the myelination of the newly formed neurons as well as significantly increased oligodendrocyte differentiation *(Hassouna et al., 2016)*. Therefore, the present work extended this to other cells present in the CA1, mainly microglia and astrocytes. To accomplish this, a staining for Iba1, a marker of microglia in the same mice was performed, which were subjected to 3-week EPO treatment (Fig. 36A-B).

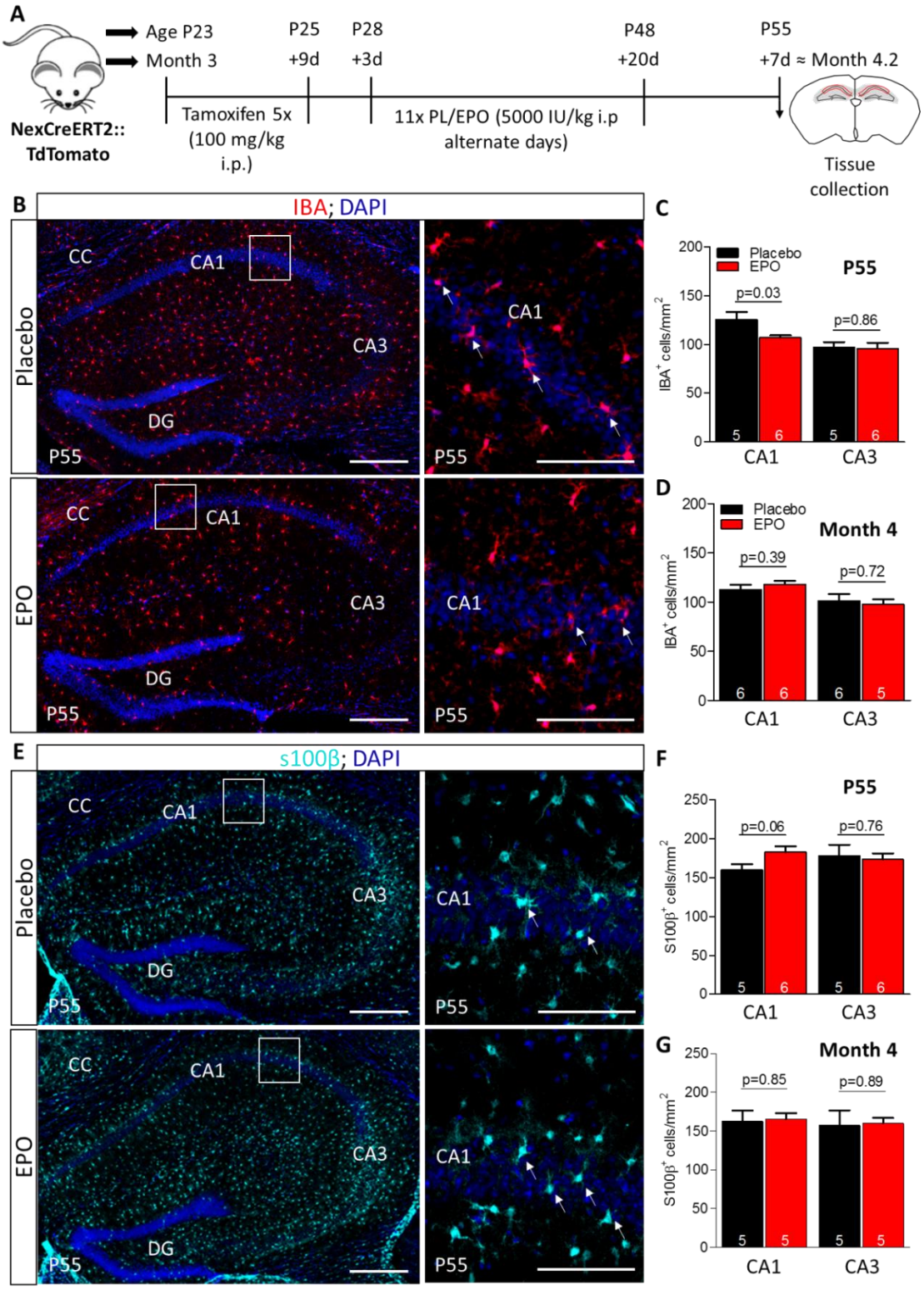
A
Age P23
Month 3
P25
+9d
P28
+3d
P48
+20d
P55
+7d ≈ Month 4.2
NexCreERT2::
TdTomato
Tamoxifen 5x
(100 mg/kg
i.p.)
11x PL/EPO (5000 IU/kg i.p
alternate days)
Tissue
collection
B
IBA; DAPI
Placebo
EPO
CC
CA1
CA3
DG
P55
C
Placebo
EPO
P55
p=0.03
p=0.86
IBA+ cells/mm2
CA1
CA3
D
Month 4
p=0.39
p=0.72
E
s100β; DAPI
F
p=0.06
p=0.76
S100β+ cells/mm2
G
p=0.85
p=0.89

Figure 36. EPO decreases the number of Iba1 positive microglia in juvenile mice in the CA1 region of the hippocampus. *(A) Experimental schematic to determine the effect of EPO on neuron numbers in 2 cohorts of NexCreERT2::TdTomato mice (starting at age P23 or month3), where tamoxifen was administered either for 5 i.p. injections in juvenile (P23) or 10x i.p. injections in adult (Month 3) mice, followed by either placebo or EPO (11 i.p; on alternate days) for three weeks. Mice were then sacrificed at P55 or at approx. Month 4.2. (B) Representative images of the hippocampus at P55 of placebo or EPO treated NexCreERT2::TdTomato mice, showing positive signal for microglial marker Iba1 (red) in the CA1 and CA3 region of the hippocampus. (C-D) Quantification of Iba1 positive microglia at P55 (C; juvenile) and at Month 4 (D; adult) in the CA1 and CA3 of placebo (black) and EPO (red) treated hippocampi of NexCreERT2::TdTomato mice. (E) Representative images of the hippocampus at P55 of placebo or EPO treated NexCreERT2::TdTomato mice, showing positive signal for astrocyte marker s100β (cyan) in the CA1 and CA3 region of the hippocampus. Nuclei were counterstained with DAPI (blue). Scale bar: 100µm. (F-G) Quantification of s100β positive astrocytes at P55 (F; juvenile) and at Month 4 (G; adult) in the CA1 and CA3 of placebo (black) and EPO (red) treated hippocampi of NexCreERT2::TdTomato mice. Data represents average number of cells ± SEM per mm^2. Quantification performed from 5-6 independent mice and p-values presented via unpaired Student's t-test.*

Upon quantification, a significant decrease in the number of microglia (Iba1$^+$) at P55 after EPO treatment was observed as compared to the placebo treated mice (Fig. 36C). This EPO induced decrease of microglia was no longer observed in adult mice (Fig. 36D) at the age of 4 months, implicating the role of EPO on microglia specifically at early developmental stages. In parallel, staining sections of hippocampi from juvenile as well as adult mice for s100β, which is a marker of mature astrocytes (Fig. 36E) did not reveal a significant change in the number of mature astrocytes, however, only a trend towards an increase in juvenile mice (Fig. 36F). This could implicate that some of the Gli precursors (demonstrated in Fig. 26 – Fig. 29), which gave rise to astrocytes upon EPO treatment. However, this effect was not observed in EPO treated adult mice (Fig. 36G), suggesting that EPO does influence microglia and astrocytes during development or adulthood.

The underlying mechanism explaining the effect of EPO on other cell types is still unknown. Therefore, to elucidate whether EPO mediated changes in the above-mentioned cell types occur via EPO-receptor (EPOR), it was imperative to determine whether EPOR is present on these cells. To achieve this, a collaboration with Synaptic Systems (SySy) was established to generate monoclonal and polyclonal antibodies

against EPOR. After several standardizing experiments, none of the generated antibodies gave reproducible results upon staining mouse brain sections with anti-EPOR antibody *(data not shown)*. Although the expression of EPOR on different cell types *in vivo* was not demonstrated, *in vitro* primary cell cultures of neurons, microglia, astrocytes and oligodendrocytes were performed. The presence of EPOR mRNA in cell cultures at different time points of development could be determined using quantitative real time PCR. To accomplish this, primary hippocampal neurons were cultured from E17 mice embryo brains (Fig. 37A) and primary microglia, astrocytes and oligodendrocytes were cultured from P1 post-natal pup brains (Fig. 37B).

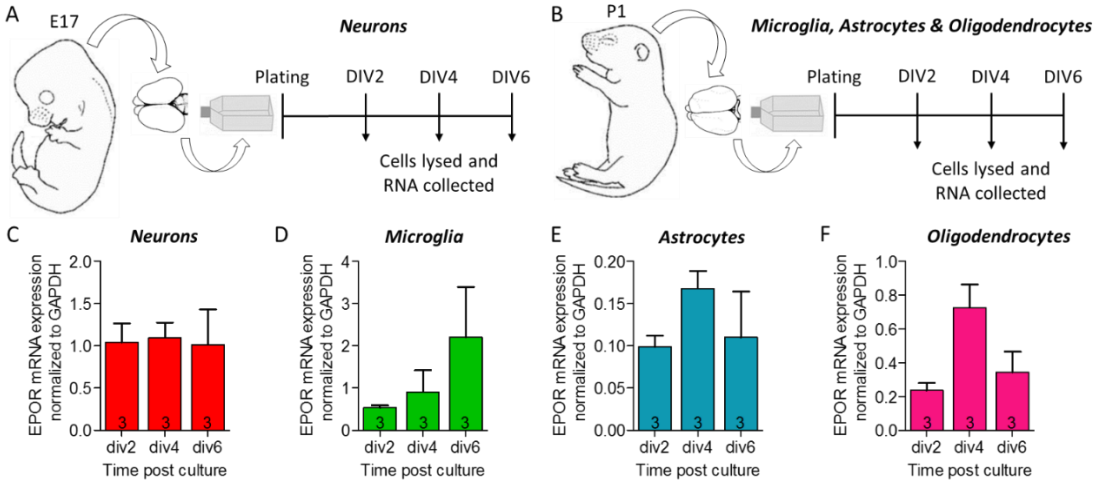

Figure 37. Endogenous mRNA levels of EPOR in cultured neurons, microglia, astrocytes and oligodendrocytes. *(A) Experimental schematic where E17 mice embryos derived hippocampal neurons were cultured for DIV 2, DIV 4 and DIV 6. Cells were lysed and RNA was collected at these time points. (B) Experimental schematic where P1 post-natal pup brain derived microglia, astrocytes or oligodendrocytes were cultured for DIV 2, DIV 4 and DIV 6. Cells were lysed and RNA was collected at these time points. (C-F) Quantification of endogenous mRNA levels of EPOR in cultured neurons (C), microglia (D), astrocytes (E) or oligodendrocytes (F) at DIV 2, DIV 4 and DIV 6 by qRT-PCR. Expression of EPOR mRNA was normalized to GAPDH, which is used as a housekeeping gene.*

In all cultures, the cells were lysed and RNA was extracted at DIV 2, DIV 4 and DIV 6 (Fig. 37A-B). Upon performing qRT-PCR with a specific EPOR primers, endogenous mRNA levels of EPOR in primary cultured hippocampal neurons (Fig. 37C), microglia (Fig. 37D), astrocytes (Fig. 37E) and oligodendrocytes (Fig. 37E) was observed. Expression of EPOR mRNA levels were normalized to GAPDH, which was used as a housekeeping gene. Interestingly, higher changes in the basal levels of EPOR mRNA in

cultured microglia and oligodendrocytes were quantified, but not in cultured neurons and astrocytes during the time course studied. Taken together, this data could indicate the role of EPO due to the presence of EPOR on these cells.

4.2.4. Drop-sequencing analysis demonstrates increase in the number of immature glutamatergic neurons after EPO treatment.

Since EPOR mRNA expression was observed in various cell types by qRT-PCR, which determines the expression of known genes with the help of specific primers, a state-of-art comprehensive approach was employed to determine the effect of EPO on the cellular heterogeneity of the CA1 region. Using this approach, the population of cells, which respond to EPO could be determined, which could not be addressed by qRT-PCR. Therefore, single cell transcriptome analysis (scRNA-Seq) was employed to explore the immediate response of EPO on the cells in the CA1 (Fig. 38A). Based on expression of previously known and well characterized cell-type markers (Fig. 38B; Wu et al. 2017), six main cell types were identified in the CA1, namely, neurons, astrocytes, microglia, oligodendrocyte precursor cells (OPCs), oligodendrocytes, and vascular endothelial cells. Feature plots marked the identity of each cluster with a specific marker. Markers that characterize each cluster are as follows: glutamatergic neurons: Camk2a (Fig. 38C) and Kif5c (Fig. 38C); GABAergic neurons: Gad1 (Fig. 38D) and Gad2 (Fig. 38D); astrocytes: Slc7a10 (Fig. 38E) and Lfng (Fig. 38E); microglia: Tmem119 (Fig. 38F) and C1qc (Fig. 38F); oligodendrocyte precursor cells: Pdgfra (Fig. 38G) and Gpr17 (Fig. 38G); mature oligodendrocytes: Mog (Fig. 38H) and Opalin (Fig. 38H); and endothelial cells: Flt1 (Fig. 38I) and Ly6c1 (Fig. 38I).

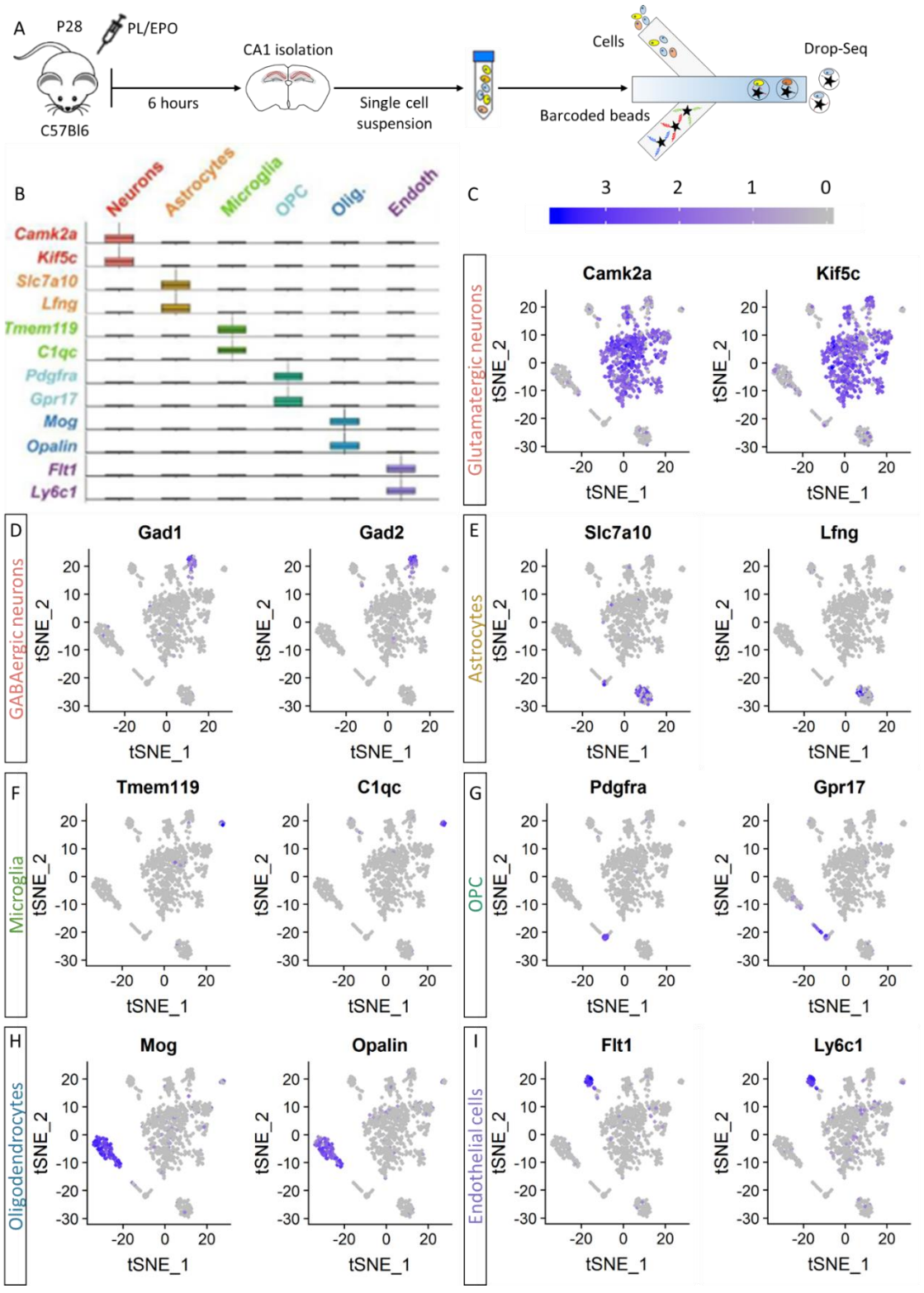
A
P28
PL/EPO
C57Bl6
6 hours
CA1 isolation
Single cell suspension
Cells
Drop-Seq
Barcoded beads
B
Neurons
Astrocytes
Microglia
OPC
Olig.
Endoth
Camk2a
Kif5c
Slc7a10
Lfng
Tmem119
C1qc
Pdgfra
Gpr17
Mog
Opalin
Flt1
Ly6c1
C
3
2
1
0
Glutamatergic neurons
Camk2a
Kif5c
D
GABAergic neurons
Gad1
Gad2
E
Astrocytes
Slc7a10
Lfng
F
Microglia
Tmem119
C1qc
G
OPC
Pdgfra
Gpr17
H
Oligodendrocytes
Mog
Opalin
I
Endothelial cells
Flt1
Ly6c1
tSNE_1
tSNE_2

Figure 38. Determination of major hippocampal cell types and cell type-specific gene markers. *(A) Experimental schematic where P28 C57Bl6 WT mice were treated with 1x i.p. injection of placebo or EPO and CA1 was isolated 6 hours later. The CA1 region was then triturated into single cell suspension and processed for Drop-Seq analysis. (B) Boxplots showing representative major cell-type of known marker genes across different cell types (Wu et al., 2017) (C-I) t-SNE plot showing cell cluster specific expression (darker signal correlates to higher expression) of known markers. Each dot is a specific cell. Known markers genes specific to mature neurons (C), GABAergic neurons (D), Astrocytes (E), Microglia (F), Oligodendrocyte precursors (G), Oligodendrocytes (H) and Endothelial cells (I). This analysis confirms that each cluster captures a particular cell. This data was generated in collaboration with Stefan Bonn's lab.*

Next, juvenile mice were treated with one injection of either placebo or EPO (5000U/kg) and dissected CA1 after 6 hours of treatment. The dissected CA1 was dissociated to obtain single cell suspension and was further analyzed by Drop-Seq. This experiment revealed alterations in the cell cluster composition (visualization of hippocampal CA1 cell clusters using t-distributed stochastic neighbor embedding, tSNE) as defined by gene expression profiles (Fig. 39A). From acutely micro-dissected and dissociated CA1 of juvenile mice, 390 and 583 single-cell transcriptomes for placebo and EPO treated mice (3 animals per group) respectively were acquired (Fig. 39B). Using principle component analysis (PCA), dimensionality reduction by t-distributed stochastic neighbor embedding (tSNE) and clustering, all the cells were unbiasedly grouped into multiple distinct clusters (Fig. 39A-B).

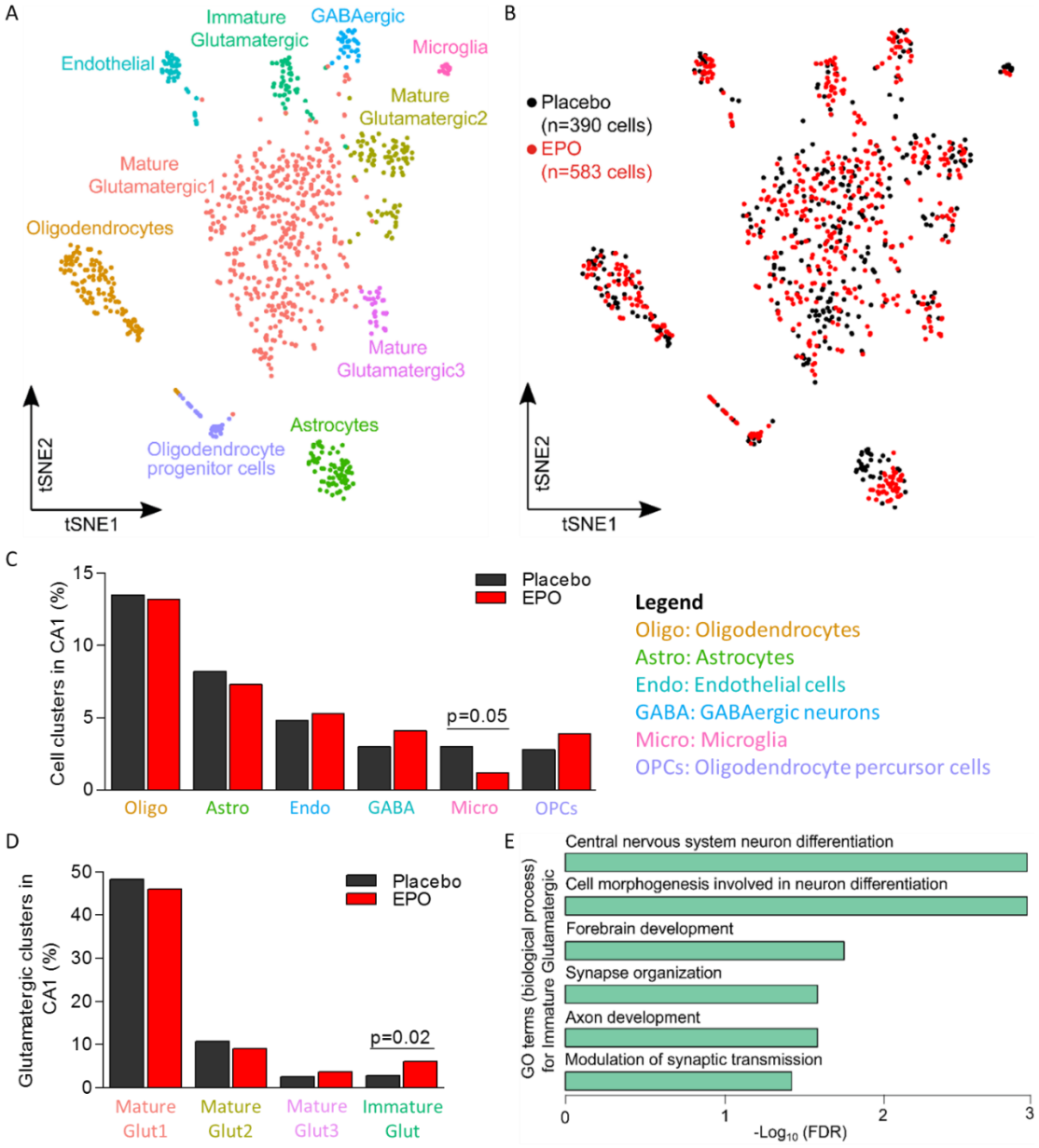

Figure 39. Drop-Sequencing analysis demonstrates increase in the number of immature glutamatergic neurons after EPO treatment. *(A) Visualization of hippocampal CA1 cell clusters using t-distributed stochastic neighbor embedding (tSNE). Each color represents a cluster of specific cells, characterized by a defined gene expression profile. (B) Based on the clusters defined in (A), individual cells derived from either placebo (black) or EPO (red) treated mice are denoted. (C) Taking the absolute number of cells (given in C) from EPO (n=583) or placebo (n=390) treated mice into account, bar graphs represents the percentage of glutamatergic clusters under each treatment condition. (D) For the immature glutamatergic cluster, significantly increased under EPO, the most relevant gene ontology terms are listed. The X-axis represents the -log10 FDR (false discovery rate adjusted p value).* (E) *The percentage of other cell types present in the CA1 under each treatment condition placebo (black) or EPO (red). Data represents the percentage of cells under each treatment conditions. Quantification performed from 3 independent mice per group and p-values presented via 2-tailed Fisher's exact test. Oligo: Oligodendrocytes; Astro: Astrocytes; Endo: Endothelial; GABA: GABAergic; Micro: Microglia; OPCs: Oligodendrocyte precursors.*

All the clusters obtained after the initial clustering and after further sub-clustering were further studied. No significant changes in the non-neuronal cell types such as astrocytes, oligodendrocytes, OPCs and endothelial cells were observed with a slight trend in the GABAergic neuronal cluster (Fig. 39C). A significant reduction in the number of microglia after EPO treatment was observed, but no effect of EPO on other cell types after 6 hours (Fig. 39C). A significant reduction in the number of microglia suggested the importance of microglia and neuron interaction at an earlier developmental time (as depicted *in vivo* in Fig. 36C).

Initial clustering of glutamatergic neurons resulted in a single cluster; however, further sub-clustering revealed multiple subpopulations, suggesting that the glutamatergic neuronal cluster does not represent homogeneous population of mature neurons but rather cells at different development stages. The clusters obtained after unbiased sub-clustering were classified as follows: (i) Glut1: Mature glutamatergic 1 expressing mature neuronal and glutamatergic signaling markers; (ii) Glut2: Mature glutamatergic 2 expressing mature neuron markers involved in processes like cytoskeleton and metabolic modifications; (iii) Glut3: Mature glutamatergic 3 involved in pre-synaptic transmission in processes like dendritic spine modification. Strikingly, along with these mature glutamatergic clusters, which did not show significant differences between EPO and placebo treatments (Fig. 39D), I observed a tiny cluster of cells, which expressed markers of immature neurons and were involved in processes of neuron differentiation. A significantly higher number of cells in the immature glutamatergic differentiation cluster after EPO treatment was observed as compared to the placebo treated CA1 (Fig. 39D). Gene Ontology (GO-terms) analysis revealed the biological relevance of transcripts involved in neuron differentiation, axon development and synapse organization for the immature glutamatergic neuronal cell cluster (Fig. 39E).

4.2.5. EPO drives maturation of immature neurons as revealed by Monocle analysis.

In order to describe the transcriptional signature that defines the immature glutamatergic vs mature glutamatergic 1 cluster, the expression of two immature neuronal markers (Tbr1 and Tle4) in combination with a known mature neuronal marker (Camkk2) was studied in our dataset. The immature glutamatergic cluster was

found to be highly specific for immature neuronal markers Tbr1 and Tle4, whereas the mature glutamatergic 1 cluster expressed the mature neuronal marker Camkk2 (Fig. 40A-C). In order to strengthen the fact that the cluster of cells, which showed an immediate response to EPO was indeed not as mature as other glutamatergic neuronal cluster, their differentiation trajectory on cells in the immature glutamatergic cluster and its neighboring cluster, mature glutamatergic 1 was determined in Monocle. To accomplish this, monocle analysis was performed wherein the single cells were ordered on a pseudo-temporal axis. The principle by which Monocle works is that, instead of tracking changes in expression as a function of time, Monocle tracks the changes as a function along the trajectory, which is termed as 'Pseudotime'. This could be defined as an abstract unit of progress, which measures the distance between a cell and the start of the trajectory. The total length of the trajectory is defined in terms of the total amount of transcription change that a particular cell undergoes when it moves from the starting state to the final state. The analysis confirmed the immature identity of cells in the immature glutamatergic cluster, reflected by a homogeneously low pseudotime of almost all cells in this cluster, which was significantly lower as compared to cells in the mature glutamatergic1 cluster (Fig. 40C-D). Importantly, a generally lower pseudotime upon EPO was observed, independent of cluster assignment, further supporting our observation of an increase in immature cells irrespective of clustering (Fig. 40E).

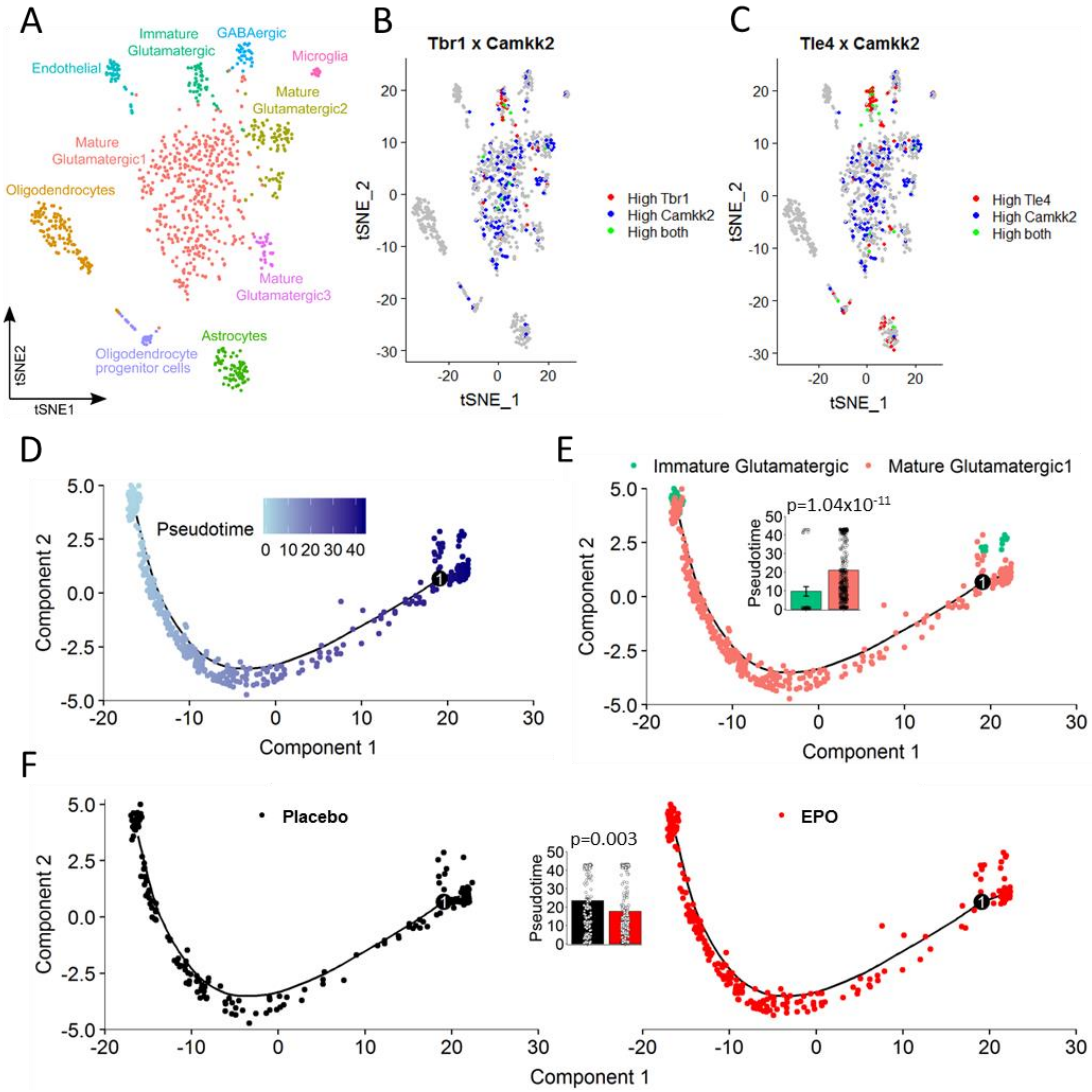

Figure 40. Trajectory analysis (Monocle) demonstrates EPO induced maturation of immature glutamatergic neurons*. (A) Visualization of hippocampal CA1 cell clusters using t-distributed stochastic neighbor embedding (tSNE). Each color represents a cluster of specific cells, characterized by a defined gene expression profile. (B-C) t-SNE plot showing bulk expression of Tbr1 (B), Tle4 (C) and Camkk2 (B-C) genes in all cell clusters of the CA1 (B-C; darker signal correlates to significant expression), where each cell is represented by a dot. Red dot represents cell, which shows the expression of Tbr1 (B) or Tle4 (C), whereas blue dot represents cell, which shows the expression of Camkk2 (B-C). In both cases, green dot represents cell, which express both Tbr1 and Camkk2 (B) or Tle4 and Camkk2 (C). (D) Trajectory analysis in Monocle 2 of cells in the 'Mature Glutamatergic1' and the 'Immature Glutamatergic' cluster colored by pseudotime (the darker the more mature). (E) Trajectory colored by cell identity. Bar graph indicates average pseudotime of the respective clusters. (F) Trajectory colored and split by placebo (black; left) versus EPO treatment (red; right). Bar graph shows average pseudotime of cells in the respective treatment groups. Data represents mean ± SEM. Quantification performed from 3 independent mice and p-values presented via 2-tailed Mann–Whitney U test. This data was generated in collaboration with Agnes Steixner.*

These results suggest that under the influence of EPO, enhanced neuro-differentiation occurs and neurons are present in a continuum, in which immature neurons progressively proceed towards neuronal maturation. This progression is characterized by expression of specific immature neuronal markers such as doublecortin (Dcx), transducin-like enhancer family member4 (Tle4), T-box brain1 (Tbr1), rhabdomyosarcoma 2-associated transcript (Rmst), SRY-Box5 (Sox5) and Stabilin1 (Satb1).

4.2.6. EPO increases the expression of immature neuronal markers such as Tbr1 and Tle4.

Certain immature neuronal markers such as Tbr1 and Tle4 were further analyzed. Tbr1 is a transcription factor expressed in the developing cerebral cortex, hippocampus and olfactory bulb *(Bulfone et al. 1995; Puelles, 2017)*. Méndez-Gómez and co-workers reported that overexpression of Tbr1 promotes generation of glutamatergic neurons without enhancing proliferation (*Méndez-Gómez et al., 2011*). Several reports have demonstrated Tbr1 to be a conserved pallial cell type *(Luzzati, 2015; Puelles, 2017)* as well as Tbr1 expressing cells regarded as conserved endogenous reserve of plastic cells *(Piumatti et al., 2018)*, which mature slowly. Using principle component analysis (PCA), dimensionality reduction by t-distributed stochastic neighbor embedding (tSNE) and clustering, the presence of Tbr1 specifically in immature glutamatergic neuronal cluster was observed as depicted by the feature plot (Fig. 41A). There was an increase in the number of Tbr1 expressing cells in the dissected CA1 upon EPO treatment as compared to the placebo treated CA1 as depicted by the violin plots in the bulk clustering (Fig. 41B) and in immature glutamatergic cluster (Fig. 41C).

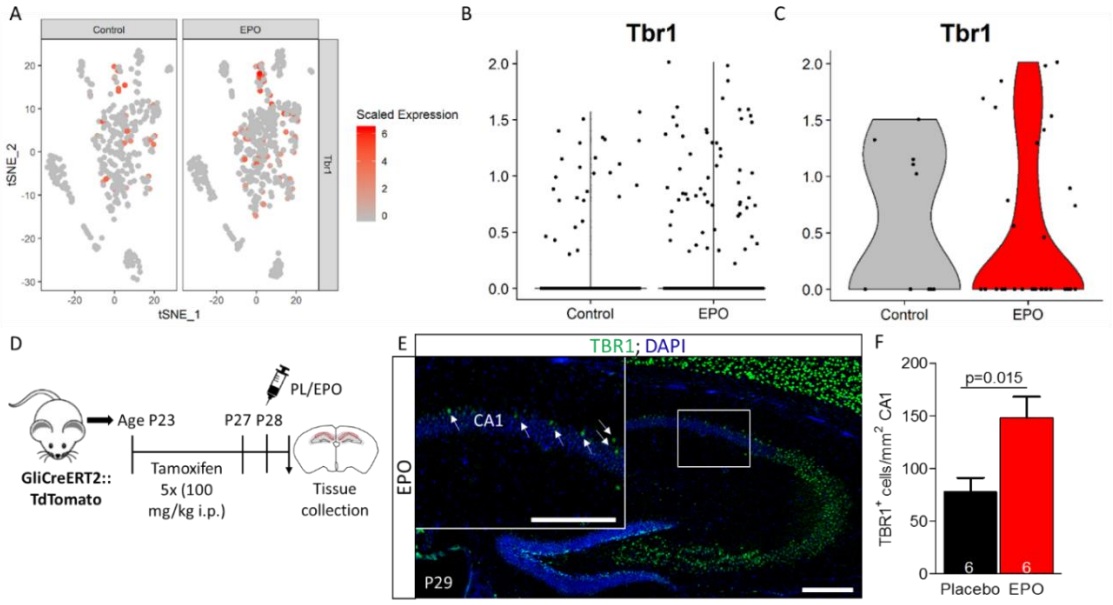

Figure 41. EPO treatment increases the expression of immature neuronal marker gene Tbr1. *(A) t-SNE plot showing bulk expression of Tbr1 gene in all cell clusters of the CA1 (A; darker signal correlates to significant expression), where each cell is represented by a dot. (B-C) Violin plot depicting the bulk expression of Tbr1 in control and EPO treatment in all cell clusters (B) and in the immature glutamatergic cell cluster (C). Data generated from 3 mice per group. (D) Experimental schematic where 5 i.p. injections of tamoxifen were administered in juvenile (P23) mice from P23-P27, followed by either placebo or EPO (1 i.p.) injection. Mice were then sacrificed at P29. (E) Representative image of the hippocampus at P29 of EPO treated GliCreERT2::TdTomato mice, showing positive signal for immature neuronal marker Tbr1 (green). Nuclei were counterstained with DAPI (blue). Insert represents the magnified image of the CA1 region of EPO treated mice, where arrows indicate positive cells. Scale bar: 100µm. (F) Quantification of Tbr1 positive cells/mm^2 at P29 in the CA1 of placebo (black) and EPO (red) treated hippocampi of GliCreERT2::TdTomato mice. Data represents average number of cells/mm^2 ± SEM. Quantification performed from 6 independent mice and p-values presented via unpaired Student's t-test.*

The expression of Tbr1 was further confirmed by immunohistochemistry in GliCreERT2::TdTomato mice after a single injection of EPO at P28 (Fig. 41D). Upon sectioning and staining with a Tbr1 specific antibody (Fig. 41E), a significant increase in the number of Tbr1 positive cells present in the CA1 region of the hippocampus of EPO treated mice was observed as compared to the control placebo treated mice (Fig. 41F).

Another differentially regulated gene in the immature cluster was Tle4. Reports have also demonstrated that Grouncho/Tle4 family, acts in conjunction with sequence specific DNA binding proteins like TCF3, Nanog, Oct4 and Sox2, to repress the embryonic stem cells (ESCs) transcription factor network in order to mediate

differentiation towards multiple lineages (*Laing et al., 2016*). Feature plot depicted the expression of Tle4 in all cell clusters (Fig. 42A), and these cells were increased in the dissected CA1 region upon EPO treatment as depicted by the violin plots in the bulk clustering (Fig. 42B) and immature glutamatergic cluster (Fig. 42C).

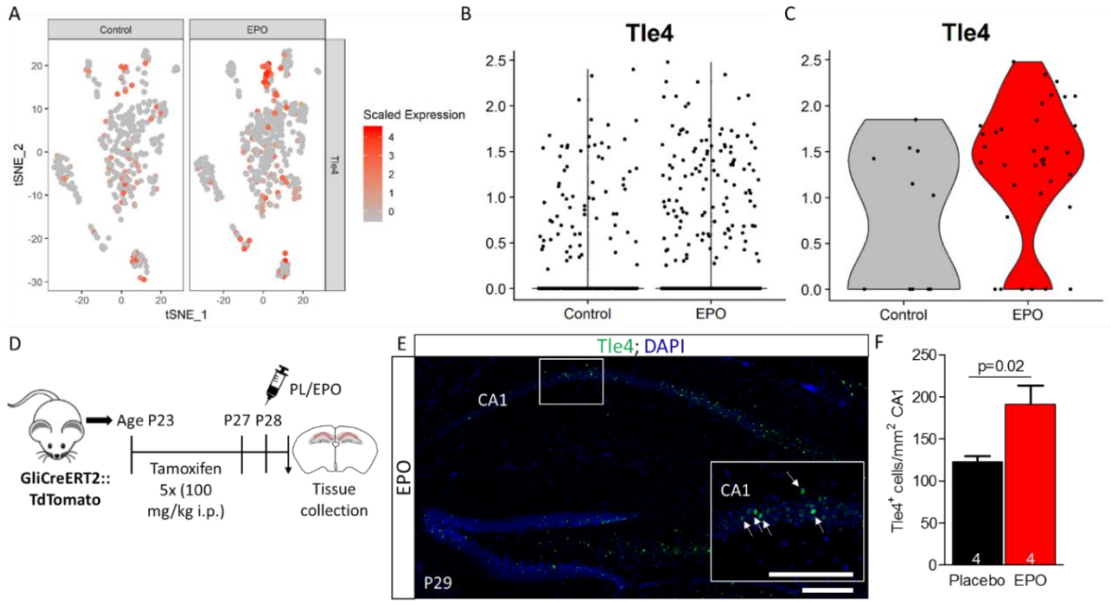

Figure 42. EPO treatment increases the expression of immature neuronal marker gene Tle4. *(A) t-SNE plot showing bulk expression of Tle4 gene in all cell clusters of the CA1 (A; darker signal correlates to significant expression), where each cell is represented by a dot. (B-C) Violin plot depicting the bulk expression of Tle4 in control and EPO treatment in all cell clusters (B) and in the immature glutamatergic cell cluster (C). Data generated from 3 mice per group. (D) Experimental schematic where 5 i.p. injections of tamoxifen were administered in juvenile (P23) mice from P23-P27, followed by either placebo or EPO (1 i.p.) injection. Mice were then sacrificed at P29. (E) Representative image of the hippocampus at P29 of EPO treated GliCreERT2::TdTomato mice, showing positive signal for immature neuronal marker Tle4 (green). Nuclei were counterstained with DAPI (blue). Insert represents the magnified image of the CA1 region of EPO treated mice, where arrows indicate positive cells. Scale bar: 100µm. (F) Quantification of Tle4 positive cells/mm^2 at P29 in the CA1 of placebo (black) and EPO (red) treated hippocampi of GliCreERT2::TdTomato mice. Data represents average number of cells/mm^2 ± SEM. Quantification performed from 6 independent mice and p-values presented via unpaired Student's t-test.*

Similar treatment scheme was followed for Tle4 quantification (Fig. 42D), and sections were stained using a Tle4 specific antibody (Fig. 42E). Here, a significant increase in the number of Tle4 positive cells in the CA1 of EPO treated mice was observed as compared to the placebo treated mice (Fig. 42F).

4.2.7. EPO increases the expression of Lnc-RNA 'RMST' in immature glutamatergic neuronal cluster.

As reported by *Hsieh and Gage, 2005* and *Yao et al., 2016*, a tight regulation of the transcriptional and epigenetic program appears to be an important player in maintaining NPCs. Moreover, transcription factors such as Sox2, Pax6, Tlx1 and REST are identified to cooperate with stage specific cofactors to induce cell fate commitment and specification. More importantly, Sox2 cooperation with various cofactors depends on the stage of that particular cell. Lodato and colleagues demonstrated that Sox2 cooperates with Oct4 in embryonic stem cells *(Lodato et al., 2013)* as well as a long non-coding RNA (lncRNAs) `RMST` to control transcriptional programs in stem cells to induce neuro-differentiation *(Ng et al., 2013)*. These publications, thereby, provide insight on relationship between Sox2 and its partners in a specifying cell state.

Using a genome-wide approach to screen for neurogenic lncRNAs, rhabdomyosarcoma 2-associated transcript (RMST) as a lncRNA required for neuronal differentiation was previously identified *(Ng & Stanton, 2013)*. RMST associated with Sox2 *(Ng et al., 2013)*, which is one of the important transcription factors controlling the fate of neural stem cells (NSCs). Therefore, this study decided to elucidate the role of RMST in modulating neurogenesis under the influence of EPO. To achieve this, similar clustering for RMST expressing cells was performed (Fig. 43A), and observed that these cells were increased in the dissected CA1 region upon EPO treatment as depicted by violin plots in the bulk clustering (Fig. 43B) and immature glutamatergic cluster (Fig. 43C), highlighting a central role for concerted Sox2-partner relationships in specifying cell state.

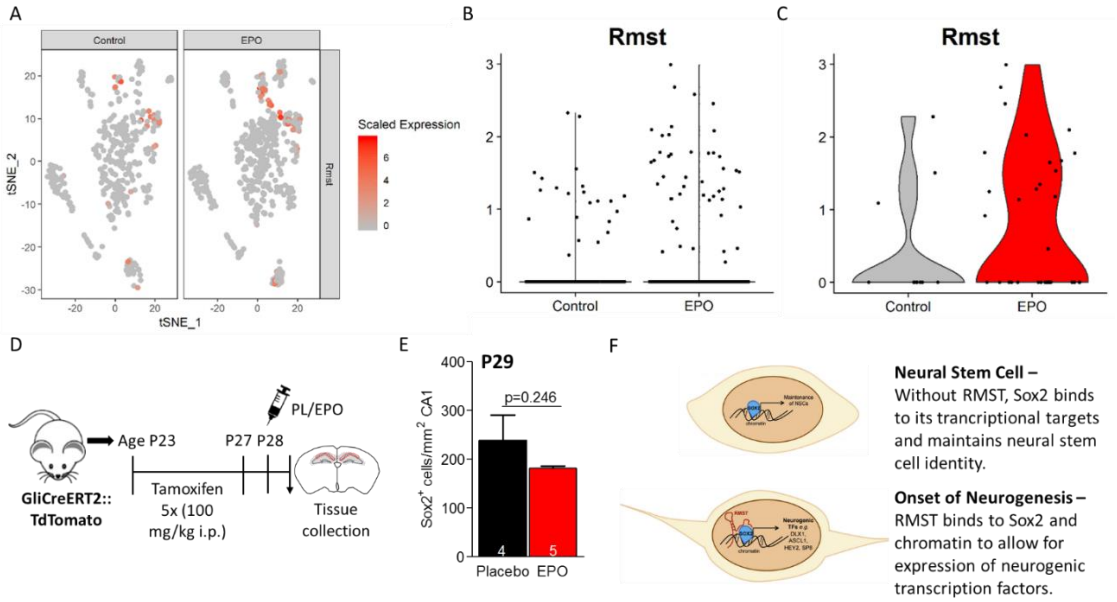

Figure 43. EPO treatment increases the expression of long noncoding RNA `RMST`.
(A) t-SNE plot showing expression of RMST in the cell clusters of the CA1 (A; darker signal correlates to significant expression), where each cell is represented by a dot. (B-C) Violin plot depicting the expression of RMST in control and EPO treatment in all cell clusters (B) and in the immature glutamatergic cell cluster (C). Data generated from 3 mice per group. (D) Experimental schematic where 5 i.p. injections of Tamoxifen were administered in juvenile (P23) mice from P23-P27, followed by either placebo or EPO (1 i.p.) injection. Mice were then sacrificed 6 hours later at P29. (E) Quantification of Sox2 positive cells/mm^2 at P29 in the CA1 of placebo (black) and EPO (red) treated hippocampi of GliCreERT2::TdTomato mice. Data represents average number of cells/mm^2 ± SEM. Quantification performed from 4-5 independent mice and p-values presented via unpaired Student's t-test. (F) Representative schematics demonstrating the association of RMST and Sox2 (adapted and modified from Ng et al, 2013).

As RMST is a long noncoding RNA, there are no antibodies available for immunohistochemical analysis, this study decided to determine the effect of EPO on Sox2 positive cells at a similar time (i.e. after 6 hours). Similar treatment scheme (Fig. 43D) was followed, and sections were stained using a Sox2 specific antibody. Upon quantification, a trend in decrease in the number of Sox2 positive cells in the CA1 of EPO treated mice was quantified as compared to the placebo treated mice (Fig. 43E). This is intriguing as RMST is known to interact with Sox2 and this RNA-protein complex activates the promoter of other neurogenic genes (*Ng et al., 2013*; Fig. 43F).

Other interesting markers for this study were Doublecortin (DCX), Special AT-rich DNA binding protein 1 (Satb1) and SRY-Box5 (Sox5). Dcx, facilitates microtubule

polymerization and is expressed in migrating neuroblasts and immature neurons *(Brown et al., 2003)*. Satb1 forms a positive regulatory loop with HuD, activating NeuroD1 transcription and thereby promoting neuronal differentiation *(Wang et al., 2015)*. Moreover, Sox5 cooperates with Tbr1 to regulate early born neurons during embryonic development and form a part of the same transcriptional network *(Bedogni et al., 2010)*. Other markers like DCX (Fig. 44A), Satb1 (Fig. 44D) and Sox5 (Fig. 44G) revealed that these markers were present in most of the cell clusters (Fig. 44B; 44E; 44H), with specifically more expression in immature glutamatergic cell cluster (Fig. 44C; 44F; 44I).

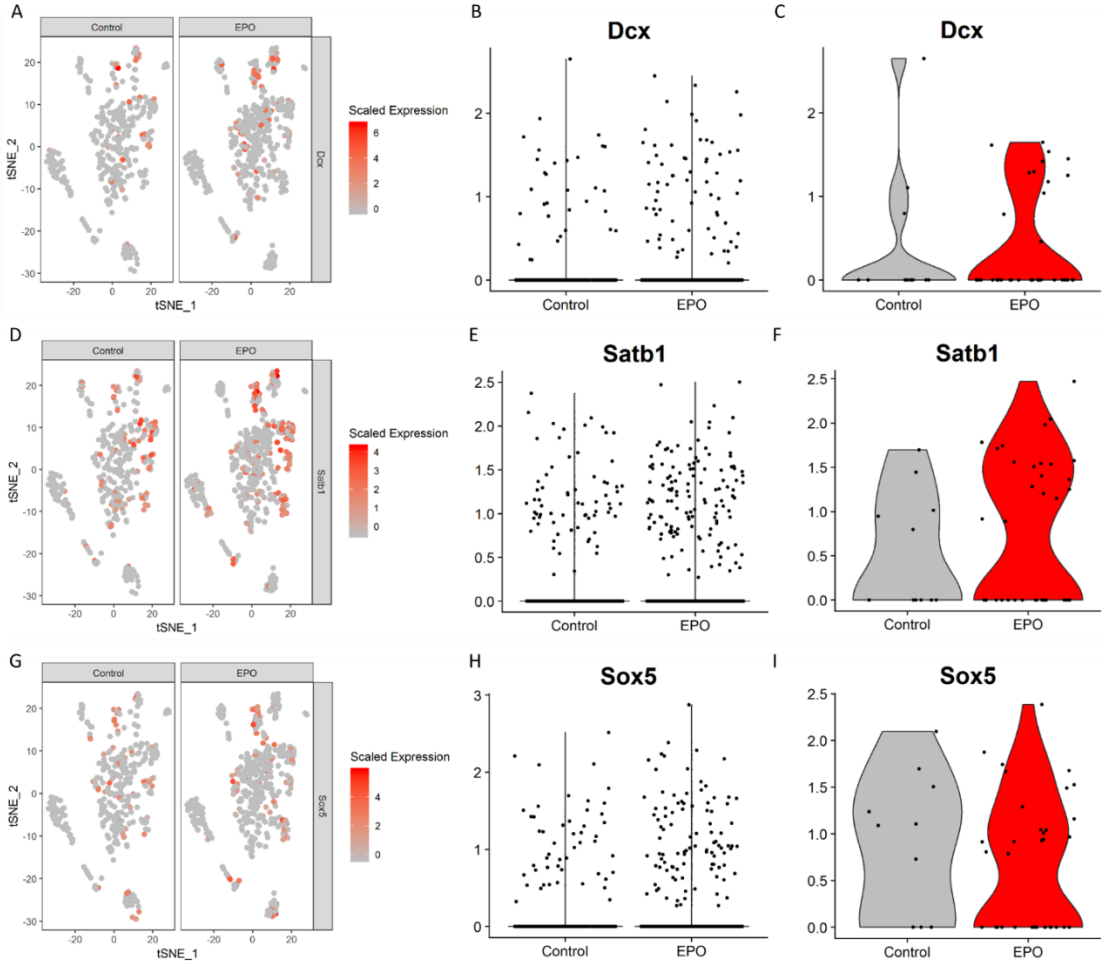

Figure 44. EPO treatment increases the expression of immature neuronal marker gene Dcx, Satb1 and Sox5. *(A; D; G) t-SNE plot showing bulk expression of Dcx (A), Satb1 (D) and Sox5 (G) genes in all cell clusters of the CA1 (A, D, G; darker signal correlates to significant expression), where each cell is represented by a dot. (B-C; E-F; H-I) Violin plot depicting the bulk expression of Dcx (B-C), Stab1 (E-F) and Sox5 (H-I) in control and EPO treatment in all cell clusters (B, E, H) and in the immature glutamatergic cell cluster (C, F, I). Data generated from 3 mice per group.*

Drop-Seq data largely corresponded with the proportion of different cell types revealed by staining. Taken together, this data provides supportive evidence of an immediate effect of EPO on pre-existing precursors to instantaneously initiate neuronal differentiation, thereby rapidly increasing the number of immature glutamatergic neurons in the CA1 region of the hippocampus. EPO and EPOR were not detected by scRNA-Seq due to their very low expression level, a known dropout effect in scRNA-Seq data.

4.3. Effect of EPO and Hypoxia on cognitive learning.

4.3.1. Elevated expression of EPO and EPOR in pyramidal neurons upon Complex Running Wheel (CRW).

Drop-Sequencing analysis is known to have dropout effects if a certain transcript is expressed in low amounts. This could be the reason why the expression of EPO and EPOR could not be detected. Therefore, an older yet highly sensitive approach of mRNA detection i.e. *in-situ* hybridization was employed. Based on the previous results, exogenous EPO induced enhancement in cognition was observed and therefore, this present study decided to explore the physiological significance of this potent effect. As it is unlikely that an organism possesses receptors and downstream mechanisms just for exogenous compounds, our group wondered whether EPO and/or EPOR are expressed in pyramidal neurons. Moreover, this thesis also decided to explore if a learning task like Complex Running Wheel (CRW) could endogenously boost EPO and/or EPOR. This could possibly provide an explanation for the improved cognition upon physical training as suggested by several publications *(Dustman et al., 1984; Gomez-Pinilla & Hillman, 2013; Kramer & Erickson, 2007; Lautenschlager & Almeida, 2006; Voelcker-Rehage & Niemann, 2013)*. It has also been reported that physical training reduces the risk for memory deficits and dementia in older adults *(Brown et al., 2013; de Bruijn et al., 2013; Larson et al., 2006; Rovio et al., 2005; van Gelder et al., 2004)*. Results from rodent studies have shown that voluntary wheel running increases neurogenesis and cell proliferation in hippocampal dentate gyrus in elderly rats *(Eadie et al., 2005; van Praag et al., 2005)*. However, the mechanisms responsible for the improvement in cognition has not been well delineated. As opposed to normal running wheels, complex running wheel (CRW) *(Liebetanz & Merkler, 2006)*, are wheels wherein the bars are irregularly spaced and the running mice are required to learn the pattern on the wheel to perform better. Therefore, WT mice were employed at P55 and exposed them to either running on CRW or without running for 5 hours, 9 hours or 13 hours (Fig. 45A). The mice were then sacrificed immediately after their running period. A highly sensitive *in-situ* hybridization method was used, which is capable of detecting even single mRNA molecules. The expression of EPO and EPOR mRNA was observed in pyramidal neurons of the CA1 region of the hippocampus (Fig. 45B).

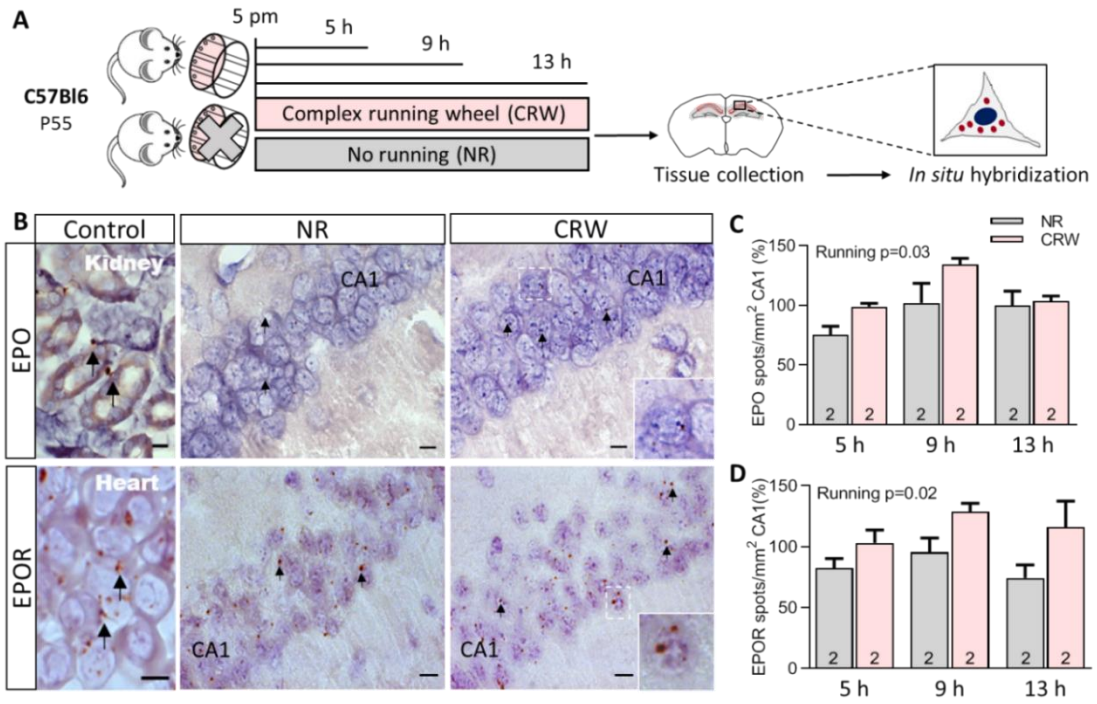

Figure 45. EPO increases the local expression of EPO/EPOR in pyramidal neurons in the CA1 region of the hippocampus. *(A) Experimental schematic of wildtype C57Bl6 mice exposed to no running (NR) or voluntary running on CRW at P55 for 5h, 9h or 13h. Mice were sacrificed at the respective time points and in-situ hybridization was performed on CA1 regions. (B) Representative in-situ hybridization images of CA1 regions of non-runners (NR) and runners (CRW) showing EPO and EPOR mRNA expression in pyramidal neurons as indicated by the brown spots. As positive controls for EPO/EPOR mRNA expression, sections of kidney (P55) and heart (E14.5) from wildtype C57Bl6 mice are presented. Scale bars: 10µm; for heart 5µm. (C-D) Quantification of total number of EPO (C) or EPOR (D) mRNA spots in CA1 of non-runners (NR) and runners (CRW), shown at 5h, 9h and 13h. Data represents average number of spots ± SEM. Quantification performed from 2 independent mice and p-values presented via two-way ANOVA.*

The mRNA expression of EPO and EPOR is reported to be very high in kidney *(Lacombe et al., 1988; Semenza et al., 1991)* and heart *(Ruifrok et al., 2008)* and therefore, their sections were used as positive controls (Fig. 45B). Upon quantification, 5-9 hours of running significantly increased the number of EPO (Fig. 45C) and EPOR (Fig. 45D) transcripts in running mice as compared to the non-running mice. Interestingly, the overall abundance of positive EPO and EPOR spots was most prominent in the *cornu ammonis* and *gyrus dentatus* but much lower in cortex and other brain regions *(data not shown)*.

4.3.2. Hypoxia inducible gene EPO and its EPOR are master regulators of enhanced learning.

First evidence of an increase in the immature neuronal markers in the CA1 like Tbr1, Dcx after a single dose of EPO was observed by single cell sequencing (Fig. 41 – Fig. 43). These represented a continuum of maturing neurons as seen by the monocle analysis (Fig. 40). Continued EPO treatment for three weeks led to an increase in mature neuronal numbers (Fig. 33) and increase in synaptic plasticity (Fig. 34). Along with these results, complex learning tasks were able to induce the expression of EPO and EPOR (Fig. 45). Moving forward, the present work wanted to decipher if these potent effects would translate into improved learning in mice treated with EPO. To determine the potential of EPO to improve cognitive performance, juvenile WT and NexCre::EPOR-KO mice were treated according to our treatment regime (Fig. 46A) where placebo or EPO was administered intraperitoneally every other day for 3 weeks, followed by a 1-week break. After the break at P55, the running-naive mice were transferred to cages containing CRW (Fig. 46B). The description of the method of generation of NexCre::EPOR-KO mice is shown below in section 4.3.5. Briefly, there is a knockdown of EPOR specifically in mature pyramidal neurons of the CA1 region of the hippocampus in these mice. However after treated with EPO, a rise in performance of EPO treated mice was observed as compared to placebo treated mice (Fig. 46C). This rise in performance was followed by a significant enhanced endurance over the whole night. However, in NexCre::EPOR-KO, EPO treatment did not show any increase in the learning and performance (Fig. 46D) as compared to placebo treated mice.

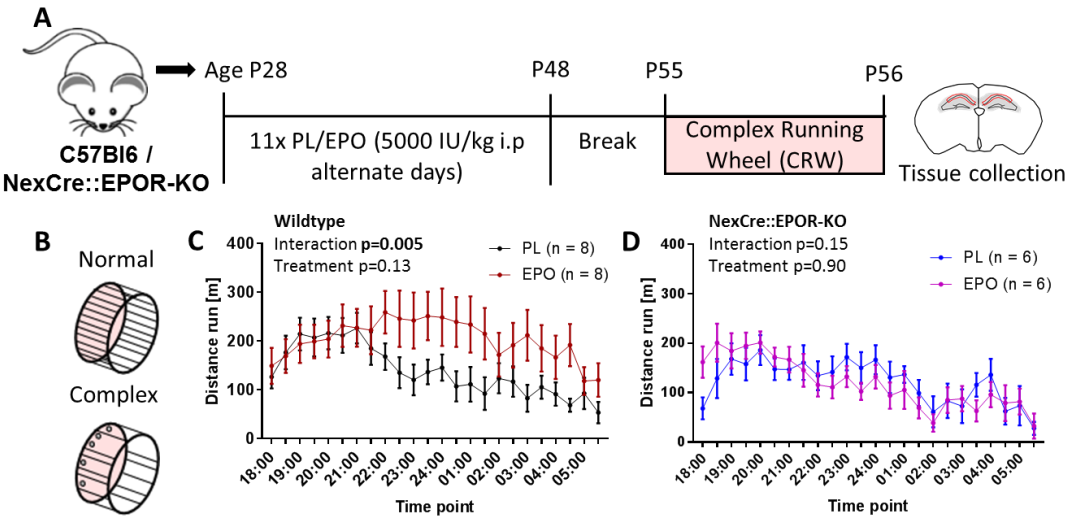

Figure 46. Learning improved upon EPO treatment. *(A) Experimental schematic to determine the effect of EPO on CRW learning. Wildtype or NexCre::EPOR-KO mice (at P28) were treated with placebo or EPO (11x i.p.) on alternate days for 3 weeks, and after 1 week of break, exposed to CRW. (B) Schematic image of standard v/s Complex Running Wheel (CRW). (C-D) Total distance run by placebo (black) and EPO (red) treated Wildtype (C) and NexCre::EPOR-KO (D) mice over the first night. Data represents average mean ± SEM. Quantification performed from 6-8 independent mice and p-values presented via two-way ANOVA. This data was generated in collaboration with Franziska Scharkowski.*

The endurance shown by EPO treated mice remained superior to the placebo treated mice over several nights *(data not shown)*. As presented in literature *(Noakes et al., 2005)*, the EPO induced increase in hematocrit, also known as `blood doping` could have contributed to the observed enhancement in performance of EPO treated mice. However, as seen by the pyramidal neuron specific knockout in Fig. 46D, this was not the case.

4.3.3. Labelling of increased hypoxic neurons in the CA1 upon CRW.

After discovering that CRW led to an increase in the endogenous EPO expression (Fig. 45), the present work decided to gain further mechanistic insight into its physiological relevance. The present work decided to focus on EPO regulation, where the underlying mechanism responsible for the upregulation of EPO in pyramidal neurons upon CRW exposure was studied. EPO was the first target gene to be identified for hypoxia-inducible factor-1 (HIF-1; *Semenza and Wang, 1992*) and is one of the best-characterized genes activated by reduced oxygen levels *(Wenger, 2002)*. Hypoxia, via hypoxia-inducible factor (HIF), has been reported to induce EPO expression in various cell types *(Jelkmann, 2007; 2011; Kietzmann et al., 2016; Krantz, 1991; Noguchi et al., 2008; Sargin et al., 2010; Sirén et al., 2009)*. A hypothesis was considered where cognitive challenge/learning of complex tasks would require more oxygen than provided steady state. This requirement of more oxygen could induce endogenous physiological hypoxia, which acts as the driving force for upregulating the endogenous EPO system in pyramidal neurons. Therefore, to prove this hypothesis, a transgenic mouse was employed, expressing a chimeric protein in which the oxygen-dependent degradation (ODD) domain of Hif-1α is fused to the tamoxifen-inducible CreERT2 recombinase *(Kimura et al., 2015)*. The CreERT2-ODD mice after crossing with R26R-TdTomato reporter mice would label every cell undergoing or responsive to hypoxia.

These CAGCreERT2-ODD::TdTomato mice (at P55) were first treated with a single injection of Tamoxifen (100mg/kg) and exposed to either overnight running on CRW or no running as controls (Fig. 47A). The mice were then sacrificed. The brains were isolated and sectioned. Upon staining with a neuronal marker NeuN (white) and TdTomato (red; Fig. 47B), labelled pyramidal neurons were observed, for the first time, to be present in a physiological hypoxic condition.

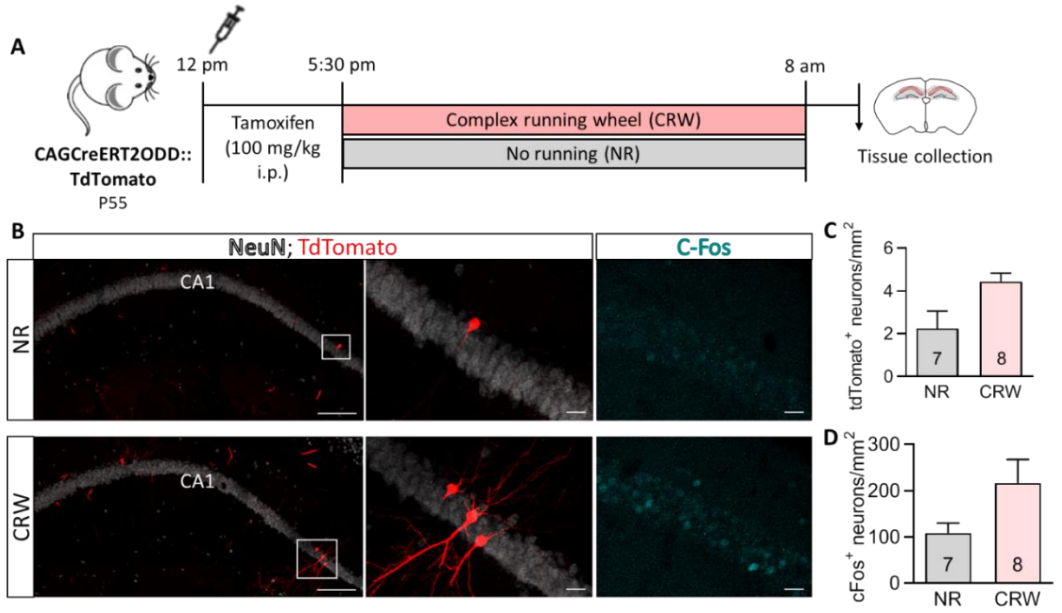

Figure 47. Voluntary running induces hypoxia in pyramidal neurons. *(A) Experimental schematic to determine the effect of running on the induction of hypoxia in the pyramidal neurons of CA1 region. CAGCreERT2-ODD:TdTomato mice were administered tamoxifen at P55 of age and exposed to either no running (NR) or overnight voluntary running (CRW). (B) Representative images of neuronal marker NeuN (white), TdTomato (red; labeling hypoxia) and C-Fos (cyan) in non-runner (NR) and runner mice (CRW). Scale bars in (B): 100µm, 10µm. (C-D) Quantification of hypoxic neurons (TdTomato$^+$) and active neurons (C-Fos$^+$) in CA1 is presented for NR or CRW over one night. Data represents average number of cells ± SEM. Quantification performed from 7-8 independent mice and p-values presented via two-way ANOVA. This data was generated in collaboration with Umer Butt.*

Upon quantification of these hypoxic pyramidal neurons, the complex wheel running over one night increased the number of 'ODD-labelled' pyramidal neurons in CA1, indicating more hypoxic neurons in animals subjected to learning of a new challenging task. (Fig. 47C). Moreover, CRW induced tendency in increased neuronal activity in the pyramidal layer (Fig. 47D) marked by the early neuronal activity marker C-Fos (cyan; Fig. 47B) was also observed.

4.3.4. Exogenous mild hypoxia acts synergistically with CRW on generation of pyramidal neurons in the CA1.

Learning to run on CRW led to relative endogenous hypoxia in pyramidal neurons as demonstrated by ODD-labeling (Fig. 47) along with upregulated EPO and EPOR mRNAs transcripts (Fig. 45) in the pyramidal neurons. Although, this short learning exposure was sufficient to cause relative endogenous hypoxia, it was not sufficient for long lasting plasticity as seen by a tendency in the C-Fos expression (Fig. 47). Therefore, whether CRW exposure for a few weeks (instead of EPO treatment) could lead to an increase in the number of pyramidal neurons, and whether sustained application of mild exogenous hypoxia in combination with running would result in similar or even synergistic effects, i.e. better learning performance together with increased neurons in the *stratum pyramidale* remained to be determined. To achieve this, NexCreERT2::TdTomato mice were employed and treated them with Tamoxifen (100mg/kg, P23-P25). From P28-P48, these mice were kept in cages with normoxic or hypoxic (12% O2) conditions (Fig. 48A). After 1-week break, these mice were exposed to either running on CRW or no running for 4 hours at the start of their night phase before sacrificing them. Immediately afterwards, the brains were processed for immunohistochemistry. Upon sectioning, staining and quantification, a significant increase in the newly formed neurons upon running was observed, which was further enhanced by exposure to mild hypoxia (Fig. 48B).

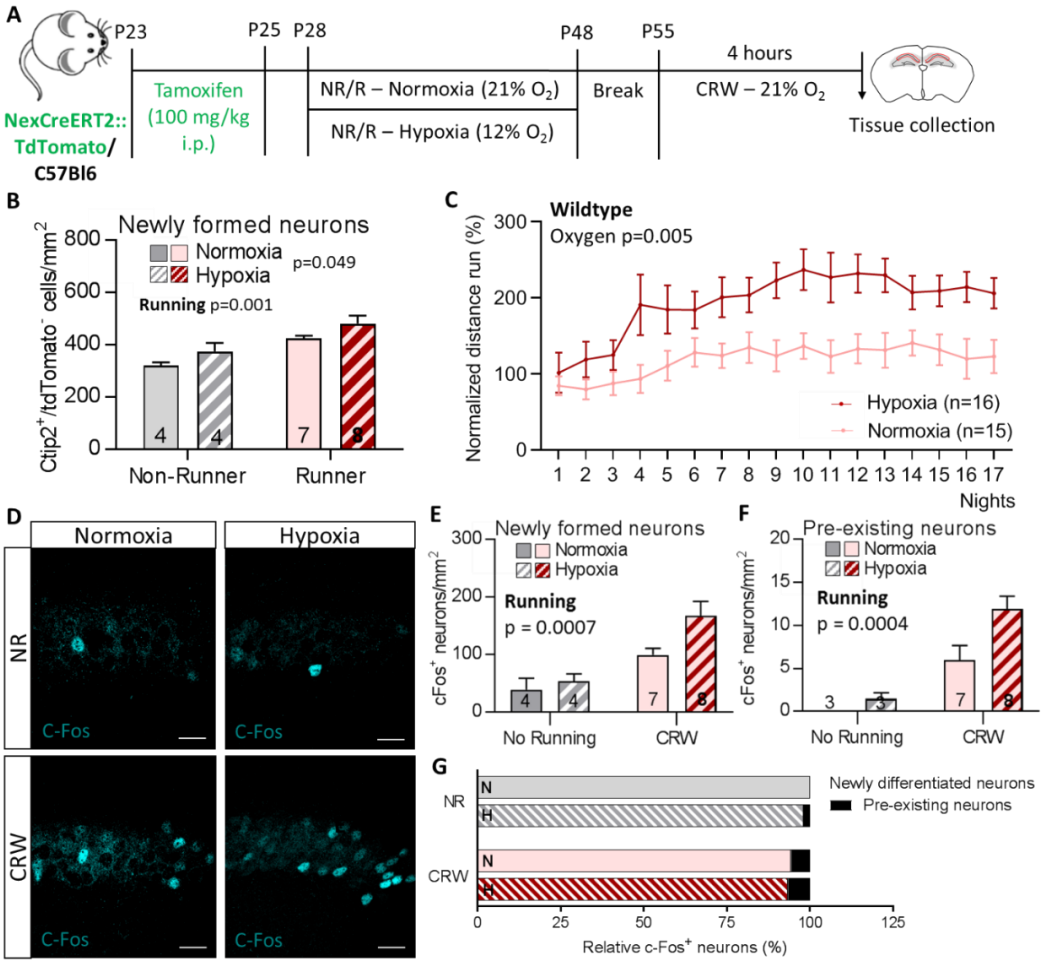

Figure 48. Voluntary running induced hypoxia gives rise to new pyramidal neurons in CA1 region. *(A) Experimental schematic to determine the effect of endogenous hypoxia on learning. NexCreERT2:TdTomato mice at P23 were injected with tamoxifen (5x i.p.) and then at P28 were exposed to NR or CRW under normoxia (21%O_2) or hypoxia (12%O_2) for 3 weeks. After 1 week of break, CRW mice were again exposed to voluntary CRW for 4h before being sacrificed at P55. (B) Quantification of newly formed neurons (Ctip2+/TdTomato-) in NR and CRW mice exposed to either normoxia or hypoxia. (C) Wildtype mice at P28 were exposed to the same experimental paradigm as shown in (A). Percent of distance run per night (normalized to mean distance run over first 3 nights) over 17 nights by WT mice exposed to either normoxia or hypoxia. (D) Representative images of active C-Fos+ neurons (cyan) in NR and CRW mice exposed to normoxia or hypoxia. Scale bars: 25µm. (E-F) Quantification of active neurons among pre-existing (F) neurons ($cFos^+/Ctip2^+/tdTomato^+$) and among newly formed (E) neurons ($cFos^+/Ctip2^+/tdTomato^-$) in CA1 region of the mice. (G) Presentation of the small percentage of pre-existing neurons among C-Fos^+ neurons. Data represents the average number of cells ± SEM. Quantification performed from 3-8 independent mice and p-values presented via 2-tailed student's t-test (E-F) or two-way repeated measures ANOVA (B-C).*

In parallel to understanding these effects, the WT mice were also monitored for their learning performance via CRW. Here, a significant improvement in motor learning/endurance in mice exposed to hypoxic conditions was observed as compared

to normoxic over three weeks (Fig. 48C). To determine the functionality of the newly differentiated/matured neurons following exposure to CRW cages with or without hypoxia for 3 weeks, the CA1 region of the hippocampus was stained with C-Fos (Fig. 48D), which is used as a readout of neuronal activity *(Morgan et al., 1987)*. A significant increase in the number of C-Fos positive neurons following running was observed, which was further enhanced by exposure to mild hypoxia (Fig. 48E). Unexpectedly, C-Fos expression was primarily detected in recently differentiated neurons (Fig. 48E), whereas the fraction of pre-existing neurons expressing C-Fos was relatively smaller (Fig. 48F; 48G).

4.3.5. Targeted deletion of EPO and EPOR in pyramidal neurons attenuates hypoxia-induced motor learning and endurance.

To pinpoint the importance of EPOR in pyramidal neurons for the enhanced motor learning and endurance, mice with targeted knockout of EPOR in pyramidal neurons were generated (NexCre::EPOR$^{fl/fl}$; as termed as EPOR-cKO). To generate this mouse model, the present work first validated whether the generated EPOR-cKO mice was indeed a functional knockout. Therefore, the female EPOR$^{fl/fl}$ mice was cross-bred with male mice homozygous for the Cre-recombinase gene under the control of the adenovirus EllA-promoter, which was used as a deleter mice. EllA-regulated Cre-recombinase was expressed in pre-implantation embryos leading to site specific deletion of LoxP flanked (fl) sequence in all tissues including the germ cells. This cross breeding generated the first familial generation (F1) of pups consisting of one EPOR allele with wild-type sequence (EPOR$^{+/+}$) and one EPOR deleted allele (EPOR$^{+/del}$). Since the EPOR$^{+/del}$ allele was present in the germ cells, a F2 cross resulted in pups possessing all possible genotypes (EPOR$^{+/+}$; EPOR$^{+/del}$ and EPOR$^{del/del}$). Interbreeding of these first generation progenies resulted in efficient germ line transmission of the deletion to subsequent generations. The presence of deleted alleles were determined by PCR based genotyping using specific primers as listed in Methods (Fig. 49B). As global deletion of EPOR is known to be lethal by E13.5 *(Lin et al., 1996; Wu et al., 1995)*, the global EPOR-cKO embryos at E12.5 were observed to be smaller and without vasculature due to the global knockout as compared to their WT littermates (Fig. 49A). A global EPOR-cKO was observed at E12.5, thereby validating the functionality of the

generated EPOR-cKO mice. After validation, the $EPOR^{fl/fl}$ mice were cross-bred with a Cre-recombinase mouse under the control of Nex promoter. This cross breeding resulted in a conditional deletion of EPOR specifically in mature pyramidal neurons. Since previously, an improved learning performance of WT mice on CRW was observed, this thesis considered a hypothesis whether this effect is attenuated with the conditional knockout of EPOR in pyramidal neurons. To achieve this, NexCre::EPOR-KO mice were exposed to CRW in normoxic or hypoxic conditions from P28-P48 followed by 1-week break (Fig. 49C; 49H).

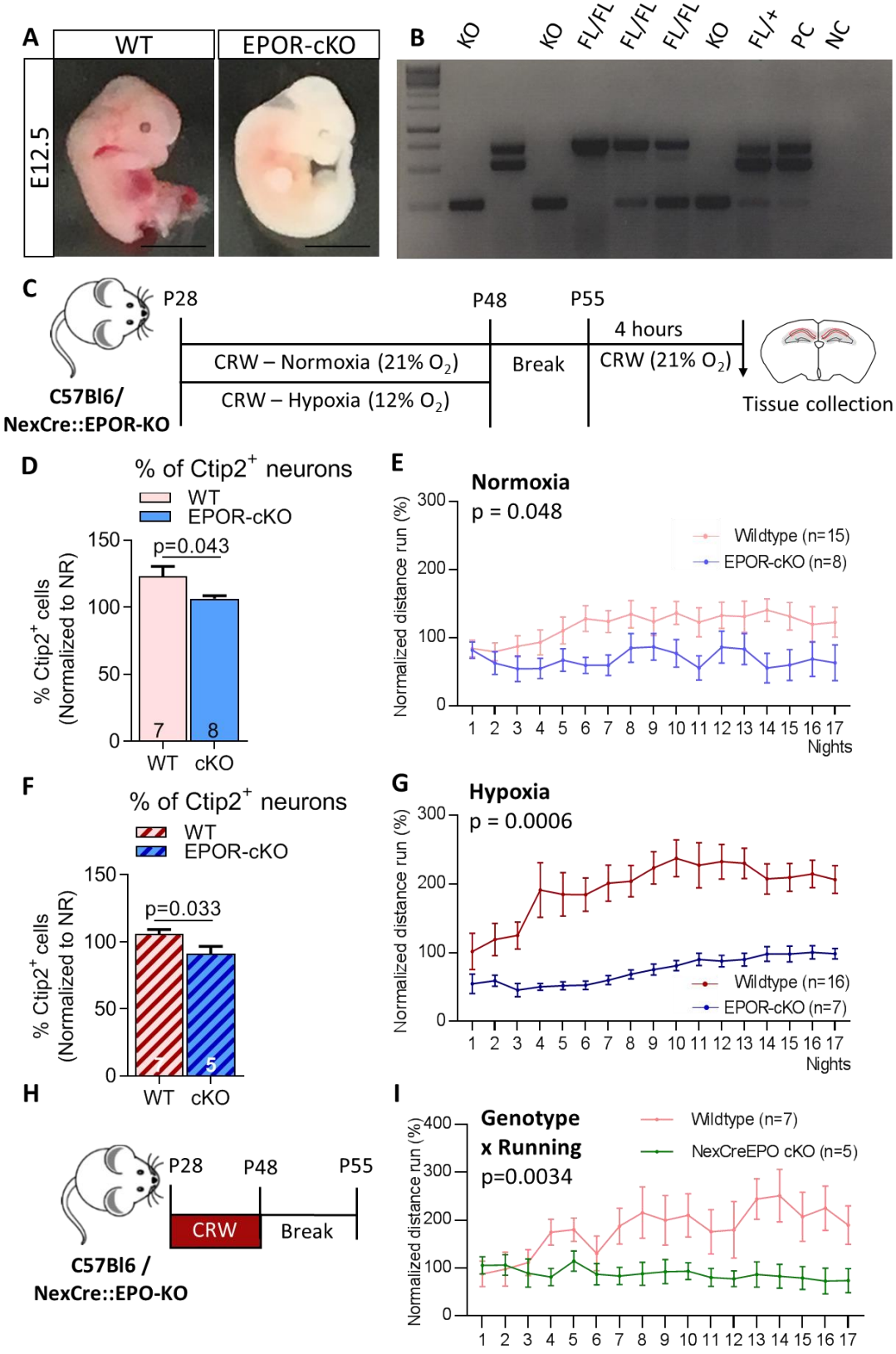
A
WT
EPOR-cKO
E12.5
B
KO
KO
FL/FL
FL/FL
FL/FL
KO
FL/+
PC
NC
C
P28
P48
P55
CRW – Normoxia (21% O2)
CRW – Hypoxia (12% O2)
Break
4 hours
CRW (21% O2)
Tissue collection
C57Bl6/
NexCre::EPOR-KO
D
% of Ctip2+ neurons
WT
EPOR-cKO
p=0.043
% Ctip2+ cells
(Normalized to NR)
WT
cKO
E
Normoxia
p = 0.048
Wildtype (n=15)
EPOR-cKO (n=8)
Normalized distance run (%)
Nights
F
% of Ctip2+ neurons
WT
EPOR-cKO
p=0.033
G
Hypoxia
p = 0.0006
Wildtype (n=16)
EPOR-cKO (n=7)
H
P28
P48
P55
CRW
Break
C57Bl6 /
NexCre::EPO-KO
I
Genotype
x Running
p=0.0034
Wildtype (n=7)
NexCreEPO cKO (n=5)

Figure 49. Voluntary running induced learning is mediated by EPOR. *(A) Representative pictures of Wildtype and E2A-Cre global KO in e12.5 embryos. Scale bars: 25µm. (B) Genotyping results depicts the functional KO using specific primers. (C) Experimental schematic to determine the effect of endogenous hypoxia on learning. WT and NexCre::EPOR-KO mice (at P28) were exposed to NR or CRW under normoxia (21%O_2) or hypoxia (12%O_2) for 3 weeks. After 1 week of break, CRW mice were again exposed to voluntary CRW for 4h before being sacrificed at P55. (D; F) Quantification of Ctip2 positive neurons (normalized to their respective NR controls) present in the CA1 region of the hippocampus of runner (CRW) exposed to either normoxic (D) or hypoxic (F) condition. Data represents average number of cells ± SEM per mm^2. Quantification performed from 3-8 independent mice and p-values presented via unpaired Student's t-test. (E; G) Percent of distance run per night (normalized to mean distance run over the first 3 nights) over 17 nights by WT and NexCre::EPOR-KO (in collaboration with Franziska Scharkowski) mice exposed to normoxia or hypoxia. Data presented as mean ± SEM. Quantification performed from 7-16 independent mice and p-values presented via 2-way repeated measures ANOVA. (H) Experimental schematic to determine the effect of endogenous hypoxia on learning. WT and NexCre::EPO-KO mice (at P28) were exposed to CRW for 3 weeks. After 1 week of break, the mice were sacrificed at P55. (I) Percent of distance run per night (normalized to mean distance run over the first 3 nights) over 17 nights by WT and NexCre::EPO-KO mice. Data presented as mean ± SEM. Quantification performed from 5-7 independent mice and p-values presented via 2-way repeated measures ANOVA.*

A significant reduction in the number of neurons (normalized to their respective NR controls) in the CA1 of NexCre::EPOR-KO mice was quantified as compared to wild-type mice exposed to either normoxic (Fig. 49D) or hypoxic conditions (Fig. 49F). Subsequently, lack of EPOR in pyramidal neurons resulted in a distinct and significant reduction of the learning curve slope over time in normoxic (Fig. 49E) as well as hypoxic conditions (Fig. 49G) compared to the respective WT controls. To further pinpoint that this enhanced learning is due to the EPO present within pyramidal neurons, NexCRE::EPO-KO mice were generated. These mice consisted of knockout of EPO specifically in pyramidal neurons. These mice along with control wild-type were subjected to endogenous hypoxia via complex running wheel. Similar to results observed in NexCre::EPOR-KO mice, significant defects in learning in NexCre::EPO-KO mice (Fig. 49I) were observed as compared to the wild-type mice. Together, these data suggests the importance of EPO and EPOR expression in pyramidal neurons to enhance learning in mice.

Discussion

5. Discussion.

Although several reports have provided individual facets of the brain EPO system, the overall view was lacking. This work contributes to the broader view by providing evidence of a novel role of EPO as a potent growth factor, which acts as a local mediator of neuronal adaptation, presumably in response to increased network activity. A new working model is proposed where cognitive challenge leads to physiological hypoxia which upregulates EPO expression in the pyramidal neurons. This induced endogenous hypoxia leads to enhanced dendritic spine growth and precursors to differentiate into neurons. This observation of substantial numbers of newly generated pyramidal neurons without proliferation may change our present concepts of adult hippocampal neurogenesis.

5.1. Role of EPO on neuronal precursors situated in adult hippocampus.

After reports from our group demonstrating the positive effect of EPO on improved cognition in man *(Ehrenreich et al., 2004; Ehrenreich et al., 2002)* and mouse *(Hassouna et al., 2016)*, our group tapped by serendipity into EPO mediated neuronal differentiation. This provided evidence that EPO treatment induced an increase in the number of pyramidal neurons and oligodendrocytes in the CA1 region of the hippocampus. Lineage tracing of newly differentiated oligodendrocytes enabled us to pinpoint the effect of EPO on NG2 positive precursors leading to their differentiation *(Hassouna et al., 2016)*. Therefore, the obvious question was to determine which neuronal precursors could give rise to EPO mediated neuronal differentiation. Although the genetic identity of EPO responsive precursors is an important aspect, the complex nature of the neuronal lineage (Fig. 50; *Rushing & Ihrie, 2016*) and the technical pitfalls precludes this thesis to make a strong conclusion. In the past, multiple transgenic mouse models of known marker proteins/genes have been developed to address similar questions.

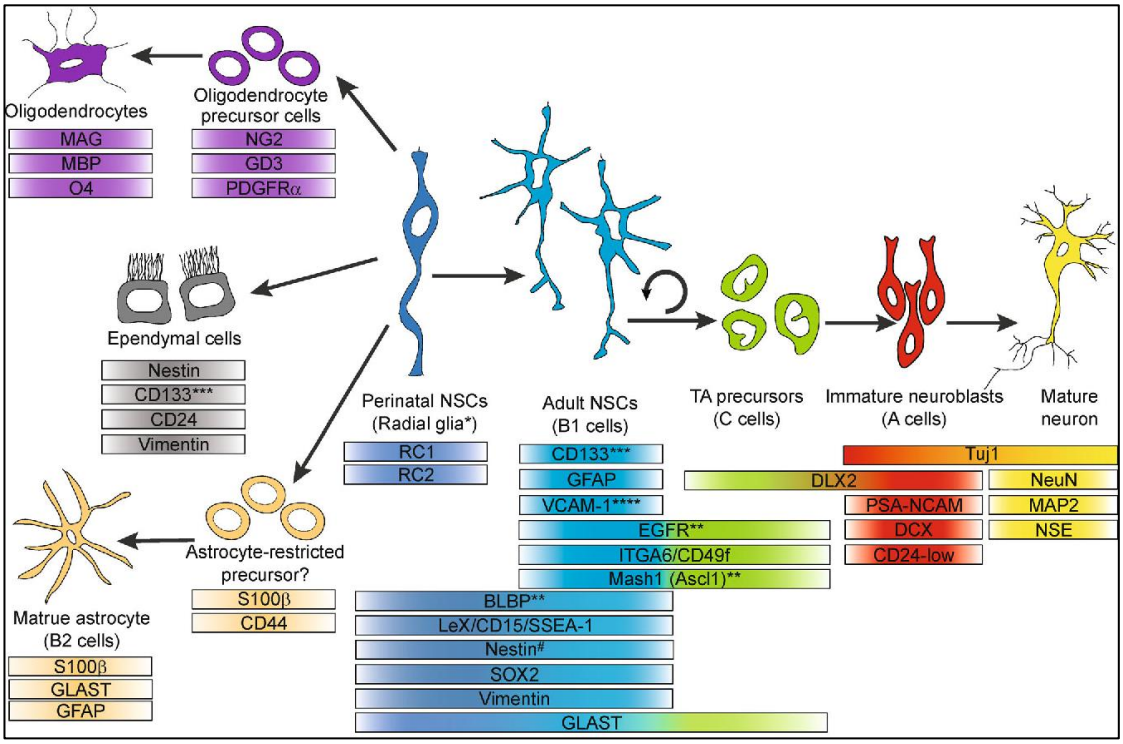

Figure 50. *Complexity of neuronal lineage as compared to oligodendrocytic lineage.*

Puelles and colleagues demonstrated that evolutionarily, Doublecortin (Dcx) positive cells are present in the pallial derivatives (homologous to the amygdala) of reptiles *(Puelles, 2017)*. These results were in congruence with the proposal put forth by Luzzati and colleagues regarding the presence of a phylogenetically conserved pallial cell type, indicating the possibility of a population of slowly maturing Dcx positive cells shared by multiple domains, which also remains conserved during evolution *(Luzzati, 2015)*. Our previous confirmatory results of EPO induced decrease in the number of transit amplifying progenitor Dcx positive cells in the CA1 region led us to consider these NSCs could give rise to pyramidal neurons. One explanation that is in line with the reports that immature Dcx positive neuronal precursors migrate through subcortical white matter tracts *(Gould et al., 1999; Gould et al., 2001; Nacher et al., 2001; Bernier et al., 2002; Luzzati et al., 2003)*, suggesting that some neurons generated in the adult SVZ may incorporate into a region(s) other than the olfactory bulb. Despite of the observed neurons using a DcxCreERT2 mouse line, the Cre background activity without tamoxifen induction limits us from conclusively labelling it as one of the EPO responsive precursor. Moreover, in addition expression of Dcx within our 'immature glutamatergic' neuronal cluster after EPO treatment was also observed by Drop-

Sequencing, thereby providing resistance for completely ruling out the possibility that EPO could mediate neuronal differentiation via Dcx positive precursors. However, six hours is a relatively short time for these precursors to migrate from the known neurogenic zones. The more plausible explanation is that these cells are generated during early development *(Luzzati et al., 2009; Bonfanti and Nacher, 2012)* and undergo slow yet delayed postnatal differentiation, which could be enhanced in need or in the presence of an EPO like factor.

Another widely accepted marker for neuronal precursor cells is Nestin. Taking hints from the literature present and employing a specific transgenic mouse line i.e. NestinCreERT2::TdTomato, which labels Nestin-expressing precursors with a TdTomato reporter, the presence of these precursors or its progeny in the CA1 region of EPO treated mice was not detected. Surprisingly, EPO had an effect on the Nestin positive precursors in the SGZ of hippocampus. This is in congruence with reports from *Bonaguidi et al., 2011*, where the authors concluded that the Nestin NSCs present in the SGZ have the ability to proliferate as well as differentiate into multi-lineage progeny. Our results are suggestive that EPO could drive these precursors to differentiate to a different progeny in other regions of the brain. However, the evidence for this hypothesis still remains to be determined and was not further explored, as it would have been outside the scope of my thesis. More than eight Nestin transgenic mouse lines have been developed. Controversial conclusions using these Nestin transgenic mouse lines revealed variations in their targets, depending on the genomic element used to drive the transgene expression *(Semerci & Maletic-Savatic, 2016)*. Using the same inducible mouse line resulted in contradictory conclusions in two different studies. Encinas and collaborators used BrdU and its analogs to suggest that these Nestin positive NSCs are disposable *(Encinas et al., 2011)*. On the other hand, Bonaguidi and colleagues used an induction protocol to activate Cre in spare, individual NSCs thereby tracing their respective lineages and claimed the indisposable nature of Nestin positive NSCs. Another NestinCreERT2 mouse line led to results that suggested external factors like social isolation or enriched environment affect these NSCs *(Dranovsky et al., 2011)*. Therefore, Nestin dependent inducible lines are a perfect example of the limitations of drawing concrete conclusions from these lines. The Nestin

transgenic inducible line used in this thesis is one of many that have been developed over the years and appears to be active mainly in type-2 progenitors. Both type-1 radial glial cells and type-2a and 2b neural precursor cells express endogenous Nestin protein *(Encinas et al., 2011; Kronenberg et al., 2003)*. A critical point in lineage tracing approaches is to determine the exact progenitor stage where CreERT2 is active and the efficiency with which it induces the reporter expression. Thus, this thesis could also not completely exclude Nestin as an EPO responsive precursor, since it could be possible that EPO does not mediate an increase in the number of neurons via Type-2 precursors in the CA1.

Sonic hedgehog (SHH) responsive NSCs have been reported to possess the ability of proliferation and differentiation into neurons, thereby increasing the NSC number as well as generating more neurons *(Ahn & Joyner, 2005)*. Gli1 is a transcription factor, which is activated by SHH signaling pathway *(Lai et al., 2003; Machold et al., 2003)*. These Gli positive precursors located in the SGZ of the hippocampus are implicated in adult neurogenesis *(Ahn et al., 2005)*. Fate mapping using GliCreERT2 inducible line, the number of Gli positive precursors significantly increased in the stratum radiatum (SR), Alveus (ALV) as well as a trend in increase in the SGZ region of the hippocampus. Surprisingly, this increase was not observed in EdU positive proliferating cells, which partially is in agreement with results previously published from *Encinas et al., 2011*, where the authors demonstrate that Gli positive NSCs are quiescent in nature, which could undergo asymmetric (direct) division to give rise to amplifying NSCs.

However, similar to the Nestin positive precursors, the presence of Gli positive precursors or their progenies in the CA1 region of the hippocampus was not detected. Interestingly, the Gli positive precursors in the SR region of EPO treated mice also showed co-expression of astrocyte marker GFAP. Surprisingly, a marker of mature astrocytes S100β was significantly reduced in the same region of the hippocampus. This finding points us in the direction that various reports have enlisted i.e. the ability of mature astrocytes to undergo dedifferentiation or transdifferentiation into other cell types in case of need such as injury *(Gotz et al., 2015; Michelucci et al., 2016; Wang et al., 2015; Yang et al., 2012)*. In conclusion, EPO seems to have an effect on SHH responsive NSCs. This has been previously reported *in vitro*, where the authors

demonstrated EPO induces SHH mediated enhanced proliferation and differentiation of adult neural progenitor cells *(Wang et al., 2007)*. Although it is undefined whether EPO induces a similar need for these mature astrocytes to dedifferentiate, this thesis could at least emphasize on the effect of EPO to regulate astrocytic differentiation via Gli positive precursors.

Yet another promising candidate is the transcription factor Sox2, which has been characterized for the generation of induced pluripotent stem cells *(Takahashi & Yamanaka, 2006)*. Since, Sox2 is an important player in maintaining stemness; the present work decided to decipher the effect of EPO on this particular precursor. Using Sox2CreERT2::TdTomato inducible mouse line, the pyramidal neurons carrying TdTomato reporter in the CA1 region was observed after using EPO as a potent molecule. The observation of Sox2 positive cells giving rise to new neurons is in accordance with multiple previous reports *(Ahlfeld et al., 2017; Suh et al., 2007)*. For instance, viral vector mediated expression of exogenous Sox2 in resident astrocytes in the adult mouse reprograms them into proliferating neuroblasts in the striatum and spinal cord, which are the regions outside canonical neurogenic niches *(Niu et al., 2013; Su et al., 2014)*. The observation that pyramidal neurons could carry over the TdTomato reporter from Sox2 labelled precursors after EPO induced differentiation interested us immensely. Unfortunately, these mice showed unspecific TdTomato signal in non-tamoxifen treated mice, thereby yet again, inhibiting us to conclusively determine whether EPO mediated increase in pyramidal neurons is via Sox2 positive precursors. However, reports suggest that Sox2 interacts with a long noncoding RNA 'RMST' to form a RNA-protein complex, which activates the promoters of various neurogenic genes *(Ng et al., 2013)*. The presence of RMST in the 'immature glutamatergic' neuronal cluster was observed upon EPO treatment using Drop-Sequencing, further strengthening the possibility of EPO mediated neuronal differentiation of Sox2 positive precursors. It remains to be elucidated whether RMST associates with Sox2 under the influence of EPO.

5.2. EPO acts on multiple precursors analogous to the hematopoietic system.

Growing evidence and our own work suggested that the neuronal lineage would be difficult to trace using transgenic mouse models. Several of these marker genes are unspecific to quiescent or amplifying progenitors, which greatly restricts their utility for such fate mapping experiments *(Hochgerner et al., 2018)*. Therefore, there is no convincing data set at present that could define EPO responsive neuronal progenitor(s) by the expression of 'unique proteins' and it remains uncertain whether such a unique marker gene exists at all. Alternatively, the molecular profile of these cells is defined by the expression level of multiple genes, as it is the case for a number of other neural cell types and their precursors, which are increasingly recognized by single cell RNA Sequencing *(Hochgerner et al., 2018; Marques et al., 2018; Zeisel et al., 2015)*. Using this approach, the known targets like Dcx, Dclk and Pax6 along with other targets like immature neuronal markers Tbr1, Tle4, Sox5, Satb1 and epigenetic players like long noncoding RNA 'RMST' were detected, all of which were present in the 'immature glutamatergic' neuronal cluster after EPO treatment. ScRNA-Sequecing has been able to reveal more markers and support a continuum of neural stem cells throughout development and adulthood as they share similar transcriptional trajectories *(Hochgerner et al., 2018; Marques et al., 2018; Zeisel et al., 2015)*.

So far, with the battery of potential markers, EPO could directly or indirectly influence the proliferation or differentiation of transit amplifying cells or neuroblasts (Dcx) and radial glial cells (Sox2 and Pax6). This thesis could partially exclude Nestin and Gli positive precursors as EPO responsive precursors that increase the number of pyramidal neurons. More importantly, using our approach, this thesis cannot exclude endothelial and astroglial cells as potential candidates. Due to the technical difficulties with the unspecific signal observed in control untreated mice, the present work cannot demonstrate with certainty that EPO has an effect on pyramidal neuronal number via particular type of precursor cell.

Moreover, this thesis also does not exclude the hypothesis that various precursors, known or unknown, could differentiate, alone or synergistically, to contribute to the increased pyramidal neuronal number upon EPO treatment. Due to the technical

difficulties, this work cannot unequivocally pinpoint these precursors, which are influenced by EPO. Moreover, this thesis could neither exclude the possibility that EPO could work on multiple precursors (Pax6, Dcx, and Sox2) in the brain to differentiate into pyramidal neurons, which reside in the CA1 region of the hippocampus nor exclude the infiltration of other resident precursors from the neighboring region. The effect of EPO on multiple progenitor cells bare similar resemblance with the differentiation observed with hematopoietic stem cells, where these cells can circumvent distinct intermediate stages and are capable of trans-differentiation. Previously, authors had proposed a continuum like view of the lineages for the hematopoietic stem cells (HSCs), where each HSC could proliferate or chooses from a spectrum of all cell fates to 'merely' differentiate. After selecting a specific cell lineage, the HSC could still 'step sideways' to an alternative, albeit closely related cell fate, suggesting that HSCs and their progenies remain versatile *(Haas et al., 2005; Pietras et al., 2015; Sanjuan-Pla et al., 2013; Yamamoto et al., 2013)*. Considering the similarities with the hematopoietic system, one could hypothesize that EPO drives neuronal differentiation without proliferation, possibly by skipping the intermediate stages of differentiation. Bernstein and colleagues provided further support to this hypothesis, where they proposed domain silence genes in embryonic stem cells, which are still 'poised' and readily activated (Bernstein et al., 2006). The triggers, which induces differentiation in these cells, could be injury or factors like EPO. If at all, this holds true, needs to be determined.

5.3. EPO mediates neurogenesis in the hippocampus.

Fate mapping neurons using additive labelling of progenitors along with their progenies have provided variable results, which might all contribute to different findings despite the use of the 'same' transgenic mouse line *(Sun et al., 2014)*. Employing inducible transgenic lines to label different precursors, the present work fails to confirm the role of EPO on either a specific type of precursor or multiple precursors present in the CA1 region of the hippocampus. This was unfortunately due to the technical difficulties and the absence of a suitable reporter line, which allowed us to fate map the newly generated neurons from a single neuronal precursor. Therefore, instead of using an

additive method, a novel subtractive approach was employed (wherein creERT2 is not expressed by progenitors but by mature neurons) to elucidate the influence of EPO on adult neurogenesis. Suh and colleagues have previously proposed the intellectual basics to this theory giving an example of a use for CaMKIIa-CreERT2 transgenic mice *(Sun et al., 2014)*. In keeping with this theory, for the first time, all embryonically born pyramidal neurons are labelled using NexCreERT2::TdTomato inducible mice both in juvenile and adult stage. The use of excitatory neuronal antibody marker like Ctip2 enabled us to distinguish the newly generated neurons obtained after EPO administration. These newly generated neurons were positive for pyramidal neuronal marker Ctip2, but were negative for TdTomato reporter as EPO treatment followed the tamoxifen administration (Fig. 51). This method does contain some limitations, like all other fate mapping approaches. The labelling efficiency upon tamoxifen induction is hardly ever 100% because some cells escape recombination. To overcome this pitfall, the percentage of unlabeled cells immediately after tamoxifen induction was estimated to be approximately 3% of cells of the total number of cells. Previous results from our group *(Hassouna et al., 2016)* have demonstrated that an increase in pyramidal neurons upon EPO treatment in the CA1 of juvenile mice occurs without an increase in proliferation. This could suggest that EPO induces asymmetric (direct) division of neural precursors to generate more pyramidal neurons on demand. EPO mediated an increase in the number of unlabeled neurons in the pyramidal layer without proliferation was demonstrated for the first time. Importantly, increased – albeit lower – numbers of newly differentiated neurons were found under these conditions even in placebo treated animals. This observation provides evidence of physiological neurogenesis throughout life outside the known neurogenic niches. Similar reports of constitutive neurogenesis in various other regions of the brain of primates and rodents have been demonstrated in neocortex *(Dayer et al., 2005; Gould et al., 1999; Gould & Kamnasaran, 2011; Kaplan, 1981)*, piriform cortex *(Bonfanti & Nacher, 2012; Rotheneichner et al., 2018)*, brain stem *(Bauer et al., 2005)* and spinal cord *(Yamamoto et al., 2001)*. Other regions of the brain where constitutive neurogenesis occurs are the substantia nigra *(Zhao et al., 2003)*, the amygdala *(Bernier et al., 2002)* and rodent CA1 region of the hippocampus *(Rietze et al., 2000)*. The

mechanism of adult neurogenesis without proliferation has been previously overlooked, but is relevant for the steady state adjustment to demand and regenerative processes in the brain. It further adds a novel perspective to the pivotal work performed by many groups who discovered adult neurogenesis in multiple regions of the brain, based on labeling the proliferating cells via integration of nucleoside analogues *(Aimone & Gage, 2011; Altman & Das, 1965; Doetsch, 2003; Gould, 2007; Kaplan, 1981; Rakic, 1985; Sanai et al., 2004)*.

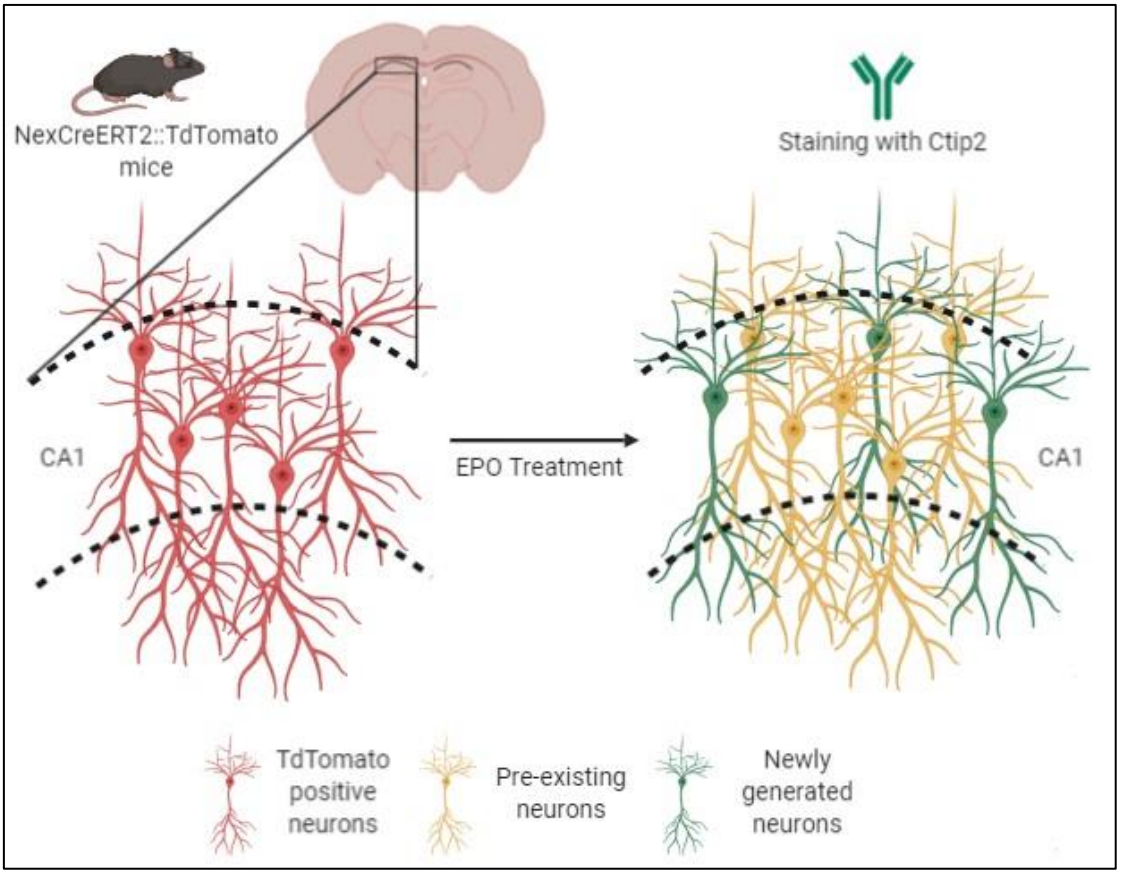

Figure 51. *EPO induced generation of newly differentiated neurons in the CA1 region of the hippocampus.*

5.4. EPO supports a continuum view for neuronal lineage.

Since the hypothesis was considered that EPO could act on multiple precursors at different stages of differentiation, this thesis argued if the continuum like view of HSCs holds true for the neuronal lineage. Firstly, the EPO mediated increase in pyramidal neurons was also confirmed on a transcriptome level, where a single dose of EPO

induced an immediate increase in the number of cells in the CA1 specifically in the 'immature glutamatergic' cluster. Secondly, questions arose about the transcript signature of this cluster. How does one define this cluster as a progenitor, neuroblasts or an immature glutamatergic cluster? In our data set, progenitor markers such as Nestin and Sox2 were not elevated, but an increase in immature neuronal markers such as Dcx, Tbr1 and Tle4 was observed *(Hochgerner et al., 2018; Piumatti et al., 2018)*. In accordance, similar marker expressions were observed to be further elevated upon EPO treatment, thereby defining this cluster as immature glutamatergic cluster. Thirdly, the immaturity of the cluster was further strengthened when Monocle analysis between immature and its neighboring mature glutamatergic cluster revealed a much lower pseudo time for the cells which were classified as immature. Lastly, to support the continuum-like view of HSCs as previously proposed *(Brown and Ceredig, 2019)*, a homogenously lower pseudotime after EPO treatment was observed where neurons are present in a continuum, in which immature neurons progressively proceed towards neuronal maturation. The presence of such a physiological neuronal continuum-like view has also been substantiated in recent reports, where the authors demonstrated that adult hippocampal neurogenesis may represent a life-long extension of development that maintains heightened plasticity *(Berg et al., 2019)*. The scRNA-Seq analysis provided sufficient evidence of an immediate effect of EPO on existing precursors to instantaneously initiate neuronal differentiation. As the expression levels of EPO and EPOR was low, they were not detected by scRNA-Seq, which is a known dropout effect.

5.5. EPO mediated enhancement in synaptic plasticity.

Several reports have successfully demonstrated enhanced neurogenesis in the hippocampus due to various factors such as VEGF, NT-3, Notch ligand Delta-like 1, IL-1b, IL-6, FGF-2 *(Barkho et al., 2006; Delgado et al., 2014; Faigle & Song, 2013; Kang & Hebert, 2015; Kawaguchi et al., 2013)*. However, the critical question often raised in the field consists of doubting the extent of positive effect of a few newly generated neurons on functional consequences. Many have reported that a small number of newly generated neurons can influence behavior as demonstrated by stimulation of

single pyramidal neurons in the rat motor cortex. These newly generated neurons could also induce whisker movements *(Brecht et al., 2004; Shadlen et al., 1996)*.

Enhanced neurogenesis and synaptic integration together could contribute to positive effects observed at functional or behavioral level. Unstimulated neurogenesis is followed by an early survival phase, where the newly generated neurons show dramatic decline in their numbers within the first few days *(Biebl et al., 2000; Kuhn et al., 2005)*. During this phase, majority of the cells are eliminated well before they could make functional connections in the target regions of the hippocampus *(Kempermann et al., 2015)*. However, it is essential that the surviving neurons integrate into the existing architecture of the hippocampus by the formation of synaptic connections with the pre-existing neurons. The initiation of dendrite and spine development generally follows the process of axonal elongation *(Sun et al., 2013)*. Once both these processes are underway, the newly generated neurons are said to be integrated and functional active. During normal neurogenesis in a healthy brain, a large proportion of neural progenitors undergo apoptosis within their first days. By rapidly removing cell debris, the scavenging properties of microglia could have an important regulatory role at early stages of neurogenesis *(Sierra et al., 2010)*. However, it is not completely understood whether the phagocytosis is beneficial for the surrounding newborn neurons by reducing pro-inflammatory mediators, or whether they are detrimental by further inducing apoptotic neuronal death *(Magnus et al., 2001; Neher et al., 2011)*.

Using transgenic mouse line (Thy1-YFP), which specifically labels dendrites and spines of pyramidal neurons, a significant increase in the density of dendrites as well as spines was observed. This result could serve as another mechanism of augmented network function and therefore strengthen the evidence of cognitive improvement upon EPO administration. This observation is in accordance with reports suggesting increase in dendritic length and complexity appears to be mediated by a cell autonomous, autocrine action of another neurotrophic factor BDNF *(Wang et al., 2015)*. In our findings, based on their morphology, the increase in the density of spines is constituted by an increase in stubby spines, which are immature in nature. The increase in immature stubby spines supports the hypothesis that the newly generated neurons form new spines, which are yet to be mature. This maturation trend is similar to that

observed with trajectory analysis in neurons, which demonstrated that these neurons are present in continuum, and are driven to maturity upon EPO administration. It is very likely, that upon appropriate cognitive stimulation, these immature stubby spines would mature into stable mushroom spines. However, evidence that this is the case, is currently the ongoing work.

Though likely, it is not established how finely tuned cross talk between microglia and adult born neurons would function and how it leads to any changes upon microglia activation. Previous work from our group also has hinted to the effect of EPO, where EPO treatment was shown to dampen microglial activity *(Mitkovski et al., 2015)*. In our present results, along with neuronal and dendritic spine increase, a reduction in the number of microglia upon EPO treatment was observed. This decrease in microglia was also corroborated by single cell RNA-Sequencing. These results together point towards enhanced neurogenesis and maybe the newly differentiated neurons do not require excessive pruning as they begin to form synaptic connections. Our findings are in accordance with Paolicelli and colleagues, where they observed a transient decrease in microglia in the first to fourth postnatal week in CXCR1 knockout mice and a corresponding increase in the dendritic spine density *(Paolicelli et al., 2011)*. An explanation could be attributed to the previously stated concept of 'pro-neurogenic' function of microglia. Disruption of the microglia expressed receptor CX3CR1 pathway in young rodents' decreased survival and proliferation of hippocampal neural progenitor cells *(Bachstetter et al., 2011)*. The other hypothetical reasoning could be that the microglia in the presence of EPO transdifferentiate and give rise to some newly generated neurons in the CA1. The microglial transdifferentiation as compared to the astrocytic transdifferentiation has not been extensively studied; however, some reports demonstrate that using 70% fetal bovine serum upregulates Sox2 in microglia, which transforms them into Map2 positive neurons *(Nonaka et al., 2008; Zhang et al., 2013)*. Our current ongoing work will attempt to shed light on this matter. On a rodent behavioral level, the increase in the number of neurons and their synaptic connections might contribute to the brain function via alteration in the structural properties of the circuitry. Enhanced synaptic plasticity is also essential for mediating pattern separation in memory formation and cognition *(Clelland et al., 2009; Nakashiba et al., 2012; Sahay*

et al., 2011). However, on an over-arching human level, these results may provide explanation of the MRI-documentable increase in the dimensions of certain brain areas *(Hassouna et al., 2016)* or the reduction of brain matter loss upon EPO treatment in mental illness *(Miskowiak et al., 2015; Wustenberg et al., 2011)*.

5.6. Mechanism of EPO action – Activity mediated adult hippocampal neurogenesis.

Adult hippocampal neurogenesis is a complex and an activity dependent process *(Kempermann et al., 2015)*. A decline in neurogenesis is observed in mice when they were not challenged to lead an active life *(Encinas et al., 2011)*. This result indicated the importance of 'use it or lose it' as a consequence of negligence *(Kempermann et al., 2015; Ott et al., 2015)*. This activity could be either physical exercise or cognitive stimulus. Ehrenreich and colleagues over the past several years have extensively demonstrated the effects of EPO on improved cognition in humans. Now these findings of increased neurodifferentiation and neuroplasticity in rodents further strengthen these claims. Here, for the first time, an endogenous mechanism of EPO mediated action on improved learning was proved. The pyramidal neurons, upon undergoing a learning task such as complex running wheel, upregulates the expression of EPO and EPOR mRNA as observed by in situ hybridization. There have been similar reports on other molecules such as Vascular Endothelial Growth Factor (VEGF). For example, on a molecular level, exercise is shown to increase the levels of insulin-like growth factor 1 (IGF-1) and VEGF, whereas inhibiting these factors led to a decrease in exercise induced adult hippocampal neurogenesis *(Fabel et al., 2003; Trejo et al., 2001)*. Subsequently, EPO treatment has shown to significantly upregulate the expression of VEGF and downstream JAK-STAT, PI3K/AKT and ERK1/2 signaling pathway in neural precursors *in vitro (Wang et al., 2007)*. Based on the evidence present in the literature and our previous work on signaling pathways, this thesis can speculate that EPO administration induces the generation of pyramidal neurons in the CA1 via upregulating certain signaling pathways in neural precursors.

Interestingly, EPO was able to increase the generation of pyramidal neurons in adult mice at almost 4 months of age. The effect of EPO in relation to aging (10 months of age) is currently being pursued. This finding enables us to emphasize the importance

of this novel mechanism of rapid local generation of neurons on demand. Adult hippocampal neurogenesis is demonstrated to decline with age in rodents *(Kuhn et al., 1996; Seki & Arai, 1995)* and in humans *(Eriksson et al., 1998)*. This decline in hippocampal neurogenesis is attributed to the reduced number of precursors as well as decline in their proliferation *(Garcia et al., 2004; Luo et al., 2006; Seki, 2002)*. It is still unclear whether EPO induces asymmetric division of neural precursors to generate pyramidal neurons in adult mice, thereby reducing the NSCs pool available for a later time point.

5.7. EPO/EPOR system central to physiological hypoxia induced hippocampal neurogenesis.

Another factor, shown to promote adult hippocampal neurogenesis, is hypoxia. Exposure to intermittent or chronic hypoxia has been demonstrated to increase neurogenesis in hippocampus *(Zhu et al., 2010)* by the activation of Wnt/β-catenin signaling *(Varela-Nallar et al., 2014)*. Moreover, localized hypoxia with the SGZ of the hippocampus has also shown to contribute to early survival of newly differentiated neurons in the adult hippocampus *(Chatzi et al., 2015)*. Similarly, hypoxia has also shown to increase neurogenesis of NSCs in vitro *(Jin et al., 2002; Shingo et al., 2001)*. Since EPO is a hypoxia inducible gene *(Semenza & Wang, 1992)*, a hypothesis was considered whether the pyramidal neurons upon a learning challenge undergo hypoxia and therefore release more EPO in vivo. This was proved using a transgenic mouse, expressing a chimeric protein in which the oxygen-dependent degradation (ODD) domain of HIF-1α is fused to the tamoxifen inducible CreERT2 recombinase *(Kimura et al., 2015)*. Upon exposure to overnight running on CRW, the labelled pyramidal neurons are present in a physiological hypoxic condition. Moreover, as mentioned above, an upregulation of EPO and EPOR mRNA levels in pyramidal neurons upon CRW was observed by insitu hybridization, thereby indicating that a cognitive challenge can increase the number of hypoxic neurons and upregulate the expression of EPO and EPOR.

Multiple reports have demonstrated the presence of EPO *(Tan & Ratcliffe, 1992)* and EPOR *(Liu & Chen, 1994)* at different developmental stages in brains of rodents.

Interestingly, EPO mRNA expression was observed in astrocyte *(Masuda et al., 1994)*, neuronal *(Bernaudin et al., 1999)* and oligodendrocyte *(Sugawa et al., 2002)* cultures. However, it is unlikely that the organism holds receptors and downstream mechanisms just for exogenous compounds, the present work hypothesized that EPOR must hold a functional relevance in the brain. Based on our findings, the present work demonstrates that the endogenous EPO system contributes to an adaptive increase in performance as shown by complex wheel running or by mild exogenous hypoxia over 3 weeks. However, to prove functional relevance of EPOR in this 'cognitive challenge or hypoxia' enhanced learning, a transgenic mouse line was employed where specific knockout EPOR in pyramidal neurons of the CA1 would enable us to understand a mechanism that is independent of the peripheral hematopoietic system. Interestingly, the increased learning is attenuated in the mice carrying EPOR deletion in pyramidal neurons. This decline in learning was not rescued even after the mice were treated with exogenous EPO. Moreover, a specific EPO deletion in pyramidal neurons led these transgenic mice to perform significantly worse as compared to the controls, indicating that the learning induced hypoxia and the regulation of its target gene EPO/EPOR is the central theme in the CNS by which EPO mediates its pro-cognitive effects.

Contrary to the more popular viewpoint that hypoxia in general is rather detrimental, recent reviews also consider that hypoxia may have beneficial effects and even a role in protecting against cognitive dysfunction *(Dale et al., 2014; Mateika et al., 2015; Watts et al., 2018; Zhang et al., 2011)*. Nevertheless, up to now, cognitive challenge has never been shown to lead to mild relative hypoxia in functionally engaged neuron populations. Along with recording increased neurodifferentiation as well as improved learning, this thesis is able to pin these effects primarily to the newly generated neurons as observed by the expression of neuronal activity marker C-Fos. This result set the basis for studying the electrophysiological properties of these newly generated neurons, which is currently in progress. Preclinical and clinical studies, however, demonstrated that the performance of sensory systems in the cerebral cortex can be substantially improved through intensive learning and practice and that these improvements are mediated by plastic changes in key neural networks *(Buonomano & Merzenich, 1998; Gilbert et al., 2001)***.** Our data using CRW would indicate that hypoxia

may act as the driving force of neuronal adaptation to increased demand. Production of EPO/EPOR in neurons likely constitutes a cell-autonomous auto/paracrine mechanism, probably in concert with other hypoxia-inducible genes, like vascular endothelial growth factor (VEGF), which has previously also been reported to enhance cognition *(Cao et al., 2004)*.

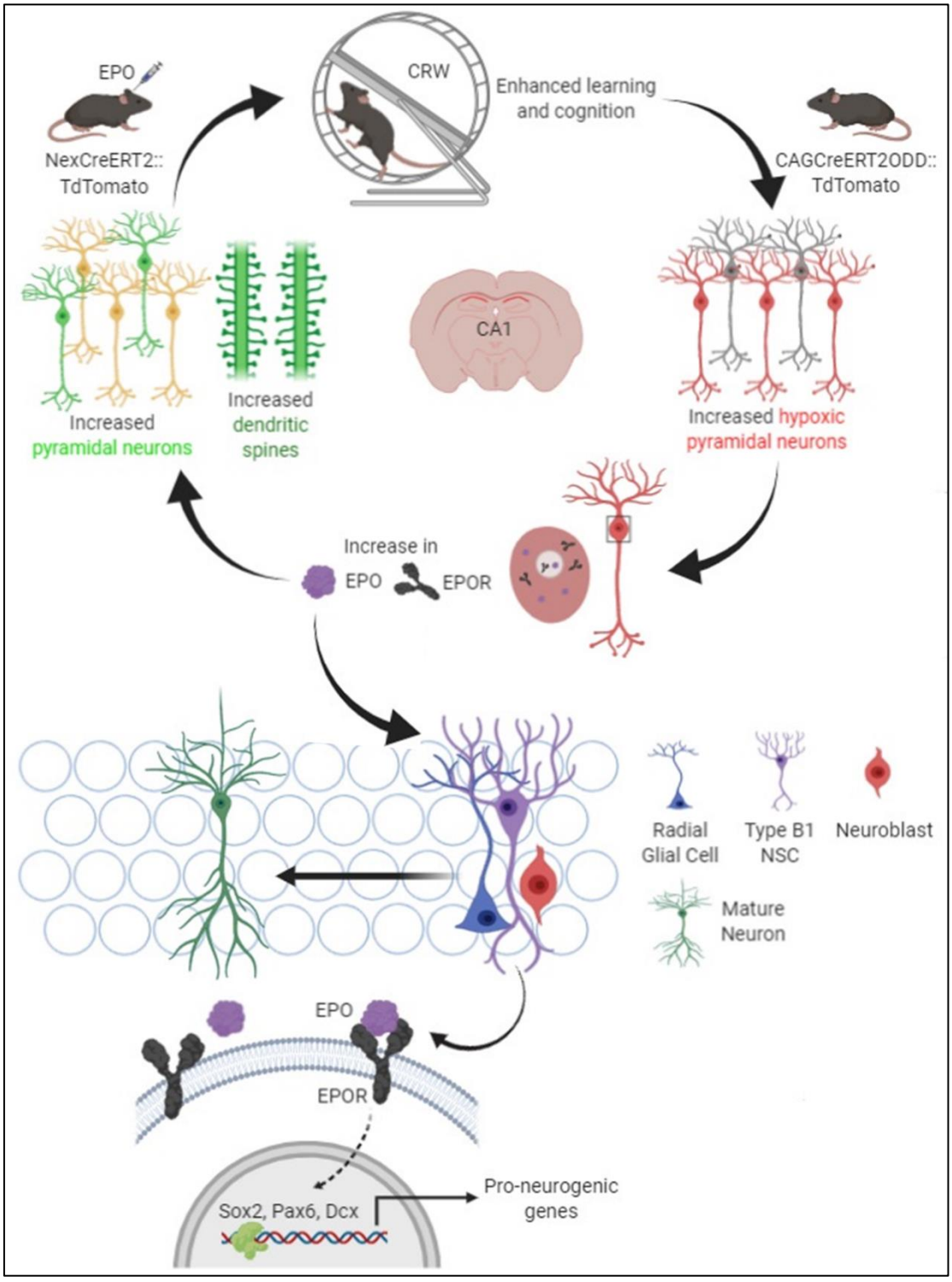

Figure 52. *Model illustrating suggested mechanisms and effects of EPO/EPOR in the CA1.*

In conclusion, my doctoral work provided first evidence that functional challenge via learning of new complex tasks induces physiological hypoxia in pyramidal neurons of the CA1. This induced hypoxia upregulates neuronal production/release of EPO, which regulates various precursors to act alone or synergistically to generate new pyramidal

neurons. Neuronal produced EPO may bind in an auto/paracrine manner to EPOR present on the pyramidal neurons leading to an increase in immature dendritic spines and thereby enhancing synaptic plasticity. EPO may also simultaneously bind to EPOR present of diverse neighboring cells, which would be ready to differentiate into neurons on demand. Taken together (Fig. 53), these integrative steps may explain the consistently enhanced cognitive function upon EPO administration as well as delineate physiological mechanisms, which would accomplish lasting adaptation to challenge via the EPO/EPOR system in the brain.

References

6. References

Abraham, A. B., Bronstein, R., Reddy, A. S., Maletic-Savatic, M., Aguirre, A., & Tsirka, S. E. (2013). Aberrant neural stem cell proliferation and increased adult neurogenesis in mice lacking chromatin protein HMGB2. *PLoS One*, **8**(12), e84838.

Abraham, B. J., Cui, K., Tang, Q., & Zhao, K. (2013). Dynamic regulation of epigenomic landscapes during hematopoiesis. *BMC Genomics*, **14**, 193.

Agarwal, A., Dibaj, P., Kassmann, C. M., Goebbels, S., Nave, K.-A., & Schwab, M. H. (2011). In vivo imaging and noninvasive ablation of pyramidal neurons in adult NEX-CreERT2 mice. *Cerebral cortex*, **22**(7), 1473-1486.

Ahlfeld, J., Filser, S., Schmidt, F., Wefers, A. K., Merk, D. J., Glass, R., . . . Schuller, U. (2017). Neurogenesis from Sox2 expressing cells in the adult cerebellar cortex. *Sci Rep*, **7**(1), 6137.

Ahn, S., & Joyner, A. L. (2005). In vivo analysis of quiescent adult neural stem cells responding to Sonic hedgehog. *Nature*, **437**(7060), 894-897.

Ahn, Y. M., Seo, M. S., Kim, S. H., Kim, Y., Yoon, S. C., Juhnn, Y. S., & Kim, Y. S. (2005). Increased phosphorylation of Ser473-Akt, Ser9-GSK-3beta and Ser133-CREB in the rat frontal cortex after MK-801 intraperitoneal injection. *Int J Neuropsychopharmacol*, **8**(4), 607-613.

Aimone, J. B., & Gage, F. H. (2011). Modeling new neuron function: a history of using computational neuroscience to study adult neurogenesis. *Eur J Neurosci*, **33**(6), 1160-1169.

Altman, J., & Das, G. D. (1965). Autoradiographic and histological evidence of postnatal hippocampal neurogenesis in rats. *J Comp Neurol*, **124**(3), 319-335.

Altman, J., & Das, G. D. (1967). Postnatal neurogenesis in the guinea-pig. *Nature*, **214**(5093), 1098-1101.

Alvarez-Buylla, A., & Lim, D. A. (2004). For the long run: maintaining germinal niches in the adult brain. *Neuron*, **41**(5), 683-686.

Amrein, I. (2015). Adult hippocampal neurogenesis in natural populations of mammals. *Cold Spring Harb Perspect Biol*, **7**(5).

Arnold, K., Sarkar, A., Yram, M. A., Polo, J. M., Bronson, R., Sengupta, S., . . . Hochedlinger, K. (2011). Sox2(+) adult stem and progenitor cells are important for tissue regeneration and survival of mice. *Cell Stem Cell*, **9**(4), 317-329.

Avilion, A. A., Nicolis, S. K., Pevny, L. H., Perez, L., Vivian, N., & Lovell-Badge, R. (2003). Multipotent cell lineages in early mouse development depend on SOX2 function. *Genes Dev*, **17**(1), 126-140.

Bachstetter, A. D., Morganti, J. M., Jernberg, J., Schlunk, A., Mitchell, S. H., Brewster, K. W., . . . Gemma, C. (2011). Fractalkine and CX 3 CR1 regulate hippocampal neurogenesis in adult and aged rats. *Neurobiol Aging*, **32**(11), 2030-2044.

Balordi, F., & Fishell, G. (2007). Hedgehog signaling in the subventricular zone is required for both the maintenance of stem cells and the migration of newborn neurons. *J Neurosci*, **27**(22), 5936-5947.

Balu, D. T., & Lucki, I. (2009). Adult hippocampal neurogenesis: regulation, functional implications, and contribution to disease pathology. *Neurosci Biobehav Rev*, **33**(3), 232-252.

Banks, W. A., Jumbe, N. L., Farrell, C. L., Niehoff, M. L., & Heatherington, A. C. (2004). Passage of erythropoietic agents across the blood-brain barrier: a comparison of human and murine erythropoietin and the analog darbepoetin alfa. *Eur J Pharmacol*, **505**(1-3), 93-101.

Barker, N., Bartfeld, S., & Clevers, H. (2010). Tissue-resident adult stem cell populations of rapidly self-renewing organs. *Cell Stem Cell*, **7**(6), 656-670.

Barkho, B. Z., Song, H., Aimone, J. B., Smrt, R. D., Kuwabara, T., Nakashima, K., . . . Zhao, X. (2006). Identification of astrocyte-expressed factors that modulate neural stem/progenitor cell differentiation. *Stem Cells Dev*, **15**(3), 407-421.

Barry, G., Guennewig, B., Fung, S., Kaczorowski, D., & Weickert, C. S. (2015). Long Non-Coding RNA Expression during Aging in the Human Subependymal Zone. *Front Neurol*, **6**, 45.

Bauer, S., Hay, M., Amilhon, B., Jean, A., & Moyse, E. (2005). In vivo neurogenesis in the dorsal vagal complex of the adult rat brainstem. *Neuroscience*, **130**(1), 75-90.

Belachew, S., Chittajallu, R., Aguirre, A. A., Yuan, X., Kirby, M., Anderson, S., & Gallo, V. (2003). Postnatal NG2 proteoglycan-expressing progenitor cells are intrinsically multipotent and generate functional neurons. *J Cell Biol*, **161**(1), 169-186.

Berg, R. W. V., Davidsson, J., Lidin, E., Angeria, M., Risling, M., & Gunther, M. (2019). Brain tissue saving effects by single-dose intralesional administration of Neuroprotectin D1 on experimental focal penetrating brain injury in rats. *J Clin Neurosci*, **64**, 227-233.

Bernaudin, M., Bellail, A., Marti, H. H., Yvon, A., Vivien, D., Duchatelle, I., . . . Petit, E. (2000). Neurons and astrocytes express EPO mRNA: oxygen-sensing mechanisms that involve the redox-state of the brain. *Glia*, **30**(3), 271-278.

Bernaudin, M., Marti, H. H., Roussel, S., Divoux, D., Nouvelot, A., MacKenzie, E. T., & Petit, E. (1999). A potential role for erythropoietin in focal permanent cerebral ischemia in mice. *J Cereb Blood Flow Metab*, **19**(6), 643-651.

Bernier, P. J., Bedard, A., Vinet, J., Levesque, M., & Parent, A. (2002). Newly generated neurons in the amygdala and adjoining cortex of adult primates. *Proc Natl Acad Sci U S A*, **99**(17), 11464-11469.

Bernstein, B. E., Mikkelsen, T. S., Xie, X., Kamal, M., Huebert, D. J., Cuff, J., . . . Lander, E. S. (2006). A bivalent chromatin structure marks key developmental genes in embryonic stem cells. *Cell*, **125**(2), 315-326.

Betizeau, M., Cortay, V., Patti, D., Pfister, S., Gautier, E., Bellemin-Menard, A., . . . Dehay, C. (2013). Precursor diversity and complexity of lineage relationships in the outer subventricular zone of the primate. *Neuron*, **80**(2), 442-457.

Biebl, M., Cooper, C. M., Winkler, J., & Kuhn, H. G. (2000). Analysis of neurogenesis and programmed cell death reveals a self-renewing capacity in the adult rat brain. *Neurosci Lett*, **291**(1), 17-20.

Boldrini, M., Fulmore, C. A., Tartt, A. N., Simeon, L. R., Pavlova, I., Poposka, V., . . . Mann, J. J. (2018). Human Hippocampal Neurogenesis Persists throughout Aging. *Cell Stem Cell*, **22**(4), 589-599 e585.

Bonaguidi, M. A., McGuire, T., Hu, M., Kan, L., Samanta, J., & Kessler, J. A. (2005). LIF and BMP signaling generate separate and discrete types of GFAP-expressing cells. *Development*, **132**(24), 5503-5514.

Bonaguidi, M. A., Wheeler, M. A., Shapiro, J. S., Stadel, R. P., Sun, G. J., Ming, G. L., & Song, H. (2011). In vivo clonal analysis reveals self-renewing and multipotent adult neural stem cell characteristics. *Cell*, **145**(7), 1142-1155.

Bonfanti, L., & Nacher, J. (2012). New scenarios for neuronal structural plasticity in non-neurogenic brain parenchyma: the case of cortical layer II immature neurons. *Prog Neurobiol*, **98**(1), 1-15.

Brecht, M., Schneider, M., Sakmann, B., & Margrie, T. W. (2004). Whisker movements evoked by stimulation of single pyramidal cells in rat motor cortex. *Nature*, **427**(6976), 704-710.

Breunig, J. J., Arellano, J. I., Macklis, J. D., & Rakic, P. (2007). Everything that glitters isn't gold: a critical review of postnatal neural precursor analyses. *Cell Stem Cell*, **1**(6), 612-627.

Brines, M. L., Ghezzi, P., Keenan, S., Agnello, D., de Lanerolle, N. C., Cerami, C., . . . Cerami, A. (2000). Erythropoietin crosses the blood-brain barrier to protect against experimental brain injury. *Proc Natl Acad Sci U S A*, **97**(19), 10526-10531.

Brines, M., & Cerami, A. (2005). Emerging biological roles for erythropoietin in the nervous system. *Nat Rev Neurosci*, **6**(6), 484-494.

Brown, B. M., Peiffer, J. J., & Martins, R. N. (2013). Multiple effects of physical activity on molecular and cognitive signs of brain aging: can exercise slow neurodegeneration and delay Alzheimer's disease? *Mol Psychiatry*, **18**(8), 864-874.

Brown, J. P., Couillard-Despres, S., Cooper-Kuhn, C. M., Winkler, J., Aigner, L., & Kuhn, H. G. (2003). Transient expression of doublecortin during adult neurogenesis. *J Comp Neurol*, **467**(1), 1-10.

Bruick, R. K. (2003). Oxygen sensing in the hypoxic response pathway: regulation of the hypoxia-inducible transcription factor. *Genes Dev*, **17**(21), 2614-2623.

Budday, S., Steinmann, P., & Kuhl, E. (2015). Physical biology of human brain development. *Front Cell Neurosci*, **9**, 257.

Buffo, A., Rite, I., Tripathi, P., Lepier, A., Colak, D., Horn, A. P., . . . Gotz, M. (2008). Origin and progeny of reactive gliosis: A source of multipotent cells in the injured brain. *Proc Natl Acad Sci U S A*, **105**(9), 3581-3586.

Bulfone, A., Smiga, S. M., Shimamura, K., Peterson, A., Puelles, L., & Rubenstein, J. L. (1995). T-brain-1: a homolog of Brachyury whose expression defines molecularly distinct domains within the cerebral cortex. *Neuron*, **15**(1), 63-78.

Buonomano, D. V., & Merzenich, M. M. (1998). Cortical plasticity: from synapses to maps. *Annual review of neuroscience*, **21**(1), 149-186.

Burton, G. J., Jauniaux, E., & Murray, A. J. (2017). Oxygen and placental development; parallels and differences with tumour biology. *Placenta*, **56**, 14-18.

Buscarlet, M., & Stifani, S. (2007). The 'Marx' of Groucho on development and disease. *Trends Cell Biol*, **17**(7), 353-361.

Bylund, M., Andersson, E., Novitch, B. G., & Muhr, J. (2003). Vertebrate neurogenesis is counteracted by Sox1-3 activity. *Nat Neurosci*, **6**(11), 1162-1168.

Cao, L., Jiao, X., Zuzga, D. S., Liu, Y., Fong, D. M., Young, D., & During, M. J. (2004). VEGF links hippocampal activity with neurogenesis, learning and memory. *Nature genetics*, **36**(8), 827.

Carmeliet, P., Dor, Y., Herbert, J. M., Fukumura, D., Brusselmans, K., Dewerchin, M., . . . Keshert, E. (1998). Role of HIF-1alpha in hypoxia-mediated apoptosis, cell proliferation and tumour angiogenesis. *Nature*, **394**(6692), 485-490.

Castaneda-Arellano, R., Beas-Zarate, C., Feria-Velasco, A. I., Bitar-Alatorre, E. W., & Rivera-Cervantes, M. C. (2014). From neurogenesis to neuroprotection in the epilepsy: signalling by erythropoietin. *Front Biosci (Landmark Ed)*, **19**, 1445-1455.

Ceredig, R., Rolink, A. G., & Brown, G. (2009). Models of haematopoiesis: seeing the wood for the trees. *Nat Rev Immunol*, **9**(4), 293-300.

Chatzi, C., Schnell, E., & Westbrook, G. L. (2015). Localized hypoxia within the subgranular zone determines the early survival of newborn hippocampal granule cells. *Elife*, **4**, e08722.

Chavez, V. M., Marques, G., Delbecque, J. P., Kobayashi, K., Hollingsworth, M., Burr, J., . . . O'Connor, M. B. (2000). The Drosophila disembodied gene controls late embryonic morphogenesis and codes for a cytochrome P450 enzyme that regulates embryonic ecdysone levels. *Development*, **127**(19), 4115-4126.

Chawana, R., Alagaili, A., Patzke, N., Spocter, M. A., Mohammed, O. B., Kaswera, C., . . . Manger, P. R. (2014). Microbats appear to have adult hippocampal neurogenesis, but post-capture stress causes a rapid decline in the number of neurons expressing doublecortin. *Neuroscience*, **277**, 724-733.

Cipolleschi, M. G., Dello Sbarba, P., & Olivotto, M. (1993). The role of hypoxia in the maintenance of hematopoietic stem cells. *Blood*, **82**(7), 2031-2037.

Clelland, C. D., Choi, M., Romberg, C., Clemenson, G. D., Jr., Fragniere, A., Tyers, P., . . . Bussey, T. J. (2009). A functional role for adult hippocampal neurogenesis in spatial pattern separation. *Science*, **325**(5937), 210-213.

Cloonan, N., Forrest, A. R., Kolle, G., Gardiner, B. B., Faulkner, G. J., Brown, M. K., . . . Grimmond, S. M. (2008). Stem cell transcriptome profiling via massive-scale mRNA sequencing. *Nat Methods*, **5**(7), 613-619.

Costa, M. R., Kessaris, N., Richardson, W. D., Gotz, M., & Hedin-Pereira, C. (2007). The marginal zone/layer I as a novel niche for neurogenesis and gliogenesis in developing cerebral cortex. *J Neurosci*, **27**(42), 11376-11388.

Costa, V., Lugert, S., & Jagasia, R. (2015). Role of adult hippocampal neurogenesis in cognition in physiology and disease: pharmacological targets and biomarkers. *Handb Exp Pharmacol*, **228**, 99-155.

Cummins, E. P., & Taylor, C. T. (2005). Hypoxia-responsive transcription factors. *Pflugers Arch*, **450**(6), 363-371.

Dale, E., Ben Mabrouk, F., & Mitchell, G. (2014). Unexpected benefits of intermittent hypoxia: enhanced respiratory and nonrespiratory motor function. *Physiology*, **29**(1), 39-48.

Dayer, A. G., Cleaver, K. M., Abouantoun, T., & Cameron, H. A. (2005). New GABAergic interneurons in the adult neocortex and striatum are generated from different precursors. *J Cell Biol*, **168**(3), 415-427.

Dayyat, E. A., Zhang, S. X., Wang, Y., Cheng, Z. J., & Gozal, D. (2012). Exogenous erythropoietin administration attenuates intermittent hypoxia-induced cognitive deficits in a murine model of sleep apnea. *BMC Neurosci*, **13**, 77.

De Bruijn, R. F., Schrijvers, E. M., de Groot, K. A., Witteman, J. C., Hofman, A., Franco, O. H., . . . Ikram, M. A. (2013). The association between physical activity and dementia in an elderly population: the Rotterdam Study. *Eur J Epidemiol*, **28**(3), 277-283.

De Filippis, L., & Delia, D. (2011). Hypoxia in the regulation of neural stem cells. *Cell Mol Life Sci*, **68**(17), 2831-2844.

Delgado, A. C., Ferron, S. R., Vicente, D., Porlan, E., Perez-Villalba, A., Trujillo, C. M., . . . Farinas, I. (2014). Endothelial NT-3 delivered by vasculature and CSF promotes quiescence of subependymal neural stem cells through nitric oxide induction. *Neuron*, **83**(3), 572-585.

Dhaliwal, J., & Lagace, D. C. (2011). Visualization and genetic manipulation of adult neurogenesis using transgenic mice. *Eur J Neurosci*, **33**(6), 1025-1036.

Digicaylioglu, M., Bichet, S., Marti, H. H., Wenger, R. H., Rivas, L. A., Bauer, C., & Gassmann, M. (1995). Localization of specific erythropoietin binding sites in defined areas of the mouse brain. *Proc Natl Acad Sci U S A*, **92**(9), 3717-3720.

Dings, J., Jager, A., Meixensberger, J., & Roosen, K. (1998). Brain tissue pO2 and outcome after severe head injury. *Neurol Res*, **20** Suppl 1, S71-75.

Doetsch, F. (2003). A niche for adult neural stem cells. *Curr Opin Genet Dev*, **13**(5), 543-550.

Doetsch, F., Caille, I., Lim, D. A., Garcia-Verdugo, J. M., & Alvarez-Buylla, A. (1999). Subventricular zone astrocytes are neural stem cells in the adult mammalian brain. *Cell*, **97**(6), 703-716.

Dranovsky, A., Picchini, A. M., Moadel, T., Sisti, A. C., Yamada, A., Kimura, S., . . . Hen, R. (2011). Experience dictates stem cell fate in the adult hippocampus. *Neuron*, **70**(5), 908-923.

Duan, X., Kang, E., Liu, C. Y., Ming, G. L., & Song, H. (2008). Development of neural stem cell in the adult brain. *Curr Opin Neurobiol*, **18**(1), 108-115.

Dupret, D., Revest, J. M., Koehl, M., Ichas, F., De Giorgi, F., Costet, P., . . . Piazza, P. V. (2008). Spatial relational memory requires hippocampal adult neurogenesis. *PLoS One*, **3**(4), e1959.

Dustman, R. E., Ruhling, R. O., Russell, E. M., Shearer, D. E., Bonekat, H. W., Shigeoka, J. W., . . . Bradford, D. C. (1984). Aerobic exercise training and improved neuropsychological function of older individuals. *Neurobiol Aging*, **5**(1), 35-42.

Eadie, B. D., Redila, V. A., & Christie, B. R. (2005). Voluntary exercise alters the cytoarchitecture of the adult dentate gyrus by increasing cellular proliferation, dendritic complexity, and spine density. *J Comp Neurol*, **486**(1), 39-47.

Ehm, O., Goritz, C., Covic, M., Schaffner, I., Schwarz, T. J., Karaca, E., . . . Lie, D. C. (2010). RBPJkappa-dependent signaling is essential for long-term maintenance of neural stem cells in the adult hippocampus. *J Neurosci*, **30**(41), 13794-13807.

Ehrenreich, H., Degner, D., Meller, J., Brines, M., Behe, M., Hasselblatt, M., . . . Siren, A. L. (2004). Erythropoietin: a candidate compound for neuroprotection in schizophrenia. *Mol Psychiatry*, **9**(1), 42-54.

Ehrenreich, H., Fischer, B., Norra, C., Schellenberger, F., Stender, N., Stiefel, M., . . . Bartels, C. (2007). Exploring recombinant human erythropoietin in chronic progressive multiple sclerosis. *Brain*, **130**(Pt 10), 2577-2588.

Ehrenreich, H., Hasselblatt, M., Dembowski, C., Cepek, L., Lewczuk, P., Stiefel, M., . . . Siren, A. L. (2002). Erythropoietin therapy for acute stroke is both safe and beneficial. *Mol Med*, **8**(8), 495-505.

Ehrenreich, H., Hinze-Selch, D., Stawicki, S., Aust, C., Knolle-Veentjer, S., Wilms, S., . . . Krampe, H. (2007). Improvement of cognitive functions in chronic schizophrenic patients by recombinant human erythropoietin. *Mol Psychiatry*, **12**(2), 206-220.

Eliasson, P., & Jonsson, J. I. (2010). The hematopoietic stem cell niche: low in oxygen but a nice place to be. *J Cell Physiol*, **222**(1), 17-22.

Encinas, J. M., Hamani, C., Lozano, A. M., & Enikolopov, G. (2011). Neurogenic hippocampal targets of deep brain stimulation. *J Comp Neurol*, **519**(1), 6-20.

Epp, J. R., Silva Mera, R., Kohler, S., Josselyn, S. A., & Frankland, P. W. (2016). Neurogenesis-mediated forgetting minimizes proactive interference. *Nat Commun*, **7**, 10838.

Erecinska, M., & Silver, I. A. (2001). Tissue oxygen tension and brain sensitivity to hypoxia. *Respir Physiol*, **128**(3), 263-276.

Eriksson, P. S., Perfilieva, E., Bjork-Eriksson, T., Alborn, A. M., Nordborg, C., Peterson, D. A., & Gage, F. H. (1998). Neurogenesis in the adult human hippocampus. *Nat Med*, **4**(11), 1313-1317.

Ernst, A., Alkass, K., Bernard, S., Salehpour, M., Perl, S., Tisdale, J., . . . Frisen, J. (2014). Neurogenesis in the striatum of the adult human brain. *Cell*, **156**(5), 1072-1083.

Fabel, K., Fabel, K., Tam, B., Kaufer, D., Baiker, A., Simmons, N., . . . Palmer, T. D. (2003). VEGF is necessary for exercise-induced adult hippocampal neurogenesis. *Eur J Neurosci*, **18**(10), 2803-2812.

Faigle, R., & Song, H. (2013). Signaling mechanisms regulating adult neural stem cells and neurogenesis. *Biochim Biophys Acta*, **1830**(2), 2435-2448.

Fandrey, J., Seydel, F. P., Siegers, C. P., & Jelkmann, W. (1990). Role of cytochrome P450 in the control of the production of erythropoietin. *Life Sci*, **47**(2), 127-134.

Feil, R., Wagner, J., Metzger, D., & Chambon, P. (1997). Regulation of Cre recombinase activity by mutated estrogen receptor ligand-binding domains. *Biochem Biophys Res Commun*, **237**(3), 752-757.

Feng, S., Wang, Q., Wang, H., Peng, Y., Wang, L., Lu, Y., . . . Xiong, L. (2010). Electroacupuncture pretreatment ameliorates hypergravity-induced impairment of learning and memory and apoptosis of hippocampal neurons in rats. *Neurosci Lett*, **478**(3), 150-155.

Ferent, J., Cochard, L., Faure, H., Taddei, M., Hahn, H., Ruat, M., & Traiffort, E. (2014). Genetic activation of Hedgehog signaling unbalances the rate of neural stem cell renewal by increasing symmetric divisions. *Stem Cell Reports*, **3**(2), 312-323.

Ferri, A. L., Cavallaro, M., Braida, D., Di Cristofano, A., Canta, A., Vezzani, A., . . . Nicolis, S. K. (2004). Sox2 deficiency causes neurodegeneration and impaired neurogenesis in the adult mouse brain. *Development*, **131**(15), 3805-3819.

Florio, M., & Huttner, W. B. (2014). Neural progenitors, neurogenesis and the evolution of the neocortex. *Development*, **141**(11), 2182-2194.

Fuchs, E., & Segre, J. A. (2000). Stem cells: a new lease on life. *Cell*, **100**(1), 143-155.

Galvin, K. E., Ye, H., Erstad, D. J., Feddersen, R., & Wetmore, C. (2008). Gli1 induces G2/M arrest and apoptosis in hippocampal but not tumor-derived neural stem cells. *Stem Cells*, **26**(4), 1027-1036.

Garcia, A. D., Doan, N. B., Imura, T., Bush, T. G., & Sofroniew, M. V. (2004). GFAP-expressing progenitors are the principal source of constitutive neurogenesis in adult mouse forebrain. *Nat Neurosci*, **7**(11), 1233-1241.

Garthe, A., Behr, J., & Kempermann, G. (2009). Adult-generated hippocampal neurons allow the flexible use of spatially precise learning strategies. *PLoS One*, **4**(5), e5464.

Ge, S., Goh, E. L., Sailor, K. A., Kitabatake, Y., Ming, G. L., & Song, H. (2006). GABA regulates synaptic integration of newly generated neurons in the adult brain. *Nature*, **439**(7076), 589-593.

Ge, S., Pradhan, D. A., Ming, G. L., & Song, H. (2007). GABA sets the tempo for activity-dependent adult neurogenesis. *Trends Neurosci*, **30**(1), 1-8.

Geil, C. R., Hayes, D. M., McClain, J. A., Liput, D. J., Marshall, S. A., Chen, K. Y., & Nixon, K. (2014). Alcohol and adult hippocampal neurogenesis: promiscuous drug, wanton effects. *Prog Neuropsychopharmacol Biol Psychiatry*, **54**, 103-113.

Gilbert, C. D., Sigman, M., & Crist, R. E. (2001). The neural basis of perceptual learning. *Neuron*, **31**(5), 681-697.

Goebbels, S., Bormuth, I., Bode, U., Hermanson, O., Schwab, M. H., & Nave, K. A. (2006). Genetic targeting of principal neurons in neocortex and hippocampus of NEX-Cre mice. *Genesis*, **44**(12), 611-621.

Gomez-Pinilla, F., & Hillman, C. (2013). The influence of exercise on cognitive abilities. *Compr Physiol*, **3**(1), 403-428.

Gopinath, S. D., Webb, A. E., Brunet, A., & Rando, T. A. (2014). FOXO3 promotes quiescence in adult muscle stem cells during the process of self-renewal. *Stem Cell Reports*, **2**(4), 414-426.

Gotz, M., & Huttner, W. B. (2005). The cell biology of neurogenesis. *Nat Rev Mol Cell Biol*, **6**(10), 777-788.

Gotz, M., Sirko, S., Beckers, J., & Irmler, M. (2015). Reactive astrocytes as neural stem or progenitor cells: In vivo lineage, In vitro potential, and Genome-wide expression analysis. *Glia*, **63**(8), 1452-1468.

Gould, E. (2007). How widespread is adult neurogenesis in mammals? *Nat Rev Neurosci*, **8**(6), 481-488.

Gould, E., Reeves, A. J., Graziano, M. S., & Gross, C. G. (1999). Neurogenesis in the neocortex of adult primates. *Science*, **286**(5439), 548-552.

Gould, E., Tanapat, P., McEwen, B. S., Flugge, G., & Fuchs, E. (1998). Proliferation of granule cell precursors in the dentate gyrus of adult monkeys is diminished by stress. *Proc Natl Acad Sci U S A*, **95**(6), 3168-3171.

Gould, E., Vail, N., Wagers, M., & Gross, C. G. (2001). Adult-generated hippocampal and neocortical neurons in macaques have a transient existence. *Proc Natl Acad Sci U S A*, **98**(19), 10910-10917.

Gould, P., & Kamnasaran, D. (2011). Immunohistochemical analyses of NPAS3 expression in the developing human fetal brain. *Anat Histol Embryol*, **40**(3), 196-203.

Graham, V., Khudyakov, J., Ellis, P., & Pevny, L. (2003). SOX2 functions to maintain neural progenitor identity. *Neuron*, **39**(5), 749-765.

Guirado, R., Perez-Rando, M., Sanchez-Matarredona, D., Castillo-Gómez, E., Liberia, T., Rovira-Esteban, L., . . . Nacher, J. (2013). The dendritic spines of interneurons are dynamic structures influenced by PSA-NCAM expression. *Cerebral cortex*, **24**(11), 3014-3024.

Gustafsson, M. V., Zheng, X., Pereira, T., Gradin, K., Jin, S., Lundkvist, J., . . . Bondesson, M. (2005). Hypoxia requires notch signaling to maintain the undifferentiated cell state. *Dev Cell*, **9**(5), 617-628.

Haas, S., Weidner, N., & Winkler, J. (2005). Adult stem cell therapy in stroke. *Curr Opin Neurol*, **18**(1), 59-64.

Harrison, S. J., Guidolin, A., Faast, R., Crocker, L. A., Giannakis, C., D'Apice, A. J., . . . Lyons, I. (2002). Efficient generation of alpha(1,3) galactosyltransferase knockout porcine fetal fibroblasts for nuclear transfer. *Transgenic Res*, **11**(2), 143-150.

Hasselblatt, M., Ehrenreich, H., & Siren, A. L. (2006). The brain erythropoietin system and its potential for therapeutic exploitation in brain disease. *J Neurosurg Anesthesiol*, **18**(2), 132-138.

Hassouna, I., Ott, C., Wustefeld, L., Offen, N., Neher, R. A., Mitkovski, M., . . . Ehrenreich, H. (2016). Revisiting adult neurogenesis and the role of erythropoietin for neuronal and oligodendroglial differentiation in the hippocampus. *Mol Psychiatry*, **21**(12), 1752-1767.

Hastings, N. B., & Gould, E. (1999). Rapid extension of axons into the CA3 region by adult-generated granule cells. *J Comp Neurol*, **413**(1), 146-154.

Hattangadi, S. M., Wong, P., Zhang, L., Flygare, J., & Lodish, H. F. (2011). From stem cell to red cell: regulation of erythropoiesis at multiple levels by multiple proteins, RNAs, and chromatin modifications. *Blood*, **118**(24), 6258-6268.

Haubst, N., Berger, J., Radjendirane, V., Graw, J., Favor, J., Saunders, G. F., . . . Gotz, M. (2004). Molecular dissection of Pax6 function: the specific roles of the paired domain and homeodomain in brain development. *Development*, **131**(24), 6131-6140.

Hevner, R. F., Hodge, R. D., Daza, R. A., & Englund, C. (2006). Transcription factors in glutamatergic neurogenesis: conserved programs in neocortex, cerebellum, and adult hippocampus. *Neurosci Res*, **55**(3), 223-233.

Hibbits, N., Pannu, R., Wu, T. J., & Armstrong, R. C. (2009). Cuprizone demyelination of the corpus callosum in mice correlates with altered social interaction and impaired bilateral sensorimotor coordination. *ASN neuro*, **1**(3), AN20090032.

Hochgerner, H., Zeisel, A., Lonnerberg, P., & Linnarsson, S. (2018). Conserved properties of dentate gyrus neurogenesis across postnatal development revealed by single-cell RNA sequencing. *Nat Neurosci*, **21**(2), 290-299.

Hodge, R. D., Kowalczyk, T. D., Wolf, S. A., Encinas, J. M., Rippey, C., Enikolopov, G., . . . Hevner, R. F. (2008). Intermediate progenitors in adult hippocampal neurogenesis: Tbr2 expression and coordinate regulation of neuronal output. *J Neurosci*, **28**(14), 3707-3717.

Holzenberger, M., Zaoui, R., Leneuve, P., Hamard, G., & Le Bouc, Y. (2000). Ubiquitous postnatal LoxP recombination using a doxycycline auto-inducible Cre transgene (DAI-Cre). *Genesis*, **26**(2), 157-159.

Hsieh, J. (2012). Orchestrating transcriptional control of adult neurogenesis. *Genes Dev*, **26**(10), 1010-1021.

Indra, A. K., Warot, X., Brocard, J., Bornert, J. M., Xiao, J. H., Chambon, P., & Metzger, D. (1999). Temporally-controlled site-specific mutagenesis in the basal layer of the epidermis: comparison of the recombinase activity of the tamoxifen-inducible Cre-ER(T) and Cre-ER(T2) recombinases. *Nucleic Acids Res*, **27**(22), 4324-4327.

Iwai, M., Stetler, R. A., Xing, J., Hu, X., Gao, Y., Zhang, W., . . . Cao, G. (2010). Enhanced oligodendrogenesis and recovery of neurological function by erythropoietin after neonatal hypoxic/ischemic brain injury. *Stroke*, **41**(5), 1032-1037.

Iyer, N. V., Kotch, L. E., Agani, F., Leung, S. W., Laughner, E., Wenger, R. H., . . . Semenza, G. L. (1998). Cellular and developmental control of O2 homeostasis by hypoxia-inducible factor 1 alpha. *Genes Dev*, **12**(2), 149-162.

Jacobs, K., Shoemaker, C., Rudersdorf, R., Neill, S. D., Kaufman, R. J., Mufson, A., . . . et al. (1985). Isolation and characterization of genomic and cDNA clones of human erythropoietin. *Nature*, **313**(6005), 806-810.

Jakovcevski, I., Mayer, N., & Zecevic, N. (2011). Multiple origins of human neocortical interneurons are supported by distinct expression of transcription factors. *Cereb Cortex*, **21**(8), 1771-1782.

Jang, M. H., Bonaguidi, M. A., Kitabatake, Y., Sun, J., Song, J., Kang, E., . . . Song, H. (2013). Secreted frizzled-related protein 3 regulates activity-dependent adult hippocampal neurogenesis. *Cell Stem Cell*, **12**(2), 215-223.

Jelkmann, W. (1992). Erythropoietin: structure, control of production, and function. *Physiol Rev*, **72**(2), 449-489.

Jelkmann, W. (2007). Erythropoietin after a century of research: younger than ever. *European journal of haematology*, **78**(3), 183-205.

Jelkmann, W. (2011). Regulation of erythropoietin production. *The Journal of physiology*, **589**(6), 1251-1258.

Jennings, B. H., & Ish-Horowicz, D. (2008). The Groucho/TLE/Grg family of transcriptional co-repressors. *Genome Biol*, **9**(1), 205.

Jin, K., Mao, X. O., Sun, Y., Xie, L., & Greenberg, D. A. (2002). Stem cell factor stimulates neurogenesis in vitro and in vivo. *J Clin Invest*, **110**(3), 311-319.

Juul, S. E., Anderson, D. K., Li, Y., & Christensen, R. D. (1998). Erythropoietin and erythropoietin receptor in the developing human central nervous system. *Pediatr Res*, **43**(1), 40-49.

Juul, S. E., Stallings, S. A., & Christensen, R. D. (1999). Erythropoietin in the cerebrospinal fluid of neonates who sustained CNS injury. *Pediatr Res*, **46**(5), 543-547

Kaelin, W. G., Jr., & Ratcliffe, P. J. (2008). Oxygen sensing by metazoans: the central role of the HIF hydroxylase pathway. *Mol Cell*, **30**(4), 393-402.

Kamachi, Y., & Kondoh, H. (2013). Sox proteins: regulators of cell fate specification and differentiation. *Development*, **140**(20), 4129-4144.

Kang, W., & Hebert, J. M. (2015). FGF Signaling Is Necessary for Neurogenesis in Young Mice and Sufficient to Reverse Its Decline in Old Mice. *J Neurosci*, **35**(28), 10217-10223.

Kaplan, M. S. (1981). Neurogenesis in the 3-month-old rat visual cortex. *J Comp Neurol*, **195**(2), 323-338.

Kasai, H., Fukuda, M., Watanabe, S., Hayashi-Takagi, A., & Noguchi, J. (2010). Structural dynamics of dendritic spines in memory and cognition. *Trends in neurosciences*, **33**(3), 121-129.

Kasai, M., Fukumitsu, H., Soumiya, H., & Furukawa, S. (2011). Caffeic acid phenethyl ester reduces spinal cord injury-evoked locomotor dysfunction. *Biomed Res*, **32**(1), 1-7.

Kästner, A., Grube, S., El-Kordi, A., Stepniak, B., Friedrichs, H., Sargin, D., ..., Nave, K., Rujescu, D., & Ehrenreich, H. (2012). Common variants of the genes encoding erythopoietin and its receptor modulate cognitive performance in schizophrenia. *Molecular Medicine*, **18**, 1029-1040.

Kawaguchi, K., Kaneko, N., Fukuda, M., Nakano, Y., Kimura, S., Hara, A., & Shimizu, M. (2013). Responses of insulin-like growth factor (IGF)-I and two IGF-binding protein-1 subtypes to fasting and re-feeding, and their relationships with individual growth rates in yearling masu salmon (Oncorhynchus masou). *Comp Biochem Physiol A Mol Integr Physiol*, **165**(2), 191-198.

Kempermann, G., Song, H., & Gage, F. H. (2015). Neurogenesis in the Adult Hippocampus. *Cold Spring Harb Perspect Biol*, **7**(9), a018812.

Kietzmann, T., Mennerich, D., & Dimova, E. Y. (2016). Hypoxia-inducible factors (HIFs) and phosphorylation: impact on stability, localization, and transactivity. *Frontiers in cell and developmental biology*, **4**, 11.

Kimura, W., Xiao, F., Canseco, D. C., Muralidhar, S., Thet, S., Zhang, H. M., . . . Sadek, H. A. (2015). Hypoxia fate mapping identifies cycling cardiomyocytes in the adult heart. *Nature*, **523**(7559), 226-230.

Kofoed, M. L., Klemp, P., & Thestrup-Pedersen, K. (1985). The Klippel-Trenaunay syndrome with acro-angiodermatitis (pseudo-Kaposi's sarcoma). *Acta Derm Venereol*, **65**(1), 75-77.

Kokaia, Z., & Lindvall, O. (2003). Neurogenesis after ischaemic brain insults. *Curr Opin Neurobiol*, **13**(1), 127-132.

Kornack, D. R., & Rakic, P. (1999). Continuation of neurogenesis in the hippocampus of the adult macaque monkey. *Proc Natl Acad Sci U S A*, **96**(10), 5768-5773.

Kramer, A. F., & Erickson, K. I. (2007). Effects of physical activity on cognition, well-being, and brain: human interventions. *Alzheimers Dement*, **3**(2 Suppl), S45-51.

Krantz, S. B. (1991). Erythropoietin. *Blood*, **77**(3), 419-434.

Kriegstein, A., & Alvarez-Buylla, A. (2009). The glial nature of embryonic and adult neural stem cells. *Annu Rev Neurosci*, **32**, 149-184.

Kronenberg, G., Reuter, K., Steiner, B., Brandt, M. D., Jessberger, S., Yamaguchi, M., & Kempermann, G. (2003). Subpopulations of proliferating cells of the adult hippocampus respond differently to physiologic neurogenic stimuli. *J Comp Neurol*, **467**(4), 455-463.

Kuhn, H. G., Biebl, M., Wilhelm, D., Li, M., Friedlander, R. M., & Winkler, J. (2005). Increased generation of granule cells in adult Bcl-2-overexpressing mice: a role for cell death during continued hippocampal neurogenesis. *Eur J Neurosci*, **22**(8), 1907-1915.

Kuhn, H. G., Dickinson-Anson, H., & Gage, F. H. (1996). Neurogenesis in the dentate gyrus of the adult rat: age-related decrease of neuronal progenitor proliferation. *J Neurosci*, **16**(6), 2027-2033.

Lacombe, C., Da Silva, J. L., Bruneval, P., Fournier, J. G., Wendling, F., Casadevall, N., . . . Tambourin, P. (1988). Peritubular cells are the site of erythropoietin synthesis in the murine hypoxic kidney. *J Clin Invest*, **81**(2), 620-623.

Lagace, D. C., Fischer, S. J., & Eisch, A. J. (2007). Gender and endogenous levels of estradiol do not influence adult hippocampal neurogenesis in mice. *Hippocampus*, **17**(3), 175-180.

Lai, K., Kaspar, B. K., Gage, F. H., & Schaffer, D. V. (2003). Sonic hedgehog regulates adult neural progenitor proliferation in vitro and in vivo. *Nat Neurosci*, **6**(1), 21-27.

Lai, P. H., Everett, R., Wang, F. F., Arakawa, T., & Goldwasser, E. (1986). Structural characterization of human erythropoietin. *J Biol Chem*, **261**(7), 3116-3121.

Larson, E. B., Wang, L., Bowen, J. D., McCormick, W. C., Teri, L., Crane, P., & Kukull, W. (2006). Exercise is associated with reduced risk for incident dementia among persons 65 years of age and older. *Ann Intern Med*, **144**(2), 73-81.

Lautenschlager, N. T., & Almeida, O. P. (2006). Physical activity and cognition in old age. *Curr Opin Psychiatry*, **19**(2), 190-193.

Lekli, I., Gurusamy, N., Ray, D., Tosaki, A., & Das, D. K. (2009). Redox regulation of stem cell mobilization. *Can J Physiol Pharmacol*, **87**(12), 989-995.

Leuner, B., Kozorovitskiy, Y., Gross, C. G., & Gould, E. (2007). Diminished adult neurogenesis in the marmoset brain precedes old age. *Proc Natl Acad Sci U S A*, **104**(43), 17169-17173.

Leung, C. T., Coulombe, P. A., & Reed, R. R. (2007). Contribution of olfactory neural stem cells to tissue maintenance and regeneration. *Nat Neurosci*, **10**(6), 720-726.

Lewczuk, P., Hasselblatt, M., Kamrowski-Kruck, H., Heyer, A., Unzicker, C., Siren, A. L., & Ehrenreich, H. (2000). Survival of hippocampal neurons in culture upon hypoxia: effect of erythropoietin. *Neuroreport*, **11**(16), 3485-3488.

Li, L., & Clevers, H. (2010). Coexistence of quiescent and active adult stem cells in mammals. *Science*, **327**(5965), 542-545.

Liebetanz, D., & Merkler, D. (2006). Effects of commissural de-and remyelination on motor skill behaviour in the cuprizone mouse model of multiple sclerosis. *Experimental neurology*, **202**(1), 217-224.

Liebetanz, D., Baier, P. C., Paulus, W., Meuer, K., Bähr, M., & Weishaupt, J. H. (2007). A highly sensitive automated complex running wheel test to detect latent motor deficits in the mouse MPTP model of Parkinson's disease. *Experimental neurology*, **205**(1), 207-213.

Lim, D. A., Tramontin, A. D., Trevejo, J. M., Herrera, D. G., Garcia-Verdugo, J. M., & Alvarez-Buylla, A. (2000). Noggin antagonizes BMP signaling to create a niche for adult neurogenesis. *Neuron*, **28**(3), 713-726.

Lin, C. S., Lim, S. K., D'Agati, V., & Costantini, F. (1996). Differential effects of an erythropoietin receptor gene disruption on primitive and definitive erythropoiesis. *Genes Dev*, **10**(2), 154-164.

Liu, C., Shen, K., Liu, Z., & Noguchi, C. T. (1997). Regulated human erythropoietin receptor expression in mouse brain. *J Biol Chem*, **272**(51), 32395-32400.

Liu, F., You, Y., Li, X., Ma, T., Nie, Y., Wei, B., . . . Yang, Z. (2009). Brain injury does not alter the intrinsic differentiation potential of adult neuroblasts. *J Neurosci*, **29**(16), 5075-5087.

Liu, H. M., & Chen, H. H. (1994). c-fos protein expression and ischemic changes in neurons vulnerable to ischemia/hypoxia, correlated with basic fibroblast growth factor immunoreactivity. *J Neuropathol Exp Neurol*, **53**(6), 598-605.

Liu, Y., & Labosky, P. A. (2008). Regulation of embryonic stem cell self-renewal and pluripotency by Foxd3. *Stem Cells*, **26**(10), 2475-2484.

Llorens-Bobadilla, E., Zhao, S., Baser, A., Saiz-Castro, G., Zwadlo, K., & Martin-Villalba, A. (2015). Single-Cell Transcriptomics Reveals a Population of Dormant Neural Stem Cells that Become Activated upon Brain Injury. *Cell Stem Cell*, **17**(3), 329-340.

Lodato, M. A., Ng, C. W., Wamstad, J. A., Cheng, A. W., Thai, K. K., Fraenkel, E., . . . Boyer, L. A. (2013). SOX2 co-occupies distal enhancer elements with distinct POU factors in ESCs and NPCs to specify cell state. *PLoS Genet*, **9**(2), e1003288.

Loike, J. D., Cao, L., Brett, J., Ogawa, S., Silverstein, S. C., & Stern, D. (1992). Hypoxia induces glucose transporter expression in endothelial cells. *Am J Physiol*, **263**(2 Pt 1), C326-333.

Luo, J., Daniels, S. B., Lennington, J. B., Notti, R. Q., & Conover, J. C. (2006). The aging neurogenic subventricular zone. *Aging Cell*, **5**(2), 139-152.

Luo, Y., Coskun, V., Liang, A., Yu, J., Cheng, L., Ge, W., . . . Li, S. (2015). Single-cell transcriptome analyses reveal signals to activate dormant neural stem cells. *Cell*, **161**(5), 1175-1186.

Luzzati, F. (2015). A hypothesis for the evolution of the upper layers of the neocortex through co-option of the olfactory cortex developmental program. *Front Neurosci*, **9**, 162.

Machold, R., Hayashi, S., Rutlin, M., Muzumdar, M. D., Nery, S., Corbin, J. G., . . . Fishell, G. (2003). Sonic hedgehog is required for progenitor cell maintenance in telencephalic stem cell niches. *Neuron*, **39**(6), 937-950.

Macosko, E. Z., Basu, A., Satija, R., Nemesh, J., Shekhar, K., Goldman, M., . . . McCarroll, S. (2015). Highly parallel genome-wide expression profiling of individual cells using nanoliter droplets. *Cell*, **161**(5), 1202-1214.

Madisen, L., Zwingman, T. A., Sunkin, S. M., Oh, S. W., Zariwala, H. A., Gu, H., . . . Zeng, H. (2010). A robust and high-throughput Cre reporting and characterization system for the whole mouse brain. *Nat Neurosci*, **13**(1), 133-140.

Magnus, T., Chan, A., Grauer, O., Toyka, K. V., & Gold, R. (2001). Microglial phagocytosis of apoptotic inflammatory T cells leads to down-regulation of microglial immune activation. *J Immunol*, **167**(9), 5004-5010.

Maherali, N., Sridharan, R., Xie, W., Utikal, J., Eminli, S., Arnold, K., . . . Hochedlinger, K. (2007). Directly reprogrammed fibroblasts show global epigenetic remodeling and widespread tissue contribution. *Cell Stem Cell*, **1**(1), 55-70.

Majmundar, A. J., Wong, W. J., & Simon, M. C. (2010). Hypoxia-inducible factors and the response to hypoxic stress. *Mol Cell*, **40**(2), 294-309.

Manalo, D. J., Rowan, A., Lavoie, T., Natarajan, L., Kelly, B. D., Ye, S. Q., . . . Semenza, G. L. (2005). Transcriptional regulation of vascular endothelial cell responses to hypoxia by HIF-1. *Blood*, **105**(2), 659-669.

Marmur, R., Mabie, P. C., Gokhan, S., Song, Q., Kessler, J. A., & Mehler, M. F. (1998). Isolation and developmental characterization of cerebral cortical multipotent progenitors. *Dev Biol*, **204**(2), 577-591.

Marques, S., van Bruggen, D., Vanichkina, D. P., Floriddia, E. M., Munguba, H., Varemo, L., . . . Castelo-Branco, G. (2018). Transcriptional Convergence of Oligodendrocyte Lineage Progenitors during Development. *Dev Cell*, **46**(4), 504-517 e507.

Marti, H. H., Gassmann, M., Wenger, R. H., Kvietikova, I., Morganti-Kossmann, M. C., Kossmann, T., . . . Bauer, C. (1997). Detection of erythropoietin in human liquor: intrinsic erythropoietin production in the brain. *Kidney Int*, **51**(2), 416-418.

Marti, H. H., Wenger, R. H., Rivas, L. A., Straumann, U., Digicaylioglu, M., Henn, V., . . . Gassmann, M. (1996). Erythropoietin gene expression in human, monkey and murine brain. *Eur J Neurosci*, **8**(4), 666-676.

Masuda, S., Okano, M., Yamagishi, K., Nagao, M., Ueda, M., & Sasaki, R. (1994). A novel site of erythropoietin production. Oxygen-dependent production in cultured rat astrocytes. *J Biol Chem*, **269**(30), 19488-19493.

Mateika, J. H., El-Chami, M., Shaheen, D., & Ivers, B. (2015). Intermittent hypoxia: a low risk research tool with therapeutic value in humans. *American Journal of Physiology-Heart and Circulatory Physiology*.

Matsumoto, K., Akao, Y., Yi, H., Shamoto-Nagai, M., Maruyama, W., & Naoi, M. (2006). Overexpression of amyloid precursor protein induces susceptibility to oxidative stress in human neuroblastoma SH-SY5Y cells. *J Neural Transm (Vienna)*, **113**(2), 125-135.

Maurice, T., Mustafa, M. H., Desrumaux, C., Keller, E., Naert, G., de la, C. G.-B. M., . . . Garcia Rodriguez, J. C. (2013). Intranasal formulation of erythropoietin (EPO) showed potent protective activity against amyloid toxicity in the Abeta(2)(5)(-)(3)(5) non-transgenic mouse model of Alzheimer's disease. *J Psychopharmacol*, **27**(11), 1044-1057.

McKenzie, I. A., Ohayon, D., Li, H., De Faria, J. P., Emery, B., Tohyama, K., & Richardson, W. D. (2014). Motor skill learning requires active central myelination. *Science*, **346**(6207), 318-322.

Meng, J. Z., Guo, L. W., Cheng, H., Chen, Y. J., Fang, L., Qi, M., . . . Hong, X. N. (2012). Correlation between cognitive function and the association fibers in patients with Alzheimer's disease using diffusion tensor imaging. *J Clin Neurosci*, **19**(12), 1659-1663.

Mercer, T. R., Dinger, M. E., Sunkin, S. M., Mehler, M. F., & Mattick, J. S. (2008). Specific expression of long noncoding RNAs in the mouse brain. *Proc Natl Acad Sci U S A*, **105**(2), 716-721.

Michelucci, A., Bithell, A., Burney, M. J., Johnston, C. E., Wong, K. Y., Teng, S. W., . . . Buckley, N. J. (2016). The Neurogenic Potential of Astrocytes Is Regulated by Inflammatory Signals. *Mol Neurobiol*, **53**(6), 3724-3739.

Milosevic, J., Schwarz, S. C., Krohn, K., Poppe, M., Storch, A., & Schwarz, J. (2005). Low atmospheric oxygen avoids maturation, senescence and cell death of murine mesencephalic neural precursors. *J Neurochem*, **92**(4), 718-729.

Ming, G. L., & Song, H. (2005). Adult neurogenesis in the mammalian central nervous system. *Annu Rev Neurosci*, **28**, 223-250.

Mira, H., Andreu, Z., Suh, H., Lie, D. C., Jessberger, S., Consiglio, A., . . . Gage, F. H. (2010). Signaling through BMPR-IA regulates quiescence and long-term activity of neural stem cells in the adult hippocampus. *Cell Stem Cell*, **7**(1), 78-89.

Miskowiak, K. W., Ehrenreich, H., Christensen, E. M., Kessing, L. V., & Vinberg, M. (2014). Recombinant human erythropoietin to target cognitive dysfunction in bipolar disorder: a double-blind, randomized, placebo-controlled phase 2 trial. *J Clin Psychiatry*, **75**(12), 1347-1355. d

Miskowiak, K. W., Macoveanu, J., Vinberg, M., Assentoft, E., Randers, L., Harmer, C. J., . . . Kessing, L. V. (2016). Effects of erythropoietin on memory-relevant neurocircuitry activity and recall in mood disorders. *Acta Psychiatr Scand*, **134**(3), 249-259.

Miskowiak, K. W., Vinberg, M., Christensen, E. M., Bukh, J. D., Harmer, C. J., Ehrenreich, H., & Kessing, L. V. (2014). Recombinant human erythropoietin for treating treatment-resistant depression: a double-blind, randomized, placebo-controlled phase 2 trial. *Neuropsychopharmacology*, **39**(6), 1399-1408.

Miskowiak, K. W., Vinberg, M., Glerup, L., Paulson, O. B., Knudsen, G. M., Ehrenreich, H., . . . Macoveanu, J. (2016). Neural correlates of improved executive function following erythropoietin treatment in mood disorders. *Psychol Med*, **46**(8), 1679-1691.

Miskowiak, K. W., Vinberg, M., Harmer, C. J., Ehrenreich, H., Knudsen, G. M., Macoveanu, J., . . . Kessing, L. V. (2010). Effects of erythropoietin on depressive symptoms and neurocognitive deficits in depression and bipolar disorder. *Trials*, **11**, 97.

Miskowiak, K. W., Vinberg, M., Macoveanu, J., Ehrenreich, H., Koster, N., Inkster, B., . . . Siebner, H. R. (2015). Effects of Erythropoietin on Hippocampal Volume and Memory in Mood Disorders. *Biol Psychiatry*, **78**(4), 270-277.

Mitkovski, M., Dahm, L., Heinrich, R., Monnheimer, M., Gerhart, S., Stegmuller, J., . . . Ehrenreich, H. (2015). Erythropoietin dampens injury-induced microglial motility. *J Cereb Blood Flow Metab*, **35**(8), 1233-1236.

Morante-Redolat, J. M., & Farinas, I. (2016). Fetal neurogenesis: breathe HIF you can. *EMBO J*, **35**(9), 901-903.

Moreno-Jimenez, E. P., Flor-Garcia, M., Terreros-Roncal, J., Rabano, A., Cafini, F., Pallas-Bazarra, N., . . . Llorens-Martin, M. (2019). Adult hippocampal neurogenesis is abundant in neurologically healthy subjects and drops sharply in patients with Alzheimer's disease. *Nat Med*, **25**(4), 554-560.

Morgan, J. I., Cohen, D. R., Hempstead, J. L., & Curran, T. (1987). Mapping patterns of c-fos expression in the central nervous system after seizure. *Science*, **237**(4811), 192-197.

Morita, M., Ohneda, O., Yamashita, T., Takahashi, S., Suzuki, N., Nakajima, O., . . . Fujii-Kuriyama, Y. (2003). HLF/HIF-2alpha is a key factor in retinopathy of prematurity in association with erythropoietin. *EMBO J*, **22**(5), 1134-1146.

Morrison, S. J., & Spradling, A. C. (2008). Stem cells and niches: mechanisms that promote stem cell maintenance throughout life. *Cell*, **132**(4), 598-611.

Mu, D., Chang, Y. S., Vexler, Z. S., & Ferriero, D. M. (2005). Hypoxia-inducible factor 1alpha and erythropoietin upregulation with deferoxamine salvage after neonatal stroke. *Exp Neurol*, **195**(2), 407-415.

Nagy, A. (2000). Cre recombinase: the universal reagent for genome tailoring. *Genesis*, **26**(2), 99-109.

Nakashiba, T., Cushman, J. D., Pelkey, K. A., Renaudineau, S., Buhl, D. L., McHugh, T. J., . . . Tonegawa, S. (2012). Young dentate granule cells mediate pattern separation, whereas old granule cells facilitate pattern completion. *Cell*, **149**(1), 188-201.

Namba, T., & Huttner, W. B. (2017). Neural progenitor cells and their role in the development and evolutionary expansion of the neocortex. *Wiley Interdiscip Rev Dev Biol*, **6**(1).

Namiki, J., Suzuki, S., Masuda, T., Ishihama, Y., & Okano, H. (2012). Nestin protein is phosphorylated in adult neural stem/progenitor cells and not endothelial progenitor cells. *Stem Cells Int*, 2012, 430138.

Neher, J. J., Neniskyte, U., Zhao, J. W., Bal-Price, A., Tolkovsky, A. M., & Brown, G. C. (2011). Inhibition of microglial phagocytosis is sufficient to prevent inflammatory neuronal death. *J Immunol*, **186**(8), 4973-4983.

Ng, S. Y., & Stanton, L. W. (2013). Long non-coding RNAs in stem cell pluripotency. *Wiley Interdiscip Rev RNA*, **4**(1), 121-128.

Nguyen, A. Q., Cherry, B. H., Scott, G. F., Ryou, M. G., & Mallet, R. T. (2014). Erythropoietin: powerful protection of ischemic and post-ischemic brain. *Exp Biol Med (Maywood)*, **239**(11), 1461-1475.

Niu, W., Zang, T., Zou, Y., Fang, S., Smith, D. K., Bachoo, R., & Zhang, C. L. (2013). In vivo reprogramming of astrocytes to neuroblasts in the adult brain. *Nat Cell Biol*, **15**(10), 1164-1175.

Noakes, M., Clifton, P. M., Doornbos, A. M., & Trautwein, E. A. (2005). Plant sterol ester-enriched milk and yoghurt effectively reduce serum cholesterol in modestly hypercholesterolemic subjects. *Eur J Nutr*, **44**(4), 214-222.

Noguchi, C. T., Wang, L., Rogers, H. M., Teng, R., & Jia, Y. (2008). Survival and proliferative roles of erythropoietin beyond the erythroid lineage. *Expert Rev Mol Med*, **10**, e36.

Nonaka, Y., Miyajima, M., Ogino, I., Nakajima, M., & Arai, H. (2008). Analysis of neuronal cell death in the cerebral cortex of H-Tx rats with compensated hydrocephalus. *J Neurosurg Pediatr*, **1**(1), 68-74.

Okita, K., Ichisaka, T., & Yamanaka, S. (2007). Generation of germline-competent induced pluripotent stem cells. *Nature*, **448**(7151), 313-317.

O'Rahilly, R., & Muller, F. (2010). Developmental stages in human embryos: revised and new measurements. *Cells Tissues Organs*, **192**(2), 73-84.

Ortega, F., & Costa, M. R. (2016). Live Imaging of Adult Neural Stem Cells in Rodents. *Front Neurosci*, **10**, 78.

Ott, C., Martens, H., Hassouna, I., Oliveira, B., Erck, C., Zafeiriou, M. P., . . . Ehrenreich, H. (2015). Widespread Expression of Erythropoietin Receptor in Brain and Its Induction by Injury. *Mol Med*, **21**(1), 803-815.

Palma, V., Lim, D. A., Dahmane, N., Sanchez, P., Brionne, T. C., Herzberg, C. D., . . . Ruiz i Altaba, A. (2005). Sonic hedgehog controls stem cell behavior in the postnatal and adult brain. *Development*, **132**(2), 335-344.

Palmer, T. D., Willhoite, A. R., & Gage, F. H. (2000). Vascular niche for adult hippocampal neurogenesis. *J Comp Neurol*, **425**(4), 479-494.

Panchision, D. M. (2009). The role of oxygen in regulating neural stem cells in development and disease. *J Cell Physiol*, **220**(3), 562-568.

Paolicelli, R. C., Bolasco, G., Pagani, F., Maggi, L., Scianni, M., Panzanelli, P., . . . Gross, C. T. (2011). Synaptic pruning by microglia is necessary for normal brain development. *Science*, **333**(6048), 1456-1458.

Pardal, R., Ortega-Saenz, P., Duran, R., & Lopez-Barneo, J. (2007). Glia-like stem cells sustain physiologic neurogenesis in the adult mammalian carotid body. *Cell*, **131**(2), 364-377.

Park, M. H., Lee, S. M., Lee, J. W., Son, D. J., Moon, D. C., Yoon, D. Y., & Hong, J. T. (2006). ERK-mediated production of neurotrophic factors by astrocytes promotes neuronal stem cell differentiation by erythropoietin. *Biochem Biophys Res Commun*, **339**(4), 1021-1028.

Parmar, K., Mauch, P., Vergilio, J. A., Sackstein, R., & Down, J. D. (2007). Distribution of hematopoietic stem cells in the bone marrow according to regional hypoxia. *Proc Natl Acad Sci U S A*, **104**(13), 5431-5436.

Pasarica, M., Sereda, O. R., Redman, L. M., Albarado, D. C., Hymel, D. T., Roan, L. E., . . . Smith, S. R. (2009). Reduced adipose tissue oxygenation in human obesity: evidence for rarefaction, macrophage chemotaxis, and inflammation without an angiogenic response. *Diabetes*, **58**(3), 718-725.

Pereira, P. S., Teixeira, A., Pinho, S., Ferreira, P., Fernandes, J., Oliveira, C., . . . Casares, F. (2006). E-cadherin missense mutations, associated with hereditary diffuse gastric cancer (HDGC) syndrome, display distinct invasive behaviors and genetic interactions with the Wnt and Notch pathways in Drosophila epithelia. *Hum Mol Genet*, **15**(10), 1704-1712.

Pietras, E. M., Reynaud, D., Kang, Y. A., Carlin, D., Calero-Nieto, F. J., Leavitt, A. D., . . . Passegue, E. (2015). Functionally Distinct Subsets of Lineage-Biased Multipotent Progenitors Control Blood Production in Normal and Regenerative Conditions. *Cell Stem Cell*, **17**(1), 35-46.

Piumatti, M., Palazzo, O., La Rosa, C., Crociara, P., Parolisi, R., Luzzati, F., . . . Bonfanti, L. (2018). Non-Newly Generated, "Immature" Neurons in the Sheep Brain Are Not Restricted to Cerebral Cortex. *J Neurosci*, **38**(4), 826-842.

Porrero, C., Rubio-Garrido, P., Avendano, C., & Clasca, F. (2010). Mapping of fluorescent protein-expressing neurons and axon pathways in adult and developing Thy1-eYFP-H transgenic mice. *Brain Res*, **1345**, 59-72.

Puelles, L. (2017). Comments on the Updated Tetrapartite Pallium Model in the Mouse and Chick, Featuring a Homologous Claustro-Insular Complex. *Brain Behav Evol*, **90**(2), 171-189.

Puthanveettil, S. V., Antonov, I., Kalachikov, S., Rajasethupathy, P., Choi, Y. B., Kohn, A. B., . . . Kandel, E. R. (2013). A strategy to capture and characterize the synaptic transcriptome. *Proc Natl Acad Sci U S A*, **110**(18), 7464-7469.

Quinones-Hinojosa, A., Sanai, N., Soriano-Navarro, M., Gonzalez-Perez, O., Mirzadeh, Z., Gil-Perotin, S., . . . Alvarez-Buylla, A. (2006). Cellular composition and cytoarchitecture of the adult human subventricular zone: a niche of neural stem cells. *J Comp Neurol*, **494**(3), 415-434.

Rakic, P. (1974). Neurons in rhesus monkey visual cortex: systematic relation between time of origin and eventual disposition. *Science*, **183**(4123), 425-427.

Rakic, P. (1985). Limits of neurogenesis in primates. *Science*, **227**(4690), 1054-1056.

Ramos, A. D., Andersen, R. E., Liu, S. J., Nowakowski, T. J., Hong, S. J., Gertz, C., . . . Lim, D. A. (2015). The long noncoding RNA Pnky regulates neuronal differentiation of embryonic and postnatal neural stem cells. *Cell Stem Cell*, **16**(4), 439-447.

Ramos, A. D., Diaz, A., Nellore, A., Delgado, R. N., Park, K. Y., Gonzales-Roybal, G., . . . Lim, D. A. (2013). Integration of genome-wide approaches identifies lncRNAs of adult neural stem cells and their progeny in vivo. *Cell Stem Cell*, **12**(5), 616-628.

Rietze, R., Poulin, P., & Weiss, S. (2000). Mitotically active cells that generate neurons and astrocytes are present in multiple regions of the adult mouse hippocampus. *J Comp Neurol*, **424**(3), 397-408.

Rimkus, T. K., Carpenter, R. L., Qasem, S., Chan, M., & Lo, H. W. (2016). Targeting the Sonic Hedgehog Signaling Pathway: Review of Smoothened and GLI Inhibitors. *Cancers (Basel)*, **8**(2).

Rodgers, J. T., King, K. Y., Brett, J. O., Cromie, M. J., Charville, G. W., Maguire, K. K., . . . Rando, T. A. (2014). mTORC1 controls the adaptive transition of quiescent stem cells from G0 to G(Alert). *Nature*, **510**(7505), 393-396.

Rotheneichner, P., Belles, M., Benedetti, B., Konig, R., Dannehl, D., Kreutzer, C., . . . Couillard-Despres, S. (2018). Cellular Plasticity in the Adult Murine Piriform Cortex: Continuous Maturation of Dormant Precursors Into Excitatory Neurons. *Cereb Cortex*, **28**(7), 2610-2621.

Rovio, S., Kareholt, I., Helkala, E. L., Viitanen, M., Winblad, B., Tuomilehto, J., . . . Kivipelto, M. (2005). Leisure-time physical activity at midlife and the risk of dementia and Alzheimer's disease. *Lancet Neurol*, **4**(11), 705-711.

Roybon, L., Deierborg, T., Brundin, P., & Li, J. Y. (2009). Involvement of Ngn2, Tbr and NeuroD proteins during postnatal olfactory bulb neurogenesis. *Eur J Neurosci*, **29**(2), 232-243.

Ruifrok, W. P., de Boer, R. A., Westenbrink, B. D., van Veldhuisen, D. J., & van Gilst, W. H. (2008). Erythropoietin in cardiac disease: new features of an old drug. *Eur J Pharmacol*, **585**(2-3), 270-277.

Rushing, G., & Ihrie, R. A. (2016). Neural stem cell heterogeneity through time and space in the ventricular-subventricular zone. *Front Biol (Beijing)*, **11**(4), 261-284.

Sahay, A., & Hen, R. (2007). Adult hippocampal neurogenesis in depression. *Nat Neurosci*, **10**(9), 1110-1115.

Sahay, A., Scobie, K. N., Hill, A. S., O'Carroll, C. M., Kheirbek, M. A., Burghardt, N. S., . . . Hen, R. (2011). Increasing adult hippocampal neurogenesis is sufficient to improve pattern separation. *Nature*, **472**(7344), 466-470.

Sanai, N., Tramontin, A. D., Quinones-Hinojosa, A., Barbaro, N. M., Gupta, N., Kunwar, S., . . . Alvarez-Buylla, A. (2004). Unique astrocyte ribbon in adult human brain contains neural stem cells but lacks chain migration. *Nature*, **427**(6976), 740-744.

Sanjuan-Pla, A., Macaulay, I. C., Jensen, C. T., Woll, P. S., Luis, T. C., Mead, A., . . . Jacobsen, S. E. (2013). Platelet-biased stem cells reside at the apex of the haematopoietic stem-cell hierarchy. *Nature*, **502**(7470), 232-236.

Sargin, D., Friedrichs, H., El-Kordi, A., & Ehrenreich, H. (2010). Erythropoietin as neuroprotective and neuroregenerative treatment strategy: comprehensive overview of 12 years of preclinical and clinical research. *Best practice & research Clinical anaesthesiology*, **24**(4), 573-594.

Sasaki, H., Bothner, B., Dell, A., & Fukuda, M. (1987). Carbohydrate structure of erythropoietin expressed in Chinese hamster ovary cells by a human erythropoietin cDNA. *J Biol Chem*, **262**(25), 12059-12076.

Scadden, D. T. (2006). The stem-cell niche as an entity of action. *Nature*, **441**(7097), 1075-1079.

Schuurmans, C., Armant, O., Nieto, M., Stenman, J. M., Britz, O., Klenin, N., . . . Guillemot, F. (2004). Sequential phases of cortical specification involve Neurogenin-dependent and -independent pathways. *EMBO J*, **23**(14), 2892-2902.

Seaberg, R. M., Smukler, S. R., & van der Kooy, D. (2005). Intrinsic differences distinguish transiently neurogenic progenitors from neural stem cells in the early postnatal brain. *Dev Biol*, **278**(1), 71-85.

Seki, T. (2002). Expression patterns of immature neuronal markers PSA-NCAM, CRMP-4 and NeuroD in the hippocampus of young adult and aged rodents. *J Neurosci Res*, **70**(3), 327-334.

Seki, T., & Arai, Y. (1995). Age-related production of new granule cells in the adult dentate gyrus. *Neuroreport*, **6**(18), 2479-2482.

Semenza, G. L. (2010). Vascular responses to hypoxia and ischemia. *Arterioscler Thromb Vasc Biol*, **30**(4), 648-652.

Semenza, G. L., & Wang, G. L. (1992). A nuclear factor induced by hypoxia via de novo protein synthesis binds to the human erythropoietin gene enhancer at a site required for transcriptional activation. *Mol Cell Biol*, **12**(12), 5447-5454.

Semenza, G. L., Koury, S. T., Nejfelt, M. K., Gearhart, J. D., & Antonarakis, S. E. (1991). Cell-type-specific and hypoxia-inducible expression of the human erythropoietin gene in transgenic mice. *Proc Natl Acad Sci U S A*, **88**(19), 8725-8729.

Semerci, F., & Maletic-Savatic, M. (2016). Transgenic mouse models for studying adult neurogenesis. *Front Biol (Beijing)*, **11**(3), 151-167.

Shadlen, M. N., Britten, K. H., Newsome, W. T., & Movshon, J. A. (1996). A computational analysis of the relationship between neuronal and behavioral responses to visual motion. *J Neurosci*, **16**(4), 1486-1510.

Sharp, F. R., Ran, R., Lu, A., Tang, Y., Strauss, K. I., Glass, T., . . . Bernaudin, M. (2004). Hypoxic preconditioning protects against ischemic brain injury. *NeuroRx*, **1**(1), 26-35.

Shen, Q., Goderie, S. K., Jin, L., Karanth, N., Sun, Y., Abramova, N., . . . Temple, S. (2004). Endothelial cells stimulate self-renewal and expand neurogenesis of neural stem cells. *Science*, **304**(5675), 1338-1340.

Shen, Q., Wang, Y., Kokovay, E., Lin, G., Chuang, S. M., Goderie, S. K., . . . Temple, S. (2008). Adult SVZ stem cells lie in a vascular niche: a quantitative analysis of niche cell-cell interactions. *Cell Stem Cell*, **3**(3), 289-300.

Shingo, T., Sorokan, S. T., Shimazaki, T., & Weiss, S. (2001). Erythropoietin regulates the in vitro and in vivo production of neuronal progenitors by mammalian forebrain neural stem cells. *J Neurosci*, **21**(24), 9733-9743.

Shweiki, D., Itin, A., Soffer, D., & Keshet, E. (1992). Vascular endothelial growth factor induced by hypoxia may mediate hypoxia-initiated angiogenesis. *Nature*, **359**(6398), 843-845.

Sidman, R. L., & Rakic, P. (1973). Neuronal migration, with special reference to developing human brain: a review. *Brain Res*, **62**(1), 1-35.

Sierra, A., Encinas, J. M., Deudero, J. J., Chancey, J. H., Enikolopov, G., Overstreet-Wadiche, L. S., . . . Maletic-Savatic, M. (2010). Microglia shape adult hippocampal neurogenesis through apoptosis-coupled phagocytosis. *Cell Stem Cell*, **7**(4), 483-495.

Siren, A. L., Knerlich, F., Poser, W., Gleiter, C. H., Bruck, W., & Ehrenreich, H. (2001). Erythropoietin and erythropoietin receptor in human ischemic/hypoxic brain. *Acta Neuropathol*, **101**(3), 271-276.

Siren, A. L., Radyushkin, K., Boretius, S., Kammer, D., Riechers, C. C., Natt, O., . . . Ehrenreich, H. (2006). Global brain atrophy after unilateral parietal lesion and its prevention by erythropoietin. *Brain*, **129**(Pt 2), 480-489.

Sirén, A.-L., Faßhauer, T., Bartels, C., & Ehrenreich, H. (2009). Therapeutic potential of erythropoietin and its structural or functional variants in the nervous system. *Neurotherapeutics*, **6**(1), 108-127.

Sirko, S., Behrendt, G., Johansson, P. A., Tripathi, P., Costa, M., Bek, S., . . . Gotz, M. (2013). Reactive glia in the injured brain acquire stem cell properties in response to sonic hedgehog. [corrected]. *Cell Stem Cell*, **12**(4), 426-439.

Snyder, J. S., Choe, J. S., Clifford, M. A., Jeurling, S. I., Hurley, P., Brown, A., . . . Cameron, H. A. (2009). Adult-born hippocampal neurons are more numerous, faster maturing, and more involved in behavior in rats than in mice. *J Neurosci*, **29**(46), 14484-14495.

Snyder, J. S., Kee, N., & Wojtowicz, J. M. (2001). Effects of adult neurogenesis on synaptic plasticity in the rat dentate gyrus. *J Neurophysiol*, **85**(6), 2423-2431.

Sorrells, S. F., Paredes, M. F., Cebrian-Silla, A., Sandoval, K., Qi, D., Kelley, K. W., . . . Alvarez-Buylla, A. (2018). Human hippocampal neurogenesis drops sharply in children to undetectable levels in adults. *Nature*, **555**(7696), 377-381.

Spalding, K. L., Bergmann, O., Alkass, K., Bernard, S., Salehpour, M., Huttner, H. B., . . . Frisen, J. (2013). Dynamics of hippocampal neurogenesis in adult humans. *Cell*, **153**(6), 1219-1227.

Spalding, K. L., Bhardwaj, R. D., Buchholz, B. A., Druid, H., & Frisen, J. (2005). Retrospective birth dating of cells in humans. *Cell*, **122**(1), 133-143.

Statler, P. A., McPherson, R. J., Bauer, L. A., Kellert, B. A., & Juul, S. E. (2007). Pharmacokinetics of high-dose recombinant erythropoietin in plasma and brain of neonatal rats. *Pediatr Res*, **61**(6), 671-675.

Stroka, D. M., Burkhardt, T., Desbaillets, I., Wenger, R. H., Neil, D. A., Bauer, C., . . . Candinas, D. (2001). HIF-1 is expressed in normoxic tissue and displays an organ-specific regulation under systemic hypoxia. *FASEB J*, **15**(13), 2445-2453.

Studer, L., Csete, M., Lee, S. H., Kabbani, N., Walikonis, J., Wold, B., & McKay, R. (2000). Enhanced proliferation, survival, and dopaminergic differentiation of CNS precursors in lowered oxygen. *J Neurosci*, **20**(19), 7377-7383.

Su, Z., Niu, W., Liu, M. L., Zou, Y., & Zhang, C. L. (2014). In vivo conversion of astrocytes to neurons in the injured adult spinal cord. *Nat Commun*, **5**, 3338.

Sugawa, M., Sakurai, Y., Ishikawa-Ieda, Y., Suzuki, H., & Asou, H. (2002). Effects of erythropoietin on glial cell development; oligodendrocyte maturation and astrocyte proliferation. *Neurosci Res*, **44**(4), 391-403.

Suh, H., Consiglio, A., Ray, J., Sawai, T., D'Amour, K. A., & Gage, F. H. (2007). In vivo fate analysis reveals the multipotent and self-renewal capacities of Sox2+ neural stem cells in the adult hippocampus. *Cell Stem Cell*, **1**(5), 515-528.

Sun, D. (2014). The potential of endogenous neurogenesis for brain repair and regeneration following traumatic brain injury. *Neural Regen Res*, **9**(7), 688-692.

Sun, M., Liao, H. G., Niu, K., & Zheng, H. (2013). Structural and morphological evolution of lead dendrites during electrochemical migration. *Sci Rep*, **3**, 3227.

Takahashi, K., & Yamanaka, S. (2006). Induction of pluripotent stem cells from mouse embryonic and adult fibroblast cultures by defined factors. *Cell*, **126**(4), 663-676.

Tam, W. L., Lim, C. Y., Han, J., Zhang, J., Ang, Y. S., Ng, H. H., . . . Lim, B. (2008). T-cell factor 3 regulates embryonic stem cell pluripotency and self-renewal by the transcriptional control of multiple lineage pathways. *Stem Cells*, **26**(8), 2019-2031.

Tan, C. C., & Ratcliffe, P. J. (1992). Rapid oxygen-dependent changes in erythropoietin mRNA in perfused rat kidneys: evidence against mediation by cAMP. *Kidney Int*, **41**(6), 1581-1587.

Tashiro, A., Sandler, V. M., Toni, N., Zhao, C., & Gage, F. H. (2006). NMDA-receptor-mediated, cell-specific integration of new neurons in adult dentate gyrus. *Nature*, **442**(7105), 929-933.

Tonchev, A. B., & Yamashima, T. (2007). "Transcribing" postischemic neurogenesis: a tale revealing hopes of adult brain repair. *J Mol Med (Berl)*, **85**(6), 539-542.

Toni, N., Laplagne, D. A., Zhao, C., Lombardi, G., Ribak, C. E., Gage, F. H., & Schinder, A. F. (2008). Neurons born in the adult dentate gyrus form functional synapses with target cells. *Nat Neurosci*, **11**(8), 901-907.

Toni, N., Teng, E. M., Bushong, E. A., Aimone, J. B., Zhao, C., Consiglio, A., . . . Gage, F. H. (2007). Synapse formation on neurons born in the adult hippocampus. *Nat Neurosci*, **10**(6), 727-734.

Trejo, J. L., Carro, E., & Torres-Aleman, I. (2001). Circulating insulin-like growth factor I mediates exercise-induced increases in the number of new neurons in the adult hippocampus. *J Neurosci*, **21**(5), 1628-1634.

Tsai, P. T., Ohab, J. J., Kertesz, N., Groszer, M., Matter, C., Gao, J., . . . Carmichael, S. T. (2006). A critical role of erythropoietin receptor in neurogenesis and post-stroke recovery. *J Neurosci*, **26**(4), 1269-1274.

van Gelder, B. M., Tijhuis, M. A., Kalmijn, S., Giampaoli, S., Nissinen, A., & Kromhout, D. (2004). Physical activity in relation to cognitive decline in elderly men: the FINE Study. *Neurology*, **63**(12), 2316-2321.

van Praag, H., Shubert, T., Zhao, C., & Gage, F. H. (2005). Exercise enhances learning and hippocampal neurogenesis in aged mice. *J Neurosci*, **25**(38), 8680-8685.

Varela-Nallar, L., Rojas-Abalos, M., Abbott, A. C., Moya, E. A., Iturriaga, R., & Inestrosa, N. C. (2014). Chronic hypoxia induces the activation of the Wnt/beta-catenin signaling pathway and stimulates hippocampal neurogenesis in wild-type and APPswe-PS1DeltaE9 transgenic mice in vivo. *Front Cell Neurosci*, **8**, 17.

Voelcker-Rehage, C., & Niemann, C. (2013). Structural and functional brain changes related to different types of physical activity across the life span. *Neurosci Biobehav Rev*, **37**(9 Pt B), 2268-2295.

Wang, C., Fong, H., & Huang, Y. (2015). Direct Reprogramming of RESTing Astrocytes. *Cell Stem Cell*, **17**(1), 1-3.

Wang, L., Zhang, Z. G., Gregg, S. R., Zhang, R. L., Jiao, Z., LeTourneau, Y., . . . Chopp, M. (2007). The Sonic hedgehog pathway mediates carbamylated erythropoietin-enhanced

proliferation and differentiation of adult neural progenitor cells. *J Biol Chem*, **282**(44), 32462-32470.

Watts, M. E., Pocock, R., & Claudianos, C. (2018). Brain Energy and Oxygen Metabolism: Emerging Role in Normal Function and Disease. *Frontiers in molecular neuroscience*, **11**.

Weidemann, A., & Johnson, R. S. (2009). Nonrenal regulation of EPO synthesis. *Kidney Int*, **75**(7), 682-688.

Wenger, R. H. (2002). Cellular adaptation to hypoxia: O2-sensing protein hydroxylases, hypoxia-inducible transcription factors, and O2-regulated gene expression. *FASEB J*, **16**(10), 1151-1162.

Wernig, M., Meissner, A., Foreman, R., Brambrink, T., Ku, M., Hochedlinger, K., . . . Jaenisch, R. (2007). In vitro reprogramming of fibroblasts into a pluripotent ES-cell-like state. *Nature*, **448**(7151), 318-324.

Wiltrout, C., Lang, B., Yan, Y., Dempsey, R. J., & Vemuganti, R. (2007). Repairing brain after stroke: a review on post-ischemic neurogenesis. *Neurochem Int*, **50**(7-8), 1028-1041.

Wu, A. R., Wang, J., Streets, A. M., & Huang, Y. (2017). Single-Cell Transcriptional Analysis. *Annu Rev Anal Chem (Palo Alto Calif)*, **10**(1), 439-462.

Wu, H., Klingmuller, U., Besmer, P., & Lodish, H. F. (1995). Interaction of the erythropoietin and stem-cell-factor receptors. *Nature*, **377**(6546), 242-246.

Wustenberg, T., Begemann, M., Bartels, C., Gefeller, O., Stawicki, S., Hinze-Selch, D., . . . Ehrenreich, H. (2011). Recombinant human erythropoietin delays loss of gray matter in chronic schizophrenia. *Mol Psychiatry*, **16**(1), 26-36, 21.

Xenocostas, A., Cheung, W. K., Farrell, F., Zakszewski, C., Kelley, M., Lutynski, A., . . . Messner, H. A. (2005). The pharmacokinetics of erythropoietin in the cerebrospinal fluid after intravenous administration of recombinant human erythropoietin. *Eur J Clin Pharmacol*, **61**(3), 189-195.

Xie, Y., & Lowry, W. E. (2018). Manipulation of neural progenitor fate through the oxygen sensing pathway. *Methods*, **133**, 44-53.

Yamamoto, R., Morita, Y., Ooehara, J., Hamanaka, S., Onodera, M., Rudolph, K. L., . . . Nakauchi, H. (2013). Clonal analysis unveils self-renewing lineage-restricted progenitors generated directly from hematopoietic stem cells. *Cell*, **154**(5), 1112-1126.

Yamamoto, S., Ooshima, Y., Nakata, M., Yano, T., Matsuoka, K., Watanabe, S., . . . Hashimoto, T. (2013). Generation of gene-targeted mice using embryonic stem cells derived from a transgenic mouse model of Alzheimer's disease. *Transgenic Res*, **22**(3), 537-547.

Yang, H., Feng, G. D., Olivera, C., Jiao, X. Y., Vitale, A., Gong, J., & You, S. W. (2012). Sonic hedgehog released from scratch-injured astrocytes is a key signal necessary but not sufficient for the astrocyte de-differentiation. *Stem Cell Res*, **9**(2), 156-166.

Ye, H., Wang, X., Li, Z., Zhou, F., Li, X., Ni, Y., . . . Lan, Y. (2017). Clonal analysis reveals remarkable functional heterogeneity during hematopoietic stem cell emergence. *Cell Res*, **27**(8), 1065-1068.

Yeo, E. J., Cho, Y. S., Kim, M. S., & Park, J. W. (2008). Contribution of HIF-1alpha or HIF-2alpha to erythropoietin expression: in vivo evidence based on chromatin immunoprecipitation. *Ann Hematol*, **87**(1), 11-17.

Yin, T., & Li, L. (2006). The stem cell niches in bone. *J Clin Invest*, **116**(5), 1195-1201.

Youssoufian, H., Longmore, G., Neumann, D., Yoshimura, A., & Lodish, H. F. (1993). Structure, function, and activation of the erythropoietin receptor. *Blood*, **81**(9), 2223-2236.

Yu, X., Shacka, J. J., Eells, J. B., Suarez-Quian, C., Przygodzki, R. M., Beleslin-Cokic, B., . . . Noguchi, C. T. (2002). Erythropoietin receptor signalling is required for normal brain development. *Development*, **129**(2), 505-516.

Zappone, M. V., Galli, R., Catena, R., Meani, N., De Biasi, S., Mattei, E., . . . Nicolis, S. K. (2000). Sox2 regulatory sequences direct expression of a (beta)-geo transgene to telencephalic neural stem cells and precursors of the mouse embryo, revealing regionalization of gene expression in CNS stem cells. *Development*, **127**(11), 2367-2382.

Zeisel, A., Munoz-Manchado, A. B., Codeluppi, S., Lonnerberg, P., La Manno, G., Jureus, A., . . . Linnarsson, S. (2015). Brain structure. Cell types in the mouse cortex and hippocampus revealed by single-cell RNA-seq. *Science*, **347**(6226), 1138-1142.

Zhang, K., Zhu, L., & Fan, M. (2011). Oxygen, a key factor regulating cell behavior during neurogenesis and cerebral diseases. *Frontiers in molecular neuroscience*, **4**, 5.

Zhang, P., Bai, Y., Lu, L., Li, Y., & Duan, C. (2016). An oxygen-insensitive Hif-3alpha isoform inhibits Wnt signaling by destabilizing the nuclear beta-catenin complex. *Elife*, **5**.

Zhang, W., Zecca, L., Wilson, B., Ren, H. W., Wang, Y. J., Wang, X. M., & Hong, J. S. (2013). Human neuromelanin: an endogenous microglial activator for dopaminergic neuron death. *Front Biosci (Elite Ed)*, **5**, 1-11.

Zhao, C., Teng, E. M., Summers, R. G., Jr., Ming, G. L., & Gage, F. H. (2006). Distinct morphological stages of dentate granule neuron maturation in the adult mouse hippocampus. *J Neurosci*, **26**(1), 3-11.

Zhao, M., Momma, S., Delfani, K., Carlen, M., Cassidy, R. M., Johansson, C. B., . . . Janson, A. M. (2003). Evidence for neurogenesis in the adult mammalian substantia nigra. *Proc Natl Acad Sci U S A*, **100**(13), 7925-7930.

Zhao, Y., Flandin, P., Long, J. E., Cuesta, M. D., Westphal, H., & Rubenstein, J. L. (2008). Distinct molecular pathways for development of telencephalic interneuron subtypes revealed through analysis of Lhx6 mutants. *J Comp Neurol*, **510**(1), 79-99.

Zhou, X., Smith, A. J., Waterhouse, A., Blin, G., Malaguti, M., Lin, C. Y., . . . Lowell, S. (2013). Hes1 desynchronizes differentiation of pluripotent cells by modulating STAT3 activity. *Stem Cells*, **31**(8), 1511-1522.

Zhu, X. H., Yan, H. C., Zhang, J., Qu, H. D., Qiu, X. S., Chen, L., . . . Gao, T. M. (2010). Intermittent hypoxia promotes hippocampal neurogenesis and produces antidepressant-like effects in adult rats. *J Neurosci*, **30**(38), 12653-12663.

7. Appendices.

7.1. List of Abbreviations.

14C – Isotope Carbon – 14

ALV – Alveus of the hippocampus

APs – Apical Progenitor cells

ARNT – Aryl Hydrocarbon Receptor Translocator

BBB – Blood Brain Barrier

BD – Bipolar Disorder

BDNF – Brain Derived Neurotrophic Factor

bFGF – basic Fibroblast Growth Factor

BMPs – Bone Morphogenetic Proteins

BPs – Basal Progenitor cells

BrdU – Bromodeoxyuridine

CBP – CREB Binding Protein

CCA – Canonical Correlation Analysis

CNS – Central Nervous System

CP – Cortical Plate

CRW – Complex Running Wheel

CSF – Cerebrospinal Fluid

CTIP2 – Chicken ovalbumin upstream promoter transcription factor interacting protein 2

DAB – 3, 3'-diaminobenzidine

DAPI – 4', 6'-diamidino-2-phenylindole

DCX – Doublecortin

DG – Dentate Gyrus

DKK1 – Dickkopf- 1

EdU – 5-Ethynyl-2'-deoxyuridine

EGF – Epidermal Growth Factor

ENs – Endothelial Cells

EP300 – E1A binding Protein p300

EPO – Erythropoietin

EPOR – Erythropoietin Receptor

EPs – Ependymal Cells

ER – Estrogen Receptor

ESCs – Embryonic Stem Cells

FBS – Fetal Bovine Serum

FCS – Fetal Calf Serum

FGF-2 – Fibroblast Growth Factor-2

FMRP – Fragile X Mental Retardation Protein

GDNF – Glial Cell Line Derived Neurotrophic Factor

GFAP – Glial Fibrillary Acidic Protein

Gli1 – Gliotactin 1

GO-terms – Gene Ontology terms

HBBS – Hanks Balanced Salt solution

HIFs – Hypoxia Inducible Factors

HMG – High Mobility Group

HPCs – Hematopoietic Progenitor Cells

HREs – Hypoxia Regulatory Elements

HSCs – Hematopoietic Stem Cells

Hsp90 – Heat Shock Protein 90

I.P. – Intraperitoneal Injection

IGF-1 – Insulin like Growth Factor-1

IHC – Immunohistochemistry

IPs – Intermediate Progenitors

IPSCs – Induced Pluripotent Stem Cells

ISH – In-Situ Hybridization

KLF4 – Krüppel-like Factor-4

LBD – Ligand Binding Domain

LncRNAs – Long Non-Coding RNAs

LTP – Long Term Potentiation

MPPs – Multipotent Precursors

MS – Multiple Sclerosis

NeuroD – Neurogenic Differentiation 1

Ngn2 – Neurogenin 2

NO – Nitric Oxide

NPCs – Neural Precursor Cells

NR – Non-Runner

NR2E1 – Nuclear Receptor Subfamily 2 Group E Member 1

NRSF – Neuron Restrictive Silencer Factor

NSCs – Neural Stem Cells

OB – Olfactory Bulb

ODD – Oxygen Dependent Degradation

OPCs – Oligodendrocyte Precursor Cells

PAA – Penicillin/Streptomycin

Pax6 – Paired-box 6

PBS – Phosphate Buffered Saline

PCA – Principle Component Analysis

PFO – Perfluro-octanol

PHD1/PHD2/PHD3 – Prolyl Hydroxylases

PNS – Peripheral Nervous System

QRT-PCR – Quantitative Real Time Polymerase Chain Reaction

REST – Repressor of Element 1-Silencing Transcription

RGCs – Radial Glial Cells

RGLs – Radial Glial Like Cells

RMS – Rostral Migratory Stream

RMST – Rhabdomyosarcoma 2-associated Transcript

Satb1 – Special AT-rich DNA binding protein 1

SCF – Stem Cell Factor

scRNA-Seq – Single Cell Transcriptome RNA sequencing

sFRP3 – Secreted Frizzled Related Protein 3

SGZ – Sub-Granular Zone

SHH – Sonic Hedgehog

SNN – Shared Nearest Neighbor

Sox2 – Sex Determining Region Y – Box 2

SP – Sub-Plate

SR – *Stratum Radiatum*

SSC – Saline-Sodium Citrate buffer

SVZ – Sub-Ventricular Zone

TAPs – Transit Amplifying Progenitors

Tbr1 – T-box Brain Gene 1

Tbr2 – T-box Brain Gene 2

TFs – Transcription Factors

Tle4 – Transducin-like enhancer family member 4

TRD – Treatment Resistant Depression

tSNE – t-distributed Stochastic Neighbor Embedding

UMI – Unique Molecular Identifier

VEGF – Vascular Endothelial Growth Factor

VHL – Von-Hippel-Lindau protein